

MD-A181 596

DEVELOPMENT OF MECHANISTIC FLEXIBLE PAVEMENT DESIGN
CONCEPTS FOR THE HEAV. (U) ILLINOIS UNIV AT URBANA
NEWMARK CIVIL ENGINEERING LAB H F KELLY SEP 86

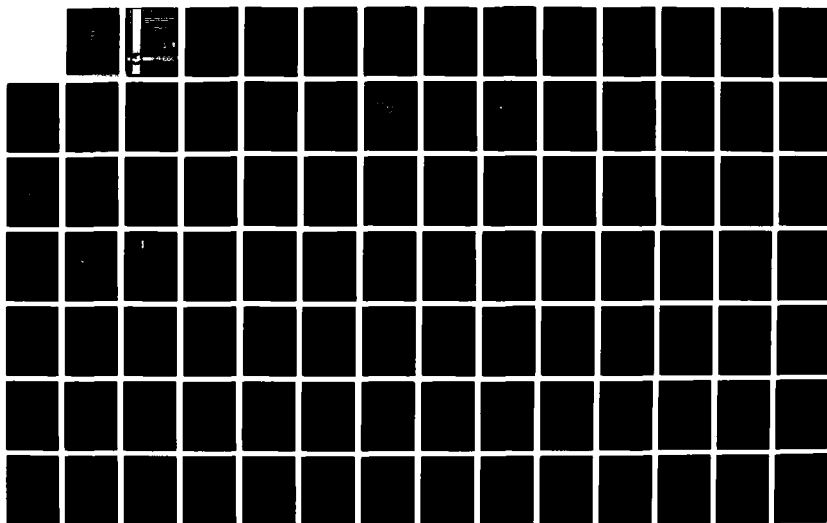
1/3

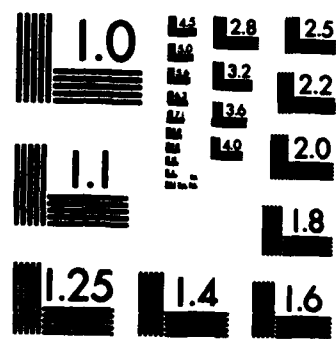
UNCLASSIFIED

AFESC/ESL-TR-86-32 F00637-85-M-6023

F/G 1/5

NL





MICROCOPY RESOLUTION TEST CHART
NATIONAL BUREAU OF STANDARDS-1963-A

AD-A181 596

DTIC FILE COPY

2

ESL-TR-86-32

Development of Mechanistic Flexible Pavement Design Concepts for the Heavyweight F-15 Aircraft

HENRY F. KELLY UNIVERSITY OF ILLINOIS
 NEWMARK CIVIL ENGINEERING LAB
 208 N. ROMINE STREET
 URBANA IL 61801

SEPTEMBER 1986

FINAL REPORT

AUGUST 1983 - MAY 1986

DTIC
SELECTED
S JUN 18 1987 D
 E

APPROVED FOR PUBLIC RELEASE: DISTRIBUTION UNLIMITED



ENGINEERING & SERVICES LABORATORY
AIR FORCE ENGINEERING & SERVICES CENTER
TYNDALL AIR FORCE BASE, FLORIDA 32403

87 0 16 001

NOTICE

PLEASE DO NOT REQUEST COPIES OF THIS REPORT FROM
HQ AFESC/RD (ENGINEERING AND SERVICES LABORATORY).
ADDITIONAL COPIES MAY BE PURCHASED FROM:

NATIONAL TECHNICAL INFORMATION SERVICE
5285 PORT ROYAL ROAD
SPRINGFIELD, VIRGINIA 22161

FEDERAL GOVERNMENT AGENCIES AND THEIR CONTRACTORS
REGISTERED WITH DEFENSE TECHNICAL INFORMATION CENTER
SHOULD DIRECT REQUESTS FOR COPIES OF THIS REPORT TO:

DEFENSE TECHNICAL INFORMATION CENTER
CAMERON STATION
ALEXANDRIA, VIRGINIA 22314

UNCLASSIFIED

SECURITY CLASSIFICATION OF THIS PAGE

REPORT DOCUMENTATION PAGE

1a. REPORT SECURITY CLASSIFICATION UNCLASSIFIED		1b. RESTRICTIVE MARKINGS	
2a. SECURITY CLASSIFICATION AUTHORITY		3. DISTRIBUTION/AVAILABILITY OF REPORT Approved for Public Release Distribution Unlimited	
2b. DECLASSIFICATION/DOWNGRADING SCHEDULE			
4. PERFORMING ORGANIZATION REPORT NUMBER(S)		5. MONITORING ORGANIZATION REPORT NUMBER(S) ESL-TR-86-32	
6a. NAME OF PERFORMING ORGANIZATION University of Illinois	6b. OFFICE SYMBOL (If applicable)	7a. NAME OF MONITORING ORGANIZATION Air Force Engineering and Services Center	
6c. ADDRESS (City, State and ZIP Code) Newmark Civil Engineering Lab 208 N. Romine Street Urbana IL 61801		7b. ADDRESS (City, State and ZIP Code) HQ AFESC/RDCP Tyndall AFB FL 32403-6001	
8a. NAME OF FUNDING/SPONSORING ORGANIZATION	8b. OFFICE SYMBOL (If applicable)	9. PROCUREMENT INSTRUMENT IDENTIFICATION NUMBER F08637-85-M-0623	
8c. ADDRESS (City, State and ZIP Code)		10. SOURCE OF FUNDING NOS.	
		PROGRAM ELEMENT NO.	PROJECT NO.
11. TITLE (Include Security Classification) Development of Mechanistic Flexible Pavement Design Concepts		62206F	2673
12. PERSONAL AUTHOR(S) for the Heavyweight F-15 Aircraft Kelly, Henry F.		13. DATE OF REPORT (Yr., Mo., Day) September 1986	14. PAGE COUNT 227
15. SUPPLEMENTARY NOTATION Availability of this report is specified on reverse of front cover.			
17. COSATI CODES		18. SUBJECT TERMS (Continue on reverse if necessary and identify by block number) Pavements Aircraft Operations Pavement Design Computer Applications	
FIELD	GROUP	SUB. GR.	
13	02		
19. ABSTRACT (Continue on reverse if necessary and identify by block number) This technical report describes a mechanistic method proposed for design of flexible airfield pavements. The report reviews the CBR Flexible Airfield Pavement Design currently used by DoD and the FAA. Then follows a description of the ILLIPAVE finite element computer model and pavement performance transfer functions developed using ILLIPAVE. Actual test data using aircraft-sized loads was used to correlate the constants used in the computer model. The proposed method was then used to design a flexible pavement to support a heavyweight F-15 (30,600 lb SWL, 355 psi). Finally, the subsequent design is compared to the design resulting from the CBR method. <i>Keywords: Computer applications, Jet fighters, Air force applications.</i>			
20. DISTRIBUTION/AVAILABILITY OF ABSTRACT UNCLASSIFIED/UNLIMITED <input type="checkbox"/> SAME AS RPT. <input checked="" type="checkbox"/> DTIC USERS <input type="checkbox"/>		21. ABSTRACT SECURITY CLASSIFICATION UNCLASSIFIED	
22a. NAME OF RESPONSIBLE INDIVIDUAL Major Robert R. Costigan		22b. TELEPHONE NUMBER (Include Area Code) 904-283-6273	22c. OFFICE SYMBOL RDCP

PREFACE

This report was submitted as a doctoral thesis to the Department of Civil Engineering, University of Illinois, funded under Contract Number F08637-85-M-0623 by the Air Force Engineering and Services Center, Engineering and Services Laboratory, Tyndall AFB, Florida 32403-6001.

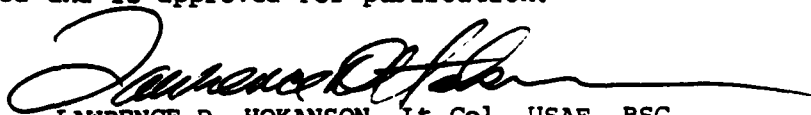
This thesis is being published in its original format by this laboratory because of its interest to the worldwide scientific and engineering community. This thesis covers work performed between August 1983 and May 1986. AFESC/RD project officer was Major Robert Costigan.

This report has been reviewed by the Public Affairs Officer (PA) and is releasable to the National Technical Information Service (NTIS). At NTIS, it will be available to the general public, including foreign nationals.

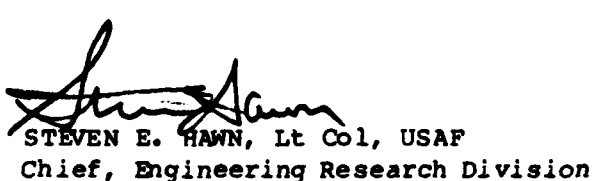
This technical report has been reviewed and is approved for publication.



ROBERT R. COSTIGAN, Major, USAF
Project Officer



LAWRENCE D. HOKANSON, Lt Col, USAF, BSC
Director, Engineering and Services
Laboratory



STEVEN E. HAWN, Lt Col, USAF
Chief, Engineering Research Division

Accession For	
NTIS GRA&I <input checked="" type="checkbox"/>	
DTIC TAB <input type="checkbox"/>	
Unannounced <input type="checkbox"/>	
Justification _____	
By _____	
Distribution/ _____	
Availability Codes	
Dist	Avail and/or Special
A-1	



TABLE OF CONTENTS

Section	Title	Page
I	INTRODUCTION.....	1
	A. OBJECTIVE.....	1
	B. BACKGROUND.....	1
	C. SCOPE/APPROACH.....	2
II	CBR FLEXIBLE AIRFIELD PAVEMENT DESIGN.....	4
	A. CBR DESIGN PROCEDURE.....	4
	B. CBR TEST.....	7
	C. ORIGINAL SELECTION OF THE CBR METHOD.....	9
	D. DEVELOPMENT OF CBR METHOD FOR AIRFIELDS.....	11
	E. TRAFFIC DISTRIBUTION - PASSES PER COVERAGE CONCEPT.....	17
	F. FIELD MOISTURE STUDIES.....	26
	G. COMMENTS CONCERNING THE CBR METHOD.....	26
III	MODELLING PAVEMENT RESILIENT STRUCTURAL RESPONSES.....	28
	A. ILLI-PAVE STRUCTURAL MODEL.....	28
	B. MATERIAL MODELS.....	32
	1. Asphalt Concrete.....	33
	2. Granular Materials.....	33
	3. Fine-Grained Soils.....	36
	C. DATA BASE FOR HEAVYWEIGHT F-15.....	36
	D. HEAVYWEIGHT F-15 DESIGN ALGORITHMS.....	41
	E. INFLUENCE OF LOAD MAGNITUDE ON STRUCTURAL RESPONSES.....	47
	F. INFLUENCE OF BASE QUALITY ON STRUCTURAL RESPONSES.....	49
	G. HEAVIER-WEIGHT F-15 DATA BASE AND DESIGN ALGORITHMS.....	50
IV	TRANSFER FUNCTIONS.....	51
	A. ASPHALT CONCRETE FATIGUE.....	51
	1. Laboratory Fatigue Testing.....	51
	2. Cumulative Damage.....	53
	3. Field Calibration of a Fatigue Equation.....	54
	4. Structural Model Responses and Correlation With Performance Data.....	54
	B. PERMANENT DEFORMATION.....	55
	1. Asphalt Concrete.....	55
	2. Granular Materials.....	56
	3. Fine-Grained Soils.....	58

TABLE OF CONTENTS
(CONTINUED)

Section	Title	Page
V	RESPONSE AND PERFORMANCE OF FULL-SCALE TEST SECTIONS.....	66
	A. OVERVIEW OF AVAILABLE TEST SECTION DATA.....	66
	B. MODELLING THE TEST SECTIONS AND CALCULATED RESPONSES.....	69
	C. TEST SECTION PERFORMANCE DATA.....	83
	D. PAVEMENT RESPONSES - PERFORMANCE CORRELATIONS.....	91
	E. DISCUSSION OF RESULTS.....	97
	1. MWHGL Test Variability.....	97
	2. Deflection Basins.....	98
	3. Subbase Stability.....	99
	4. Failure Criteria.....	100
VI	COMPONENTS OF A MECHANISTIC DESIGN PROCEDURE FOR CONVENTIONAL FLEXIBLE AIRFIELD PAVEMENTS.....	101
	A. TRAFFIC ANALYSIS.....	101
	B. CLIMATIC AND SEASONAL CONSIDERATIONS.....	109
	C. STRUCTURAL MODEL AND PAVEMENT RESPONSES.....	111
	D. MATERIALS CHARACTERIZATION.....	113
	E. TRANSFER FUNCTIONS.....	114
	F. PERFORMANCE ANALYSIS.....	116
	F. BASIC STEPS IN THE DESIGN PROCESS.....	116
VII	COMPARISON OF PROPOSED PROCEDURES AND DESIGNS WITH CBR METHOD.....	118
	A. MECHANISTIC DESIGN EXAMPLE.....	118
	B. COMPARISON OF MECHANISTIC DESIGN WITH CBR DESIGN.....	119
	C. CORRELATION OF COMPUTED RESPONSES WITH CBR DESIGNS.....	125
	D. COMPARISON OF PROPOSED PROCEDURES WITH CBR DESIGN PROCEDURE.....	132
VIII	SUMMARY, FINDINGS AND CONCLUSIONS, AND RECOMMENDATIONS.....	137
	A. SUMMARY.....	137
	B. FINDINGS AND CONCLUSIONS.....	137
	C. RECOMMENDATIONS.....	139
APPENDIX		
A	ILLI-PAVE DATA BASE.....	141
B	ILLI-PAVE DESIGN ALGORITHMS.....	195
	LIST OF REFERENCES.....	210

LIST OF FIGURES

Figure	Title	Page
1	FLEXIBLE PAVEMENT DESIGN CURVES FOR LIGHT-LOAD PAVEMENT.....	6
2	PROCEDURE FOR DETERMINING CBR OF SUBGRADE SOILS.....	8
3	TOTAL THICKNESS OF BASE AND SURFACING IN RELATION TO CBR VALUES.....	12
4	EXTRAPOLATION OF HIGHWAY PAVEMENT THICKNESS BY THE ELASTIC THEORY.....	14
5	TENTATIVE DESIGN OF FOUNDATIONS FOR FLEXIBLE PAVEMENTS.....	14
6	PERCENTAGE OF DESIGN THICKNESS VERSUS COVERAGES.....	18
7	LOAD REPETITIONS FACTOR VERSUS COVERAGES FOR VARIOUS LANDING GEAR TYPES.....	19
8	COMPARISON OF CBR DESIGN EQUATIONS TO PAVEMENT BEHAVIOR DATA.....	20
9	GENERAL NORMAL DISTRIBUTION (GND) CURVE.....	22
10	GND CURVE AS RELATED TO AIRCRAFT TRAFFIC DISTRIBUTION.....	22
11	GND CURVE FOR OVERLAPPING TIRE PRINTS, TWIN WHEELS.....	24
12	MAXIMUM ORDINATE ON CUMULATIVE TRAFFIC DISTRIBUTION CURVE FOR TWO WHEELS VERSUS WHEEL SPACING.....	25
13	CYLINDRICAL PAVEMENT CONFIGURATION.....	29
14	RECTANGULAR SECTION OF AN AXISYMMETRIC SOLID.....	29
15	SYSTEM CONFIGURATION.....	30
16	TYPICAL ASPHALT CONCRETE MODULUS - TEMPERATURE RELATIONSHIP...	34
17	RELATIONSHIP BETWEEN K AND N VALUES FOR GRANULAR MATERIALS IDENTIFIED BY RADA AND WITCZAK.....	35
18	TYPICAL REPRESENTATION OF THE RESILIENT MODULUS-REPEATED DEVIATOR STRESS RELATIONSHIP FOR FINE-GRAINED SOILS.....	37
19	SUBGRADE MATERIAL MODELS USED WITH ILLI-PAVE.....	38
20	AC TENSILE STRAIN VERSUS AC THICKNESS, $E_{Ri}=3.02$ KSI, $E_{AC}=100$ KSI.....	44

LIST OF FIGURES
(CONTINUED)

Figure	Title	Page
21	AC TENSILE STRAIN VERSUS AC THICKNESS, $E_{Ri}=3.02$ KSI, $E_{AC}=500$ KSI.....	45
22	SUBGRADE STRESS RATIO VERSUS AC THICKNESS, $E_{Ri}=3.02$ KSI, $E_{AC}=500$ KSI.....	46
23	TYPICAL PERMANENT DEFORMATION BEHAVIOR FOR A DENSE-GRADED LIMESTONE.....	57
24	TYPICAL PERMANENT DEFORMATION BEHAVIOR FOR A FINE-GRAINED SOIL.....	59
25	STRESS LEVEL-PERMANENT STRAIN RELATIONS FOR A FINE-GRAINED SOIL.....	61
26	INFLUENCE OF MOISTURE CONTENT ON THE PERMANENT STRAIN RESPONSE OF A FINE-GRAINED SOIL.....	62
27	EFFECT OF ONE FREEZE-THAW CYCLE ON PERMANENT DEFORMATION FOR A FINE-GRAINED SOIL.....	63
28	SUBGRADE STRAIN CRITERIA.....	64
29	RELATIONSHIPS BETWEEN PLASTIC STRAIN AND ELASTIC STRAIN FOR FINE-GRAINED SOIL AT 1000 REPETITIONS.....	65
30	APPROXIMATE E_{Ri} - CBR RELATIONSHIP.....	72
31	MWHGL ITEM 1 "DYNAMIC" DEFLECTIONS UNDER 30-KIP STATIC WHEEL LOAD.....	74
32	MWHGL ITEM 2 "DYNAMIC" DEFLECTIONS UNDER 30-KIP STATIC WHEEL LOAD.....	75
33	MWHGL LANE 2 ITEM 1 "DYNAMIC" DEFLECTIONS UNDER 50-KIP STATIC WHEEL LOAD.....	76
34	MWHGL LANE 2A ITEM 1 "DYNAMIC" DEFLECTIONS UNDER 50-KIP STATIC WHEEL LOAD.....	77
35	MWHGL LANE 2 ITEM 2 "DYNAMIC" DEFLECTIONS UNDER 50-KIP STATIC WHEEL LOAD.....	78
36	MWHGL LANE 2A ITEM 2 "DYNAMIC" DEFLECTIONS UNDER 50-KIP STATIC WHEEL LOAD.....	79
37	MWHGL ITEM 1 DEFLECTIONS UNDER 3988-LB PEAK-TO-PEAK VIBRATORY LOAD.....	80

**LIST OF FIGURES
(CONTINUED)**

Figure	Title	Page
38	MWHGL ITEM 2 DEFLECTIONS UNDER 3805-LB PEAK-TO-PEAK VIBRATORY LOAD.....	81
39	MWHGL ITEM 2 DEFLECTIONS UNDER 11.4-KIP PEAK-TO-PEAK VIBRATORY LOAD.....	82
40	REFERENCE 74 ITEM 1 DEFLECTIONS UNDER 9000-LB FWD LOAD.....	84
41	REFERENCE 74 ITEM 2 DEFLECTIONS UNDER 9000-LB FWD LOAD.....	85
42	REFERENCE 74 ITEM 3 DEFLECTIONS UNDER 9000-LB FWD LOAD.....	86
43	SUBGRADE STRESS RATIO VERSUS COVERAGES, SUBGRADE FAILURES ONLY.....	95
44	SUBGRADE STRAIN VERSUS COVERAGES, SUBGRADE FAILURES ONLY.....	96
45	MECHANISTIC DESIGN METHOD.....	102
46	TYPICAL TRAFFIC DISTRIBUTION CURVE FOR TAXIWAY, $\sigma=30$ INCHES...	105
47	TRAFFIC DISTRIBUTION USING DISCRETE LANES, $\sigma=30$ INCHES.....	106
48	AC TENSILE STRAIN VERSUS OFFSET DISTANCE.....	107
49	SUBGRADE DEVIATOR STRESS AND STRESS RATIO VERSUS OFFSET DISTANCE.....	108
50	RESILIENT MODULUS - % SATURATION RELATIONS FOR FINE-GRAINED SOILS.....	110
51	INFLUENCE OF CYCLIC FREEZE-THAW ON THE RESILIENT BEHAVIOR OF A FINE-GRAINED SOIL.....	112
52	CUMULATIVE AC FATIGUE DAMAGE VERSUS GRANULAR BASE THICKNESS FOR 32,000 COVERAGES OF HEAVYWEIGHT F-15 AIRCRAFT.....	120
53	SUMMER SUBGRADE STRESS RATIO VERSUS GRANULAR BASE THICKNESS ($E_{Ri}=3.1$ KSI).....	121
54	SOAKED CBR OF AASHO ROAD TEST SUBGRADE SOIL.....	123
54	FLEXIBLE PAVEMENT DESIGN CURVE FOR F-15, TYPE A TRAFFIC AREA.....	124
56	EFFECT OF ASPHALT CONCRETE MODULUS UPON REPETITION - SUBGRADE STRESS RATIO RESULTS.....	130

LIST OF FIGURES
(CONTINUED)

Figure	Title	Page
57	EFFECT OF ASPHALT CONCRETE MODULUS UPON REPETITION - VERTICAL SUBGRADE STRAIN RESULTS.....	131
B-1	AC TENSILE STRAIN VERSUS AC THICKNESS, VARYING GRANULAR BASE THICKNESS.....	204
B-2	AC TENSILE STRAIN VERSUS AC THICKNESS, VARYING AC MODULUS.....	205
B-3	AC TENSILE STRAIN VERSUS AC THICKNESS, VARYING SUBGRADE MODULUS.....	206
B-4	SUBGRADE STRESS RATIO VERSUS AC THICKNESS, VARYING GRANULAR BASE THICKNESS.....	207
B-5	SUBGRADE STRESS RATIO VERSUS AC THICKNESS, VARYING AC MODULUS.....	208
B-6	SUBGRADE STRESS RATIO VERSUS AC THICKNESS, VARYING SUBGRADE MODULUS.....	209

LIST OF TABLES

Table	Title	Page
1	SUBBASE REQUIREMENTS, MAXIMUM PERMISSIBLE VALUES.....	10
2	DESIGN CBR FOR BASE COURSES.....	10
3	ILLI-PAVE VARIABLES FOR 4X5X5X4 FACTORIAL.....	39
4	SUMMARY OF MATERIAL PROPERTIES FOR ILLI-PAVE SOLUTIONS.....	40
5	ILLI-PAVE VARIABLES FOR 3 ⁴ FACTORIAL.....	48
6	TEST SECTION ANALYSIS RESULTS.....	70
7	SUMMARY OF TRANSFER FUNCTIONS DEVELOPED FROM ALL FAILED TEST SECTIONS.....	93
8	SUMMARY OF TRANSFER FUNCTIONS DEVELOPED FROM SUBGRADE FAILURES.....	94
9	DESIGN FOR 32,000 COVERAGES OF HEAVYWEIGHT F-15 AIRCRAFT.....	122
10	MECHANISTIC ANALYSIS OF CBR DESIGN FOR 32,000 COVERAGES OF HEAVYWEIGHT F-15 AIRCRAFT.....	126
11	TOTAL PAVEMENT THICKNESS ACCORDING TO CBR DESIGN FOR HEAVYWEIGHT F-15 AIRCRAFT.....	128
12	CORRELATION OF ILLI-PAVE RESPONSES WITH CBR DESIGN.....	129
13	SUBGRADE STRESS RATIO CRITERIA FROM REFERENCE 71 STRAIN CRITERIA.....	133
14	ASPHALT CONCRETE FATIGUE DAMAGE EXPECTED FROM MECHANISTIC ANALYSIS OF CBR DESIGNS FOR HEAVYWEIGHT F-15.....	134
15	SUBGRADE STRESS RATIO FOR "HOT" SUMMER DAY FROM MECHANISTIC ANALYSIS OF CBR DESIGNS FOR HEAVYWEIGHT F-15.....	135
A-1	ILLI-PAVE DATA BASE, STRUCTURAL RESPONSES TO 30-KIP/355-PSI LOAD.....	143
A-2	ILLI-PAVE DATA BASE, STRUCTURAL RESPONSES TO 24-KIP/355-PSI LOAD.....	153
A-3	ILLI-PAVE DATA BASE, STRUCTURAL RESPONSES TO 36-KIP/355-PSI LOAD.....	156
A-4	COMPARISON OF AC TENSILE STRAIN (MEAC) AT 24-, 30-, AND 36-KIP LOAD.....	159

**LIST OF TABLES
(CONTINUED)**

Table	Title	Page
A-5	COMPARISON OF SUBGRADE STRAIN (EZ) AT 24-, 30-, AND 36-KIP LOAD.....	162
A-6	COMPARISON OF SUBGRADE DEVIATOR STRESS (SDEV) AT 24-, 30-, AND 36-KIP LOAD.....	165
A-7	ILLI-PAVE DATA BASE, STRUCTURAL RESPONSES TO 30-KIP/355-PSI LOAD (LOW-QUALITY BASE COURSE).....	168
A-8	ILLI-PAVE DATA BASE, STRUCTURAL RESPONSES TO 30-KIP/355-PSI LOAD (HIGH-QUALITY BASE COURSE).....	171
A-9	COMPARISON OF AC TENSILE STRAIN (MEAC) AT 30-KIP/355-PSI LOAD WITH LOW-, MEDIUM-, AND HIGH-QUALITY BASE COURSE.....	174
A-10	COMPARISON OF SUBGRADE STRAIN (EZ) AT 30-KIP/355-PSI LOAD WITH LOW-, MEDIUM-, AND HIGH-QUALITY BASE COURSE.....	177
A-11	COMPARISON OF SUBGRADE DEVIATOR STRESS (SDEV) AT 30-KIP/355-PSI LOAD WITH LOW-, MEDIUM-, AND HIGH-QUALITY BASE COURSE.....	180
A-12	ILLI-PAVE DATA BASE, STRUCTURAL RESPONSES TO 36-KIP/395-PSI LOAD.....	183
A-13	COMPARISON OF AC TENSILE STRAIN (MEAC) AT 30-KIP/355-PSI AND 36-KIP/355-PSI LOAD TO 36-KIP/395-PSI LOAD.....	186
A-14	COMPARISON OF SUBGRADE STRAIN (EZ) AT 30-KIP/355-PSI AND 36-KIP/355-PSI LOAD TO 36-KIP/395-PSI LOAD.....	189
A-15	COMPARISON OF SUBGRADE DEVIATOR STRESS (SDEV) AT 30-KIP/ 355-PSI AND 36-KIP/355-PSI LOAD TO 36-KIP/395-PSI LOAD.....	192
B-1	REGRESSION EQUATIONS WITH "ENGINEERING MEANINGFUL" VARIABLES DEVELOPED FROM FULL FACTORIAL MINUS SUBGRADE FAILURES (373 CASES).....	197
B-2	REGRESSION EQUATIONS WITH MORE "COMPLICATED" VARIABLES DEVELOPED FROM FULL FACTORIAL MINUS SUBGRADE FAILURES (372 CASES).....	198
B-3	REGRESSION EQUATIONS DEVELOPED FROM 3^4 FACTORIAL MINUS SUBGRADE FAILURES (70 CASES).....	199
B-4	REGRESSION EQUATIONS DEVELOPED FOR 24-KIP/355-PSI LOADING DEVELOPED FROM 3^4 FACTORIAL MINUS SUBGRADE FAILURES (73 CASES).....	200

LIST OF TABLES
(CONTINUED)

Table	Title	Page
B-5	REGRESSION EQUATIONS DEVELOPED FOR 36-KIP/355-PSI LOADING DEVELOPED FROM 3 ⁴ FACTORIAL MINUS SUBGRADE FAILURES (66 CASES).....	201
B-6	REGRESSION EQUATIONS DEVELOPED INCLUDING LOAD VARIABLE FROM 3 ⁵ FACTORIAL MINUS SUBGRADE FAILURES (209 CASES).....	202
B-7	REGRESSION EQUATIONS DEVELOPED FOR HEAVIER-WEIGHT F-15 DEVELOPED FROM 3 ⁴ FACTORIAL MINUS SUBGRADE FAILURES (66 CASES).....	203

SECTION I
INTRODUCTION

A. OBJECTIVE

The primary goals of this research are to develop mechanistic design algorithms and a tentative proposed design procedure for the current heavyweight and proposed heavier-weight F-15. The algorithms will provide the capability to estimate critical pavement structural responses (stresses, strains, deflections) given the pavement layer geometry and material characteristics. These responses can then be used to predict pavement performance by using appropriate transfer functions.

B. BACKGROUND

The United States Air Force is using a new heavyweight F-15 aircraft. The plane has a 30,000-lb single-wheel load with a 355-psi tire inflation pressure. The Air Force has proposed using a heavier-weight F-15 aircraft which would have a 36,000-lb single-wheel load with a 395-psi tire inflation pressure. Therefore, the F-15 replaces the F-4 as the controlling aircraft for the design of Light-Load Pavements. The F-4E/G currently operates with a maximum wheel load of 25,400 pounds and a 265-psi tire inflation pressure (Reference 1). The actual load and configuration parameters of the critical aircraft are defined in Reference 2.

The current Department of Defense (DOD) criteria and procedure for design of flexible airfield pavements are outlined in a Tri-Services (Navy, Army, and Air Force) Manual (Reference 3). The procedure uses the California Bearing Ratio (CBR) for determining the strengths of soils (fine-grained and granular). A detailed discussion of the CBR design method for flexible

airfield pavements is contained in Section II.

Field tests have not been conducted using the new and proposed F-15 aircraft. Thus, CBR design curve development will require extrapolations. In some cases, extrapolations can be misleading, particularly when the pavement systems contain stress-dependent material and are subjected to heavy wheel loads and high tire pressures. Furthermore, field tests are expensive and time consuming to run, and provide only minimum amounts of basic data.

Development of a mechanistic flexible airfield design procedure would allow relatively quick and inexpensive quantitative evaluation of desired pavement response parameters (stresses, strains, and deflections) as the pavement layer geometry, material characteristics, and/or loading change. However, a mechanistic design procedure must be verified by field test data. If DOD adopted such a mechanistic design procedure, design equations, curves, tables, etc., could be developed for the heavyweight F-15, or any other aircraft loading, with a minimum of additional field testing.

In this research, the ILLI-PAVE finite element program (discussed in Section III) is used as the structural model to calculate pavement responses. ILLI-PAVE has been validated for highway loading (9-kip) for conventional flexible pavement (References 4, 5, 6, and 7), for full-depth asphalt concrete pavements (Reference 8), and for flexible pavements containing lime-stabilized layers (Reference 9). ILLI-PAVE has also been validated for F-4 aircraft loading of flexible pavements containing cement- and lime-stabilized layers (Reference 10).

C. SCOPE/APPROACH

Section II describes the present DOD design method of conventional flexible airfield pavement. It also summarizes the original adoption and

adaptation of the method by the U.S. Army Corps of Engineers.

Section III describes the ILLI-PAVE structural model. Material characterization is considered for each of the pavement layers in a conventional flexible pavement (asphalt concrete, granular base/subbase, and subgrade soil). Algorithms are developed by stepwise multiple regression analyses relating pavement variables (thicknesses and moduli) to pavement response. Some sensitivity analyses are presented.

Section IV considers transfer functions. Methods of estimating asphalt concrete fatigue and methods to limit permanent deformation within each pavement layer are presented.

Section V presents a validation of the ILLI-PAVE structural model based on existing full-scale test section data.

Section VI considers the components of a mechanistic design procedure for conventional flexible pavement.

Section VII presents a mechanistic design example and compares the proposed procedures with the existing CBR design method.

Section VIII presents conclusions, recommendations, and suggestions for Air Force implementation and future research.

SECTION II

CBR FLEXIBLE AIRFIELD PAVEMENT DESIGN

The flexible pavement CBR design methods utilized by the Department of Defense (Army, Navy, and Air Force) and the Federal Aviation Administration (FAA) are similar. The methods consider three requirements for flexible pavement designs (Reference 11):

1. Each layer must be thick enough to distribute traffic induced stresses so that the underlying layer is not overstressed and excessive shear deformation in the underlying layer will not occur. The CBR procedures are used to determine the layer thickness required to prevent excessive shear deformation in the underlying layer. This section is concerned primarily with this problem, which is termed "thickness design."
2. Each layer must be compacted adequately so that traffic does not produce an intolerable amount of added consolidation and/or rutting. The modified AASHTO laboratory compaction test and construction specifications requiring the proper percentage of laboratory density are used to control consolidation under traffic.
3. The surface must be stable, wear resistant, and weather resistant. Design procedures using the Marshall stability test are used to design the bituminous paving mixtures to produce a wear and weather resistant surfacing that will not rut excessively under traffic.

A. CBR DESIGN PROCEDURE

The current Department of Defense (DOD) criteria and procedure for CBR design is outlined in the Tri-Services (Navy, Army, and Air Force) Manual entitled, "Flexible Pavement Design for Airfields," (Reference 3). To use

the procedure, enter the top of the design curve (see example, Figure 1) with the design CBR and follow it downward to the intersection with appropriate gross weight curve, then horizontally to appropriate aircraft passes curve, then down to required total pavement thickness above subgrade. The same procedure is applied to successive layers. Each layer of the pavement must be of higher quality (increased CBR) than the layer below it. It is assumed that stress distribution through the pavement is independent of the quality of the various layers (Reference 11).

The Air Force categorizes airfield pavements into one of three load conditions. The categories are Light Load, Medium Load, and Heavy Load. Each category, in turn, has a set of critical aircraft load and configuration parameters that are used to establish the design thicknesses. The design curve for the Light-Load Pavement is shown in Figure 1. The present controlling aircraft for Light-Load Pavements is the F-4 and is defined in Reference 2 as having, for Type B traffic area, a gross aircraft weight of 60,000 pounds supported on two nontracking main landing gears each having a single wheel with a tire contact area of 100 in.² and a nose gear. The Light-Load Pavement is designed for 300,000 passes of the specified light aircraft load and 1000 passes of the specified medium aircraft load. Type B traffic areas for Light-Load Pavement are (Reference 2):

1. The first 1000 feet of runway ends.
2. Primary taxiways.
3. Connecting taxiways, short lengths of primary taxiway turns, and intersections of primary taxiways.
4. All aprons and hardstands.
5. Power check pads.

Minimum asphalt concrete (AC) surface and granular base thicknesses for

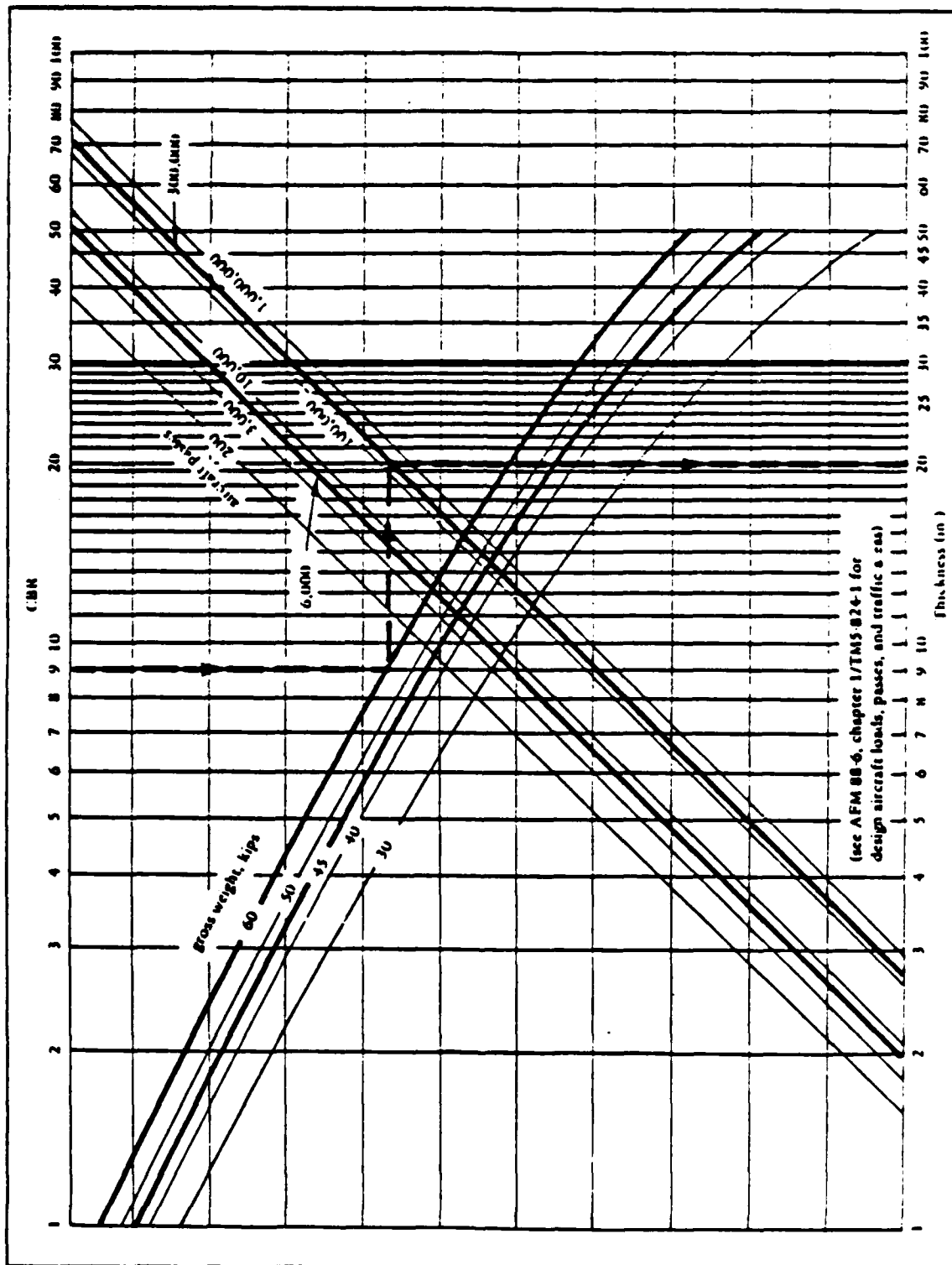


Figure 1. Flexible Pavement Design Curves for Light-Load Pavement (Reference 3).

fighter aircraft (Light-Load Pavements) are:

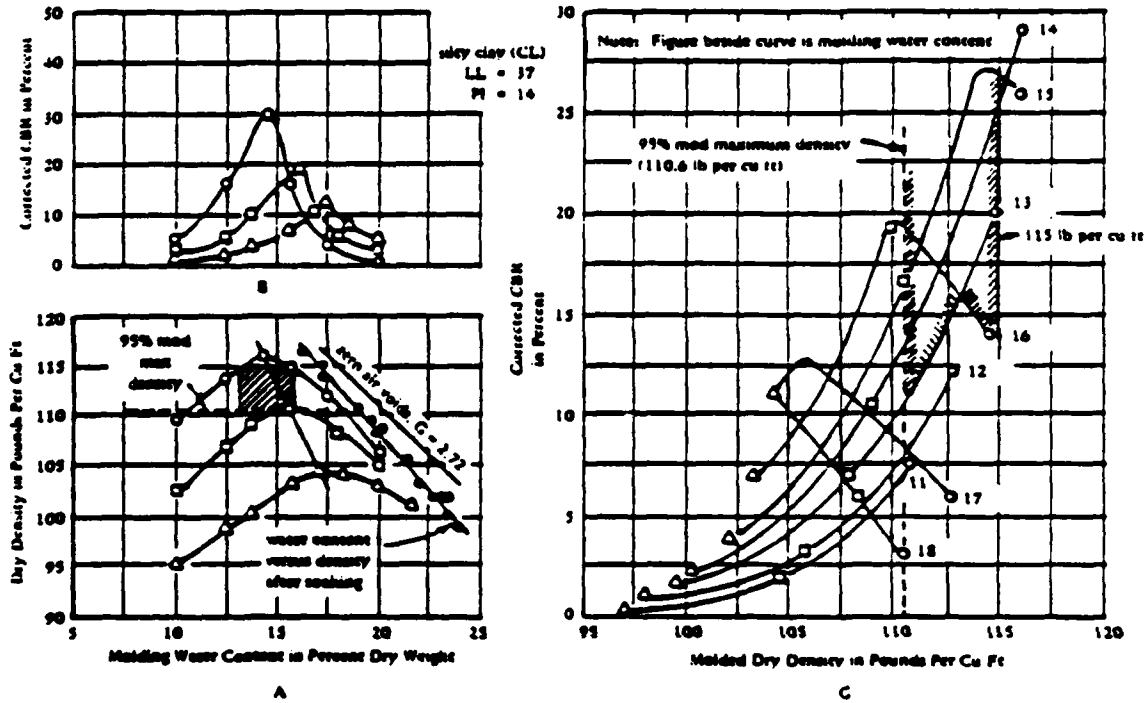
<u>100-CBR Base</u>		<u>80-CBR Base</u>	
<u>AC</u>	<u>Base</u>	<u>AC</u>	<u>Base</u>
3"	6"	4"	6"

The new heavyweight F-15, with a single-wheel load of 30,000 pounds and tire pressure of 355 psi, will become the controlling aircraft for Light-Load Pavements.

B. CBR TEST

The CBR test can be performed on samples compacted in test molds, on material in-place, or on undisturbed samples. However, for design the latter test is used only in special cases. To represent the prototype condition that will be the most critical for design, the test is normally performed on compacted samples of subgrade soil after a four-day soak under a surcharge representing the weight of the pavement. Samples are prepared at varying moisture contents and three different compactive efforts. The complete procedure is illustrated in Figure 2 and details of the test methods are presented in Military Standard 621A, Method 101. When laboratory CBR tests on compacted samples are used, at least two complete series of tests, as outlined in Figure 2, should be performed for each distinct subgrade soil type. Careful engineering judgement is then used in selecting the design CBR values.

Supplementary requirements are used for granular materials because laboratory CBR tests on these materials show CBR values higher than those obtained in the field. This is because of the confining effect of the 6-inch-diameter CBR mold (References 12 and 13). Therefore, the laboratory tests are supplemented by gradation and Atterberg limits requirements shown



Legend

- - 35 Blow/layer compactive effort
- - 26 blow/layer compactive effort
- △ - 12 blow/layer compactive effort
- G - Specific gravity of soil

1. Step A. Determine moisture/density relationship (MIL-STD-621 Method 100) at 12, 26 and 35 blows/layer. Plot dryness to which soil can be compacted in the field - for clay of example use 95% of maximum density. Plot desired moisture content range - for clay of example use $\pm 1-1/2\%$ of optimum moisture content for approximately 13 and 16%. Shaded area represents compactive effort greater than 95% and within $\pm 1-1/2\%$ of optimum moisture content.
2. Step B. Plot laboratory CBR (MIL-STD-621 Method 101) for 12, 26 and 35 blows/layer.
3. Step C. Plot CBR versus dry density at constant moisture content. Plot attainable limits of compaction from graph A-110.6 and 115 pounds per cubic foot for example. Hatched area represents attainable CBR lines for desired compaction (110.6 to 115 lb per cu ft) and moisture content (13 to 16%). CBR varies from 11 (95% compaction and 13% moisture content) to 26 (15% moisture content and maximum compaction). For design purposes use a CBR at low end of range-in example use CBR of 12 with moisture content specified between 13 and 16%.

Figure 2. Procedure for Determining CBR of Subgrade Soils (Reference 3).

in Table 1. If the laboratory CBR exceeds the maximum permissible values in the range shown, use the value shown in Table 1. Design CBR values for base course materials are shown in Table 2. Definitions/requirements for base course materials are contained in Table 6-1 of Reference 3.

C. ORIGINAL SELECTION OF THE CBR METHOD

The adoption of the CBR method of thickness design for flexible airfield pavements is discussed by McFadden and Pringle in the CBR Symposium (Reference 14) and is summarized in this section. They state that during the latter part of November 1940, the responsibility for the design and construction of military airfields was assigned to the U.S. Army Corps of Engineers. It was concluded that there was insufficient time to develop a purely theoretical design method due to the war emergency program then being faced. Therefore, adaptation of an empirical method that had been successfully used for highway loading appeared to be the only solution. Some of the controlling reasons for adopting the CBR method were:

1. The CBR method had been correlated to the service behavior of flexible pavements and construction methods and successfully used by the State of California for a number of years.
2. It could be more quickly adapted to airfield pavement design for immediate use than any other method.
3. It was thought to be as reasonable and as sound as any of the other methods investigated.
4. Two other states were known to have methods of a similar nature that had been successful.
5. The subgrade could be tested with simple portable equipment either in the laboratory or in the field.

TABLE 1. SUBBASE REQUIREMENTS, MAXIMUM PERMISSIBLE VALUES (REFERENCE 3).

Material	Design CBR	Size (in.)	Percent Passing		Plasticity Requirements	
			No. 10	No. 200	LL	PI
Subbase	50	3	50	15	25	5
Subbase	40	3	80	15	25	5
Subbase	30	3	100	15	25	5
Select material	20	3	--	25 ^a	35 ^a	12 ^a

Note: LL signifies liquid limit; PI signifies plasticity index

^a Suggested limits

TABLE 2. DESIGN CBR FOR BASE COURSES (REFERENCE 3).

Type	Design CBR
Graded crushed aggregate	100
Water-bound macadam	100
Dry-bound macadam	100
Bituminous intermediate and surface courses, central plant, hot mix	100
Limerock	80
Mechanically stabilized aggregate	80

6. Testing could be done on samples of soil in the condition representative of the foundation-moisture state under most pavements.

D. DEVELOPMENT OF CBR METHOD FOR AIRFIELDS

Adaptation of CBR highway design to design of airfield pavements is discussed by Middlebrooks and Bertram in Reference 14. Investigations made from 1928 to 1942, on both adequate pavements and flexible pavements that failed, furnished considerable empirical data for correlation of the CBR requirements with service behavior. From these data, curves were formulated such as curves A and B, Figure 3, which show the minimum thickness of base and surfacing used in 1942 for light and medium heavy traffic on the California highway system.

It was believed that curve A, Figure 3, was the most reliable, so it was used as a basis for conversions. This curve was originally drawn for lighter wheel loads, but it was known from service behavior of the pavements that 9000-pound truck wheel loads were supported without distress throughout the life of the pavement. It was decided that curve A could be assumed to represent a 12,000-pound airplane wheel. There were two reasons for this decision: 1) highway loadings were carried on tires with a deformation of less than 10 percent whereas airplane tires had a deformation of 35 percent, thus resulting in larger contact area, and 2) highway traffic is channelized whereas runway traffic is fairly well spread out. Curve B was judged on the same basis to represent a 7000-pound wheel load.

Empirical curves were developed for heavier airplane loadings by extrapolating the original data on the basis of the elastic theory and a one-layer (Boussinesq) system. Shear stresses were used as a guide in making the extrapolations. A uniform tire pressure of 60 psi covered the entire

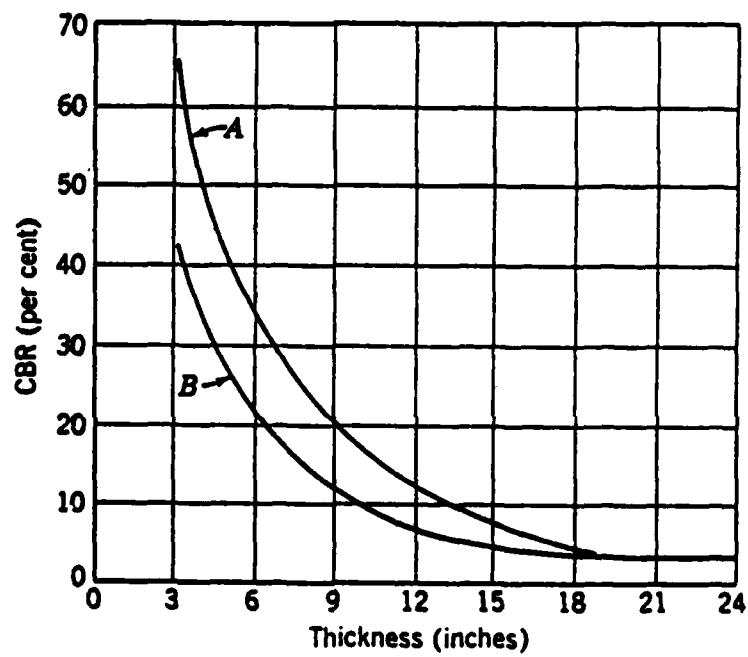


Figure 3. Total Thickness of Base and Surfacing in Relation to CBR Values (Reference 14).

group of planes in use. Wheel loads of 25,000 lb, 40,000 lb, and 70,000 lb were selected to cover the range of heavy aircraft loads. Circular areas were used for ease of computation and also because the difference in shear stresses in base course and subgrade did not vary materially for elliptical and circular areas. Shear stresses were computed as shown in Figure 4 by the use of stress tables. The thicknesses of base course and pavement corresponding to CBRs of 3, 5, 7, and 10 were located on the stress curve for the 12,000-lb load curve and the stresses corresponding to these thicknesses were noted. On the basis that these stresses should not be exceeded for other wheel loads to retain a uniform standard of design, the stress values were located on the curves for 25,000-lb, 40,000-lb, and 70,000-lb wheel loads (Figure 4). The thickness corresponding to these stresses was transferred to the graph of thickness versus CBR, and curves similar to those shown in Figure 5 were drawn.

A series of accelerated traffic tests was immediately initiated to validate the extrapolations. Test sections were subjected to accelerated traffic with wheel loads up to 200,000 pounds (References 15 through 22). The pavements were considered to be failed when either of the following conditions occurred (Reference 23):

1. Surface upheaval of 1 inch or greater of the pavement adjacent to the traffic load (pavement shear failure).
2. Severe surface cracking to significant depths. Surface rutting that is not associated with upheaval results from compaction deficiency and was not considered in the failure criteria.

These studies permitted comparison between the thickness design curves and the performance during traffic. The comparisons were based on the in-place CBR that existed during the traffic period. The results of these

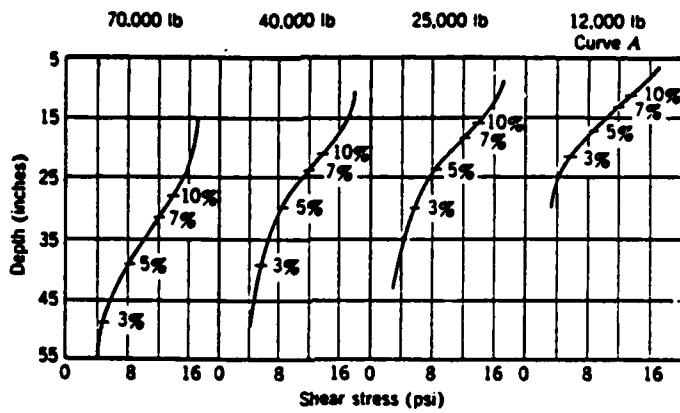


Figure 4. Extrapolation of Highway Pavement Thickness by the Elastic Theory (Reference 14).

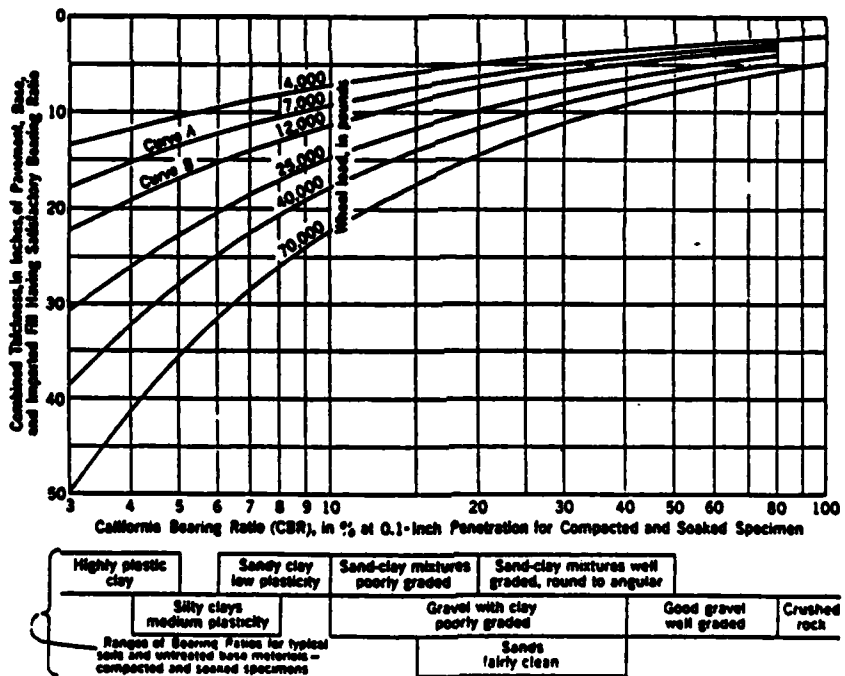


Figure 5. Tentative Design of Foundations for Flexible Pavements (Reference 14).

tests were in good agreement with existing design curves for loads below 30,000 pounds, but the data indicated additional thicknesses were needed for heavier loads. Design curves were adjusted accordingly. Tire pressures during these tests were generally 100 psi or less (Foster in Reference 14).

When the B-29 plane was introduced with dual wheel assemblies, it was necessary to evaluate the effect of the multiple wheel assemblies in comparison with the single wheel. Original work, described by Boyd and Foster in Reference 14, resulted in adopting an Equivalent Single-Wheel Load (ESWL) based on equal vertical subgrade stress. An ESWL is defined as the load on a single tire that will cause an equal magnitude of a preselected parameter (stress, strain, deflection, or distress) at a given location within a specific pavement system to that resulting from a multiple-wheel load at the same location within the pavement structure (Reference 13). Calculations were made using one-layer elastic theory (Boussinesq) and assuming the contact area of the ESWL is equal to that of one tire of the multiple-wheel gear assembly.

Further tests (Reference 24) indicated that using an ESWL based on subgrade stress gave thicknesses which were slightly unconservative. A complete reanalysis (Reference 25) of all data resulted in developing multiple-wheel design curves by adjusting the thickness for a given multiple-wheel load on a given subgrade to produce a deflection in the subgrade equal to that produced by a load when carried on a single wheel (i.e., equal subgrade deflection ESWL).

A similar procedure was developed for adjusting the existing design curves for higher tire pressures (Reference 26). First it had to be determined what tire pressure the existing design curves represented. Although original extrapolations were based on 60-psi tire pressures, traffic

data used in correlation of the curves consisted of tire pressures ranging from 55 to 110 psi. Since no particular effect of variations of this magnitude was observed from the traffic data, the existing curves were considered adequate for tire pressures up to 100 psi. The resulting higher tire pressure curves for lighter wheel loads and the lower CBR values (thick bases) were only slightly changed. For the heavier loads and higher CBR values (thinner bases), the thickness requirements for the 200- and 300-psi pressures are as much as 20 percent in excess of the required thicknesses for the 100-psi pressures. Tests were conducted at the Waterways Experiment Station from 1949-1951 (References 27, 28 and 29) with tire pressures up to 240 psi. As a result of these studies, the design curves were considered adequate for tire pressures up to 200 psi. These studies also established requirements for asphalt pavement surface thickness and quality, and base course quality.

Studies conducted in 1956 (Reference 30) indicated that the CBR relationship for airfield pavement design in the range of subgrade CBR values from 3 to about 10 to 12, could be expressed as:

$$T = \sqrt{P(1/8.1CBR - 1/p\pi)} = \sqrt{P/8.1CBR - A/\pi} \quad (1)$$

where, T = thickness in inches,

P = total load in pounds,

p = tire pressure in psi,

A = tire contact area in in.^2 , and

CBR = strength of soil as determined by MIL-STD-621A, Method 101.

The design thickness of a pavement layer was later represented by the expression (Reference 31):

$$T = (0.23 \log C + 0.15) t \quad (2)$$

where t is the standard thickness for a particular aircraft as calculated

from Equation (1) and C is the number of coverages.

This equation was derived from Figure 6 which is a plot of the percentage of design thickness versus coverages required to produce failure. The curve was prepared for "theater of operations" design. It is not considered to be conservative because it is believed that the importance of the time element and the fact that high maintenance can be accepted warranted a reasonable element of unconservatism (Closure to Reference 14).

Further research resulted in a statistical equation of the best-fit curve, that is appropriate for all CBR values (Reference 31):

$$T = \alpha_i \{ \sqrt{A} [-0.0481 - 1.562 (\log CBR/p_e) - 0.6414 (\log CBR/p_e)^2 - 0.4730 (\log CBR/p_e)^3] \} \quad (3)$$

where, CBR and A are as previously defined,

α_i = load repetition factor, which is dependent on number of coverages and number of wheels on main landing gear assemblies (see Figure 7), and

p_e = equivalent single-wheel load or single-wheel load tire pressure, in psi.

Figure 8 shows Equations (1) and (3) based upon Corps of Engineers test section performance.

Use of the CBR design procedure has been extended to unsurfaced soil and expedient surface (matting) "theater of operations" airfields.

E. TRAFFIC DISTRIBUTION - PASSES PER COVERAGE CONCEPT

The design procedures used by DOD and FAA account for the effect of lateral distribution of traffic on runways and taxiways by using the passes per coverage ratio to relate the number of operations of an aircraft to the number of design stress applications to the pavement. The incremental detriment to a pavement resulting from a particular aircraft wheel at a

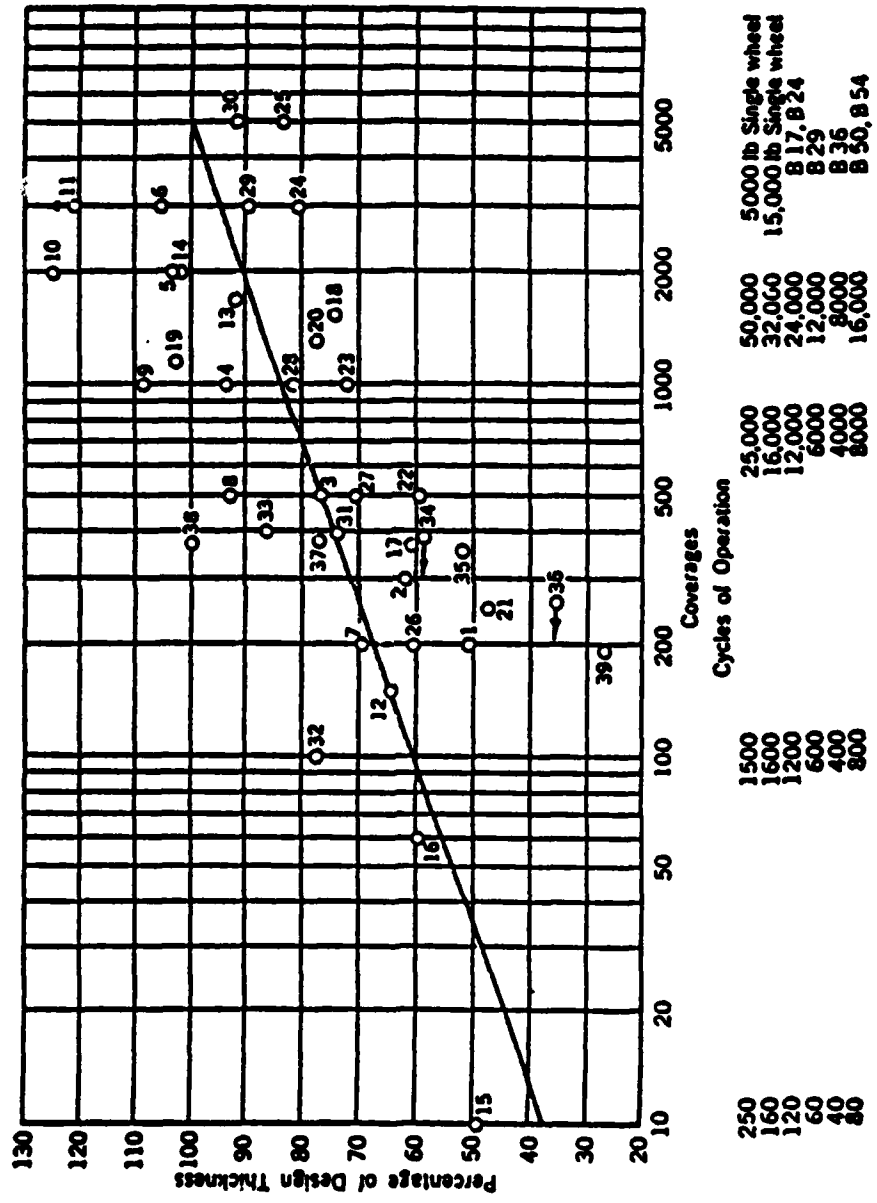


Figure 6. Percentage of Design Thickness Versus Coverages (Reference 14).

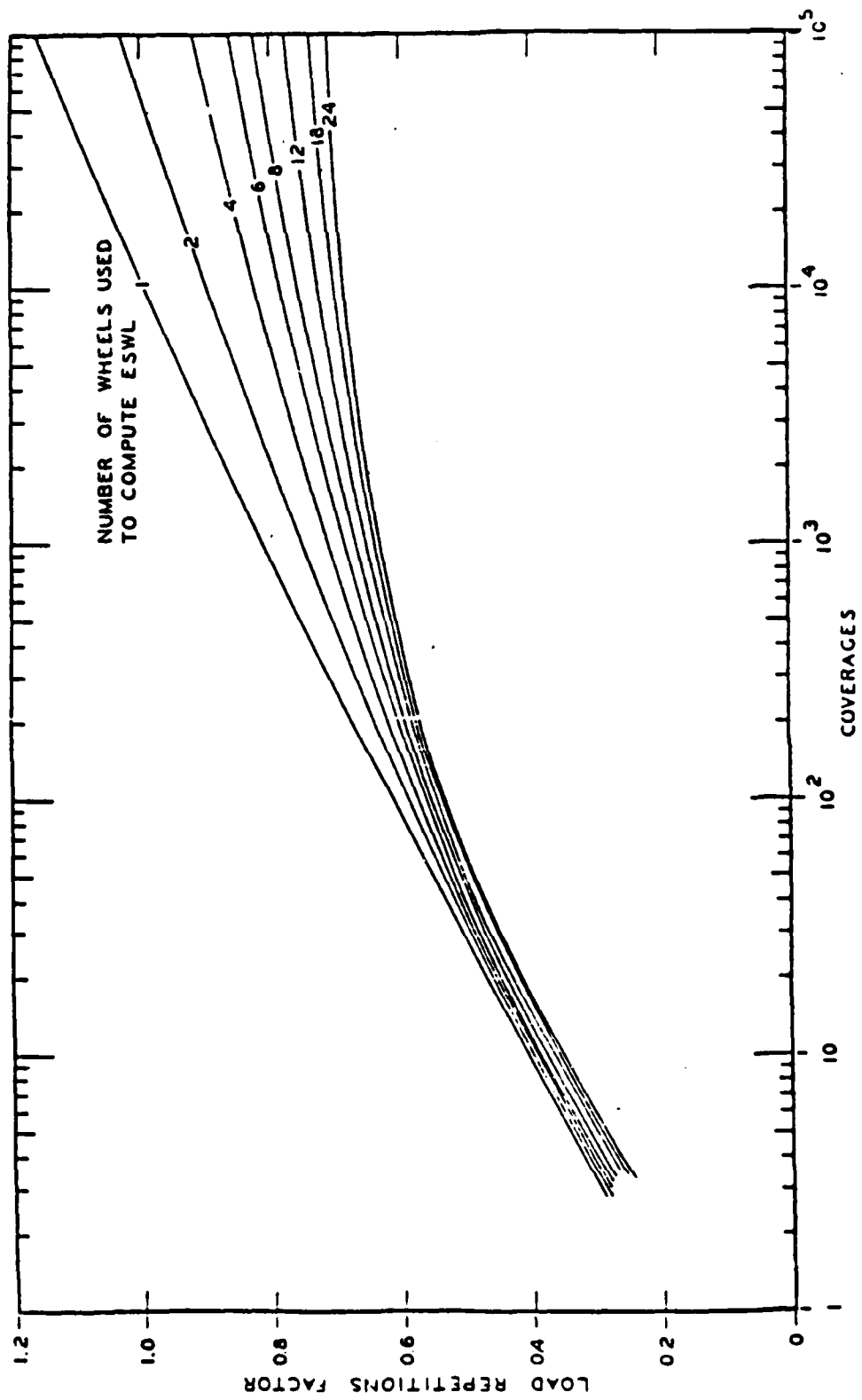


Figure 7. Load Repetitions Factor Versus Coverages for Various Landing Gear Types (Reference 31).

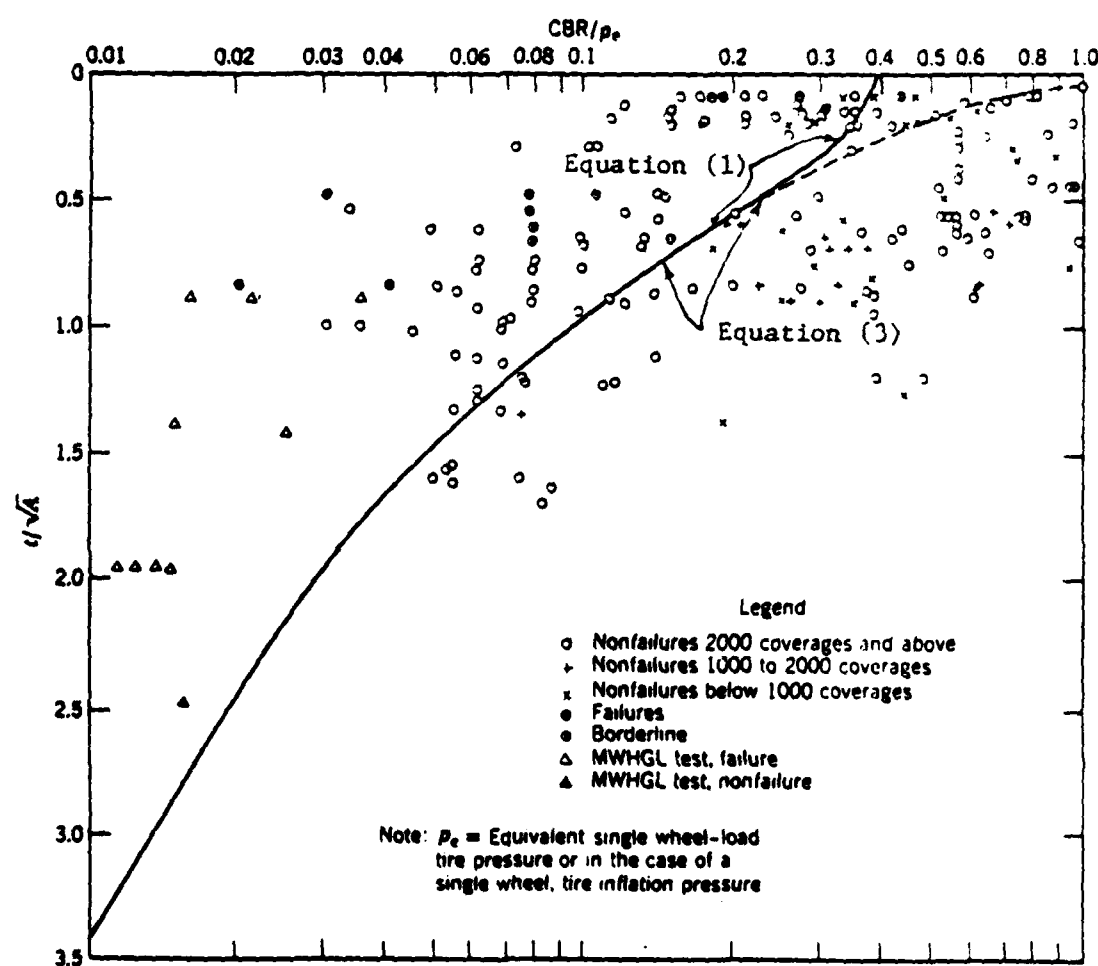


Figure 8. Comparison of CBR Design Equations to Pavement Behavior Data (Reference 13).

specified location on pavements is influenced by many factors. Some of the more important factors are (Reference 31): (1) number of wheels, (2) wheel configuration, (3) tire contact area, (4) tire inflation pressure, and (5) location of wheel on pavement.

The lateral distribution of aircraft traffic on runways and taxiways may be represented by a general normal distribution (GND) curve (Figure 9). The ordinate represents the frequency of the passes of the aircraft center line at a certain distance from the pavement center line. This distance from the center line is plotted as the abscissa. Two definitions are needed to further explain the passes per coverage concept:

1. Wander is defined as the width over which the center line of aircraft traffic is distributed 75 percent of the time (Reference 33). The same concept may be extended to the center line of one tire. A wander width of 70 inches is used for taxiways and the first 1000 feet of each runway end. A wander width of 140 inches is used for the runway interior. These values are based on actual traffic observations (Reference 33).

2. Coverage is defined as the application of the maximum stress on a point in a pavement surface. Therefore, when a pavement is designed for a particular wheel load, one coverage is being applied to a point on the pavement each time this wheel load passes over that point (Reference 33). By definition, for a wander width of 70 inches, 75 percent of the passes (or 75 percent of the GND curve area) lie in the interval between $x = -35$ inches and $x = 35$ inches (see Figure 10). From a standard normal distribution (SND) curve table, 75 percent of the SND curve lies in the interval between $z = -1.15$ and $z = 1.15$. So for this particular situation

Standard Deviation = $(x - \text{Mean})/z = (35 - 0)/1.15 = 30.43$ inches
If the tire width is W_t , then the tire applies coverages on the point $x=0$

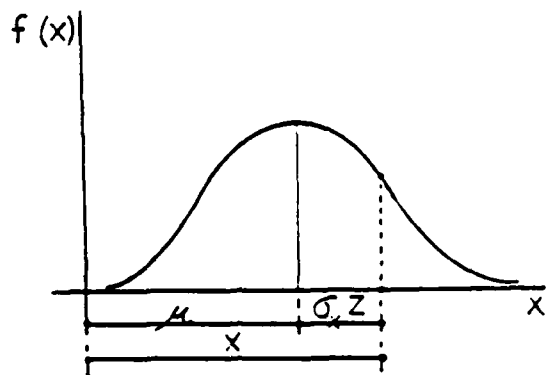


Figure 9. General Normal Distribution (GND) Curve (Reference 32).

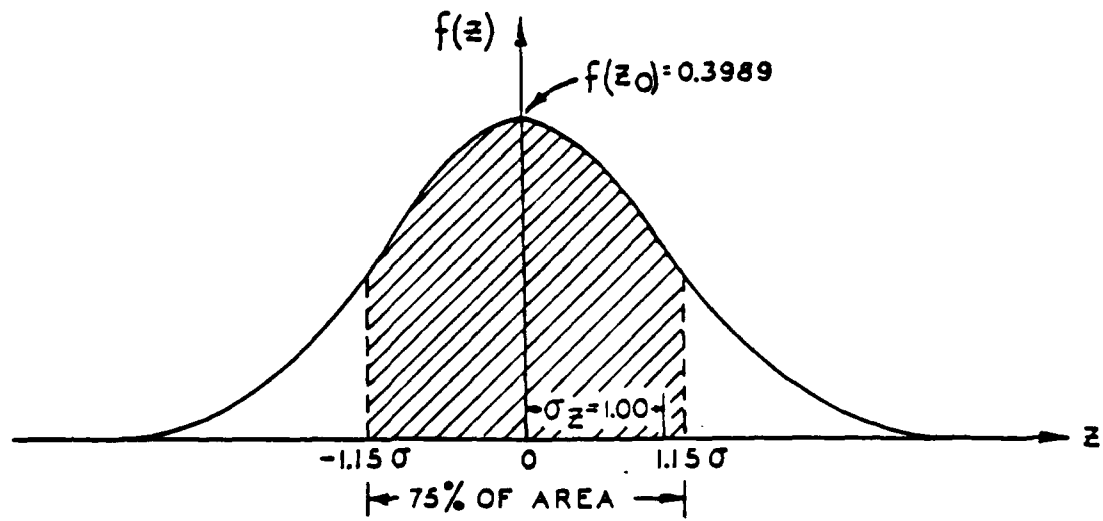


Figure 10. GND Curve as Related to Aircraft Traffic Distribution (Reference 32).

at every position of its own center line within the interval

$$-W_t/2 \leq x \leq +W_t/2$$

So, the number of coverages per pass (c/p) applied by one tire on the point $x=0$ is given by the expression

$$c/p = \int_{-W_t/2}^{+W_t/2} f(x) dx \quad (4)$$

Example Calculation

For the new heavyweight F-15, $A=85 \text{ in.}^2$ ($P=30 \text{ kips}$, $p=355 \text{ psi}$)

$$W_t = 0.878 \times \text{Tire Contact Area} \quad (\text{when } W_t \text{ is not known, Reference 32})$$
$$= 8.08 \text{ in.}$$

$$\text{Coverage/Pass} = .3989 W_t / 30.43 = .106$$

In computing the number of coverages applied by passes of a multiple-wheel gear aircraft, all the wheels on the main gears, as well as their arrangements, must be considered. Usually there is overlap among the GND curves of the several tires in the same assembly. Figure 11 shows an example of a GND curve for overlapping tire prints of a twin-wheel aircraft. The solid lines represent the individual GND curves and the dashed lines represent the combined effect of two wheels. In studying the combined effect of the wheels on a multiple-wheel gear aircraft, the individual curves can be drawn and the ordinates added graphically in the overlapping areas, and the maximum ordinate of the cumulative curve obtained. For tandem wheels which track each other, the maximum ordinate of the cumulative curve equals two times the maximum ordinate of an individual curve. The maximum ordinate of the cumulative curve for any two wheels may be obtained from Figure 12. For wheel arrangements that do not follow the pattern of single, twin, and twin-tandem, the maximum ordinates of the cumulative curves must be

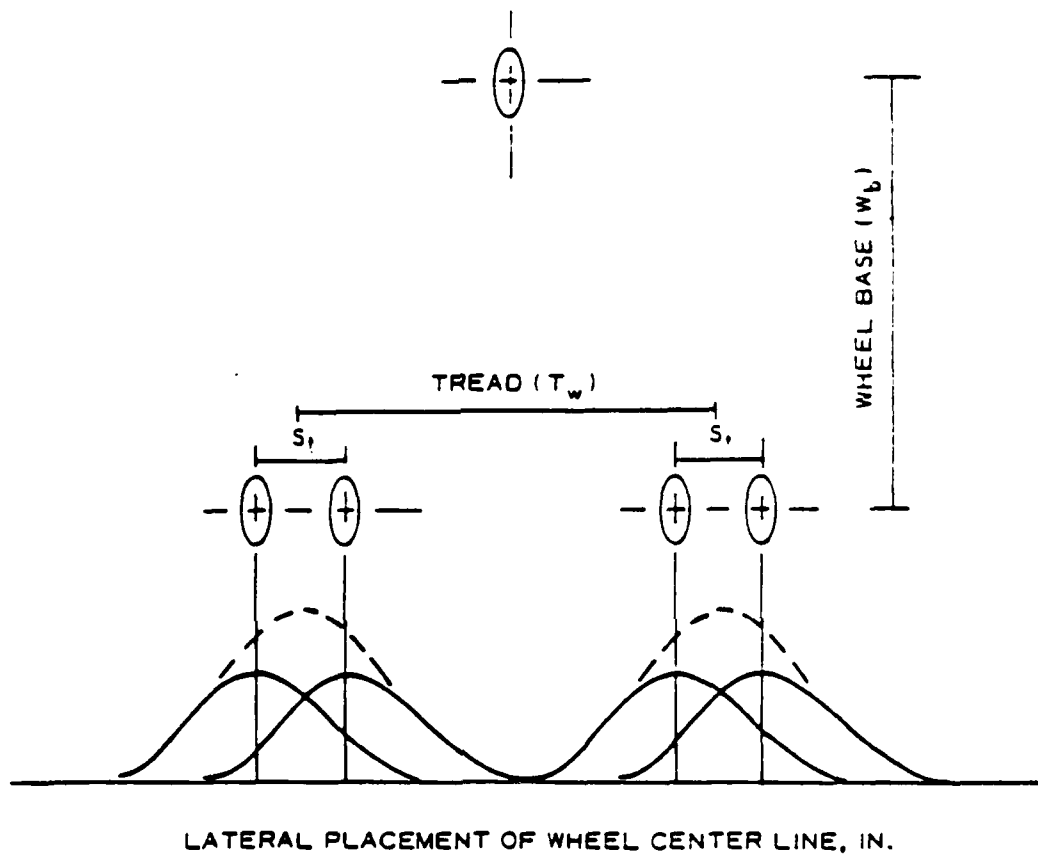


Figure 11. GND Curve for Overlapping Tire Prints, Twin Wheels (Reference 32).

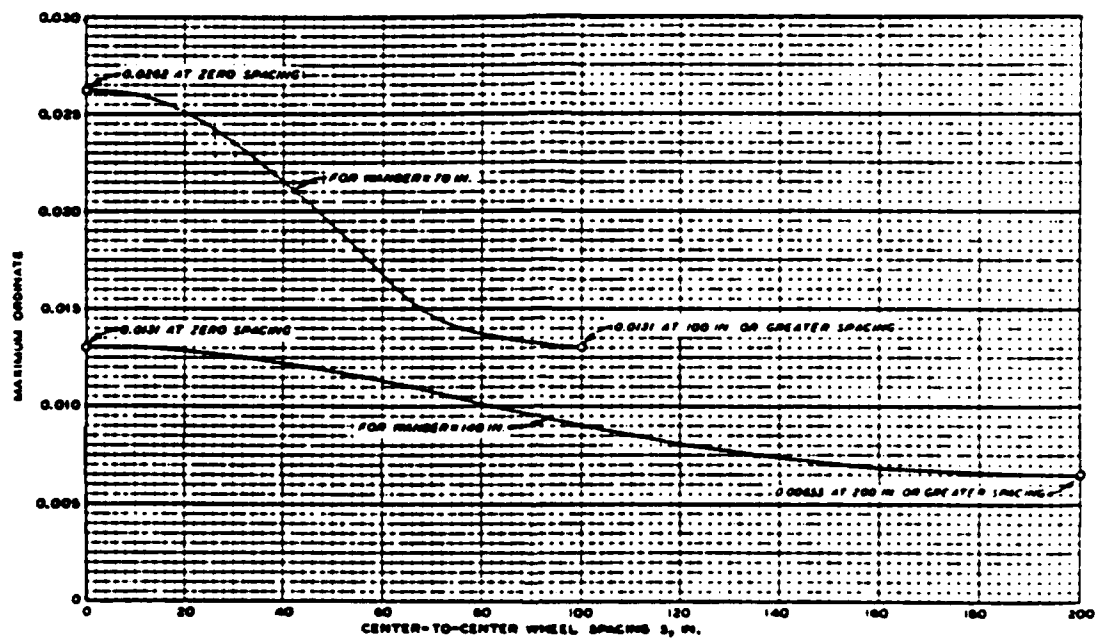


Figure 12. Maximum Ordinate on Cumulative Traffic Distribution Curve for Two Wheels Versus Wheel Spacing (Reference 32).

determined from their combined distribution curves.

F. FIELD MOISTURE STUDIES

In February 1945 the Flexible Pavement Laboratory of the U.S. Army Engineer Waterways Experiment Station undertook a field moisture study to develop a better understanding of moisture conditions under flexible pavements. Airfields in various climatic zones were visited repeatedly in various seasons and in successive years. Test pits were opened and samples taken to evaluate moisture, density and CBR. It was concluded (References 34, 35, and 36) that moisture contents and CBR values of four-day laboratory soaked samples were generally conservative compared to those obtained in the field for base course, and conservative or approximate to those obtained for subgrade materials. Variations in moisture content with time followed no prescribed pattern of increase or decrease.

The procedure for determining the soaked CBR value to be used for design is shown in Figure 2. In the Figure 2 example, at 95 percent of maximum density the CBR value ranges from 3 to 19 when molding water content varies from 11 to 18 percent.

G. COMMENTS CONCERNING THE CBR METHOD

The following points are offered:

1. Advantages of the CBR method are the wide spread familiarity of the CBR test and the simplicity of the CBR design method itself.
2. The CBR method is empirical, or in part empirical, and therefore, the production of design criteria for loadings not covered in field tests requires interpolations and/or extrapolations. Since pavement design involves several parameters (load, material strength, tire contact pressure,

number of wheels, spacing of wheels, and repetitions of load), interpolations and extrapolations can be considerably involved.

3. The CBR test is not a measure of any "fundamental" soil property.

4. CBR is a static test. Repeated load soil response/behavior is more representative of field loading. The consensus of studies compiled in Reference 37 is that "the response of granular materials to repeated loading is different from their response to static loading." For fine-grained soils, it has been shown (Reference 38) that equivalent resilient moduli are not always obtained for soils with the same CBR value.

5. Selection of the "four-day soaked CBR" value to use for design is very dependent upon the molding water content and compacted density. Very conservative designs may result if the lowest CBR is selected as the design value for the entire life of the pavement.

6. Stress distribution through the pavement is assumed to be independent of the quality of the various layers (Reference 11). A granular (unbound) base composed of high-quality material is not considered to have any advantage over the same thickness of unbound layered base with high-quality material in the top and inferior material in the lower part.

7. Asphalt concrete fatigue cracking was not considered in determining minimum surface thickness. Minimum asphalt concrete thickness was based only on providing adequate resistance against weathering and abrasion over a period of years (Reference 26).

8. Stress-dependent behavior of granular materials and fine-grained soils is not considered.

SECTION III

MODELLING PAVEMENT RESILIENT STRUCTURAL RESPONSES

In this section the structural model used in this study is described. The models used to characterize the pavement materials are presented. Structural response algorithms are developed that relate pavement variables (thicknesses and moduli) to the response parameters. Sensitivity analyses are performed to determine effect of load magnitude and granular base quality on structural responses.

A. ILLI-PAVE STRUCTURAL MODEL

The ILLI-PAVE computer program developed at the University of Illinois is a modified version of the finite element program originally presented by Wilson (Reference 39) and later modified and/or adapted by Barksdale (Reference 40); Duncan, Monismith, and Wilson (Reference 41); the research staff of the U.S. Army Construction Engineering Laboratory at Champaign, Illinois; and the Transportation Facilities Group, Department of Civil Engineering, University of Illinois at Urbana-Champaign. The current version (Reference 42) available at the University of Illinois incorporates an improved user oriented format as well as additional material models.

The pavement is modelled with a two-dimensional finite solid of revolution as shown in Figure 13. By symmetry, the solution of the three-dimensional solid may be specified in terms of a plane radial section, rectangular configuration as shown in Figure 14. This rectangular section is then divided into a set of rectangular elements connected at their nodal points. Figure 15 shows a typical system configuration.

The nodes at the inner and outer vertical boundaries are constrained to

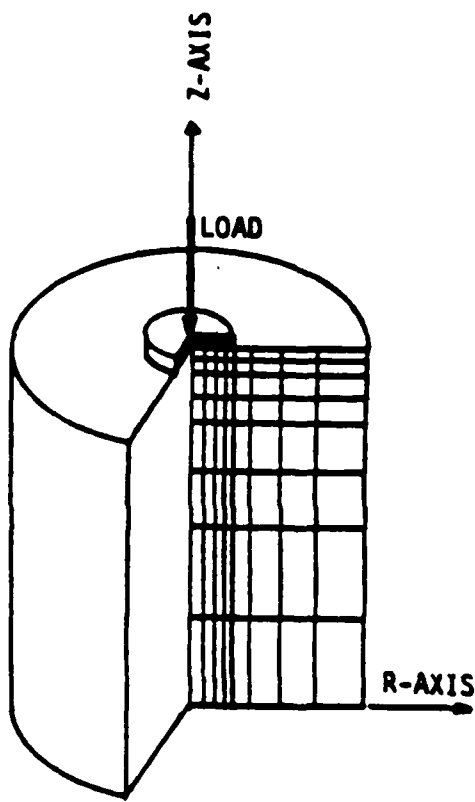


Figure 13. Cylindrical Pavement Configuration (Reference 42).

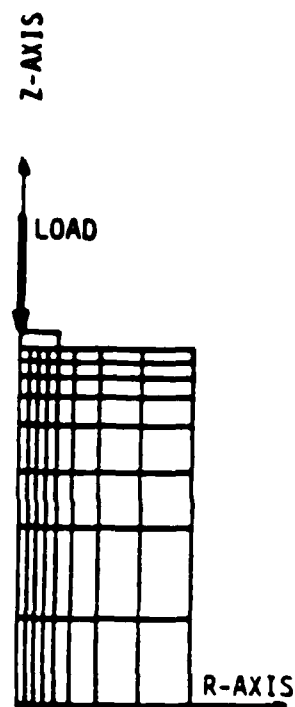


Figure 14. Rectangular Section of an Axisymmetric Solid (Reference 42).

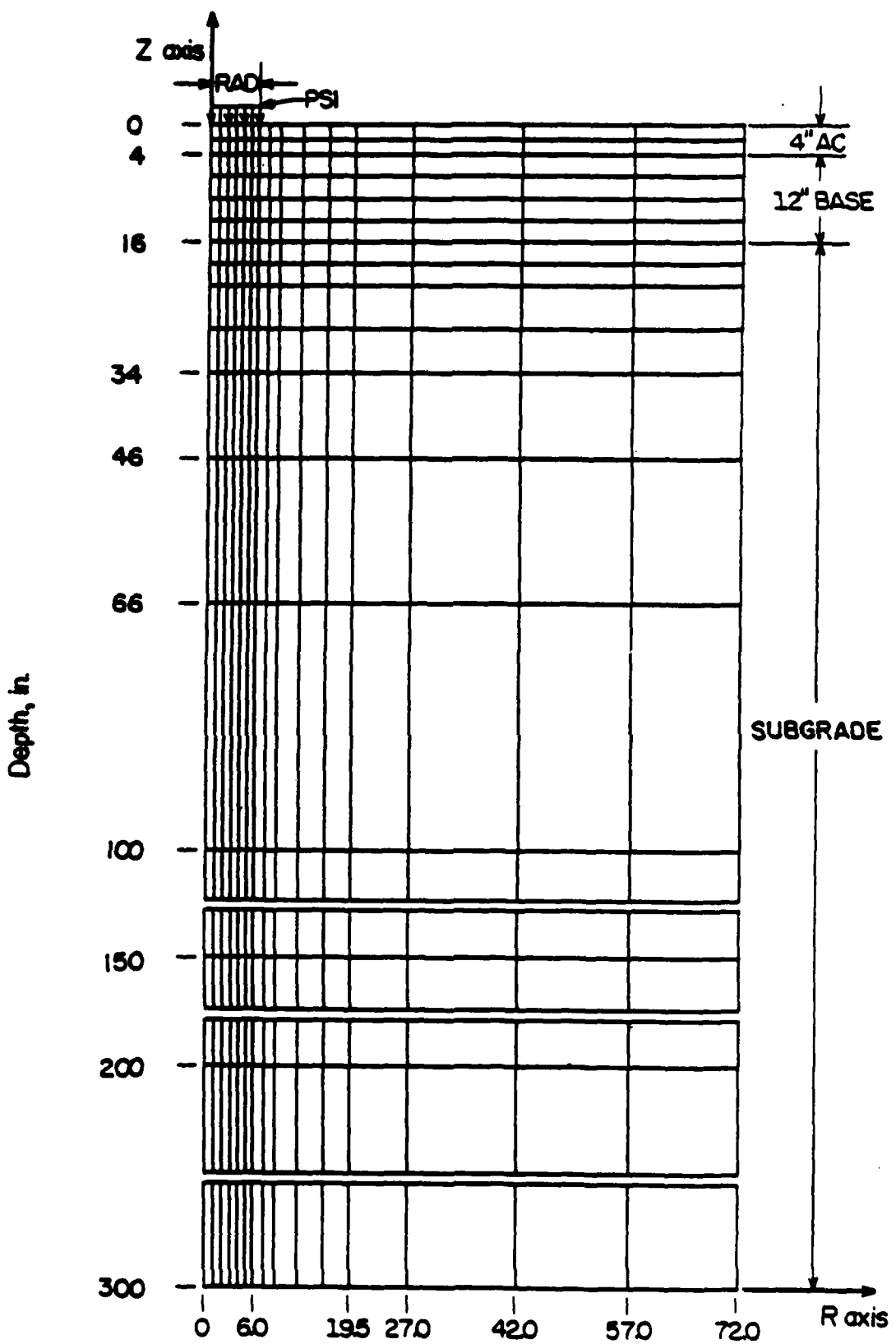


Figure 15. System Configuration (Reference 42).

move only in the vertical direction. The lower boundary is constrained of both vertical and horizontal movement. All other elements and nodes are free to move vertically and horizontally.

Good approximation using the finite element technique can be obtained for most problems in solid mechanics, provided a sufficient number of elements are selected and any required fictitious rigid boundaries are placed at a sufficient distance from the applied load. The smaller and more numerous the elements, the greater the accuracy, but the higher the cost. A compromise between these two conflicting factors was developed by Duncan, Monismith, and Wilson (Reference 41). Their criteria are:

1. The element stresses will be sufficiently accurate so long as the length (vertical) to width (horizontal) ratio of the elements do not exceed five to one.
2. Smaller elements near the load will increase accuracy where the influences of the applied load are more significant.
3. The rigid lower boundary should be placed at least an approximate depth of 50 times the radius of the applied load.
4. The outer side boundary should be specified at a minimum distance of 12 radii of the applied load.

ILLI-PAVE incorporates a method of principal stress correction for both fine-grained and granular materials based on the Mohr-Coulomb theory of failure. This procedure is described in Reference 4. For a given state of stress, failure occurs when:

$$\sigma_1 = \sigma_3 \tan^2 (45^\circ + \phi/2) + 2c \tan (45^\circ + \phi/2) \quad (5)$$

where, σ_1 = major principal stress,

σ_3 = minor principal stress,

c = cohesion, and

ϕ = angle of internal friction.

This equation defines a circle which is tangent to the Mohr-Coulomb envelope.

It is common to assume no cohesion exists in granular materials ($c=0$) and undrained conditions prevail for fine-grained materials ($\phi=0$).

A major advantage of the stress correction procedure is the assignment of realistic resilient modulus values. Conventional elastic layer structural models frequently predict stresses for typical flexible pavement materials that exceed their strengths. For example, a tensile radial stress is often predicted in the granular (non-cohesive) base course. ILLI-PAVE uses an iterative approach to predicting responses. Moduli values are assumed for the first iteration. The predicted stresses are then examined and adjusted as necessary. The adjusted stresses are used to calculate the resilient modulus values used in the next iteration. This procedure is accomplished for each individual element.

The prediction of actual measured stresses and deflections with the finite element analysis has been shown to be more accurate than the n-layered elastic system or than any other available methods (References 40 and 41). Furthermore, the ILLI-PAVE response deflections adequately represent dynamic deflections generated by moving wheel loads (References 4 through 10).

B. MATERIAL MODELS

The ILLI-PAVE structural model inputs are the material characteristics of the various layers. Material characteristics may be determined from direct laboratory testing, backcalculated from non-destructive testing (NDT) data, or estimated.

A measure of the elastic modulus of untreated granular and fine-grained materials is the resilient modulus, E_r . It is determined from repeated load

tests and is defined by:

$$E_r = \text{Repeated Axial Compressive Stress}/\text{Recoverable Axial Strain} \quad (5)$$

E_r is recommended for use in elastic analysis of pavements subjected to moving wheel loads. ILLI-PAVE can accommodate stress-dependent modulus relationships for granular and fine-grained materials.

1. Asphalt Concrete

The stiffness of any given asphalt concrete (AC) mixture is primarily dependent upon temperature and rate of loading. A constant linear resilient modulus was used to represent the asphalt concrete layer at a specified temperature. Work done by Brown (Reference 43) and Chou (Reference 37) show that at the short loading time associated with normal vehicle speeds, an assumption of linear elastic behavior is reasonable. Therefore, AC modulus was considered to be directly related to temperature (Figure 16).

2. Granular Materials

The resilient modulus of granular materials is modelled as:

$$E_r = K \theta^n \quad (7)$$

where, E_r is the resilient modulus, in psi

K and n are constants determined from testing, and

θ is the sum of the three principal stresses, in psi.

Rada and Witczak (Reference 45) investigated six different granular material types. A plot of K - n relation for all aggregates is shown in Figure 17. A mid-range of values of $K=5000$ and $n=0.5$ (from Figure 17) were selected for these analyses. In Section III.F, effects of using other values for K and n are reported. An angle of internal friction of 40° was selected for the analyses.

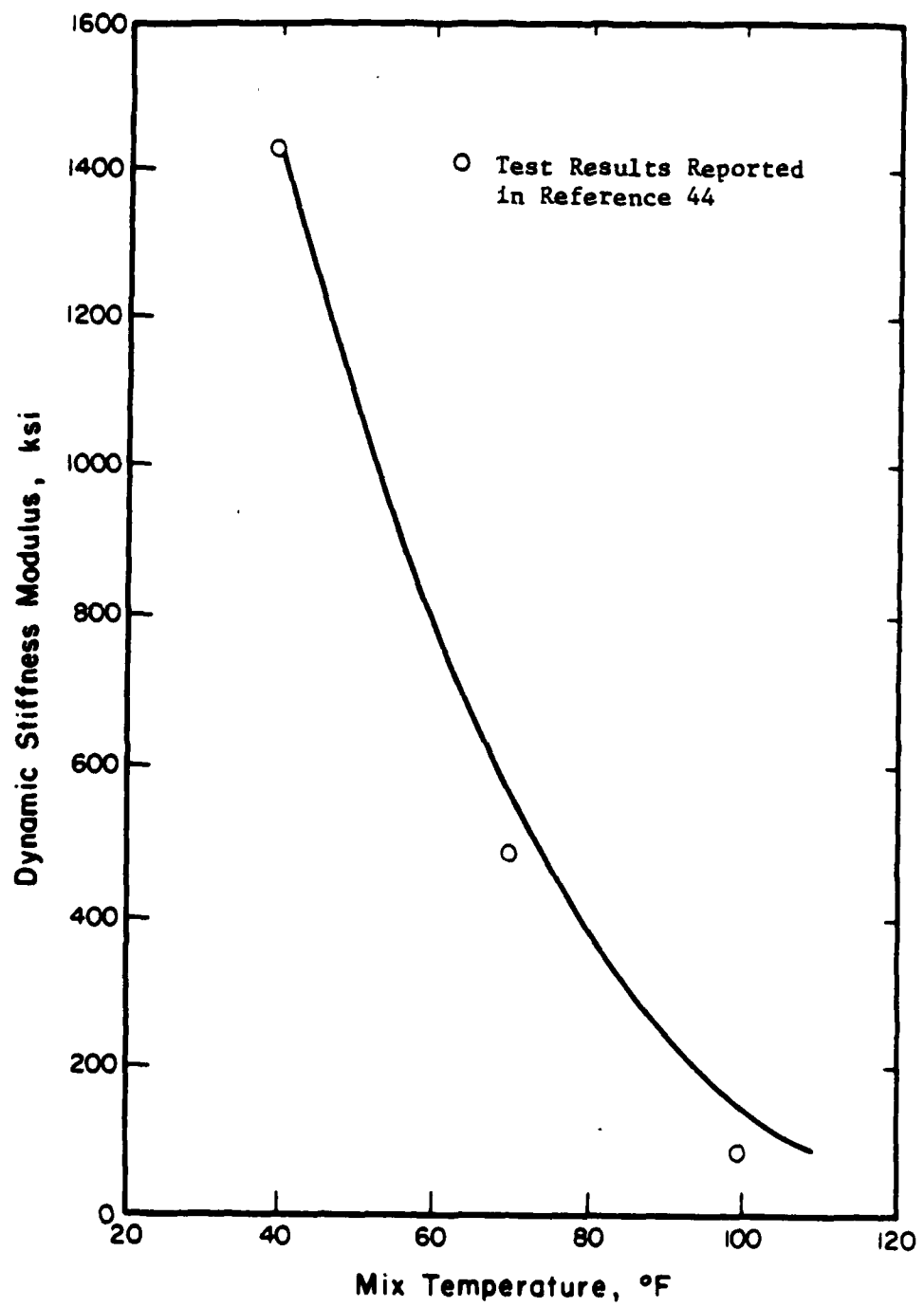


Figure 16. Typical Asphalt Concrete Modulus - Temperature Relationship (Reference 7).

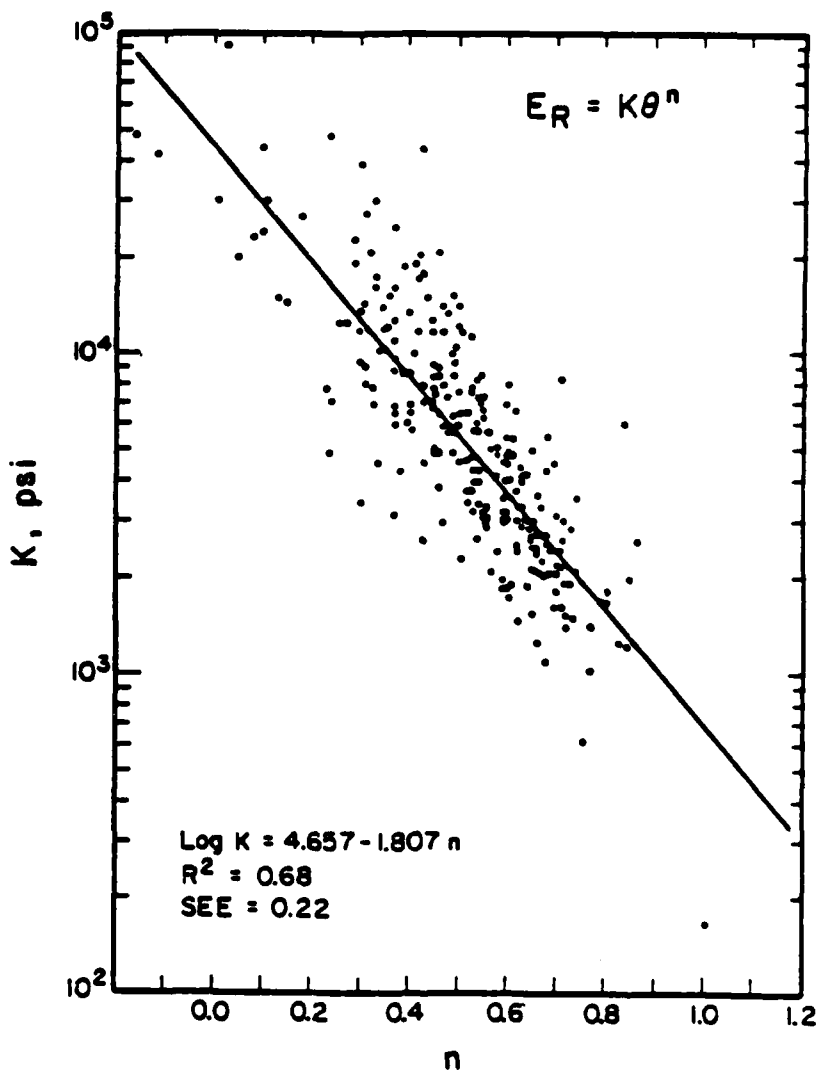


Figure 17. Relationship Between K and n Values for Granular Materials Identified by Rada and Witczak (Reference 45).

3. Fine-Grained Soils

In general, the resilient modulus of fine-grained soils decreases with increasing deviator stress and is relatively unaffected by small changes in the confining pressure (Reference 38). A typical response relationship is displayed in Figure 18. This figure shows a substantial change in slope at a certain point called the "breakpoint." The subgrade resilient modulus at this "breakpoint" is noted as E_{Ri} . Thompson and Robnett (Reference 38) found that the slopes (K_1 and K_2) and the "breakpoint" deviator stress (σ_{Dj}) did not vary appreciably between soil types and soil conditions. Therefore, E_{Ri} is the most significant property of the subgrade influencing resilient responses. The four resilient modulus models for fine-grained soils used in the computer analyses are shown in Figure 19. These models were developed (Reference 46) based on the work done by Thompson and Robnett (Reference 38). The VERY SOFT subgrade accounts for those soils highly susceptible to high moisture and/or freeze-thaw cycling effects.

C. DATA BASE FOR HEAVYWEIGHT F-15

Heavyweight F-15 aircraft loading conditions are 30,000-lb circular wheel load with a 355-psi contact pressure (radius of loaded area of 5.19 inches). The pavement variables and ranges used in the analyses are:

- (1) Thickness of Asphalt Concrete - 3 to 9 inches,
- (2) Modulus of Asphalt Concrete - 100 to 1500 ksi,
- (3) Thickness of Granular Base - 6 to 24 inches, and
- (4) Resilient Modulus of Subgrade at Breakpoint - 1.00 to 12.34 ksi.

Table 3 shows the specific values of the pavement variables. These values allow for the formation of a 4x5x5x4 full factorial totalling 400 cases.

Table 4 is a summary of material properties used for the analyses. A summary

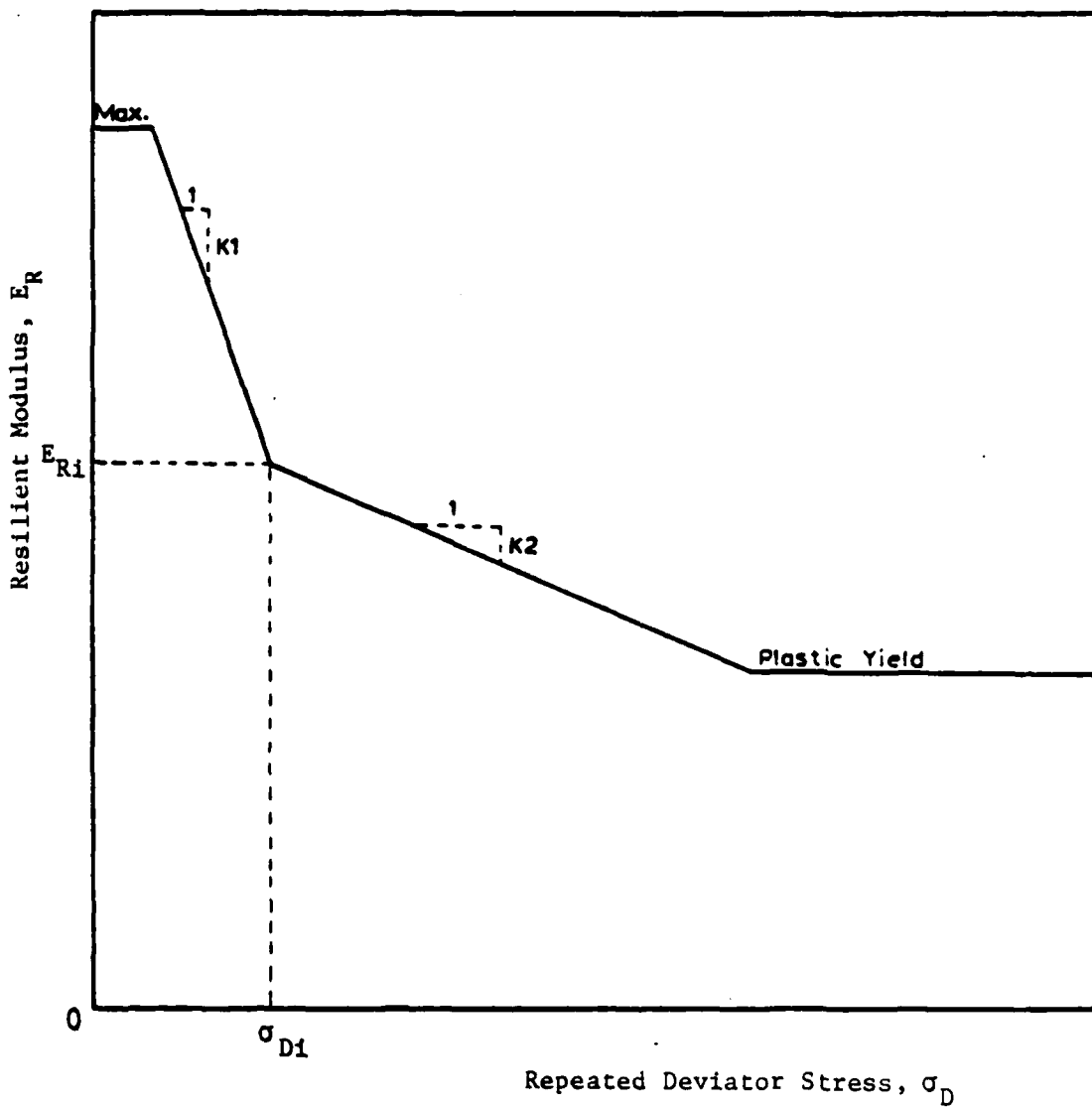


Figure 18. Typical Representation of the Resilient Modulus-Repeated Deviator Stress Relationship for Fine-Grained Soils (Reference 7).

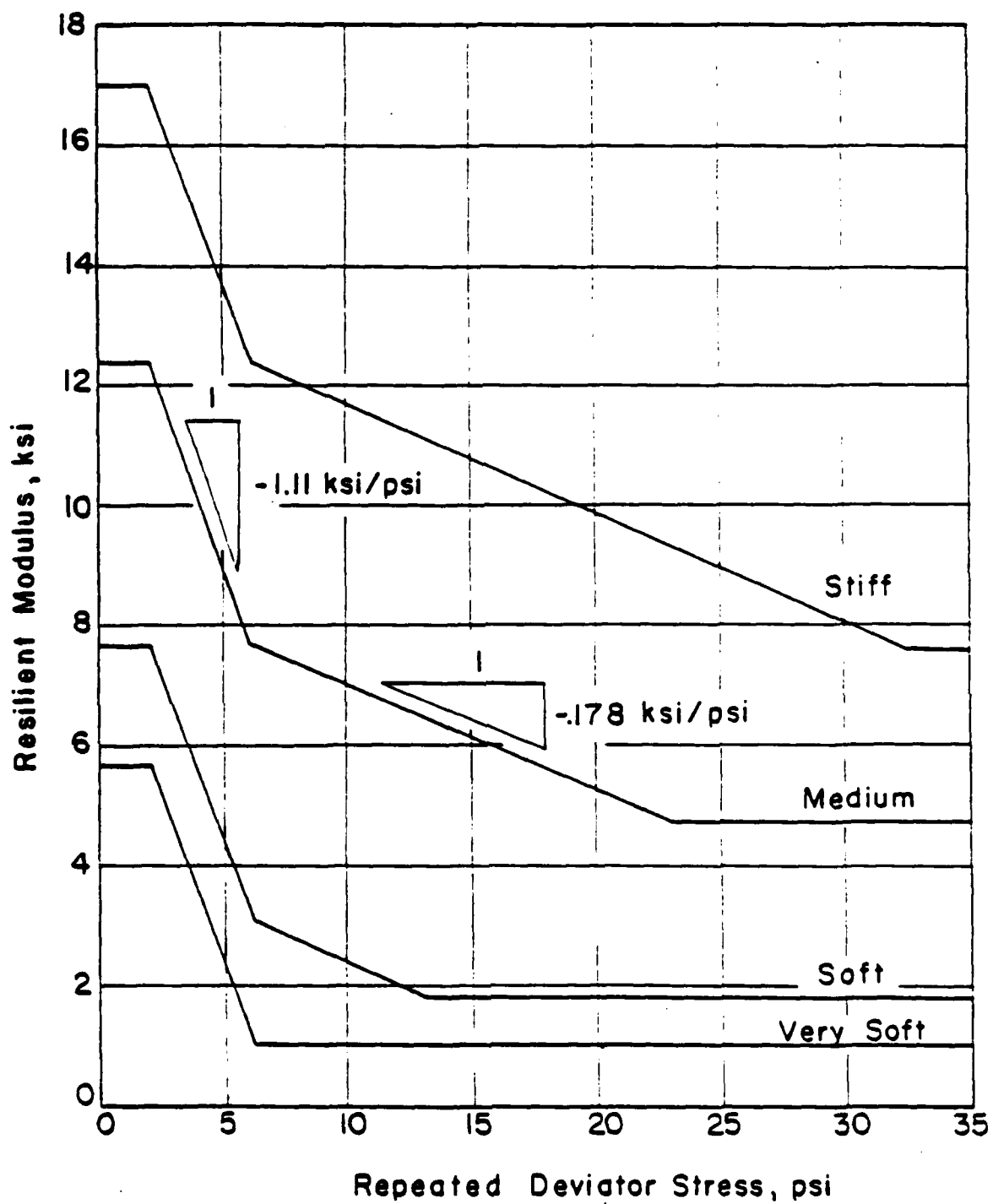


Figure 19. Subgrade Material Models Used With ILLI-PAVE (Reference 46).

TABLE 3. ILLI-PAVE VARIABLES FOR 4x5x5x4 FACTORIAL.

FACTOR	VALUES
1. Thickness of Asphalt Concrete,	3, 5, 7, and 9 inches
2. Modulus of Asphalt Concrete,	100, 300, 500, 1000, and 1500 ksi
3. Thickness of Granular Base,	6, 9, 12, 18, and 24 inches
4. Subgrade Resilient Modulus at Breakpoint	1.00 ksi (Very Soft Subgrade) 3.02 ksi (Soft Subgrade) 7.68 ksi (Medium Subgrade) 12.34 ksi (Stiff Subgrade)

TABLE 4. SUMMARY OF MATERIAL PROPERTIES FOR ILLI-PAVE SOLUTIONS.

	Asphalt	Concrete	Granular	Subgrade						
	40°F	50°F	70°F	85°F	100°F	Base	Stiff	Medium	Soft	V. Soft
Unit Weight (pcf)	145.0	145.0	145.0	145.0	145.0	135.0	125.0	120.0	115.0	110.0
Lateral Pressure										
Coef. at Rest	0.37	0.50	0.67	0.76	0.60	0.60	0.82	0.82	0.82	0.82
Poisson's Ratio	0.27	0.33	0.40	0.43	0.46	0.38	0.45	0.45	0.45	0.45
Unconfined Compress. Strength (psi)	--	--	--	--	--	--	32.8	22.8	12.8	6.2
Deviator Stress	--	--	--	--	--	--	32.8	22.8	12.8	6.2
Upper Limit (psi)	--	--	--	--	--	--	2.0	2.0	2.0	2.0
Deviator Stress										
Lower Limit (psi)	--	--	--	--	--	--	6.2	6.2	6.2	6.2
Deviator Stress @ "Breakpoint" (psi)	--	--	--	--	--	--	12.34	7.68	3.02	1.00
E _{ri} (ksi)	--	--	--	--	--	4.0	7.605	4.716	1.827	1.00
E-Failure (ksi)	--	--	--	--	--	--	--	--	--	--
E-Const. Mod. (ksi)	1500.0	1000.0	500.0	300.0	100.0	--	--	--	--	--
E-Model (psi)	--	--	--	--	--	50000 ^{0.5}	--	--	--	--
Frict. Angle (deg)	--	--	--	--	--	40.0	0.0	0.0	0.0	0.0
Cohesion (psi)	--	--	--	--	--	0.0	16.4	11.4	6.4	3.1

of the ILLI-PAVE computer outputs for the 400 cases of the full factorial design is listed in Table A-1. Table A-1 presents the following response parameters in conjunction with the independent variables (thicknesses and moduli) used in each computer run:

- (1) Deflection at surface, under the center of loaded area (D0),
- (2) Deflection at surface, 12 inches from center of loaded area (D1),
- (3) Deflection at surface, 24 inches from center of loaded area (D2),
- (4) Deflection at surface, 36 inches from center of loaded area (D3),
- (5) Deflection basin area = $6(1 + 2xD1/D0 + 2xD2/D0 + D3/D0)$,
- (6) Maximum tensile strain at the bottom of the asphalt concrete layer,
- (7) Maximum tensile stress at the bottom of the asphalt concrete layer,
- (8) Maximum octahedral stress within the asphalt concrete layer =

$$1/3 \sqrt{(\sigma_z - \sigma_r)^2 + (\sigma_r - \sigma_t)^2 + (\sigma_t - \sigma_z)^2 + 6\tau_{rz}} \quad (8)$$

where, σ_z = vertical normal stress,

σ_r = radial normal stress,

σ_t = tangential normal stress, and

τ_{rz} = shear stress.

- (9) Deflection at the top of the subgrade,
- (10) Maximum compressive vertical strain at top of subgrade,
- (11) Maximum subgrade normal stress,
- (12) Maximum subgrade deviator stress (SDEV), and
- (13) Subgrade stress ratio = SDEV/Unconfined Compressive Strength.

D. HEAVYWEIGHT F-15 DESIGN ALGORITHMS

Design algorithms were developed by applying the Statistical Package for the Social Sciences (SPSS) stepwise regression program (Reference 47) to the ILLI-PAVE generated response data (Section III.C). The regression equation

is developed in a series of steps with the independent variables being entered one at a time. At each step the variable entered is the one that makes the greatest improvement in the prediction of the dependent variable. This provides an indication of the relative significance of each variable. The precision of a regression equation may be measured by the correlation coefficient (R), the coefficient of determination (R^2), and the standard error of estimate (SEE).

Initially the independent variables used in the analyses were thickness of AC, AC modulus, thickness of granular base, subgrade modulus at breakpoint (E_{Ri}), log 10 transformations of these variables, reciprocal transformation of these variables, square root transformations of these variables, and two-way interactions of these transformed and untransformed variables. Some three-way interactions were tried and, as expected, their effects were negligible.

The recommended algorithms based on "engineering meaningful" variables are shown in Table B-1. Included in the Tables are statistics that indicate the precision of the equations. The first line beneath each design algorithms are the statistics based upon comparing log of the predicted response (dependent variable of algorithm) with log of the ILLI-PAVE response. For comparison, the algorithms using more "complicated" variables are presented in Table B-2. The precision of the resulting equations using "complicated" variables is insignificantly greater than equations using more "engineering meaningful" variables. Additionally, the precision of equations developed using five variables were only slightly greater than those developed using four variables. Cases where subgrade failure occurred (i.e., stress ratio = 1.0) were deleted from the analyses (leaving 372 cases), resulting in greater precision. This was a reasonable assumption since

designs predicting subgrade failure would not be acceptable. However, equations developed from the entire data base were very similar.

The antilog of the standard error of estimate provides meaningful data and is shown in parenthesis. For perfect prediction, the standard error of estimate would be 0.000. The antilog of this is 1.000. For other values of the antilog (the value will never be less than one), the amount greater than one provides a fractional measure of the error of the estimate. For example, the standard error of estimate for the AC strain equation is 0.0320. The antilog of this 1.076. This indicates that the prediction standard error of estimate is 7.6 percent of the actual ILLI-PAVE AC strain.

The second line beneath each design algorithms are the statistics based upon comparing the arithmetic value of the predicted response (antilog of dependent variable) with the arithmetic value of the ILLI-PAVE response.

Examination of the statistics shows that the algorithms developed are very good. In fact, the standard errors of estimate for the algorithms are generally within the accuracy of the ILLI-PAVE model itself.

The precision of the AC strain equation for cases where AC modulus = 100 ksi is low ($R^2 = .356$ and SEE = 142 microstrain). The cause for this can be seen by examining Figure 20. At low AC thicknesses (i.e., less than 5 inches) and AC modulus = 100 ksi, computed AC tensile strain actually drops. This drop is difficult to account for in an algorithm equation. Since the algorithms predict close or conservative values, there is little need for concern. However, in general, the algorithms predict ILLI-PAVE model responses much better at AC moduli greater than 100 (for example, see Figure 21). An example of a subgrade stress ratio plot is presented in Figure 22. Example plots of predicted AC tensile strain and subgrade stress ratio, obtained from the algorithms, are presented in Figures B-1 through B-6.

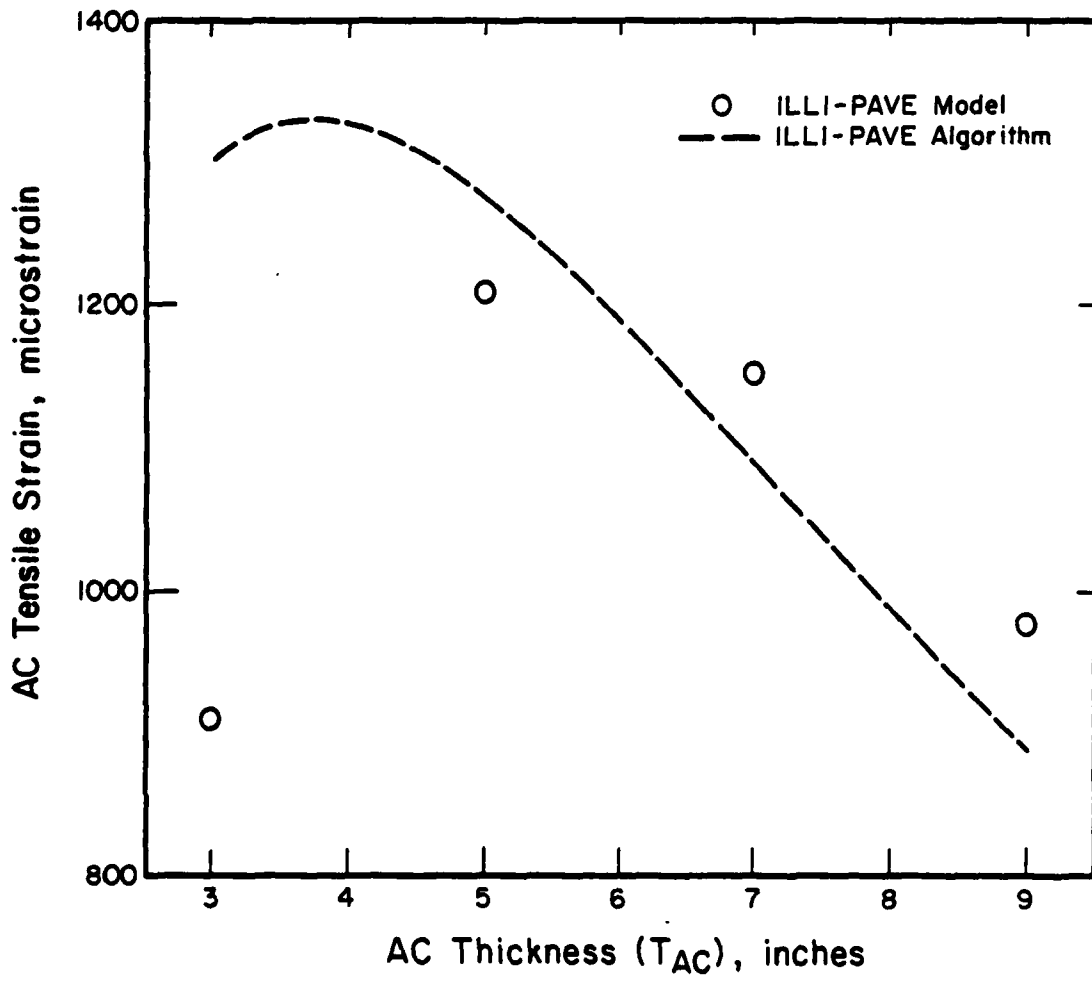


Figure 20. AC Tensile Strain Versus AC Thickness,
 $E_{Ri} = 3.02$ ksi, $E_{AC} = 100$ ksi.

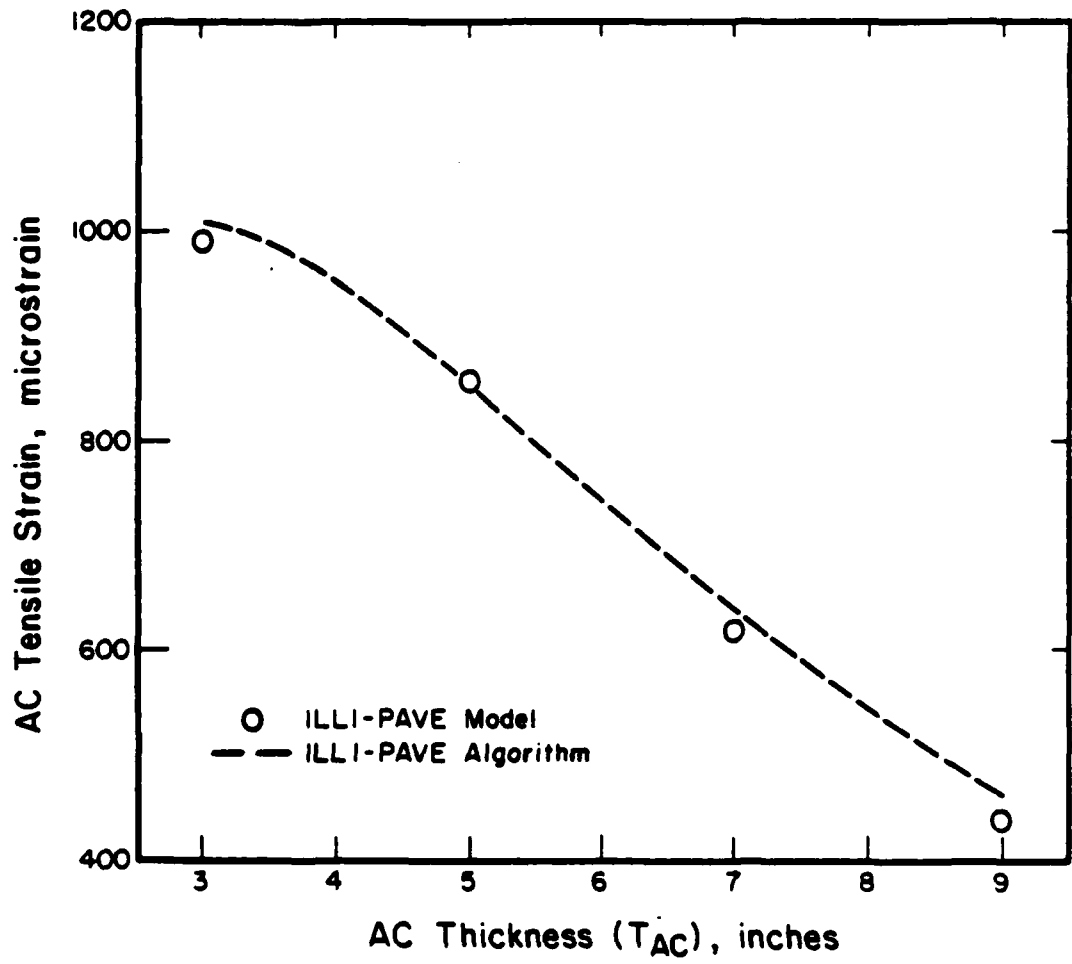


Figure 21. AC Tensile Strain Versus AC Thickness,
 $E_{Ri} = 3.02$ ksi, $E_{AC} = 500$ ksi.

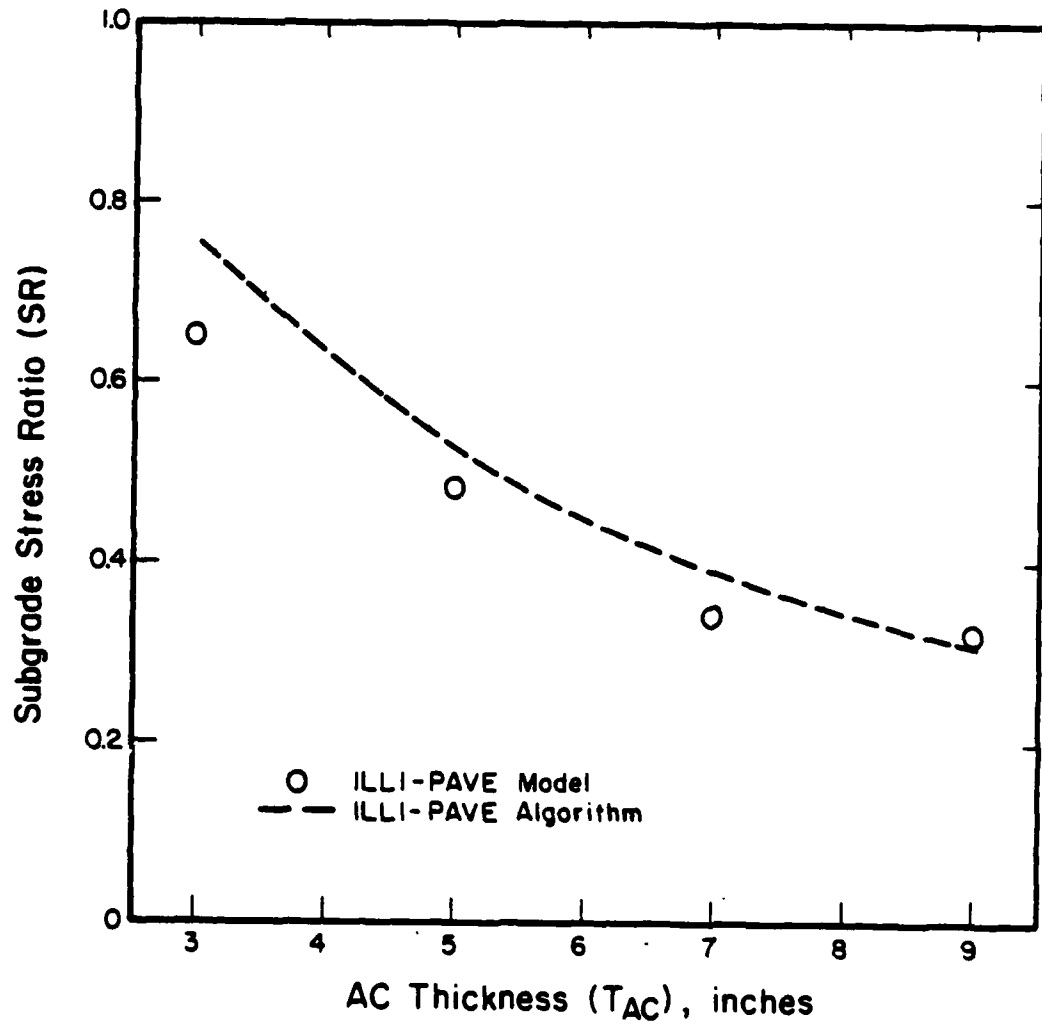


Figure 22. Subgrade Stress Ratio Versus AC Thickness,
 $E_{Ri} = 3.02$ ksi, $E_{AC} = 500$ ksi.

These plots show the interactions between the four variables: AC thickness, granular base thickness, AC modulus, and subgrade modulus at breakpoint.

It was desired to reduce the number of runs required for other analyses. However, a partial factorial design of this magnitude is quite complicated. Therefore, the $4 \times 5 \times 5 \times 4$ factorial was reduced to a 3^4 factorial (81 cases). The values of variables used are contained in Table 5. Regression analyses were performed on this reduced data base, again without subgrade failure cases (leaving 70 cases). The algorithms developed are presented in Table B-3. The statistics contained in the Table are based upon applying the algorithms to the full data base (372 cases). Examination of the statistics shows that these algorithms can still be considered "good," thus the 3^n factorials provided acceptable results.

E. INFLUENCE OF LOAD MAGNITUDE ON STRUCTURAL RESPONSES

When an aircraft traverses a surface, whether smooth or rough, the interaction of the aircraft and the surface causes dynamic responses in the aircraft. These responses increase and decrease the gear load on the pavement. Additionally, aircraft may operate at other than the maximum static load of 30,000 pounds (more armament during a wartime emergency, less weight when fuel has been expended). The effect of gear loads other than 30,000 pounds was analyzed to determine the sensitivity of the pavement responses to a load variable.

A 3^4 factorial was run with the wheel load at 24,000 pounds and at 36,000 pounds. Contact pressure remained constant at 355 psi, resulting in radii of loaded areas of 4.64 inches (24,000-lb load) and 5.68 inches (36,000-lb load). A summary of the ILLI-PAVE computer outputs for the 24,000-lb and 36,000-lb loads are listed in Tables A-2 and A-3 respectively.

TABLE 5. ILLI-PAVE VARIABLES FOR 3^4 FACTORIAL.

FACTOR	VALUES
1. Thickness of Asphalt Concrete,	3, 5, and 9 inches
2. Modulus of Asphalt Concrete,	100, 500, and 1500 ksi
3. Thickness of Granular Base,	6, 12, and 24 inches
4. Subgrade Resilient Modulus at Breakpoint	1.00 ksi (Very Soft Subgrade) 7.68 ksi (Medium Subgrade) 12.34 ksi (Stiff Subgrade)

A comparison of some critical responses (i.e., tensile strain in AC, compressive strain in subgrade, and deviator stress in subgrade) from 24-, 30-, and 36-kip loads are contained in Tables A-4, A-5, and A-6. As approximations, these guidelines can be used:

<u>Response</u>	<u>Comparing 24-kip to 30-kip Response</u>	<u>Comparing 36-kip to 30-kip Response</u>
AC Strain	10-15 % less	10-15 % greater
Subgrade Strain	15-20 % less	15-20 % greater
Subgrade Deviator Stress	15-20 % less	10-15 % greater

Algorithms developed for the 24- and 36-kip loads are contained in Tables B-4 and B-5 respectively. Additionally, algorithms were developed using the variable of load magnitude (P), which are contained in Table B-6.

F. INFLUENCE OF BASE QUALITY ON STRUCTURAL RESPONSES

Granular base characterization was discussed in Section III.B.2. The resilient modulus is modelled as:

$$E_r = K \theta^n$$

where, E_r is the resilient modulus, in psi

K and n are constants, and

θ is the sum of the principal stresses, in psi.

Values of $K=5000$ and $n=0.5$ were assumed in developing the data base.

References 7 and 48 reported little sensitivity of the pavement's structural responses when K and n were varied over typical values for aggregate base material. However, the studies only considered highway loading (9-kip). A similar study using the heavyweight F-15 loading was conducted.

Typical K and n values are shown in Figure 17. For higher quality base material, $K=9000$ and $n=0.33$ were selected. For lower quality base material,

$K=3000$ and $n=0.65$ were selected. The angle of internal friction was kept constant at 40° . A 3^4 factorial was run for each base material quality. Therefore, including $K=5000/n=0.5$ data, a 3^5 factorial was run. The data bases for the lower and higher quality base materials are listed in Tables A-7 and A-8 respectively. Comparisons of some critical responses using different base material qualities (similar to those presented in Section III.E for different load magnitudes) are contained in Table A-9, A-10, and A-11.

Except at AC modulus = 100 ksi and AC thickness = 3 inches (i.e., when granular stresses/moduli are high), there is little effect on AC tensile strain (Table A-9). For subgrade compressive strain (Table A-10) and subgrade deviator stress (Table A-11) there is little difference in response even at low AC thickness and moduli values. No combinations of higher quality material in the upper portion of base and lower quality in the lower portion were tried. Based on this analysis, it was concluded that $K=5000$ and $n=0.5$ were acceptable values for general use.

G. HEAVIER-WEIGHT F-15 DATA BASE AND DESIGN ALGORITHMS

The loading for the proposed heavier-weight F-15 aircraft is a 36,000-lb circular wheel load with a contact pressure of 395 psi giving a 5.39-inch radius of loaded area. The data base obtained using ILLI-PAVE is listed in Table A-12. The algorithms developed are listed in Table B-7.

Comparisons of some critical responses at 30-kip/355-psi and 36-kip/355-psi to 36-kip/395-psi loadings are contained in Tables A-13, A-14, and A-15. Generally, computed responses for the 36-kip/395-psi loading are only 1-5 percent greater than under the 36-kip/355-psi loading. The additional 40 psi contact pressure produces little difference in pavement response.

SECTION IV

TRANSFER FUNCTIONS

A transfer function relates pavement structural responses (stress, strain, deflection) to pavement distress and performance. It is also called a distress function or performance model. The two predominate modes of distress in flexible pavements are:

- (1) Cracking of the asphalt concrete layer, and
- (2) Rutting.

In this section some AC fatigue transfer functions are considered. Also, rutting transfer functions and design approaches to limit rutting are presented. More detailed discussions of transfer functions are presented in References 7 and 8.

A. ASPHALT CONCRETE FATIGUE

"Fatigue is the phenomena of repetitive load-induced cracking due to a repeated stress or strain level below the ultimate strength of the material," (Reference 13). Under traffic loading, the pavement is subjected to repetitive flexing creating tensile stresses/strains. The magnitude of the flexural stresses/strains are dependent on the overall stiffness and nature of the pavement construction.

1. Laboratory Fatigue Testing

Fatigue tests may be conducted by several test methods and various specimen sizes. A common test used is a repeated load flexure device with beam specimens. Repeated load indirect tensile (split tensile) tests have also been used.

Fatigue testing may be conducted under either controlled stress or controlled strain loading. In the controlled stress mode, a constant load is continuously applied to the specimen. Because of the progressive damage to the specimen, a decrease in stiffness results. This, in turn, causes an increase of the actual flexural strain with load applications. For the controlled strain approach, the load is continuously changed to yield a constant beam deflection. This results in a stress that continuously decreases with load application. Yoder and Witczak (Reference 13) suggest applying controlled strain tests to thin asphalt layer pavements (less than 2 inches) and controlled stress conditions to thicker asphalt pavement layers (greater than 6 inches). At intermediate thicknesses, the probable fatigue response is governed by something intermediate to these two test modes. Since controlled stress conditions give more conservative estimates of the fatigue life, this test may be safely employed for these cases.

Chou (Reference 37) points out that investigators have defined the failure or end point of a fatigue test in many different ways. It has been taken as the point corresponding to complete fracture of the test specimen, the point at which a crack is first observed or detected, or the point at which the stiffness or some other property of the specimen has been reduced by a specific amount from its initial value.

Investigators have generally used two forms of equations to relate the fatigue testing results to the number of repetitions until failure (N_f). The difference of opinion arises over the importance of the AC stiffness. With AC stiffness effect, the fatigue relationship is of the form:

$$N_f = K (1/\epsilon_{AC})^a (1/E_{AC})^b \quad (9)$$

where, ϵ_{AC} = magnitude of load induced strain,

E_{AC} = AC dynamic stiffness modulus, and

K, a, b = constants determined by testing and/or pavement performance analysis.

Bonnaure, et al. (Reference 49), Finn, et al. (Reference 50), Kingham (Reference 51), Witczak (Reference 52), and the Asphalt Institute thickness design procedure (Reference 53) indicate AC stiffness is important. Without AC stiffness effect, the fatigue relationship is of the form:

$$N_f = K (1/\epsilon_{AC})^a \quad (10)$$

where all terms are as defined for Equation (9). Pell (Reference 54), Thompson (Reference 55), and the Federal Highway Administration overlay design procedure (Reference 56) indicate this form of the equation is adequate.

2. Cumulative Damage

To account for the strain variations, Miner's hypothesis of damage accumulation has been used by many researchers (e.g., References 57, 58, and 59) to evaluate the effects of repeated load applications on the fatigue properties of pavement materials. Miner's hypothesis can be expressed mathematically in terms of relative damage factors. The equation for the damage factor is:

$$D_i = n_i/N_i \quad (11)$$

where, D_i = the relative damage during some period i ,

n_i = the number of load applications during the period, and

N_i = the total number of load applications the pavement could carry for the strain induced under the conditions prevailing during the period.

Cracking is expected to occur when the sum of the damage factors equals one (i.e., $\sum D_i = 1.0$). In Equation (11), N_i is determined from a fatigue equation, N_f in Equation (9) or (10).

3. Field Calibration of a Fatigue Equation

Laboratory fatigue tests of bituminous mixes do not adequately represent the boundary conditions in an existing pavement (e.g., simply supported versus continuously supported). Brown and Pell (Reference 57) suggest that in-service pavement life (repetitions to failure for a given strain level) is on the order of 20 times the life of a test specimen in the laboratory. Thus, it is necessary to calibrate the laboratory fatigue curves with the performance of in-service pavements. Calculation of the tensile strain at the bottom of the AC layer must be done using the structural model that will be used for design (ILLI-PAVE, elastic layer, etc.). A different response will normally be calculated for each structural model (model dependency).

4. Structural Model Responses and Correlation With Performance Data

Another method of developing transfer functions is by directly correlating the AC tensile strain calculated using an appropriate structural model with corresponding field performance. The objective is to select the values of K, a, and b in Equations (9) or (10) to provide the best prediction of actual data. Pavement properties may vary over the period of the test, thus AC tensile strain would not necessarily remain constant. Transfer functions developed in this manner are also structural model dependent.

Elliot and Thompson (Reference 7) applied this method using the ILLI-PAVE model to the AASHO Road Test data. They derived the following equations:

$$\log N_{2.5} = -4.4856 - 2.92 \log \epsilon_{AC} \quad (12)$$

$$\log N_{1.5} = -5.5204 - 3.27 \log \epsilon_{AC} \quad (13)$$

where, $N_{2.5}$ and $N_{1.5}$ = the number of load applications to a Present Serviceability Index of 2.5 and 1.5 respectively, and

ϵ_{AC} = predicted AC tensile strain in inch/inch.

The constants 2.92 and 3.27 are analogous to the "a" constant of Equation (10).

When the AC stiffness effects were considered, the following equation was developed:

$$\log N = 2.4136 - 3.16 \log \epsilon_{AC} - 1.4 \log E_{AC} \quad (14)$$

where, N = the predicted number of load applications to crack appearance,

ϵ_{AC} = predicted AC tensile strain in inch/inch, and

E_{AC} = dynamic stiffness modulus of the AC in psi.

B. PERMANENT DEFORMATION

The rutting in flexible pavements results from the accumulation of small permanent deformations associated with repetitive traffic loading (Reference 60). Each layer of a flexible pavement and the subgrade contribute to the development of rutting in the pavement surface. Experience indicates that under normal pavement conditions, deformation within asphaltic materials primarily occurs during warm weather. Under cold weather conditions, little deformation occurs because of the stiff condition of the asphalt material. In some cases, the subgrade soil may be frozen in winter and provide firm support for the overlying asphalt concrete layer and thus reduce pavement deformation. While rutting and fatigue are two separate modes of distress, rutting can contribute to fatigue failure of a pavement due to tensile strains in the surfacing which result from bending caused by rutting in the base and subgrade.

1. Asphalt Concrete

AC rutting prediction is not considered in the mechanistic design procedure developed in this study. It is assumed, as is the case with the

Asphalt Institute highway pavement thickness design procedure, that rutting can be controlled on the basis of mixture design procedures, policies, and practices. The DOD uses the Marshall Mix Design procedure for design of bituminous mixes of airfield pavements (Reference 3). Investigations are underway by the U.S. Army and Air Force to develop suitable AC mixes for the heavyweight F-15 aircraft.

2. Granular Materials

A ϵ_p (permanent strain) - $\log N$ (number of load repetitions) relation adequately represents the permanent deformation behavior of granular materials. A typical plot is shown in Figure 23. The general form of the equation is:

$$\epsilon_p = a + b \log N \quad (15)$$

where, ϵ_p = permanent strain,

N = number of load repetitions, and

a, b = experimentally derived factors from repeated load testing data.

The plastic strains of granular materials have been found (References 61 through 66) to increase with load repetitions, increase with increasing deviator stress, decrease with increasing confining pressures, increase significantly with increasing fines, increase with increasing degree of saturation, increase drastically if the base is compacted at 95 instead of 100 percent of maximum density, and are also dependent on the stress repetition sequence and magnitude. A limited number of large stress repetitions can effect a large permanent strain. In general, the factors that increase the shear strength of a granular material (particularly increased density) will decrease permanent deformation accumulation. The actual plastic deformation could be more serious than predicted in the

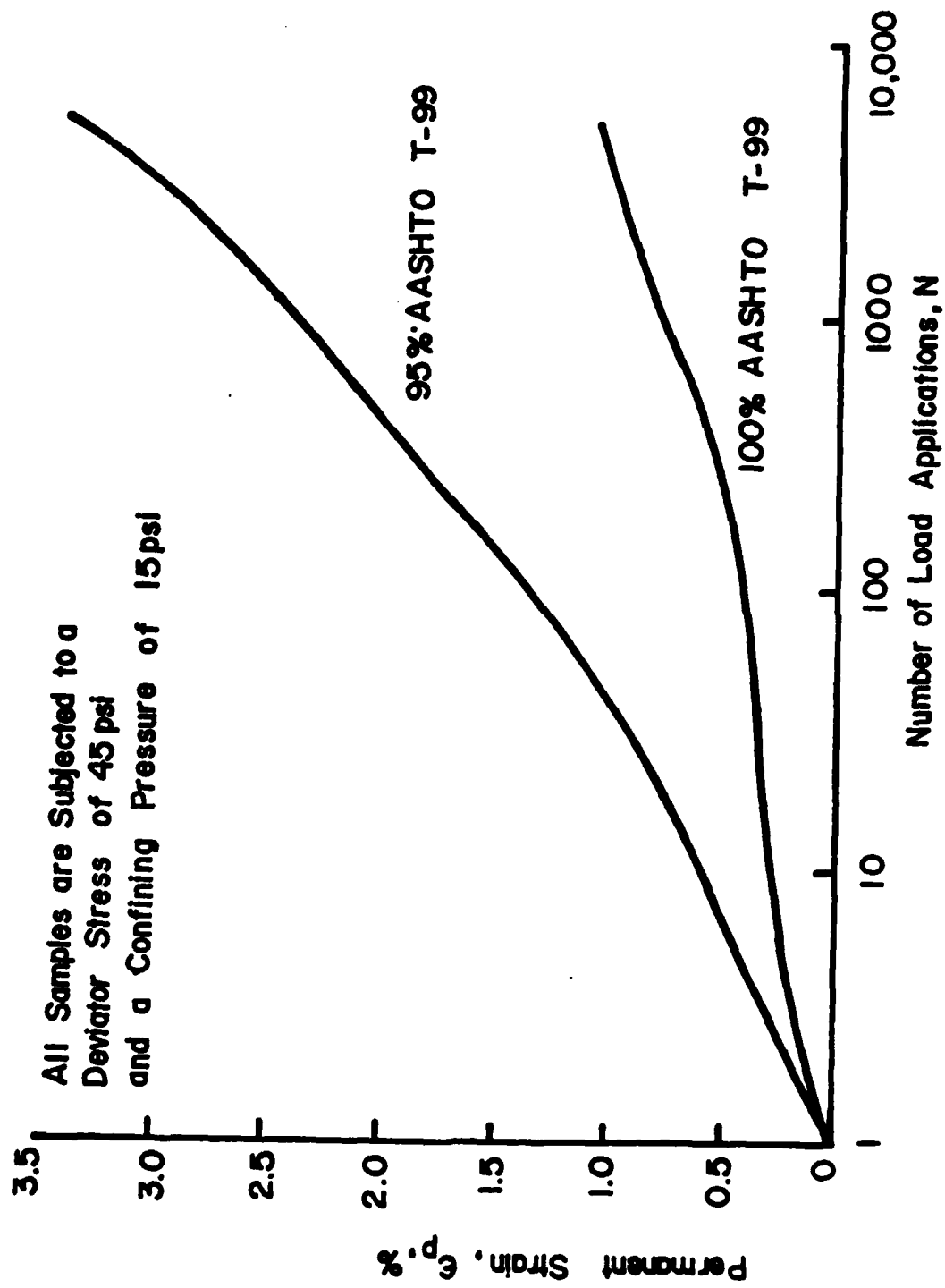


Figure 23. Typical Permanent Deformation Behavior for a Dense-Graded Limestone (Reference 66).

laboratory under repetitive loading tests if a significant buildup of pore pressures should occur in the field due to poor drainage conditions.

Chou (Reference 63) concluded that the response of granular materials to repeated applications of aircraft loads in an actual runway are extremely complicated and are not fully understood. The response of the granular materials to repeated applications of aircraft loads cannot be simulated by the laboratory repeated load triaxial tests. Stress states in the granular layers cannot be accurately predicted using existing computer programs (elastic layer, nonlinear finite element, etc.). To minimize the potential of permanent deformation in untreated granular materials, it may be best for design purposes, at least at the present time, to specify strict compaction requirements and select materials with higher modulus values/shear strengths.

3. Fine-Grained Soils

A $\log \epsilon_p - \log N$ relation is generally satisfactory to represent the permanent deformation behavior of fine-grained soils. A typical plot is shown in Figure 24. The general form of the equation is:

$$\epsilon_p = A N^b \quad (16)$$

where, ϵ_p = permanent strain,

N = number of load repetitions, and

A, b = experimentally derived factors from repeated load testing data.

The "b factor" generally ranges between 0.1 and 0.2 (Reference 66). "A" varies considerably as a function of magnitude of the repeated stress. For stress ratios (repeated stress/strength) greater than about 0.5-0.67, "A" may increase rapidly with only a small additional increase in the repeated stress level (Reference 66). Limiting the stress ratio to acceptable levels is a good concept for general design. Figure 25 illustrates the "limiting stress

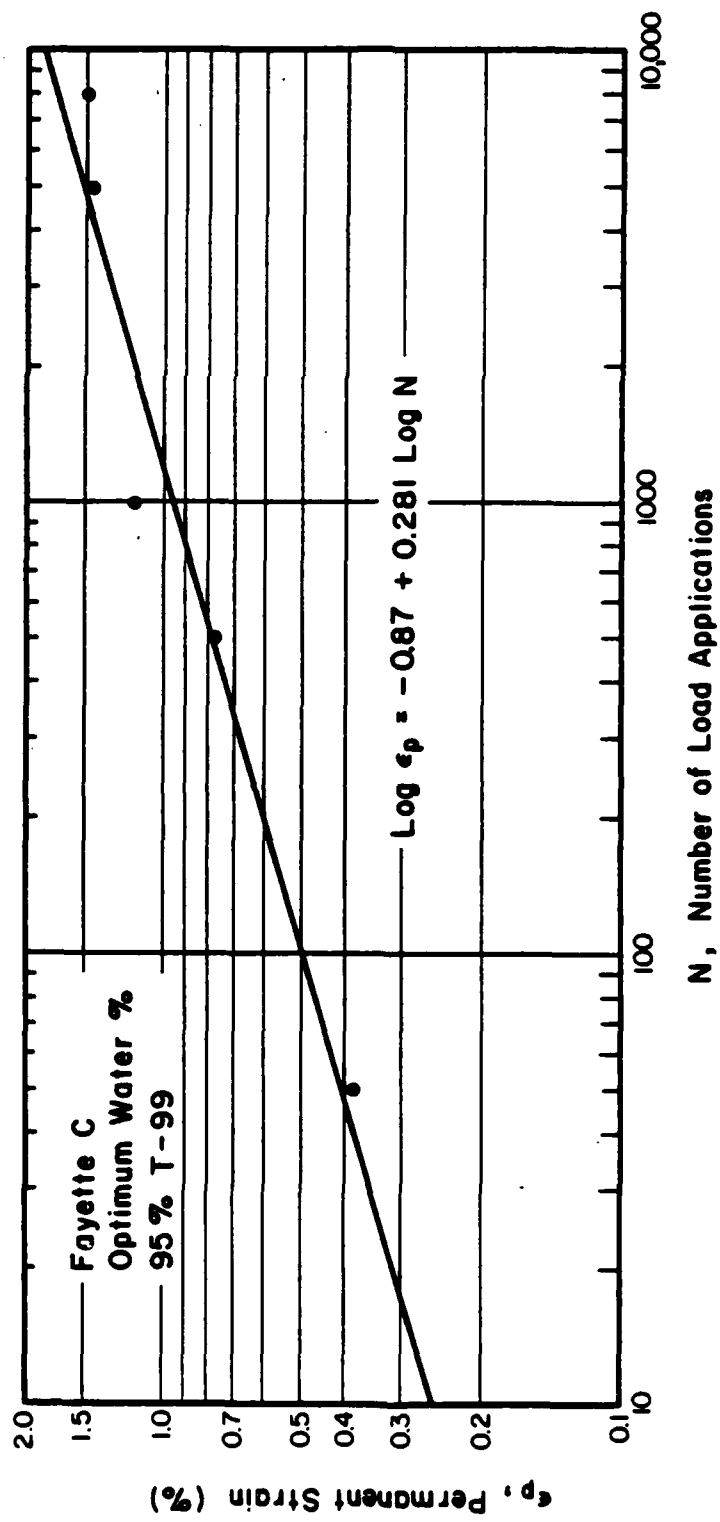


Figure 24. Typical Permanent Deformation Behavior for a Fine-Grained Soil (Reference 66).

ratio" concept.

In general, factors that cause a decrease in shear strength increase the accumulation of permanent deformation. The detrimental effects of moisture increase in excess of optimum are shown in Figure 26. One freeze-thaw cycle has destructive effects as demonstrated in Figure 27. Subgrade permanent strain is also stress history dependent.

The compressive vertical subgrade strain is a design criterion adopted by various investigators (References 52, 57, and 68) and agencies (Asphalt Institute - Reference 53, Shell - Reference 69). Other investigators limit the vertical compressive stress on top of the subgrade (Reference 70) or subgrade deviator stress ratio (References 7, 8, and 66). Barker and Brabston (Reference 71) present limiting subgrade strain criteria as a function of subgrade modulus (Figure 28). This criteria is discussed in more detail in Section VII.C.

Chou (Reference 63) found that the concept of controlling subgrade rutting through limiting subgrade strains in flexible pavements is not strictly correct. Laboratory repeated load test results shown in Figure 29 indicate that, for a given value of elastic strain, the permanent strain of the subgrade increases with decreasing CBR values. Based on these findings, a transfer function to limit rutting containing both subgrade strain/stress and subgrade modulus/strength variables would be more appropriate. The stress ratio (repeated deviator stress/compressive strength) accounts for both stress intensity and subgrade strength.

The subgrade design criterion adopted in this study is the limitation of the subgrade stress ratio. This design stress ratio is selected to limit rutting to an acceptable level for design circumstances.

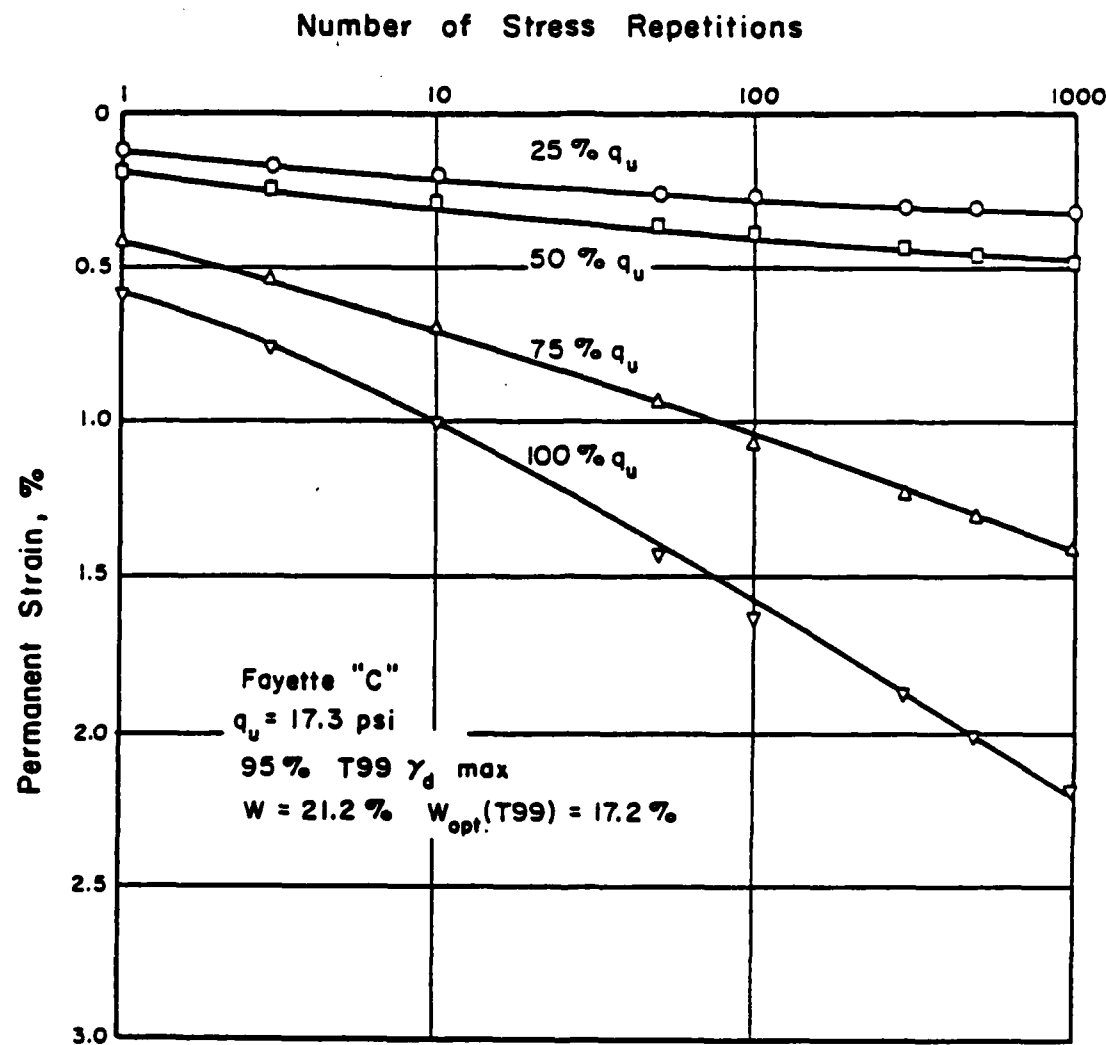


Figure 25. Stress Level-Permanent Strain Relations for a Fine-Grained Soil (Reference 66).

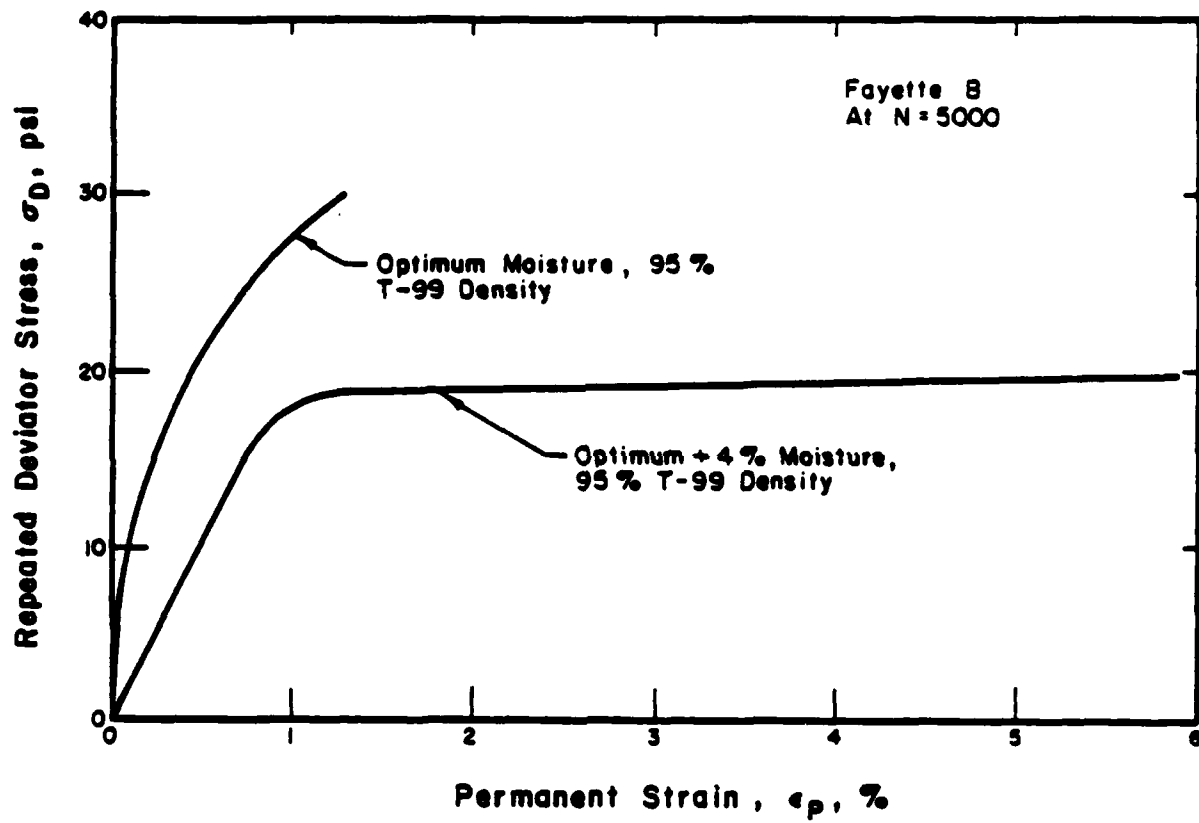


Figure 26. Influence of Moisture Content on the Permanent Strain Response of a Fine-Grained Soil (Reference 66).

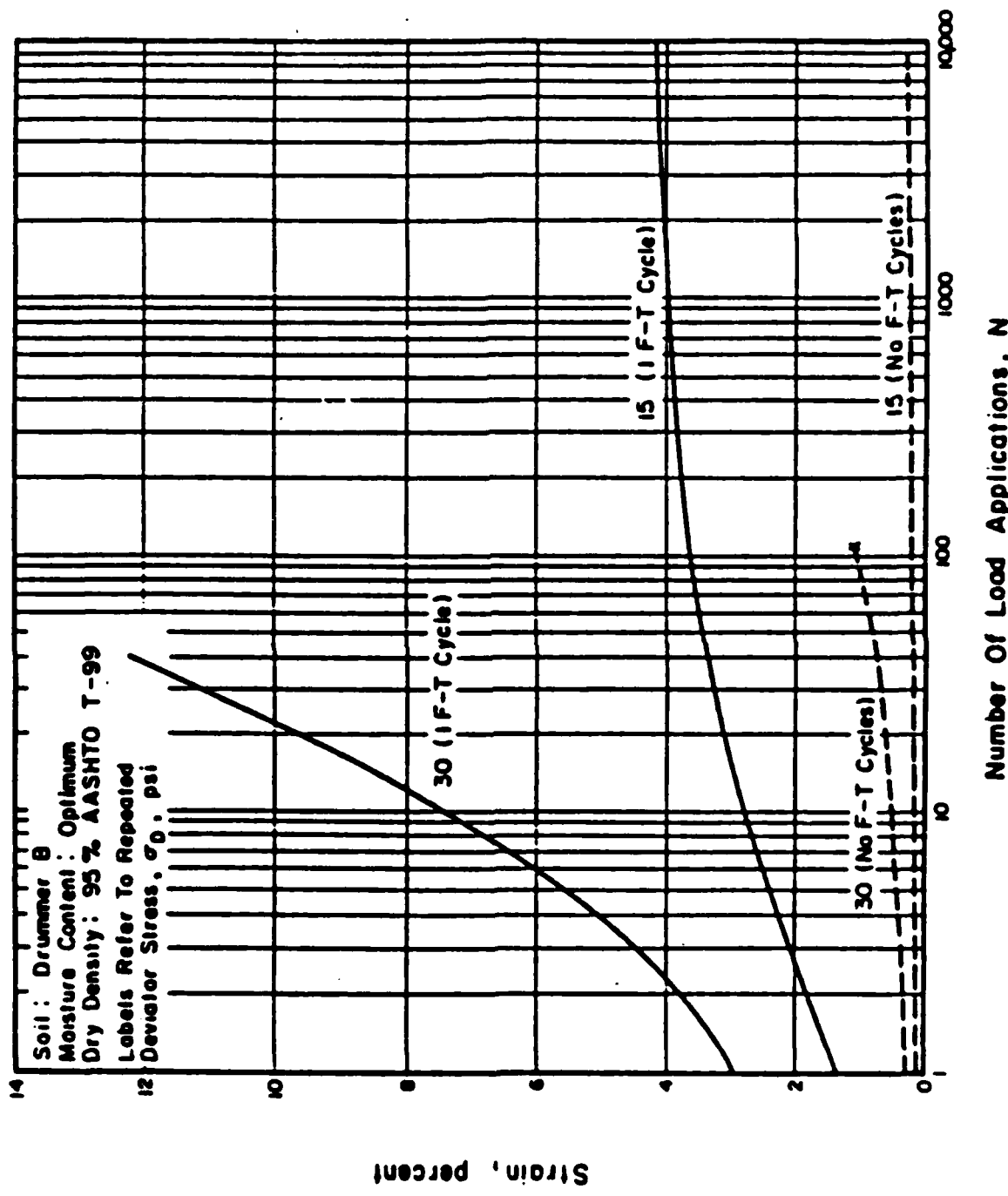


Figure 27. Effect of One Freeze-Thaw Cycle on Permanent Deformation for a Fine-grained Soil (Reference 66).

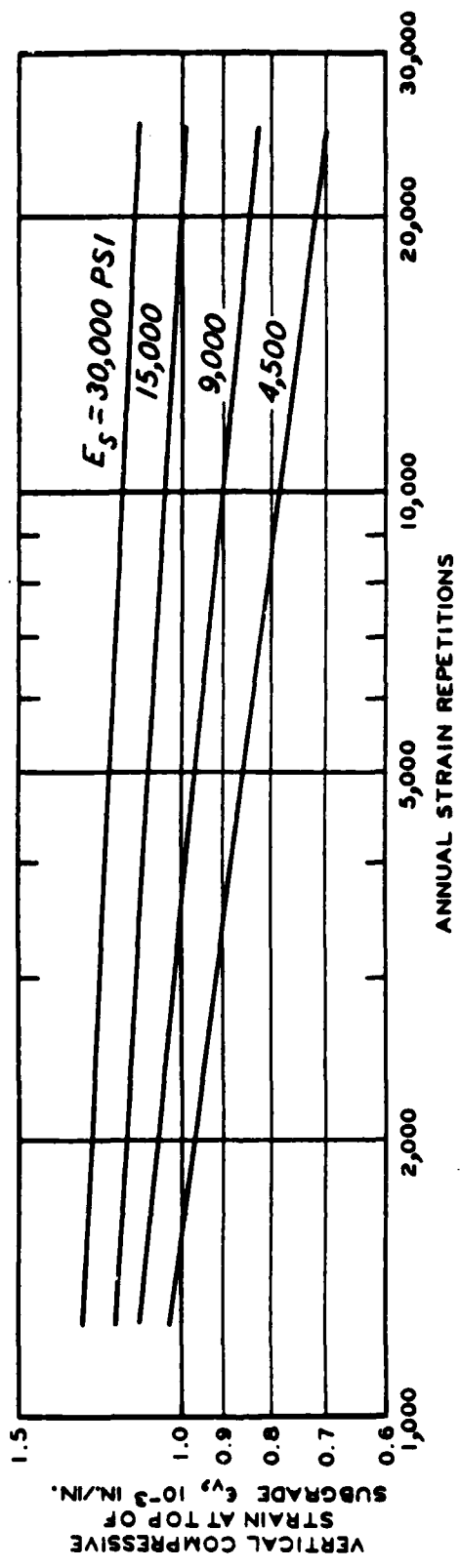


Figure 28. Subgrade Strain Criteria (Reference 71).

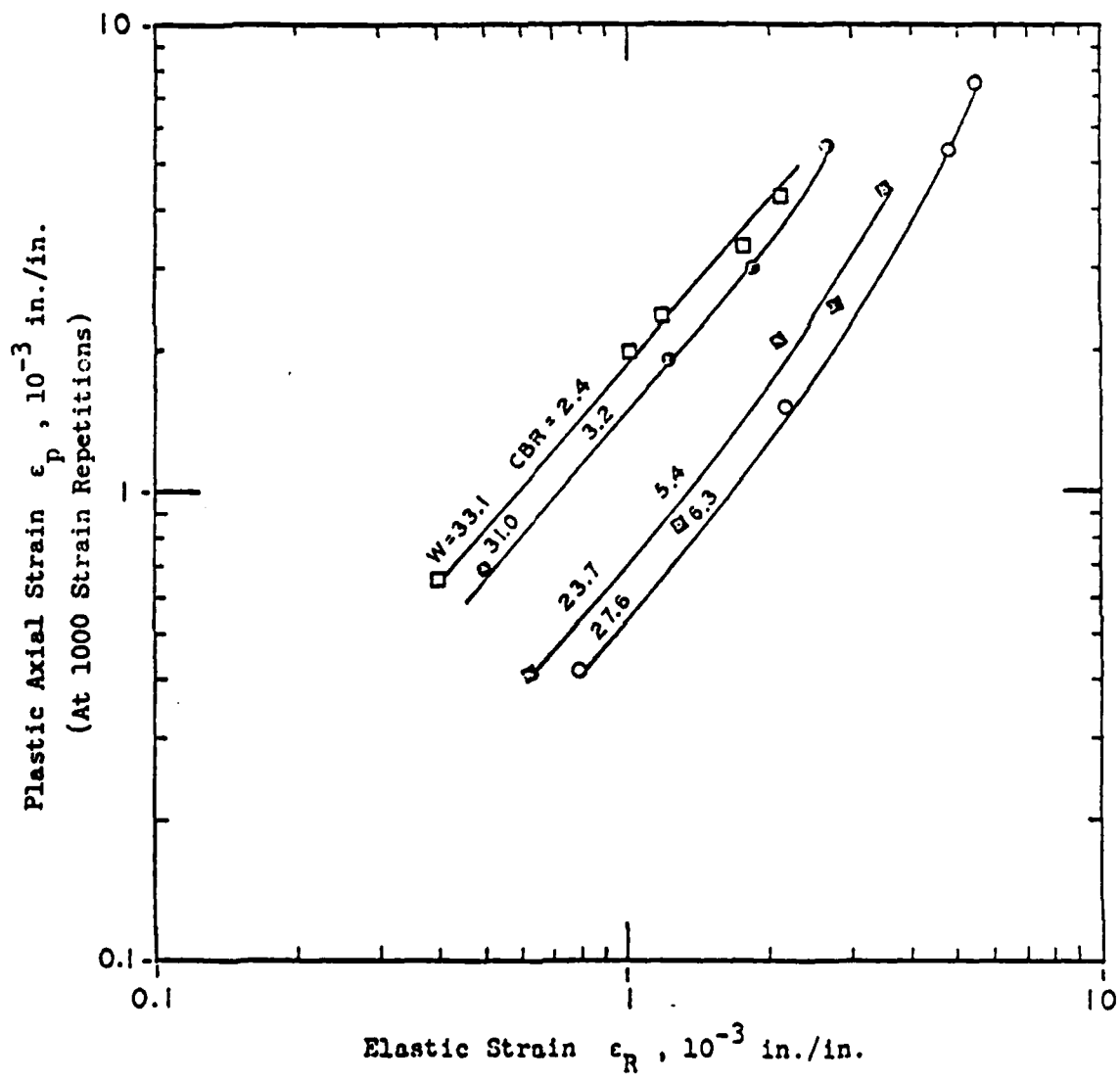


Figure 29. Relationships Between Plastic Strain and Elastic Strain for Fine-Grained Soil at 1000 Repetitions (Reference 65).

SECTION V

RESPONSE AND PERFORMANCE OF FULL-SCALE TEST SECTIONS

This section presents an overview of available data for single-wheel, high tire pressure aircraft trafficking of conventional flexible pavement test sections. These test sections are then modeled using ILLI-PAVE to calculate pavement responses (stresses, strains, deflections). Finally, critical responses are correlated with performance (number of coverages until failure).

A. OVERVIEW OF AVAILABLE TEST SECTION DATA

The majority of available information relates to roads and streets trafficked with relatively light loads and low tire pressures (cars, trucks, etc.). Even the test sections constructed in the early 1940s during the development of the CBR method were generally trafficked with tire pressures at 60-100 psi. These early test sections were not analyzed.

Reference 22 presents the results of an investigation of asphalt paving mixtures. Traffic tests included 37,000-lb single-wheel loads at 110 psi tire pressure. Test sections had various asphalt mixes (different asphalt and filler contents), pavement surface thicknesses and types (surface treatment, sand asphalt, or asphalt concrete with crushed limestone or uncrushed gravel aggregate), and base course thicknesses and qualities (crushed limestone, sand-loess, or sand-loess-clay). The investigation was concerned primarily with the pavement surface. Subgrade conditions were of little concern except that subgrade shear deformation development was undesirable. Therefore, a high strength subgrade was used. The subgrade was classified as a lean clay (CL) with liquid limit (LL) of 47 and plasticity

index (PI) of 23. The "as constructed" subgrade surface CBRs (excluding turnaround areas) range from 9 to 31 with an average of 20.7 and standard deviation of 7.3 (CV=35.4 %). Since the variability of the subgrade was so high, these tests were also not analyzed.

Further traffic tests were conducted five years later (1949) on previously untrafficked portions of these test sections (Reference 27). Traffic tests included 30,000-lb single-wheel load at 200 psi tire pressure. Reference 27 reports that the subgrade was non-uniform and high deflections occurred throughout the test. Reported CBR values, just within the area receiving the single-wheel traffic, range from 6 to 26. However, because of the relative uniformity of moisture content and densities (coefficients of variation respectively of 4.5 and 2.3 %), E_{Ri} could be estimated (see Section V.B). Pavement surface thicknesses were 1.5 and 2.0 inches and base course ranged from 10 to 11.5 inches thick.

Later that same year (1949), more of these previously untrafficked test sections were trafficked with small high-pressure tires for the Navy (Reference 28). The traffic load was 8000-lb single-wheel load with a tire pressure of 240 psi. The subgrade could be modelled with the same E_{Ri} as previously determined. Pavement surfaces were 1.5, 3.0 and 5.0 inches thick. Total pavement thickness (surface + granular base) was 9 inches.

Reference 72 presents the results of 10,000-lb, 110 psi wheel load traffic. The intent of this test was to determine the effect of mixed traffic. One lane received only the 10-kip traffic, another lane received both 10- and 25-kip traffic, the final lane received a combination of 10-, 25-, and 50-kip traffic. The three test sections were 5 inches, 8 inches, and 11 inches of well-graded crushed limestone surfaced with a bituminous surface treatment on a CH subgrade (heavy clay) having a 6 CBR.

The Multiple Wheel Heavy Gear Load (MWHGL) test (Reference 31) included trafficking with 30,000-lb and 50,000-lb single-wheel loads. For the test, the natural soil at and near the site was used for the bottom portion of the controlled-strength subgrade. This soil was classified as a CL and had a LL of 34 and PI of 12. The top three feet of subgrade consisted of a heavy clay (CH) commonly called "Vicksburg Buckshot," with a LL of 73 and PI of 48. A target CBR of 4 was set, except in Item 4 which had 2 feet of CBR 2 material. Items receiving single-wheel traffic had 3 inches of asphalt concrete and 6 inches of high-quality base with 6 or 15 inches of gravelly-sand subbase.

Construction control of the subgrade was excellent with average water content of 32.5 % ($CV=4.9\%$) and average dry density of 85.6pcf ($CV=2.7\%$). However, there was a large spread of CBR values (see Section V.E.1 for analysis of MWHGL test statistics). Only Items 1 and 2 received single-wheel traffic. Item 1 had an average CBR of 3.5 ($CV=21.1\%$) and Item 2 had an average CBR of 4.5 ($CV=25.6\%$).

In a bituminous stabilization study (Reference 73), four conventional flexible pavement test sections were trafficked with a 75,000-lb single-wheel load at 278 psi contact pressure. The MWHGL test subgrade was used for this study. Previously untrafficked portions of Items 4 and 5 of the MWHGL test were trafficked in addition to the two sections constructed as part of this study. One item consisted of a 15-inch full-depth high-quality asphalt concrete. The other item consisted of a 9-inch high-quality asphalt concrete surface over a gravelly-sand subbase material. The MWHGL test items had 3 inches of asphalt concrete and 6 inches of high-quality base with 24 or 33 inches of gravelly-sand subbase.

One conventional flexible pavement test section was also trafficked and

reported in Reference 74. Traffic applied was a 75,000-lb load and 278 psi contact pressure. The test section consisted of 3 inches of high-quality asphalt concrete over 21 inches of high-quality crushed stone. The MWHGL test subgrade was used.

The final test sections analyzed are reported in Reference 75. Three test sections were trafficked with simulated F-4 aircraft loading (27,000-lb, 265 psi wheel load). The goal of this effort was to determine the minimum AC thickness required to withstand 150 passes of an F-4. One item had a double-bituminous surface treatment, another item had 1-inch high-quality AC surface, the final item had 2-inch high-quality AC. Note, the present DOD requirement for the F-4 is 3 inches of AC over a 100 CBR base (Reference 3). The subgrade was "Vicksburg Buckshot Clay," with a CBR of 6.

B. MODELLING THE TEST SECTIONS AND CALCULATED RESPONSES

The pavement test sections discussed in Section V.A were modelled using the ILLI-PAVE finite element program (discussed in Section III.A). The AC surface was characterized as a linear elastic material, bituminous-surface treatment thickness was treated as part of the granular base thickness, and the base course and subgrade were characterized as stress-dependent material as discussed in Section III.B. Pavement temperatures during deflection basin measurements were not reported for any of the test sections analyzed. AC modulus values were assigned based upon estimated temperatures. A summary of ILLI-PAVE input values and calculated responses for test sections analyzed are contained in Table 6.

The subgrade values reported in Reference 27 varied greatly. However, E_{Ri} could be estimated from the following regression equation for cohesive soils contained in Table 18 of Reference 38:

TABLE 6. TEST SECTION ANALYSIS RESULTS.

Test Point	Reference	Wheel Load (kips)	Contact Area (in. ²)	Cover-ages	ILLI-PAVE INPUT				ILLI-PAVE RESULTS			Failure Mode
					TAC (in.)	EAC (ksi)	TGR (in.)	E _{Ri} (ksi)	00 (mils)	ε _{AC}	σ _D (psi)	
1	27	30	150	220	1.5	100	11.5	11.3	81.6	426	24.4	0.79
2	27	30	150	216	2.0	100	10.0	11.3	83.6	516	26.1	0.84
3	27	30	150	178	1.5	100	10.5	11.3	84.4	412	26.0	0.84
4	27	30	150	178	2.0	100	10.0	11.3	83.6	516	26.1	0.84
5	27	30	150	203	2.0	100	10.0	11.3	83.6	516	26.1	0.84
6	28	8	37	1400 ^a	1.5	200	7.5	11.3	37.1	703	18.3	0.59
7	28	8	37	1276	3.0	200	6.0	11.3	29.5	834	15.2	0.49
8	28	8	37	1264	5.0	200	4.0	11.3	21.5	600	11.2	0.36
9	72	10	91	40	--	--	5.0	9.0	60.3	--	24.6	0.96
10	72	10	91	400	--	--	8.0	9.0	47.4	--	18.2	0.71
11	72	10	91	1400 ^a	--	--	11.0	9.0	42.0	--	14.2	0.56
12	31	30	285	120	4.0	100	11.0	5.0	91.8	506	11.7	0.69
13	31	30	285	450 ^a	4.0	100	20.0	7.0	67.5	458	9.6	0.45
14	31	50	285	6	4.0	100	11.0	5.0	152.6	649	15.5	0.91
15	31	50	285	200	4.0	100	20.0	7.0	105.3	584	13.4	0.62
16	31	50	285	6	4.0	500	11.0	5.0	120.0	708	12.9	0.76
17	31	50	285	200	4.0	500	20.0	7.0	90.3	556	11.6	0.54
18	73	75	270	8	15.0	100	--	5.0	143.1	1613	13.8	0.81
19	73	75	270	12	9.0	100	15.0	5.0	151.6	1115	12.5	0.73
20	73	75	270	18	4.0	100	29.0	5.0	147.2	723	10.5	0.62
21	73	75	270	70	4.0	100	37.0	5.0	135.7	738	8.5	0.50
22	74	75	270	50	3.0	400	21.0	5.0	165.1	609	12.9	0.76
23	75	27	111	20	1.7	100	8.2	9.0	102.4	526	25.6	1.00
24	75	27	111	14	1.4	100	9.0	9.0	100.3	438	25.6	1.00
25	75	27	111	2	--	--	9.9	9.0	104.8	--	25.6	1.00

^a Not Failed^b Binder Course Mix Failure

$$E_{Ri} = 25.51 - .466\theta \quad (17)$$

where, $\theta = w\gamma_d/\gamma_w$ (volumetric water content)

w = gravimetric water content in percent

γ_d = dry density in pounds per cubic feet (pcf)

γ_w = 62.4 pcf (unit weight of water), and

E_{Ri} = subgrade modulus at intercept in ksi.

For $\gamma_d = 110.9$ pcf and $w = 17.1\%$, E_{Ri} would be 11.3 ksi. Using the approximate relationship between E_{Ri} and CBR (Figure 30), CBR is between 7 and 8. The AC modulus was estimated at 100 ksi since all the traffic was applied during the summer.

The test sections reported in Reference 28 were modelled with the same E_{Ri} as previously determined (11.3 ksi) since the same subgrade was used with only a few months separating the tests. Traffic was applied September 26-November 8 when pavement temperatures were 80-95°F. An AC modulus of 200 ksi was assigned. The only failure data used were from test sections that had high-quality AC; sections containing AC with uncrushed gravel as the aggregate or sand asphalt were not considered.

The in place subgrade of the test reported in Reference 72 had a CBR of 6. An E_{Ri} of 9 ksi was assigned based upon the E_{Ri} - CBR plot contained in Figure 30.

The variability of pavement layer thicknesses reported in the MWHGL test (Reference 31) appears to be high. Asphalt concrete thickness averaged 3.9 inches with a 95 percent confidence interval of 3.7-4.1 inches, but 3 inches was the target value. A 4-inch AC surface was used for response calculations. The average thickness of pavement (AC + granular base + granular subbase) was presumably determined from several unreported measurements.

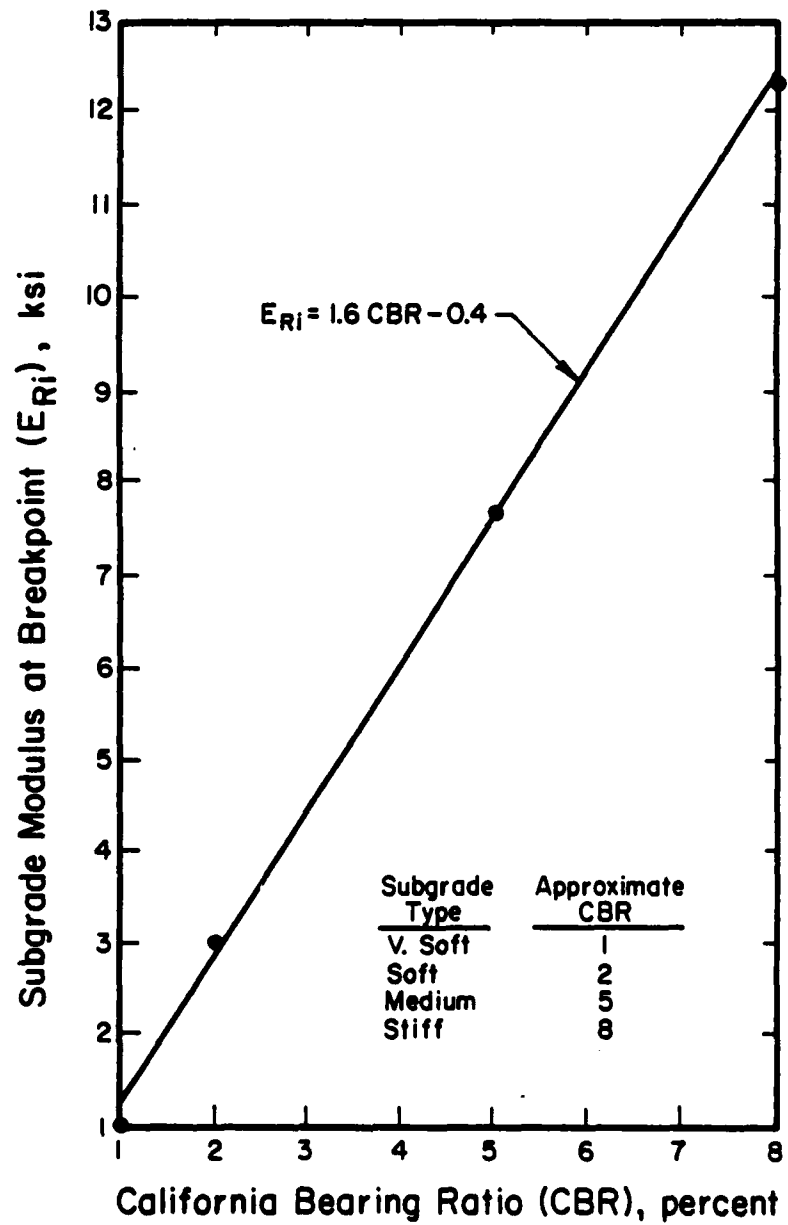


Figure 30. Approximate E_{Ri} - CBR Relationship.

The MWHGL report contains static deflection basins measured under both the 30- and 50-kip loading. The "static" deflections were converted to "dynamic" deflections by multiplying by 0.6. The factor 0.6 is the average ratio of moving wheel load deflections to the Benkelman beam, creep speed deflections measured during the AASHO Road Test (Reference 7). Under the 30-kip loading, an $E_{Ri} = 5$ ksi was backcalculated for Item 1 (Figure 31). An $E_{Ri} = 7$ ksi was backcalculated for Item 2 (Figure 32). These values of E_{Ri} correspond very well with the average CBR values of 3.5 and 4.5 measured in Items 1 and 2, respectively. However, under the 50-kip static loading (Figures 33 through 36), the match between ILLI-PAVE calculated deflections and measured "dynamic" deflections are not as good. It appears that there was considerable plastic deformation occurring under the 50-kip loading. ILLI-PAVE calculates resilient (rebound) deflections. Notice the large difference between the deflection basins measured transverse to traffic and parallel to traffic. Apparently there is more plastic deformation occurring parallel to traffic.

Attempts to match deflection basins measured under a vibratory loading were also unsuccessful (Figures 37, 38, and 39). This is attributed to the 9000-lb static weight of the vibratory testing equipment. The ILLI-PAVE deflections shown in Figures 37, 38, and 39 are the difference between deflections calculated at 9000 pounds plus half the peak-to-peak dynamic force and 9000 pounds minus half the peak-to-peak force.

AC temperatures for four of the test sections were high (90-115°F) during trafficking and an AC modulus of 100 ksi was assigned. The other two test sections were only trafficked when AC temperatures were between 60 and 70°F, and an AC modulus of 500 ksi was assigned.

For the test sections reported in References 73 and 74, an E_{Ri} of 5 ksi

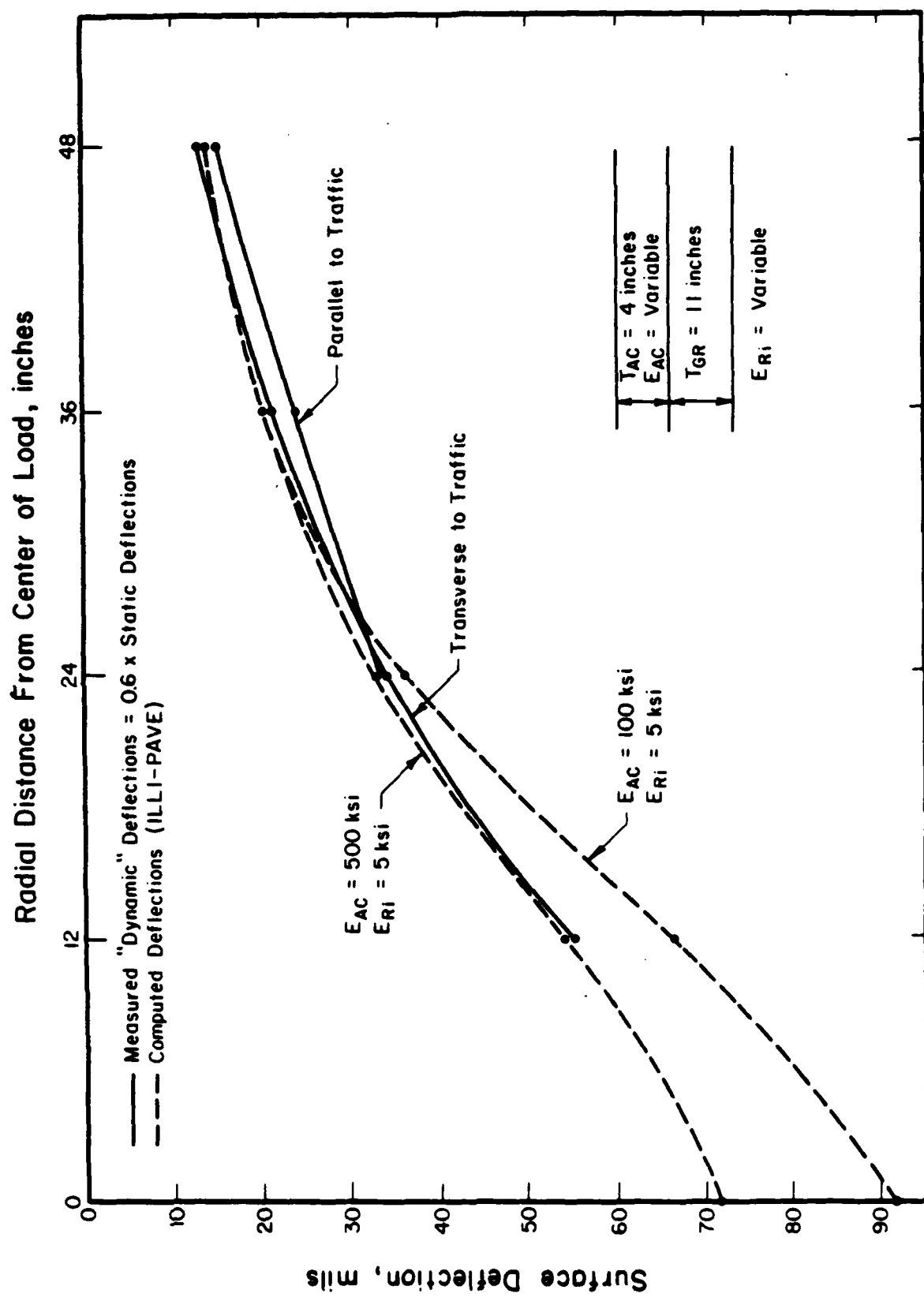


Figure 31. MWHCL Item 1 "Dynamic" Deflections Under 30-kip Static Wheel Load.

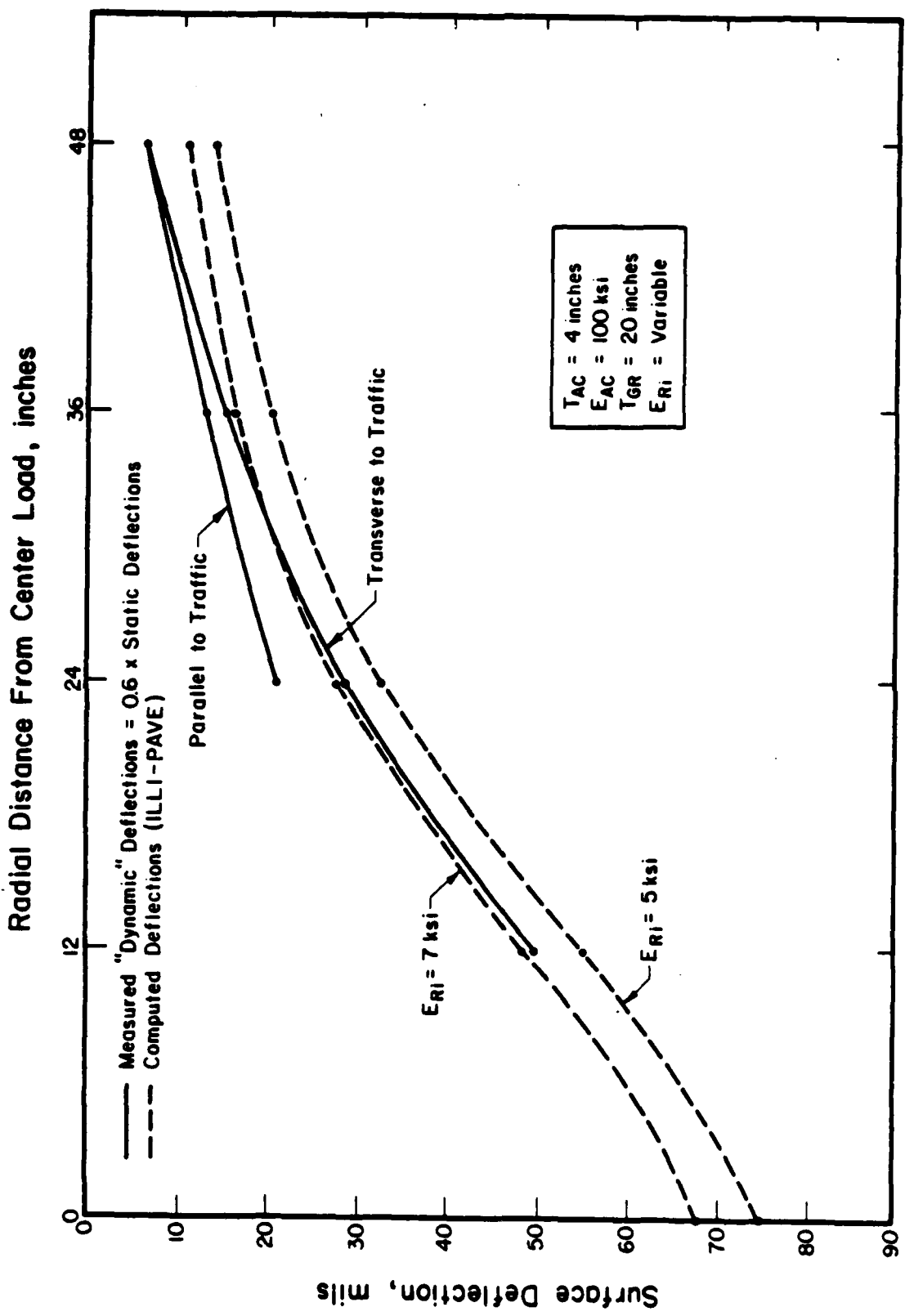


Figure 32. NWHCL Item 2 "Dynamic" Deflections Under 30-kip Static Wheel Load.

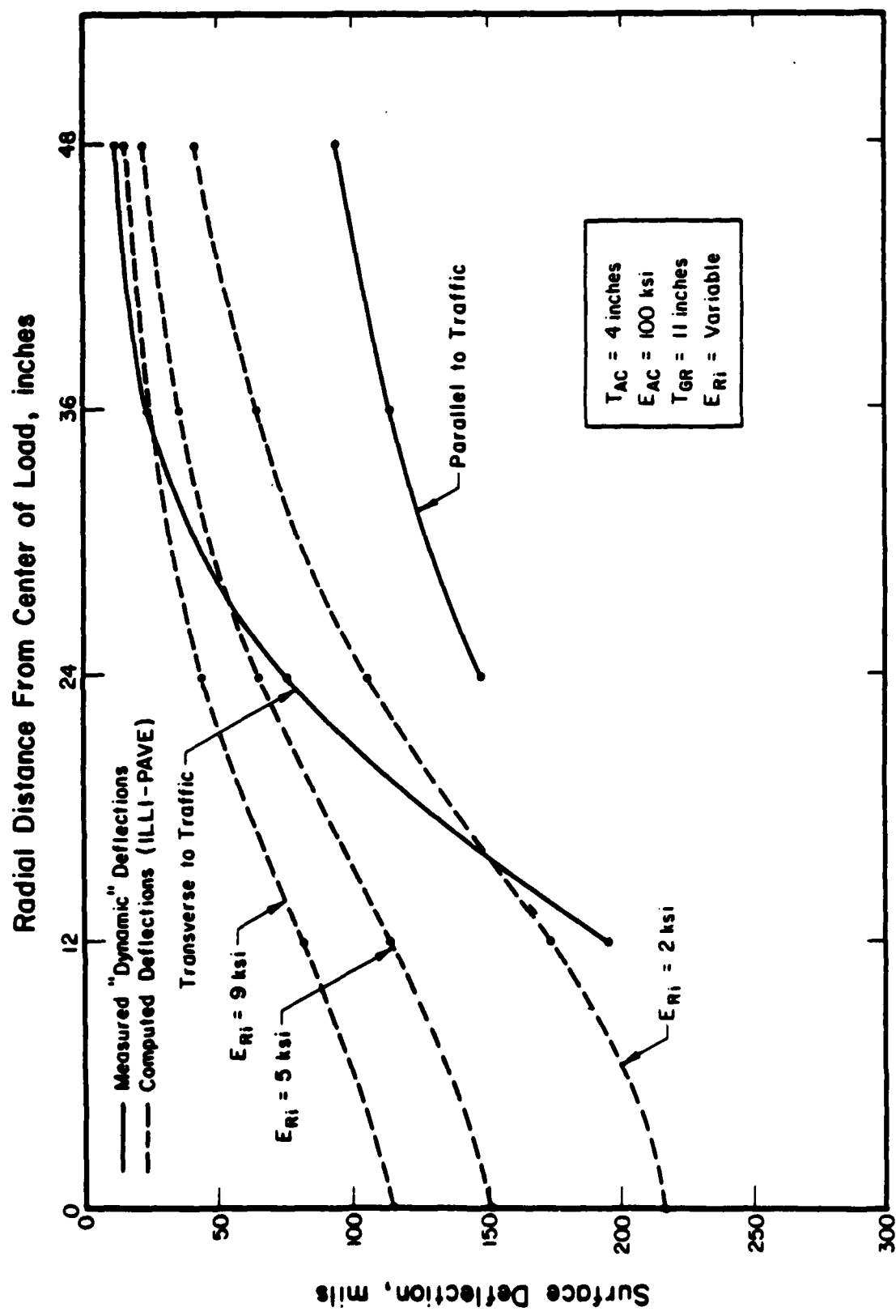


Figure 33. NWHCL Lane 2 Item 1 "Dynamic" Deflections Under 50-kip Static Wheel Load.

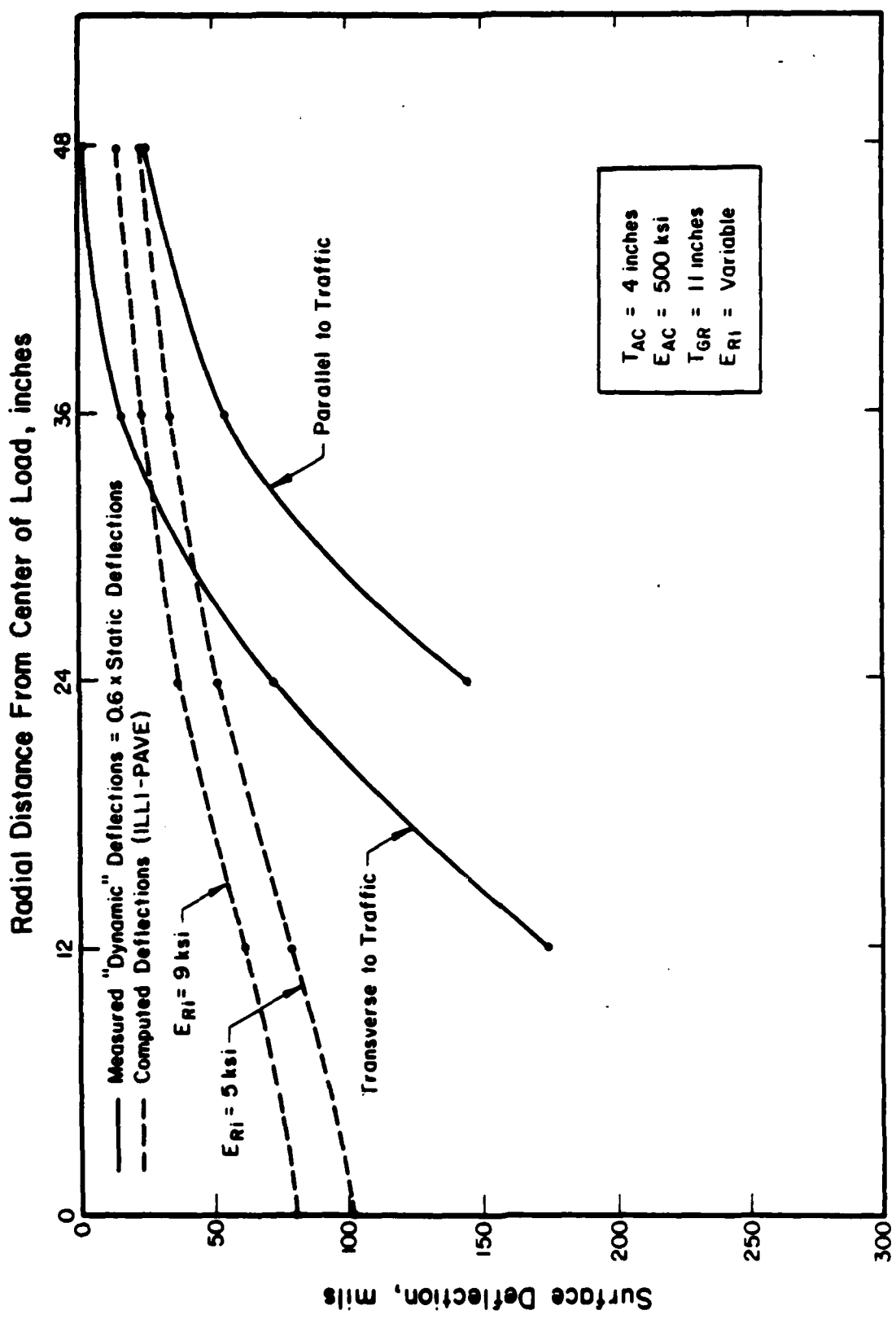


Figure 14. FHWICL Lane 2A Item 1 "Dynamic" Deflections Under 50-kip Static Wheel Load.

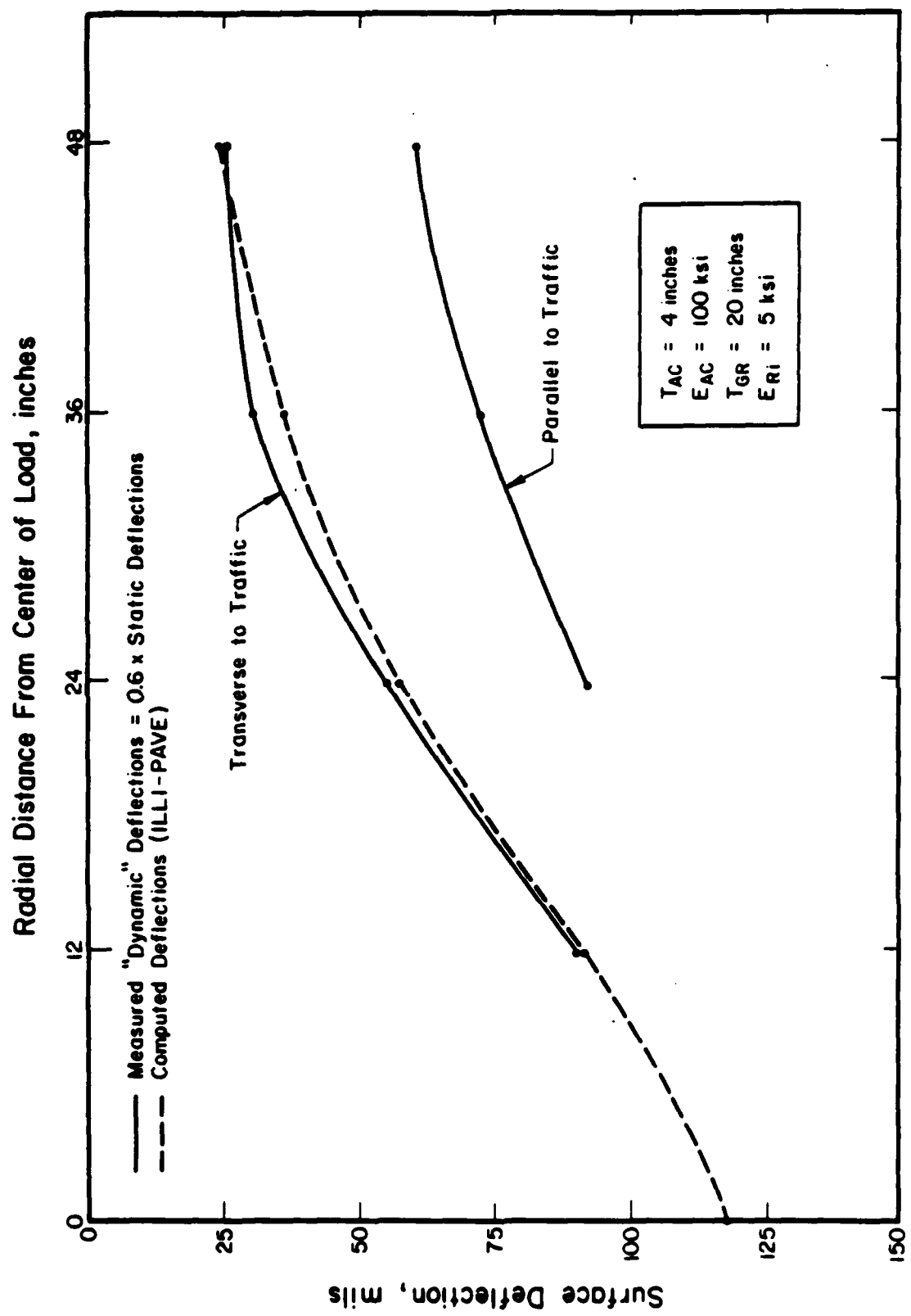


Figure 35. NWHGL Lane 2 Item 2 "Dynamic" Deflections Under 50-kip Static Wheel Load.

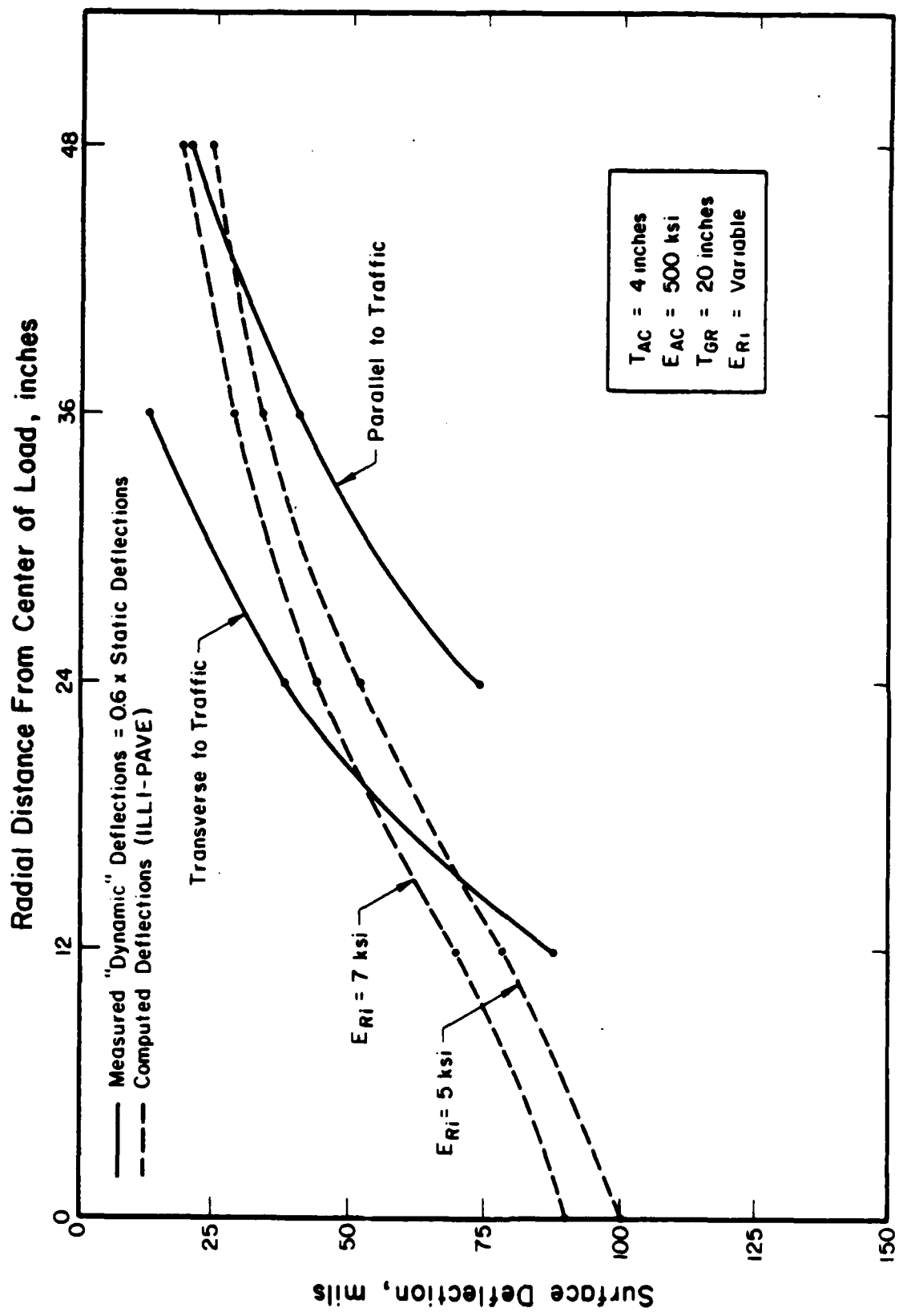


Figure 36. MWIGL Lane 2A Item 2 "Dynamic" Deflections Under 50-kip Static Wheel Load.

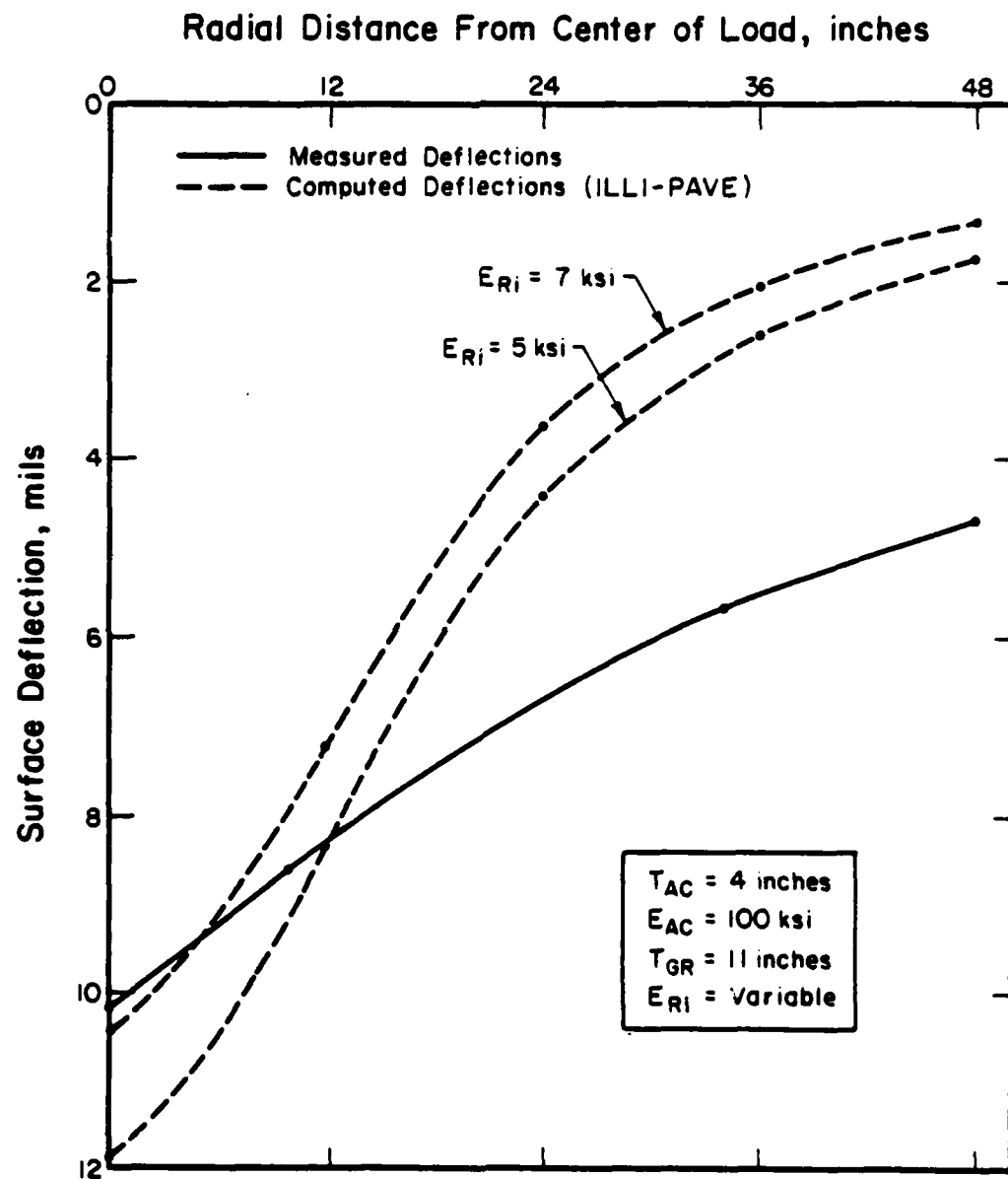


Figure 37. MWHGL Item 1 Deflections Under 3988-lb Peak-to-Peak Vibratory Load.

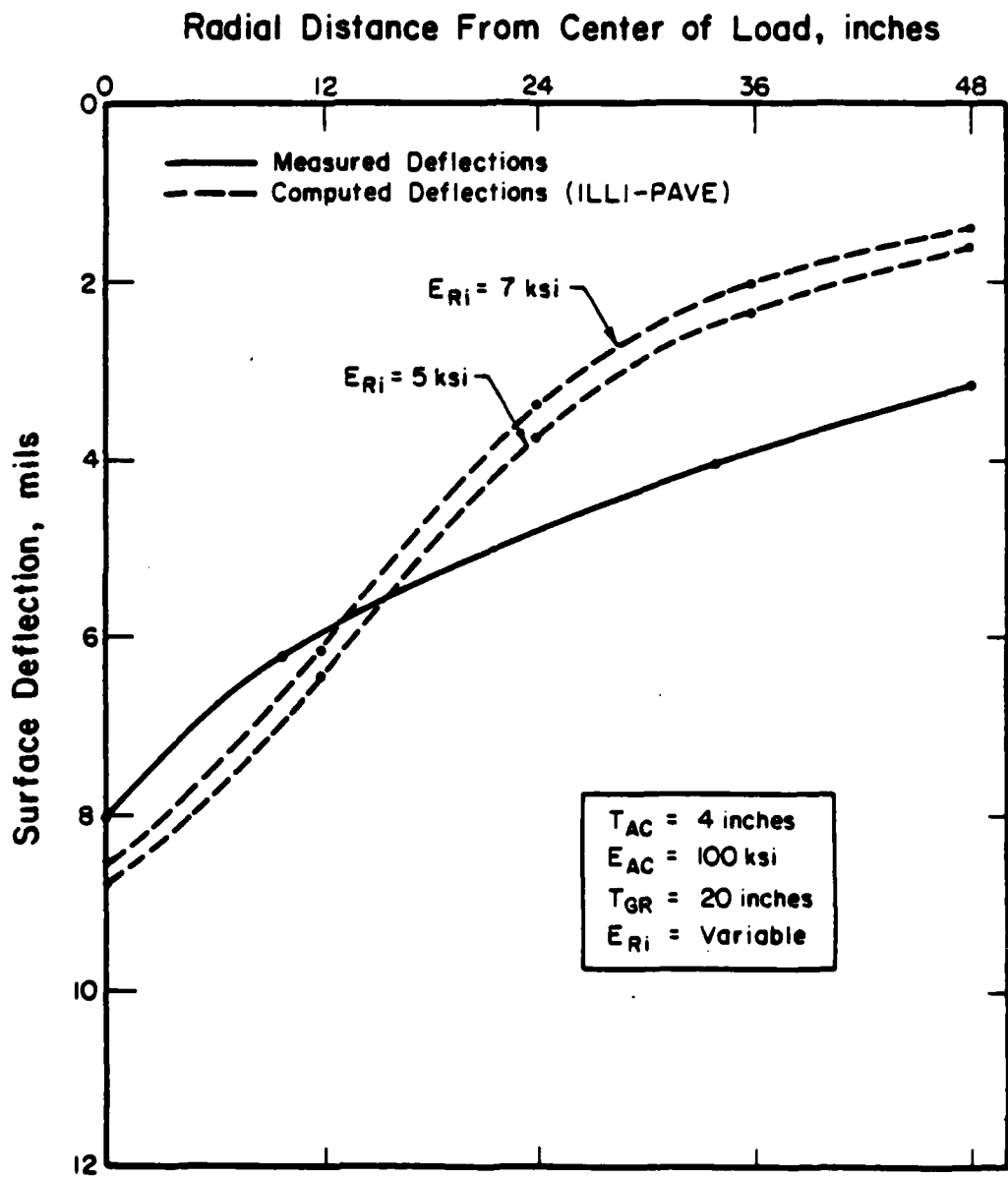


Figure 38. MWHGL Item 2 Deflections Under 3805-lb Peak-to-Peak Vibratory Load.

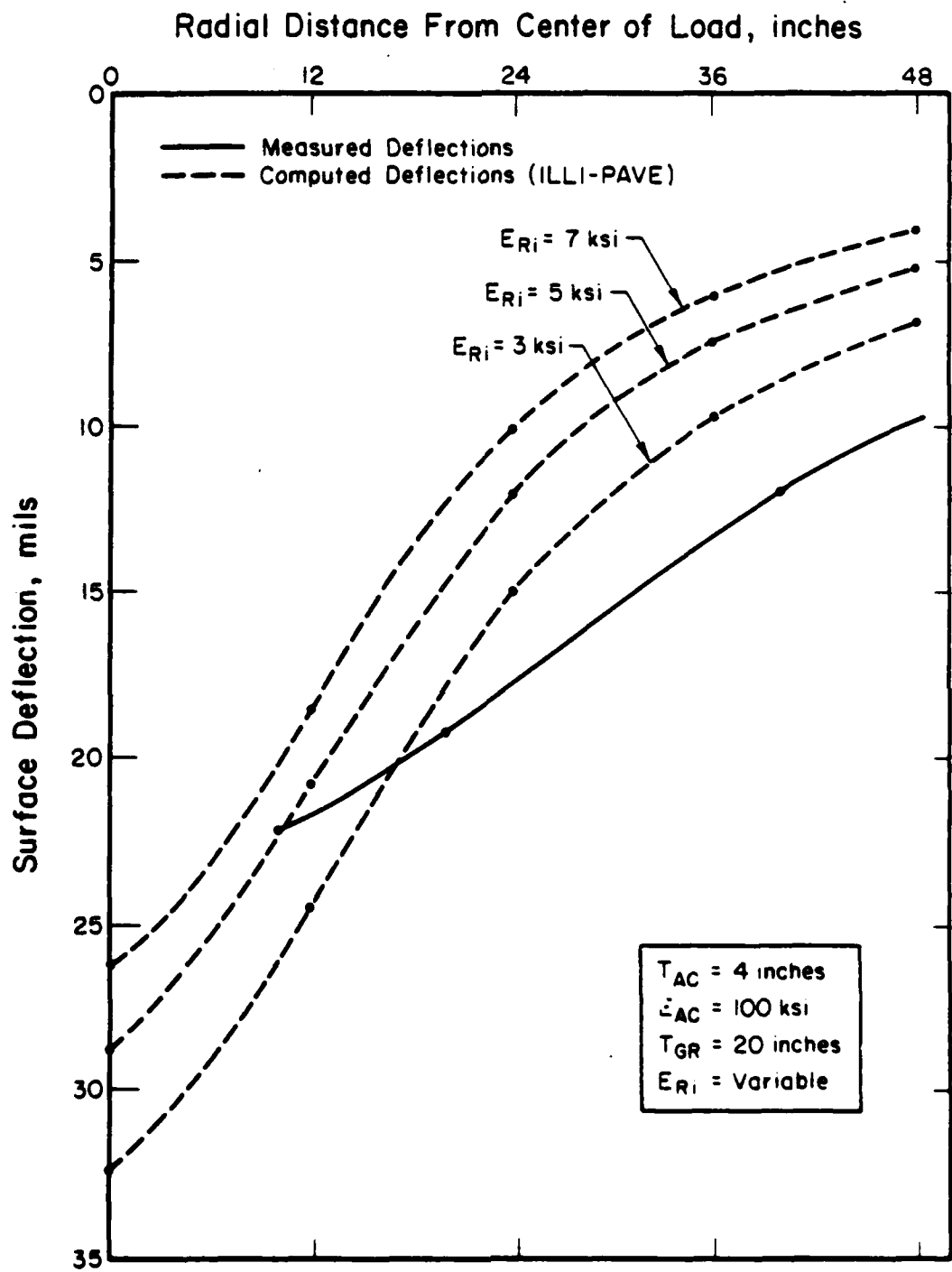


Figure 39. MWHGL Item 2 Deflections Under 11.4-kip Peak-to-Peak Vibratory Load.

was assigned since the MWHGL subgrade was used. The measured "dynamic" deflection basins under the 75-kip static load do not match well with ILLI-PAVE calculated deflections. This is believed to be caused by large plastic deformations produced by the high magnitude of loading. The tests reported in Reference 73 were conducted with AC temperatures 90-115°F. Therefore an AC modulus of 100 ksi was assigned. The tests reported in Reference 74 were conducted with AC temperatures 60-90°F; an AC modulus of 400 ksi was assigned.

Falling Weight Deflectometer (FWD) data is included in Reference 75. The following values of E_{Ri} were backcalculated:

Item 1 - $E_{Ri} = 5.0$ ksi (Figure 40),

Item 2 - $E_{Ri} = 2.4$ ksi (Figure 41), and

Item 3 - $E_{Ri} = 1.7$ ksi (Figure 42).

Since these E_{Ri} values were very low for the 6 CBR measured, an E_{Ri} of 9 ksi was assigned. It was assumed there was an instrumentation error since the 9000-lb FWD deflections were close to reported static deflections under an F-4 load cart. Since trafficking occurred in summer, an AC modulus of 100 ksi was assigned.

C. TEST SECTION PERFORMANCE DATA

The observed performance and results of failure investigation, if available, are reported for each test section analyzed. Test points referred to in this section correspond to the test points contained in Table 6. All data were extracted from the corresponding reference in Table 6.

Test Point 1 - Trafficking produced high deflections at 77 coverages and rutting at 91 coverages. By 200 coverages, the pavement was showing longitudinally under each pass of the wheel. Pavement was considered to be

AD-A181 596

DEVELOPMENT OF MECHANISTIC FLEXIBLE PAVEMENT DESIGN
CONCEPTS FOR THE HEAV. (U) ILLINOIS UNIV AT URBANA
NEWMARK CIVIL ENGINEERING LAB H F KELLY SEP 86

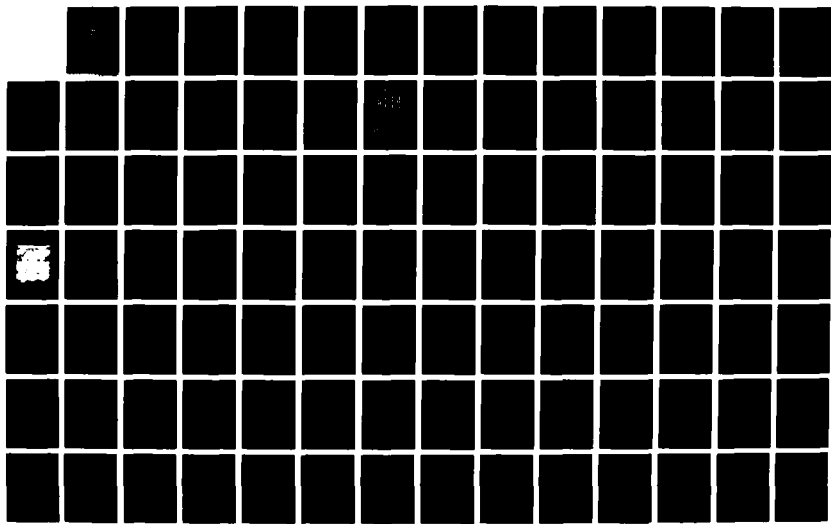
2/3

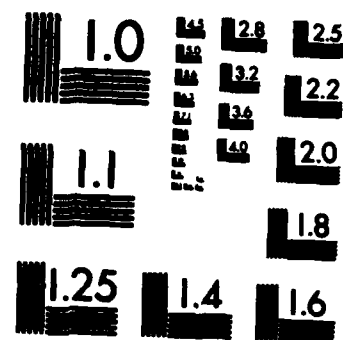
UNCLASSIFIED

AFESC/ESL-TR-86-32 F08637-85-M-6023

F/G 1/5

NL





MICROCOPY RESOLUTION TEST CHART
NATIONAL BUREAU OF STANDARDS-1963-A

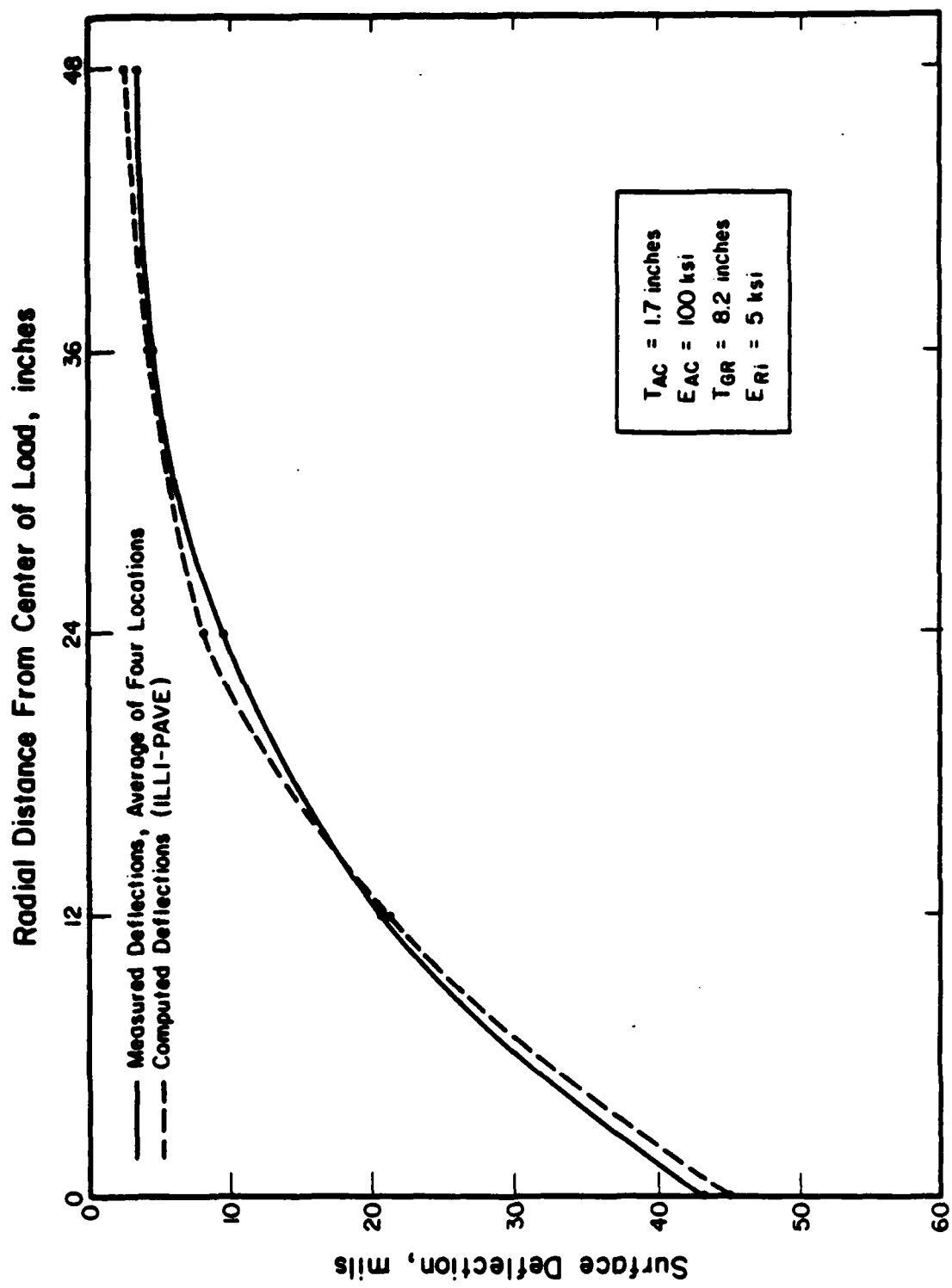


Figure 40. Reference 74 Item 1 Deflections Under 9000-lb FWD Load.

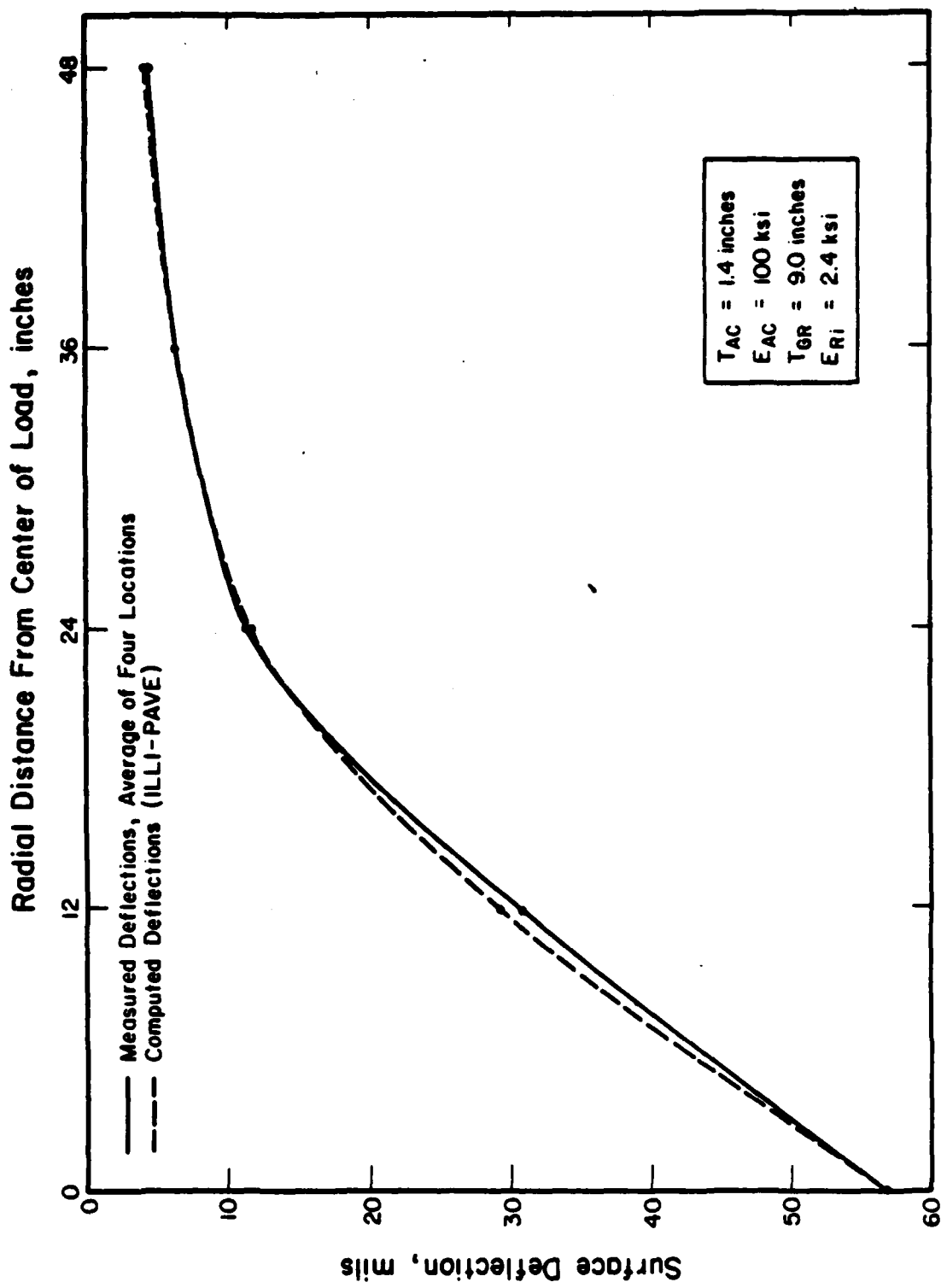


Figure 41. Reference 74 Item 2 Deflections Under 9000-lb FWD Load.

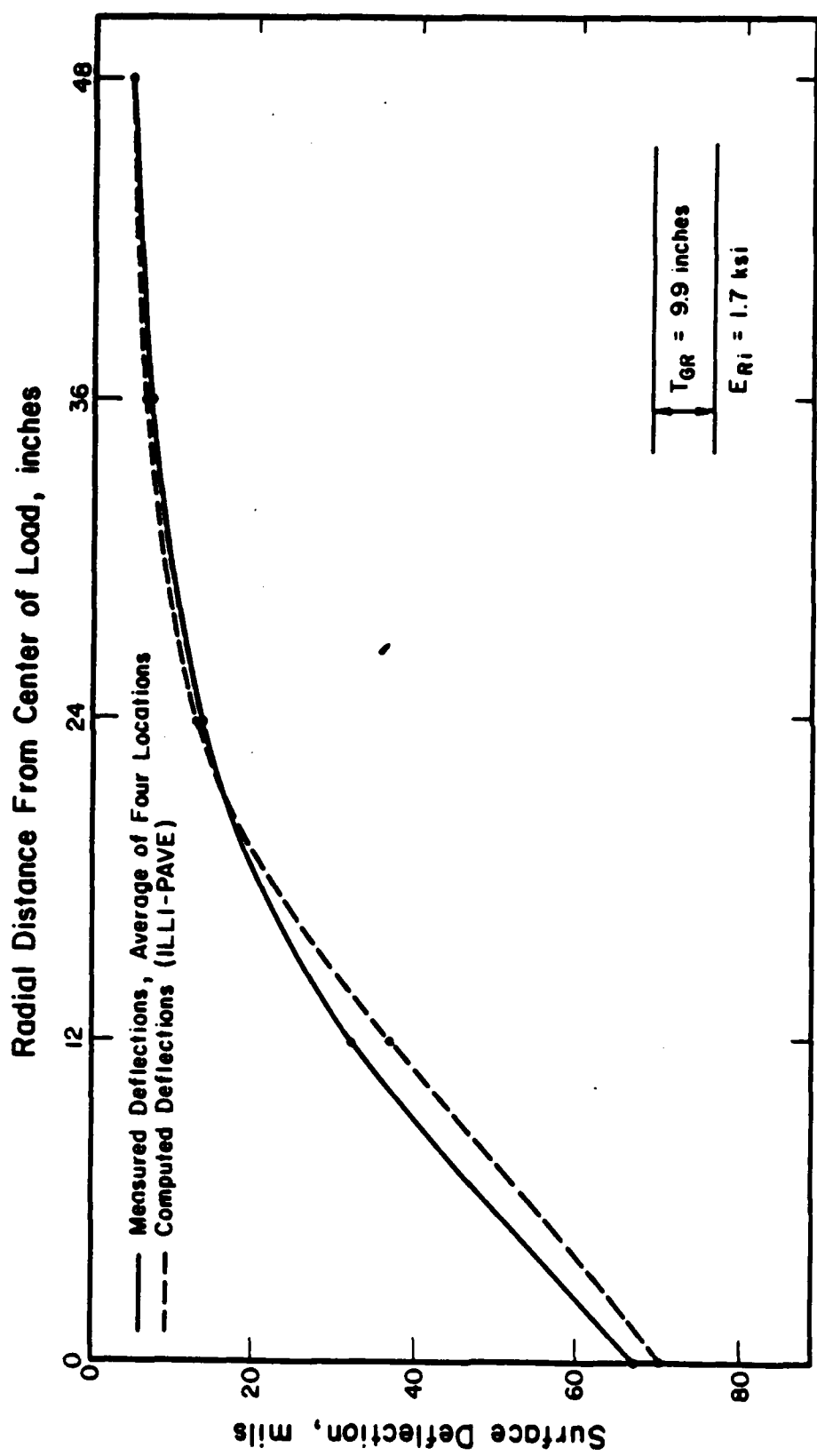


Figure 42. Reference 74 Item 3 Deflections Under 9000-lb FWD Load.

after 220 coverages.

Test Points 2-5 - Behavior under traffic was characterized by high deflections and longitudinal cracking at the edge of the traffic lane. There was a definite depression in the traffic lane throughout. By 100 coverages, test points 2, 3, and 4 showed a definite depression in the traffic lane, and by 150 coverages, cracking had started in test points 3, 4, and 5. By 216 coverages, all 4 test points showed faint to pronounced cracking. The cracking and settlement were more or less uniform throughout the traffic lane.

Test point 6 - Hairline longitudinal cracking was noted at 1349 coverages. Well-defined rutting (1/4- to 1/2-inch) was noted at 1400 coverages. The pavement was not considered failed.

Test Point 7 - Hairline longitudinal cracking was noted at 1174 coverages. Pronounced rutting (1/2-inch or greater) was noted at 1276 coverages.

Test Point 8 - Pronounced longitudinal cracking was noted at 1400 coverages and pronounced rutting (1/2-inch or greater) was noted at 1264 coverages.

Test Point 9 - Subgrade shear cracks became visible on the surface of the test section at 40 coverages. Inability to continue application of traffic due to rutting occurred at 160 coverages.

Test Point 10 - First indication of subgrade shear cracks occurred at 400 coverages. Test section was trafficked for 1700 coverages without complete failure occurring.

Test Point 11 - Test section was trafficked with 1700 coverages without any distress.

Test Point 12 - Hairline longitudinal cracks in the asphaltic concrete

were first noticed after 10 coverages of traffic. At 38 coverages, hairline alligator cracking was noted in the entire width of the lane between Stations 3+04 and 3+30. By 44 coverages, there was alligator cracking throughout the item and a longitudinal crack running parallel to the direction of traffic for the entire length of the item. This long crack would open slightly and then close as the test cart traversed the lane. The hairline cracks in the center 2 feet of the lane had expanded to a width of about 1/8 inch after 95 coverages. By 120 coverages, some of the cracks extended through the full thickness of asphalt concrete, and the item was considered failed.

A trench was excavated after completion of traffic and revealed that shear deformation occurred in the subgrade material. Permanent deformation also occurred in the asphalt concrete, base, and subbase material, and was caused by shear failure in the subgrade and by some consolidation in the upper layers. The maximum permanent deformation was 1.4 inches and upheaval was 0.1 inches.

Test Point 13 - Test section was not considered failed after 450 coverages of traffic. Maximum permanent deformation was 0.8 inches and upheaval was 0.1 inches.

Test Point 14 - As the test vehicle made the first pass, small cracks appeared on the pavement surface along side the test wheel. These cracks became wider as the test vehicle traversed the traffic lane. After 6 coverages, the item was rated as failed. There was alligator cracking in the center 5 feet throughout the traffic lane. Some cracks in the center of the lane were 3/8-inch wide and base material could be seen. Maximum permanent deformation was 1.2 inches with upheaval of 0.6 inches.

Test Point 15 - After 34 coverages, hairline cracks were observed at the center line and along both edges of the traffic lane. Slight upheaval of the

outside edges and permanent deformation of about 1 inch at the center line of the lane were also noticed at this time. As traffic continued, the center portion and the area 1 foot from the edges of the lane began to deteriorate rapidly. After 132 coverages, there were 1/6-inch-wide cracks located in the center and edges of the lane. After 200 coverages, the wider cracks extended through the AC layer and the item was considered failed. The item was considered failed due to severe alligator cracking between Stations 2+40 and 2+60.

Failure investigation showed an upheaval of about 1.2 inches located outside the traffic lane and deformation of the base and subbase course. No distinct deformation of the subgrade material was evidence. Permanent deformation above the subgrade was due primarily to lateral movement of the subbase material, which resulted in surface upheaval. Maximum permanent deformation was 2.4 inches and upheaval of 0.6 inches.

Test Point 16 - After six coverages, this item was rated as failed. Traffic was stopped due to 1/4- and 1/2-inch-wide longitudinal cracks between Stations 3+25 and 3+35. There was severe alligator cracking throughout the item. Maximum permanent deformation was 1.5 inches with 1.2 inches of upheaval.

Test Point 17 - Very little damage was noticed on the pavement surface until about 124 coverages. At this time, 1/4-inch-wide longitudinal cracks near the center of the lane and 1/32-inch-wide cracks approximately 2 feet from one edge of the traffic lane were detected. The item was considered failed after 200 coverages. The pavement had severe alligator cracking throughout the entire center portion of the lane at this time. Most longitudinal cracks were 3/8-inch-wide. Maximum permanent deformation was 1.5 inches with 0.4 inches of upheaval.

Test Point 18 - The asphalt concrete started cracking on the first pass of the wheel load. Grooving behind the load wheel indicated that a major part of total deflection was permanent. The item was considered failed after 8 coverages. Failure investigation showed that permanent deformation extended through the pavement structure and into the subgrade. The total pavement thickness above the subgrade decreased within the traffic lane and increased outside the traffic lane. These changes were caused by plastic flow of the asphalt concrete. Maximum permanent deformation was 2.2 inches with no upheaval.

Test Point 19 - The item withstood only 12 coverages of the load wheel. Failure was due to excessive permanent deformation and cracking of the asphalt concrete. Failure investigation revealed considerable settlement inside the traffic lane and upheaval adjacent to the traffic lane. This settlement and upheaval appeared to be due primarily to lateral shifting of the unbound gravelly-sand subbase material. Maximum permanent deformation was 1.6 inches with 0.5 inches of upheaval.

Test Point 20 - Hairline longitudinal pavement cracks and noticeable ruts were observed at the end of 2 coverages. The rutting of the pavement and cracking of the asphalt concrete increased rapidly with load repetitions, and was considered failed after 18 coverages. Maximum permanent deformation was 1.6 inches with 0.6 inches of upheaval.

Test Point 21 - This item was still in good condition at the end of 18 coverages. As traffic continued, the deflections and permanent deformations increased and resulted in cracking of the AC. The item was considered failed at the end of 70 coverages. Maximum permanent deformation was 2.0 inches with 0.5 inches of upheaval.

Test pits were not excavated for Test Points 20 and 21. However, these

were Test Items 4 and 5 of the MWHGL test, which were investigated after trafficking with a 240-kip twin-tandem assembly. The findings showed that deformation in the base and subbase courses and slight deformation of the subgrade occurred. Slight upheaval of the various layers was noted at the outside edges of the traffic lane.

Test Point 22 - After 10 coverages, small hairline longitudinal cracks were observed in the center of the traffic lane. The test item was considered failed after 50 coverages. At failure, there were 1/4- to 3/8-inch wide cracks extending through the AC layer with 2.88 inches of permanent deformation and a 0.48-inch upheaval.

Test Point 23 - Under distributed traffic, failure occurred at 44 coverages with the observance of a 3 3/4-inch rut. Channelized traffic caused failure after 54 passes when a 3 3/16-inch rut was measured. One inch of permanent deformation occurred at 20 coverages during both channelized and distributed traffic.

Test Point 24 - Distributed traffic caused failure after 20 coverages with a 3-inch rut depth (14 coverages for 1-inch rut depth). Failure under channelized traffic occurred at 41 passes with a 3-inch rut depth (24 passes for 1-inch rut depth).

Test Point 25 - Failure under distributed traffic occurred at 6 coverages with a 3-inch rut depth (2 coverages for 1-inch rut depth). Channelized traffic failed the item after 29 passes with a 3 5/16-inch rut depth (9 passes for a 1-inch rut depth).

D. PAVEMENT RESPONSES - PERFORMANCE CORRELATIONS

Regression analyses were conducted to predict coverages to failure as a function of calculated pavement responses. A summary of the results using

all failed sections is contained in Table 7. This table shows very little correlation of coverages with AC strain. This is not surprising since none of the failures were judged to be caused by fatigue of the AC. The best straight line regression equation was developed using maximum surface deflection (D0). Multiple variable regression equations developed as a function of both subgrade modulus at breakpoint (E_{Ri}) and calculated subgrade response (strain, deviator stress, or stress ratio) show better precision.

Further regression analysis was accomplished using only those test points identified as subgrade failures. The failure mode for each test section is contained in Table 6. Fifteen of the failures were attributed to subgrade failure. The result of this analysis is presented in Table 8. Plots of subgrade stress ratio and strain versus coverages are presented in Figures 43 and 44, respectively. The precision of these equations are acceptable except for coverages as a function of subgrade stress ratio only. As discussed in Section IV.B.3, subgrade permanent deformation increases rapidly when the stress ratio exceeds 0.5-0.6. Therefore, the relationship is not a linear one. It may be possible, however, to approximate a straight-line relationship at stress ratios below the threshold of 0.5-0.6.

Only two types of subgrade were used in the test sections analyzed. Test Points 1 thru 8 were constructed on a lean clay subgrade. All other test sections were built on a heavy clay "buckshot" subgrade. The results may not be applicable to other types of subgrade soils.

Note that the data only covers the low end of the scale for coverages (less than 1000). Extrapolations beyond the ranges included in the analysis could be misleading.

TABLE 7. SUMMARY OF TRANSFER FUNCTIONS DEVELOPED
FROM ALL FAILED TEST SECTIONS.

A	B ₁	X ₁	B ₂	X ₂	R ²	SEE	Number of Cases
2.567	-9.8x10 ⁻⁴	ϵ_{AC}	--	--	0.126	0.735	19
3.578	-5.1x10 ⁻⁴	ϵ_z	--	--	0.572	0.539	22
1.899	-2.4x10 ⁻³	σ_D	--	--	0.000	0.823	22
3.973	-2.825	SR	--	--	0.385	0.646	22
6.976	-2.643	log D0	--	--	0.587	0.529	22
1.851	-9.7x10 ⁻⁴	ϵ_{AC}	0.3309	log E_{AC}	0.137	0.751	19
2.115	5.0x10 ⁻⁴	log ϵ_{AC}	-0.1396	T _{AC}	0.173	0.736	19
2.162	-4.6x10 ⁻⁴	ϵ_z	0.1509	E_{Ri}	0.830	0.348	22
0.855	-0.109	σ_D	0.3624	E_{Ri}	0.773	0.402	22
2.521	-2.986	SR	0.1911	E_{Ri}	0.806	0.371	22
6.955	-2.625	log D0	-0.0040	T _{AC}	0.587	0.542	19

Equations of Form: log coverages = A + B₁X₁ + B₂X₂

ϵ_{AC} = Asphalt concrete tensile strain, in microstrain

ϵ_z = Subgrade compressive strain, in microstrain

D0 = Surface deflection, in mils

SR = Subgrade stress ratio

σ_D = Subgrade deviator stress, in psi

T_{AC} = Asphalt concrete thickness, in inches

E_{AC} = Asphalt concrete modulus, in ksi

E_{Ri} = Subgrade modulus at breakpoint, in ksi

R² = Coefficient of determination

SEE = Standard error of estimate

TABLE 8. SUMMARY OF TRANSFER FUNCTIONS DEVELOPED FROM SUBGRADE FAILURES.

A	B ₁	X ₁	B ₂	X ₂	R ²	SEE	Number of Cases
26.58	-6.930	log ϵ_z	--	--	0.645	0.452	15
4.774	-3.681	SR	--	--	0.272	0.647	15
8.009	-3.215	log D0	--	--	0.404	0.585	15
22.99	-6.196	ϵ_z	0.1118	E_{Ri}	0.808	0.346	15
5.414	-11.10	log σ_D	11.85	log E_{Ri}	0.800	0.353	15
2.963	-5.426	SR	3.6521	log E_{Ri}	0.807	0.346	15

Equations of Form: $\log \text{coverages} = A + B_1 X_1 + B_2 X_2$

ϵ_z = Subgrade compressive strain, in microstrain

D0 = Surface deflection, in mils

SR = Subgrade stress ratio

σ_D = Subgrade deviator stress, in psi

E_{Ri} = Subgrade modulus at breakpoint, in ksi

R² = Coefficient of determination

SEE = Standard error of estimate

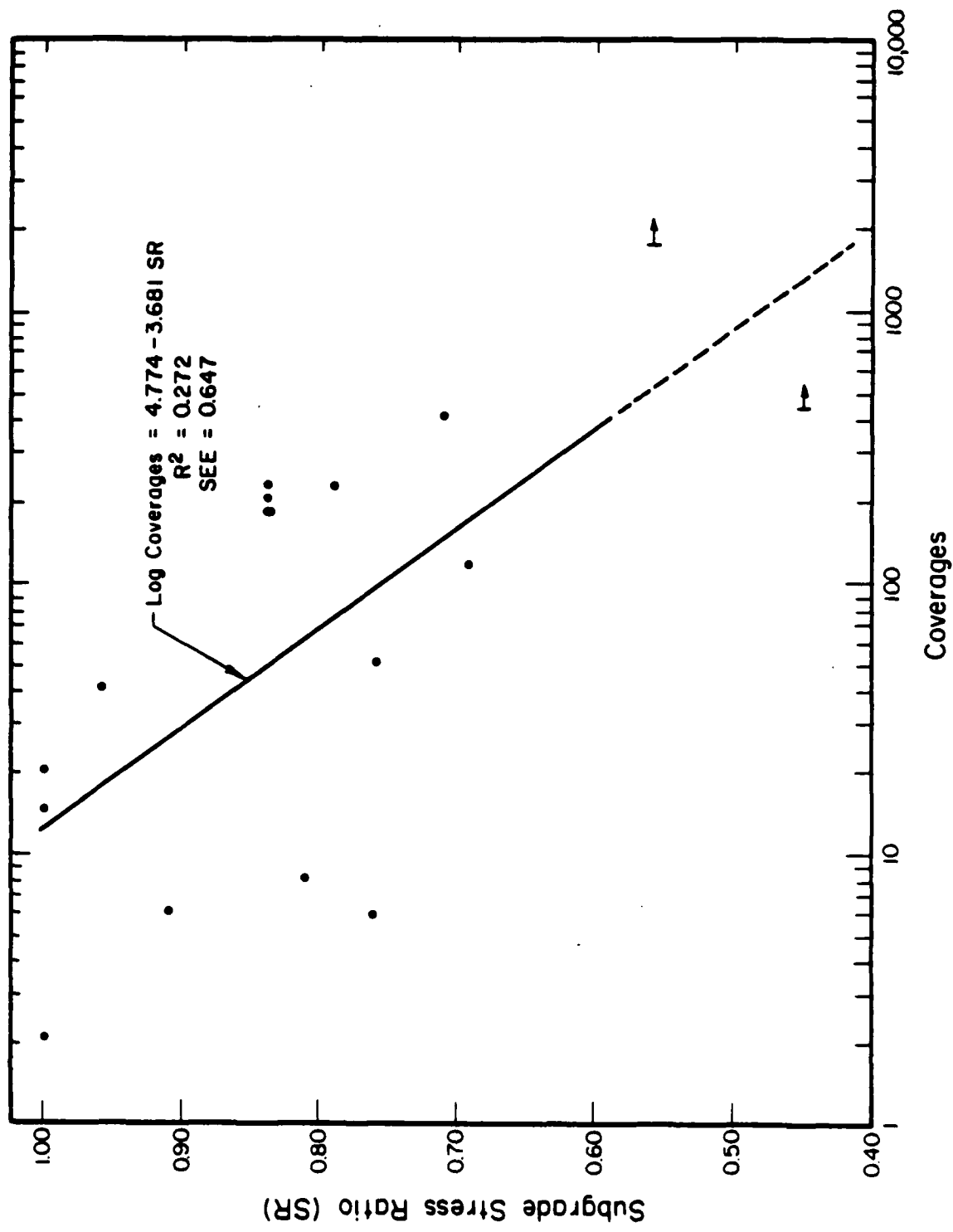


Figure 43. Subgrade Stress Ratio Versus Coverages, Subgrade Failures Only.

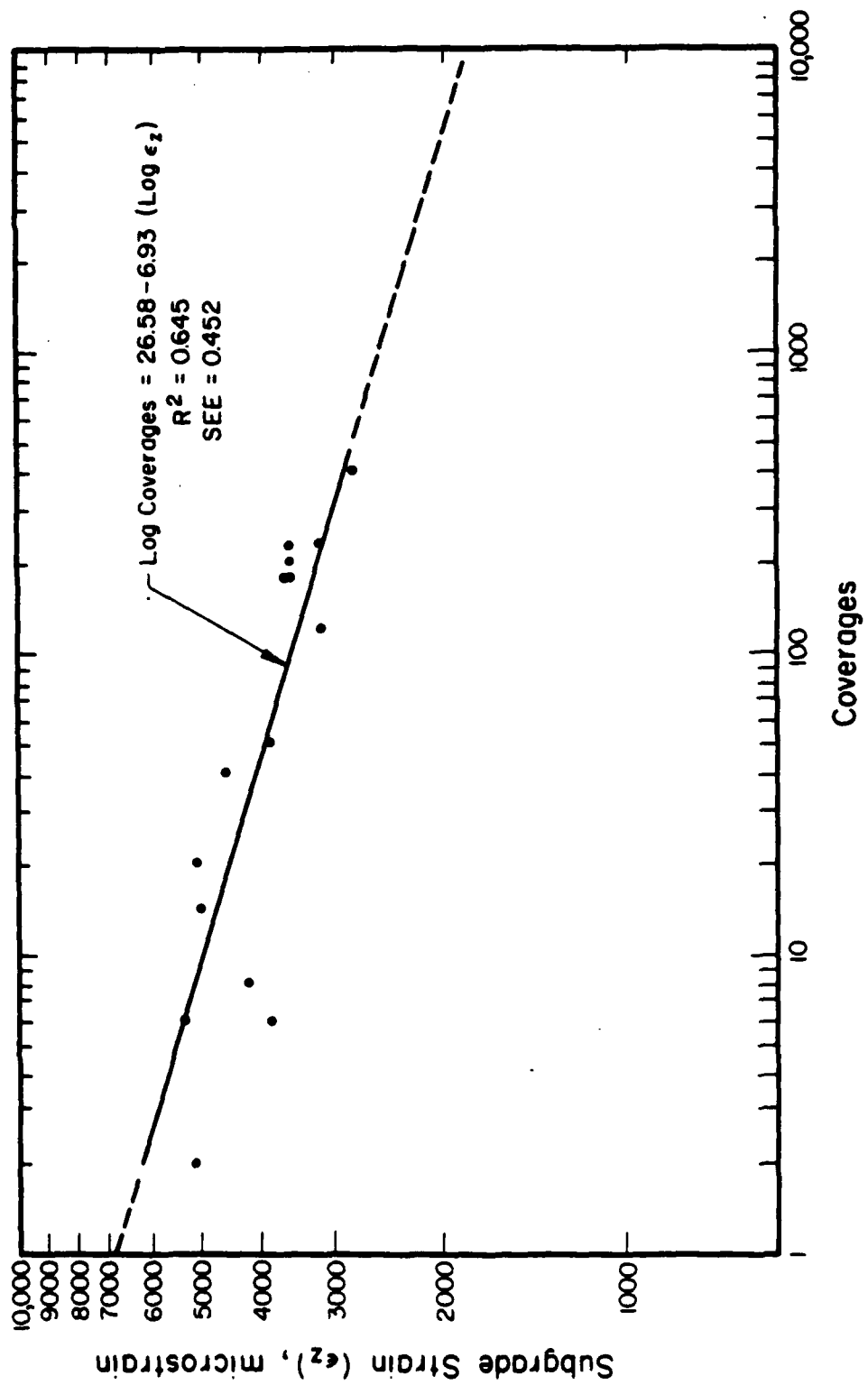


Figure 44. Subgrade Strain Versus Coverages, Subgrade Failures Only.

E. DISCUSSION OF RESULTS

The pavement sections analyzed were constructed and tested over a period of approximately 40 years dating back to 1944. Backcalculation of pavement properties under these circumstances can only be considered an estimate. However, the results are good, especially considering:

- (1) Lack of AC temperature data (see Section V.B),
- (2) Normal test variability,
- (3) Inherent variability of soil and pavement materials,
- (4) Errors associated with estimating dynamic properties based upon heavy static loading,
- (5) Inadequate compaction of low-quality subbase, in some cases, because of poor subgrade stability, and
- (6) Inconsistent failure criteria.

The regression equations that relate pavement response to pavement performance (i.e., transfer functions), presented in Section V.D, show the general relationships expected.

1. MWHGL Test Variability

The Multiple Wheel Heavy Gear Load (MWHGL) test was the largest and probably most tightly controlled of any involving airfield pavement design and loading. Yet, high variability is characteristic, particularly for AC thickness and subgrade CBR. Because of the variability, it is difficult to make statistical conclusions. Student T-tests and F-tests were conducted on the MWHGL test data statistics. Conclusions that can be made based on $\alpha = 95\%$ are as follows:

- (1) There is a statistically significant difference in before and after traffic CBR for the CH (heavy clay) subgrade.

(2) There is a statistically significant difference in before and after traffic CBR, water content, and dry density for the CL (lean clay) subgrade.

(3) There is a statistically significant difference between the Items' CBR and degree of saturation after traffic for combined CH and CL subgrade. (There was not enough data to evaluate just the CL subgrade.)

(4) There is a statistically significant difference between the average AC thickness and the target value of 3 inches. The 95 % confidence interval is 3.7-4.1 inches.

For one-tailed hypotheses (e.g., CBR is greater after traffic, not just different) and $\alpha = 95\%$, the following additional conclusions may be made:

(1) Item 3 CH subgrade CBR increased and degree of saturation decreased during traffic.

(2) The subbase dry density increased during traffic.

(3) Item 5 CH subgrade degree of saturation increased in the traffic lane.

(4) CL subgrade degree of saturation decreased in the traffic lane.

Variability of material properties is expected. Yoder and Witczak (Reference 13) report typical standard deviations for 2.5 to 7.5-inch AC layer thicknesses are 0.3-0.8 inches and for unbound granular layer thicknesses is 0.75-1.5 inches. Average strength (e.g., CBR) coefficient of variation (CV) is about 30 % with typical range 15-40 %. For the typical highway sections, average rebound deflection CV is about 25 % with typical range of 10-35 %.

2. Deflection Basins

Based upon the discussions in the preceding section, variability in pavement properties (thicknesses and moduli) are inherent and must be

anticipated. Backcalculating modulus values based upon one deflection basin reading can be misleading. Pavement properties can only be estimated at that one particular location, which might happen to be the strongest or weakest place in the pavement. Taking deflection basin readings at several locations with multiple independent readings at each location is necessary to confidently estimate the pavement properties. Note the statistic presented in Section V.E.1, typical CV for rebound deflections is 25 %.

Backcalculating dynamic modulus values cannot accurately be done using deflections under loads where considerable permanent deflections are imposed. For this analysis, "dynamic deflection" was estimated to be 0.6 of the static deflection. This is a common value for highway loading on well-designed pavement sections. A well-designed pavement section suffers very little permanent deformation per load. However, the test sections analyzed were designed to fail prematurely, at less than 5000 coverages. Considerable permanent deformation occurred under both static and dynamic wheel loading.

3. Subbase Stability

The subbase used for Test Points 12 through 17 and 19 through 21 was a low-quality material consisting of gravelly sand (Unified classification SP). The average in-place CBR on the top of the layer was 14. This material had a low shear strength when well compacted. Since the subgrade CBR values were low, it is likely that inadequate compaction was obtained in the subbase, further reducing its shear strength. This would explain why there appeared to be an increase in subbase dry density during traffic (MWHGL Test) and why many of the test sections failed due to lateral movement of the subbase and not due to subgrade permanent deformation or AC fatigue.

A minimum CBR of 6-8 is required to provide the ability to place and compact overlying material layers (Reference 76). If the subgrade soil at the granular material-subgrade interface has a very low shear strength, it may not be possible to develop the full potential of the frictional stress needed to resist the radial displacement of the granular layer and decompaction may result. The Air Force recognized stability problems during recent construction of the SALTY DEMO airfield pavements. The subgrade in this case had to be stabilized with lime to achieve adequate stability to provide a working platform for construction (Reference 77).

4. Failure Criteria

There appeared to be inconsistent failure criteria for the different tests. Some sections were considered failed with a 1/2-inch rut while another was not considered failed until a 2.88-inch rut had been achieved and the pavement was severely cracked. The pavement would have been considered hazardous to aircraft long before such a large rut occurred.

The Air Force uses the Pavement Condition Index (PCI) to gage the structural integrity and surface operational conditions. The PCI is based upon the types of distress, severity of distress, and amount or density of distress. Rutting is one type of distress used for input. When a rut exceeds 1 inch in depth, it is considered of high severity. Major rehabilitation is needed when the PCI rating falls below 70. If the PCI falls below 55, repair costs rise dramatically. The Air Force generally schedules maintenance work before ruts become 1 inch deep, yet the CBR equation was originally developed assuming a 1-inch rut was failure. Transfer functions in which failure is defined as dropping to a specific PCI level, would be useful.

SECTION VI

COMPONENTS OF A MECHANISTIC DESIGN PROCEDURE FOR CONVENTIONAL FLEXIBLE AIRFIELD PAVEMENTS

A mechanistic or analytic design procedure includes the following steps (see Figure 45):

- (1) Characterize AC material, granular material and subgrade soil. Evaluation of materials can be accomplished by laboratory simulation or estimated based upon tests done on similar materials. However, the key is projecting what the field conditions will be (temperature, moisture, density, loading conditions, strength/stiffness, etc.) for the materials selected.
- (2) Use a suitable structural model for calculating the critical responses (stresses, strains, deflections) in the pavement structure.
- (3) Consider the performance characteristics of the materials and their likely mode(s) of failure by using calculated structural responses in appropriate transfer functions.
- (4) Repeat Steps 1 through 3 as necessary to provide the desired level of service for some predicted traffic.

In this section, all of the components of a mechanistic design procedure for pavements are discussed.

A. TRAFFIC ANALYSIS

For design of airfield pavements, engineers must determine the number of load repetitions of each load configuration that will be applied to the pavement. In this study, only the heavyweight F-15 aircraft loading is considered. For design purposes, the maximum wheel load is generally used, but only takeoff operations are considered. Landings are made at a reduced

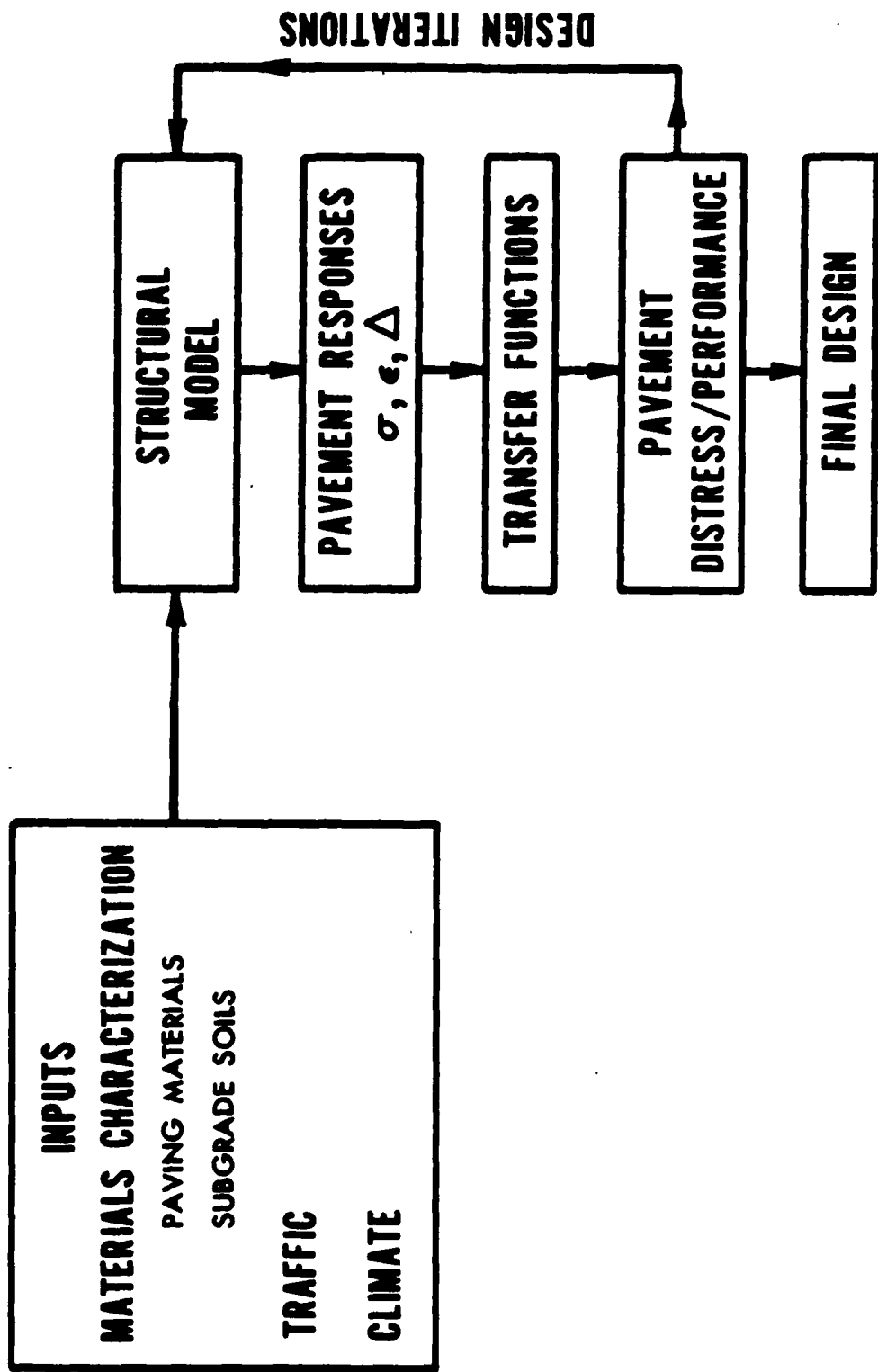


Figure 45. Mechanistic Design Method.

weight due to expenditure of fuel and are disregarded. For example, the maximum takeoff weight for the F-15 A/B (Reference 1) is 54 kips (wheel load of 22.1 kips) but maximum landing weight is 39 kips (wheel load of 16.0 kips), a 38 percent decrease.

The number of operations is converted to number of coverages. For flexible pavements, a coverage is a measure of the number of maximum stress applications that occur on the surface of the pavement due to the applied traffic. A coverage occurs when all points on the pavement surface within the traffic lane have been subjected to one application of maximum stress, assuming that stress is equal under the tireprint (Reference 32). Traffic on airfields is distributed over a wide area. The work reported by Brown and Thompson (Reference 33) is incorporated in the present DOD method and was discussed in Section II.E.

To account for the wander effect and also for the reduced wheel load caused by wing lift of a rapidly moving aircraft, the DOD design method (Reference 2) divides airfields into traffic areas. These areas attempt to categorize common areas of anticipated distress and are divided as follows:

(1) Type A traffic areas are subjected to the greatest concentration of maximum loaded aircraft. Normally these are primary taxiways and the first 500-foot ends of runways.

(2) Type B traffic areas are subjected to the normal distribution of maximum loaded aircraft. These areas normally include the second 500-foot ends of runways, aprons, parking, or aircraft maintenance pavements. These areas are designed for fewer coverages of the maximum loaded aircraft.

(3) Type C Traffic areas are those having a reduced loading of the aircraft or where the speed of the aircraft results in less than maximum stresses in the pavement. Pavement areas include runway interior and

secondary taxiways. These pavements are designed for the same number of coverages as Type B Traffic areas, but for 75 percent of maximum aircraft gross load.

(4) Type D traffic areas are those in which the traffic volume is extremely low and/or the weight of operating aircraft is considerably less than maximum gross load. These areas are the outside edges of the runway (outside the center 75-foot width).

The traffic distribution curve (Figure 46) can be broken up into separate traffic lanes, each the width of the aircraft wheel (8.08 inches for the heavyweight F-15, see Section II.E). Figure 47 shows that 10.7 percent of the total traffic will traverse the center traffic lane. A standard deviation of 30 inches was assumed. Yoder and Witczak (Reference 13) report common standard deviations of traffic distribution for taxiways is between 2 and 3.5 feet, and for runways is from about 7.5 to 15 feet on takeoff and from 13 to 20 feet on landing.

This approach assumes that the critical damage point is near the centerline of the center traffic lane and that damage is caused only by traffic applied to the center traffic lane. ILLI-PAVE runs show that this is a reasonable assumption for AC tensile strain (see Figure 48). However, for subgrade deviator stress/stress ratio, this assumption is not as good. Figure 49 shows that subgrade deviator stress only drops four percent from the maximum value at the center of the loaded area to a lateral distance of one tire width away. Therefore, for considering subgrade rutting, it might be necessary to use the cumulative traffic percentage for the center three traffic lanes (i.e., $10.3 + 10.7 + 10.3 = 31.3\%$).

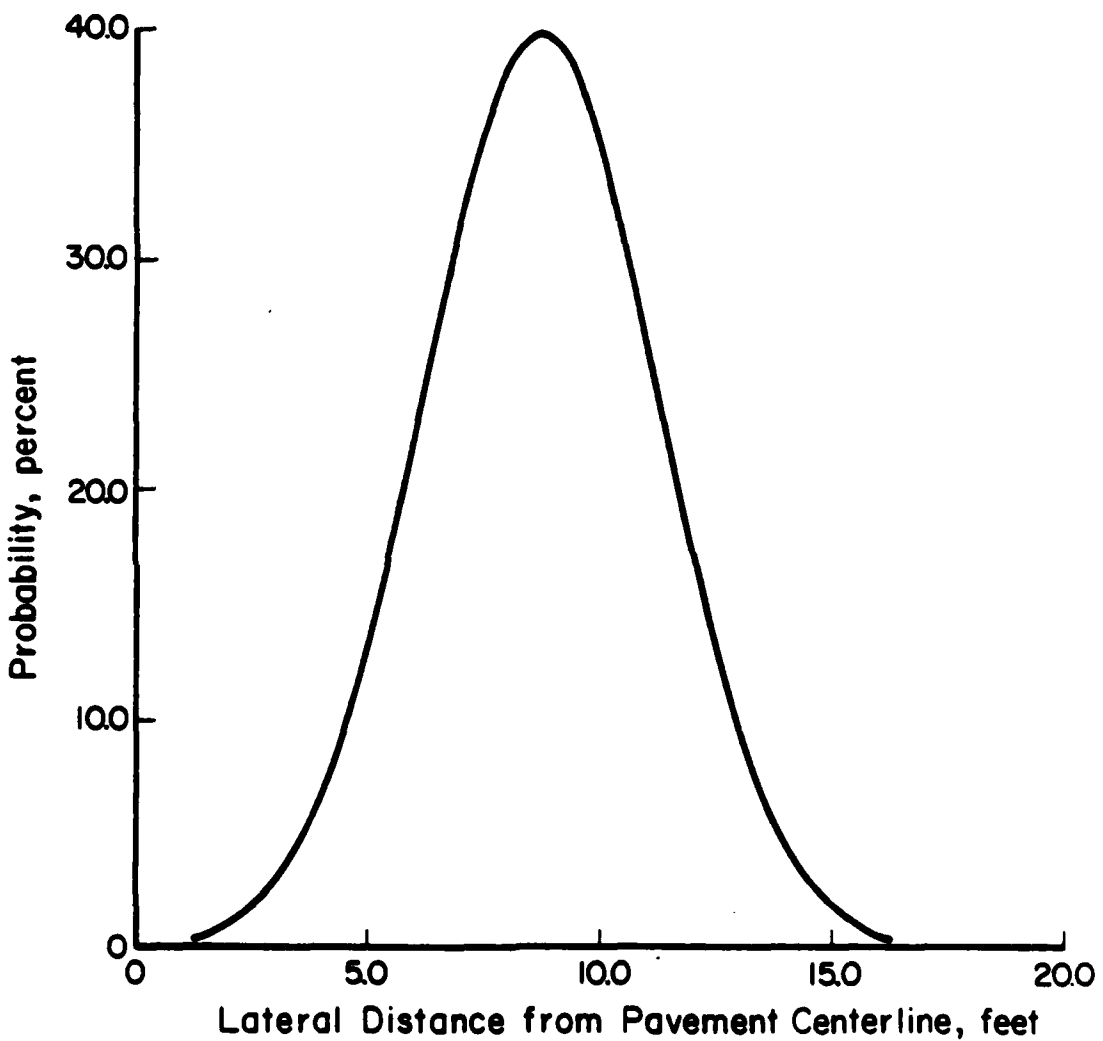


Figure 46. Typical Traffic Distribution Curve for Taxiway, $\sigma=30$ Inches.

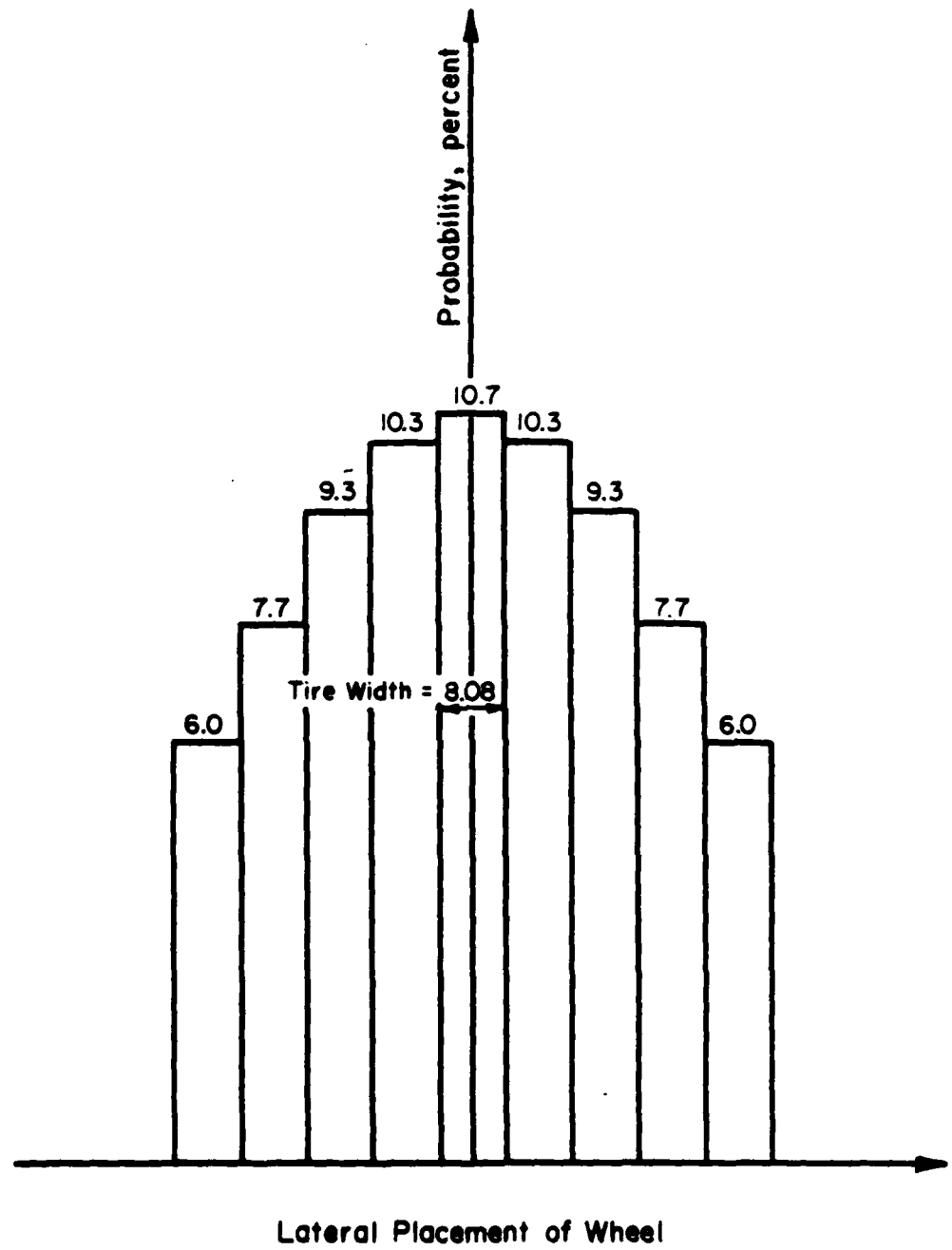


Figure 47. Traffic Distribution Using Discrete Lanes, $\sigma=30$ Inches.

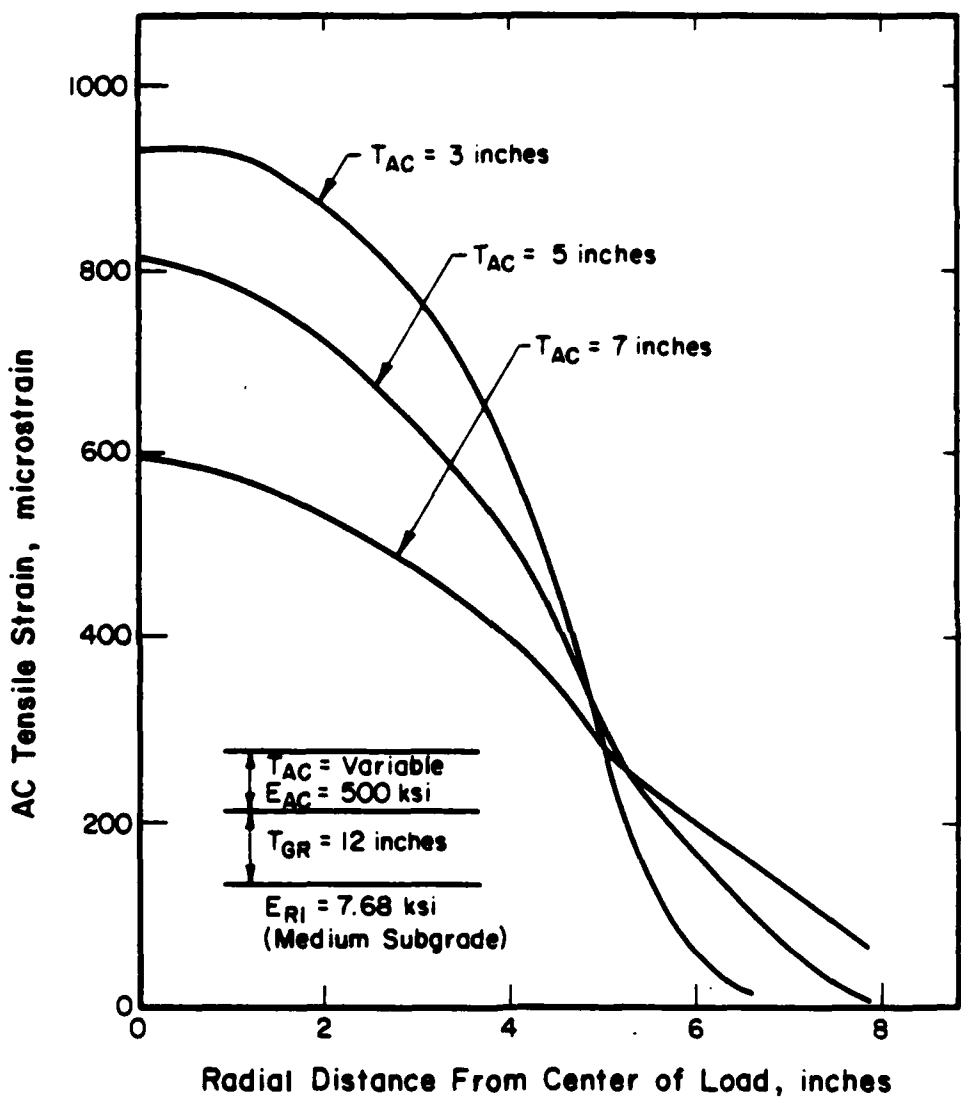


Figure 48. AC Tensile Strain Versus Offset Distance.

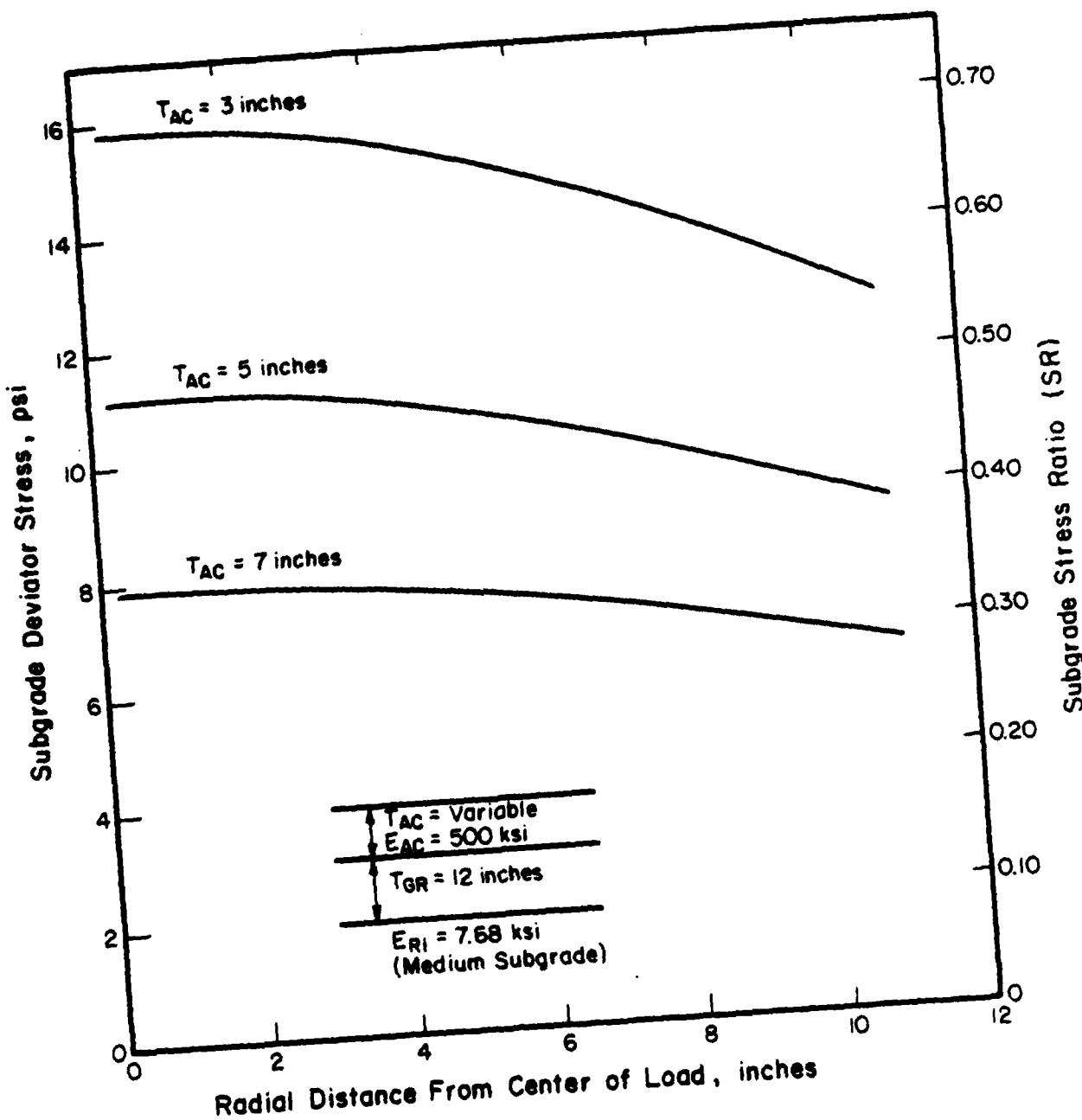


Figure 49. Subgrade Deviator Stress and Stress Ratio Versus Offset Distance.

B. CLIMATIC AND SEASONAL CONSIDERATIONS

Pavement system response and performance are influenced by local climatic conditions which vary with the seasons. The effect of various climatic factors must be considered and included in the mechanistic design procedure.

Factors that must be considered for conventional flexible pavements are:

- (1) Seasonal temperature variations,
- (2) Frost penetration depth and duration,
- (3) Freeze-thaw cycles,
- (4) Precipitation frequency, amount and seasonal distribution, and
- (5) Areal and system drainage characteristics.

Asphalt concrete modulus is primarily a function of the pavement temperature (see Section III.B.1). A relationship between AC modulus and temperature was shown in Figure 16. Temperature variations throughout the year and the resulting change of AC modulus should be considered in a mechanistic design procedure.

A high-quality granular material contains little water and, therefore, is little affected by freeze and thaw. Subgrade soils are greatly affected by moisture. E_Ri is strongly correlated with degree of saturation. The regression equations shown in Figure 50 indicate that E_Ri can be estimated based on degree of saturation. Thompson and Robnett (Reference 38) found that soils containing higher clay contents and increased plasticity tend to be less sensitive to changes in degree of saturation.

The modulus of frozen soils increases sharply (as high as 50-100 ksi). Generally it can be considered that no load related damage is done to pavements when the subgrade is frozen. However, environmental damage caused by frost heave must be considered. Generally, in a conventional flexible pavement, a large thickness of clean granular material is used to reduce or

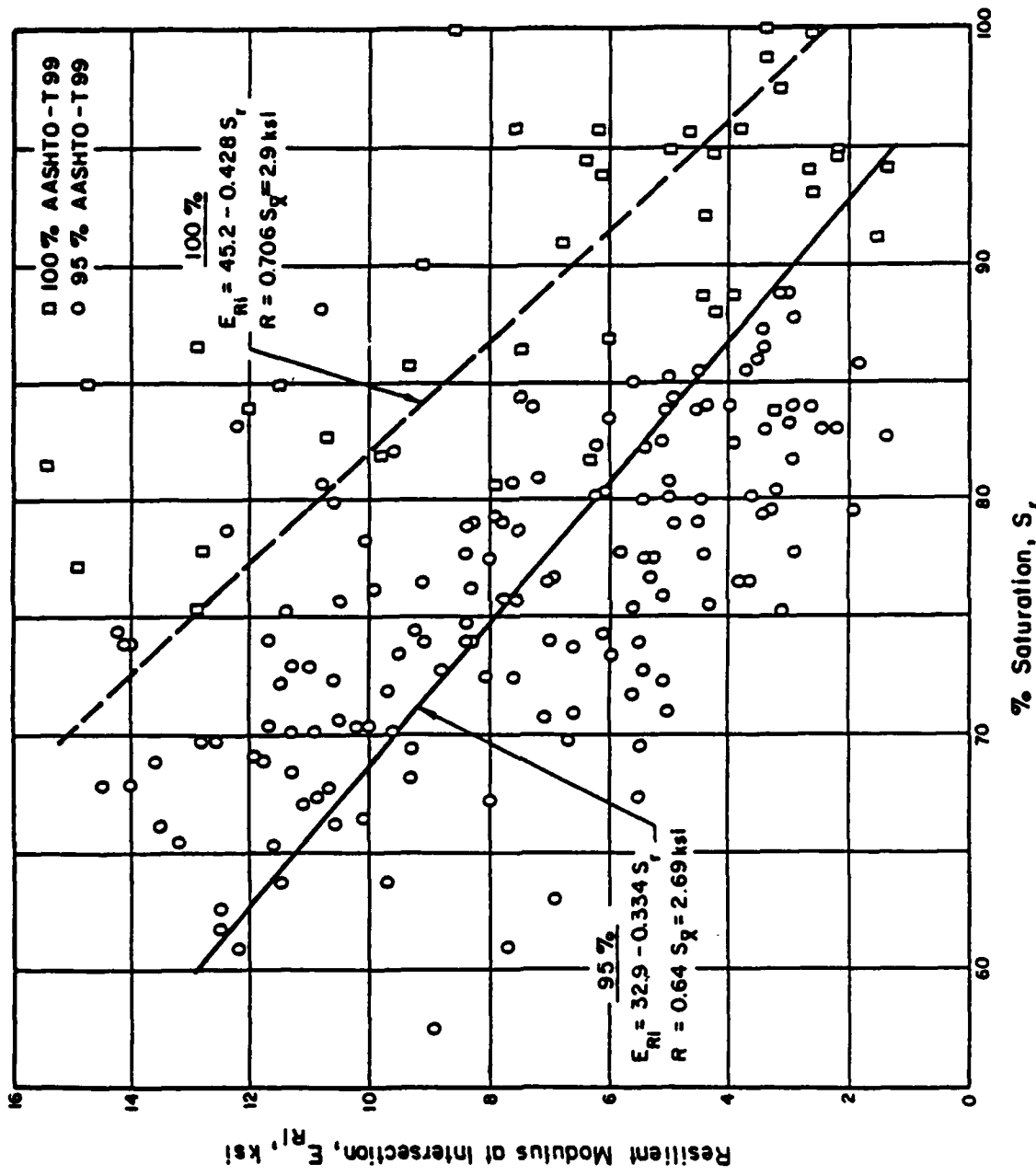


Figure 50. Resilient Modulus - % Saturation Relations for Fine-Grained Soils (Reference 38).

even prevent frost penetration into frost susceptible subgrade. An alternate method of design is to allow the subgrade to freeze and then design for the resulting low subgrade strength during thaw. The DOD uses both of these methods (Reference 78).

Studies have shown (Reference 79 through 84) that substantial increases in resilient deformation (reduced resilient moduli) were caused by the imposition of a small number of freeze-thaw cycles, even though no gross moisture changes were allowed (closed system freeze-thaw). Typical data illustrating the freeze-thaw effect are shown in Figure 51. It is significant to note that one freeze-thaw cycle is sufficient to drastically reduce the resilient modulus of the soil.

The most common approach for incorporating seasonal effects into a design procedure is to establish some single design condition that represents the overall annual effect (e.g., a single AC modulus and a single subgrade modulus). This approach is used in highway design procedures developed by the Asphalt Institute (Reference 53) and Shell (Reference 69). Gomez-Achecar and Thompson (Reference 8) demonstrated that a single design condition (AC modulus and subgrade E_{Ri}) can be used effectively for full-depth AC pavement design. However, Elliott and Thompson (Reference 7) found that no single set of design conditions could approximate the same cumulative load damage as determined from summing weekly load damage factors for all conventional flexible pavements (thicknesses and moduli). The study did determine that seasonal values of AC modulus and E_{Ri} could represent all the conventional flexible pavement designs.

C. STRUCTURAL MODEL AND PAVEMENT RESPONSES

In Section III, an appropriate structural model was selected for

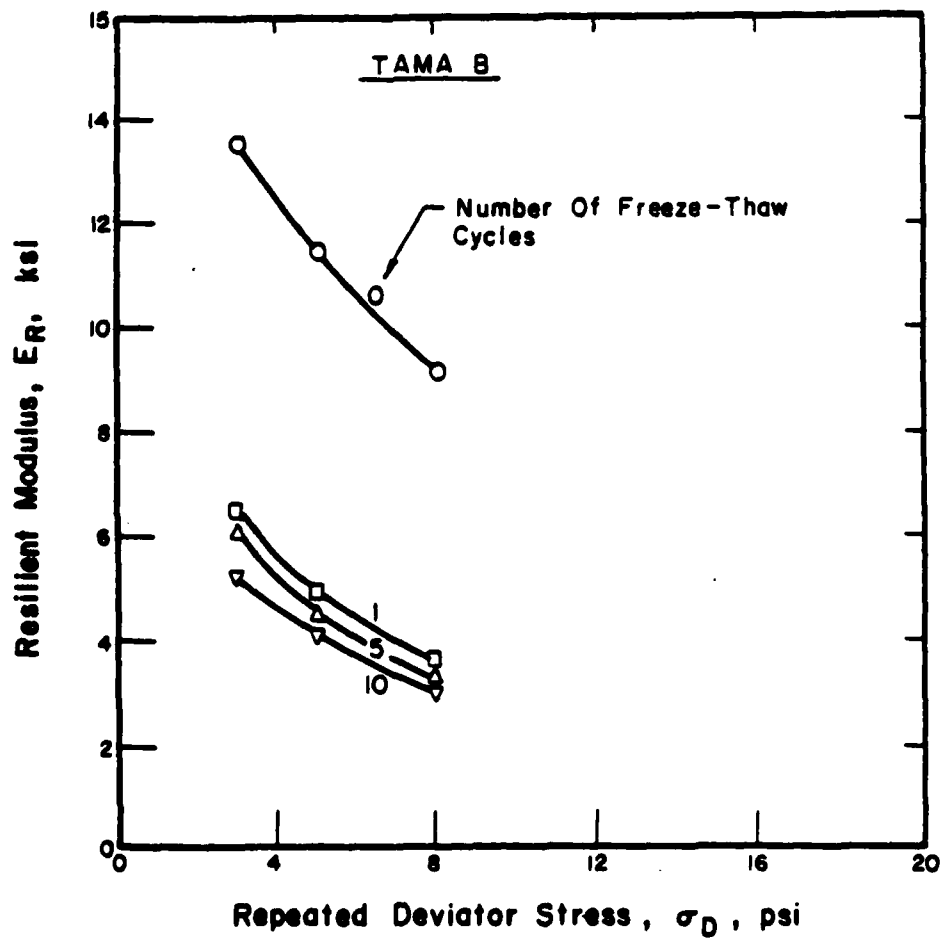


Figure 51. Influence of Cyclic Freeze-Thaw on the Resilient Behavior of a Fine-Grained Soil (Reference 84).

estimating the pavement responses (deflections, stresses, and strain) that control pavement performance. The material characterization models, the ILLI-PAVE structural model, and the ILLI-PAVE algorithms provide reliable estimates of the flexible pavement structural responses to a specified load application. In this study, the heavyweight F-15 aircraft (30-kip/355-psi loading) and the heavier-weight F-15 (36-kip/395-psi loading) are investigated. The discussions of transfer functions (Section IV) and analyses of single-wheel aircraft loading on test sections (Section V) show that pavement performance is related to:

- (1) Tensile strain in the bottom of the AC layer, and
- (2) Subgrade deviator stress ratio.

On the basis of these findings, structural response design algorithms (Table B-1) for AC strain and subgrade stress ratio (or subgrade deviator stress/compressive strength) are recommended for use in the design procedure.

Design algorithms similar to those developed in this study for F-15 aircraft loading and for highway loading (Reference 7) of conventional flexible pavement can be developed for other type of loadings and pavement configurations (e.g., full-depth asphalt, Reference 8).

D. MATERIALS CHARACTERIZATION

Material characterization models for AC, granular bases, and subgrade soils were discussed in detail in Section III. The recommended material characterization models were used in developing the ILLI-PAVE algorithms. The material characteristics required to complete a design analysis using the algorithms are:

- (1) Thickness of asphalt concrete,
- (2) Thickness of granular base,

(3) Asphalt concrete modulus, and

(4) Subgrade E_{Ri} .

AC modulus and subgrade E_{Ri} are not unique values, but are a range of values that change with time and are a function of climatic conditions. For practical design purposes, these variations can be incorporated into the design procedure. A practical approach to selection of AC modulus is use of a single AC modulus-temperature relationship (such as Figure 16). For more precision, an AC modulus-temperature relationship can be developed for each climatic zone based on the "typical" mix used in the area. For even further refinement, the AC modulus can be predicted from the mix properties using, for example, the Asphalt Institute equation (Reference 53). Subgrade E_{Ri} is dependent upon many factors, such as soil type, applied deviator stress, density, moisture, plasticity, carbon content, etc. A complete series of soil surveys and testing may not be successful in predicting what the E_{Ri} would be several years after construction.

The DOD method of material characterization was discussed in Section II. AC modulus is not considered in the design procedure. The same minimum AC thickness is used for all climatic areas. All other layers in a flexible pavement are characterized by its CBR. The CBR value determined after four days of soaking is used as the subgrade design CBR. However, this value varies greatly with molding density and moisture content (see Figure 2). It is difficult to predict CBR, density, and water content as a function of time (days, months, years).

E. TRANSFER FUNCTIONS

Transfer functions are the link between the pavement response predicted by an appropriate structural model and pavement distress or expected service

life. Flexible pavement design procedures normally consider two types of distress - fatigue cracking and surface rutting.

Fatigue cracking is evaluated in terms of the predicted load induced tensile strain in the bottom of the AC surfacing. Fatigue transfer functions are generally of the form:

$$N_f = K (1/\epsilon_{AC})^a (1/E_{AC})^b \quad (18)$$

or

$$N_f = K (1/\epsilon_{AC})^a \quad (19)$$

where, N_f = the predicted number of load applications until "failure"

ϵ_{AC} = magnitude of load induced tensile strain in the AC

E_{AC} = AC dynamic stiffness modulus, and

K, a, b = constants determined by testing and/or pavement performance analysis.

These equations may be developed originally by laboratory fatigue testing with field calibration (adjusted to field performance) or by direct correlation of predicted strain (and modulus) in the pavement with field performance.

Surface rutting is normally considered in terms of subgrade stress or strain. In reality, surface rutting is the summation of the consolidation and displacement of the materials in all of the pavement layers and subgrade. Most design procedures attempt to control rutting by limiting subgrade compressive strain. Generally rutting within the pavement structure (surfacing, base and subbase) is controlled by proper mix design, material specifications, and construction control. Subgrade compressive strain may not be a good indication of permanent deformation for all subgrades (see Section IV.B.3). A better indication of subgrade permanent deformation includes both stress/strain and modulus/strength. Therefore, a subgrade

deviator stress ratio transfer function is recommended. The relationship between permissible stress ratio and coverages is a nonlinear one. Permanent subgrade deformations increase sharply for stress ratios greater than about 0.6-0.7. Therefore, until validated stress ratio transfer functions are developed, it seems reasonable to limit maximum predicted subgrade stress ratios to 0.5-0.6 for long-term stable performance.

F. PERFORMANCE ANALYSIS

The final step in the design process is the comparison of the predicted allowable load applications with the required number of load applications. Iteration of the design procedure with a new pavement design is required if the pavement is not adequate for the expected traffic. Since there is no one combination of pavement layer thicknesses and moduli that is appropriate for controlling both fatigue and rutting, life-cycle cost analyses should also be performed to determine the optimum pavement cross section. It may be more economic to increase pavement life by increasing surface thickness rather than base thickness. Increasing base or subgrade strength by stabilization/modification may also be a viable option.

G. BASIC STEPS IN THE DESIGN PROCESS

The basic steps in the design process (refer to Figure 45) are listed below:

1. Determine the required number of load applications for each aircraft (in this study, only the heavyweight F-15 is considered).
2. Select appropriate subgrade E_Ri and AC modulus values based on subgrade type and climatic conditions.
3. Calculate the AC tensile strain and subgrade deviator stress ratio

using ILLI-PAVE or ILLI-PAVE design algorithms.

4. Determine the predicted allowable number of load applications (for both AC fatigue and subgrade rutting) for the trial design using Step 3 results with the appropriate transfer functions.

5. Compare the predicted allowable number of load applications to the required number of load applications. If both are satisfactory, the design is acceptable (not necessarily optimal). If not, another trial design is selected and Steps 2 through 5 are repeated.

SECTION VII
COMPARISON OF PROPOSED PROCEDURES
AND DESIGNS WITH CBR METHOD

This section summarizes the use of the proposed mechanistic design procedure by presenting an example problem. A comparison is also made between the proposed procedures and the DOD design method.

A. MECHANISTIC DESIGN EXAMPLE

The following data are assumed for the pavement design example:

Location: Ottawa, Illinois

Traffic: 300,000 Passes of Heavyweight F-15 Aircraft

Subgrade: AASHTO A-6, UNIFIED CL, LL=28, PI=13

Seasonal Values (From Reference 7):

	Asphalt Concrete Modulus	Subgrade E_{Ri}
Spring	1300 ksi	1.4 ksi
Summer	300 ksi	3.1 ksi
Fall	700 ksi	5.4 ksi
Winter	1800 ksi	6.5 ksi

The 300,000 aircraft passes are converted to approximately 32,000 coverages. The procedure presented in Section VI.A with an assumed standard deviation of wander of 30 inches results in a coverage to pass ratio of 0.107. Assuming equal distribution of traffic over the year, approximately 8000 coverages will occur during each season.

Figure 52 is a plot of cumulative asphalt concrete fatigue damage for various granular base and AC thicknesses. Figure 53 is a plot of subgrade

stress ratios. AC tensile strain and subgrade stresss ratios were computed from the corresponding algorithms shown in Table B-1. The number of repetitions until AC fatigue failure was calculated using Equation (14) developed by Elliott and Thompson (Reference 7):

$$\log N = 2.4136 - 3.16 \log \epsilon_{AC} - 1.4 \log E_{AC} \quad (20)$$

where, N = the predicted number of load applications to crack appearance,

ϵ_{AC} = predicted AC tensile strain in inch/inch, and

E_{AC} = dynamic stiffness of the AC in psi.

Figure 52 shows that AC thickness of 6 inches with granular base thickness of 14 inches is just satisfactory for AC fatigue. An alternate design for the same cumulative damage is 5 inches of AC with 42 inches of granular base. In Figure 53, plots of subgrade stress ratio for "average" summer day ($E_{AC}=300$ ksi) and for "hot" summer day ($E_{AC}=100$ ksi) conditions are presented. Limiting the subgrade stress ratio to 0.5 during a "hot" summer day requires 6 inches of AC with 24 inches of granular base. The calculations for this pavement section are presented in Table 9.

B. COMPARISON OF MECHANISTIC DESIGN WITH CBR DESIGN

The first step in using the DOD design method is determining the four-day soaked CBR of the subgrade. For the as constructed soil conditions (dry density of 116 pcf and moisture content of 14.3 %), the soaked CBR of the AASHO test subgrade soil is approximately 2 (see Figure 54). From Figure 55, the total required pavement thickness for the CBR design is 45 inches. Minimum AC thickness is 4 inches. However, frost design must be considered according to the frost design procedures contained in Reference 78.

Mean Freezing Degree Days = 500

Design Freezing Degree Days (Average of 3 Coldest Winters in 30) = 900

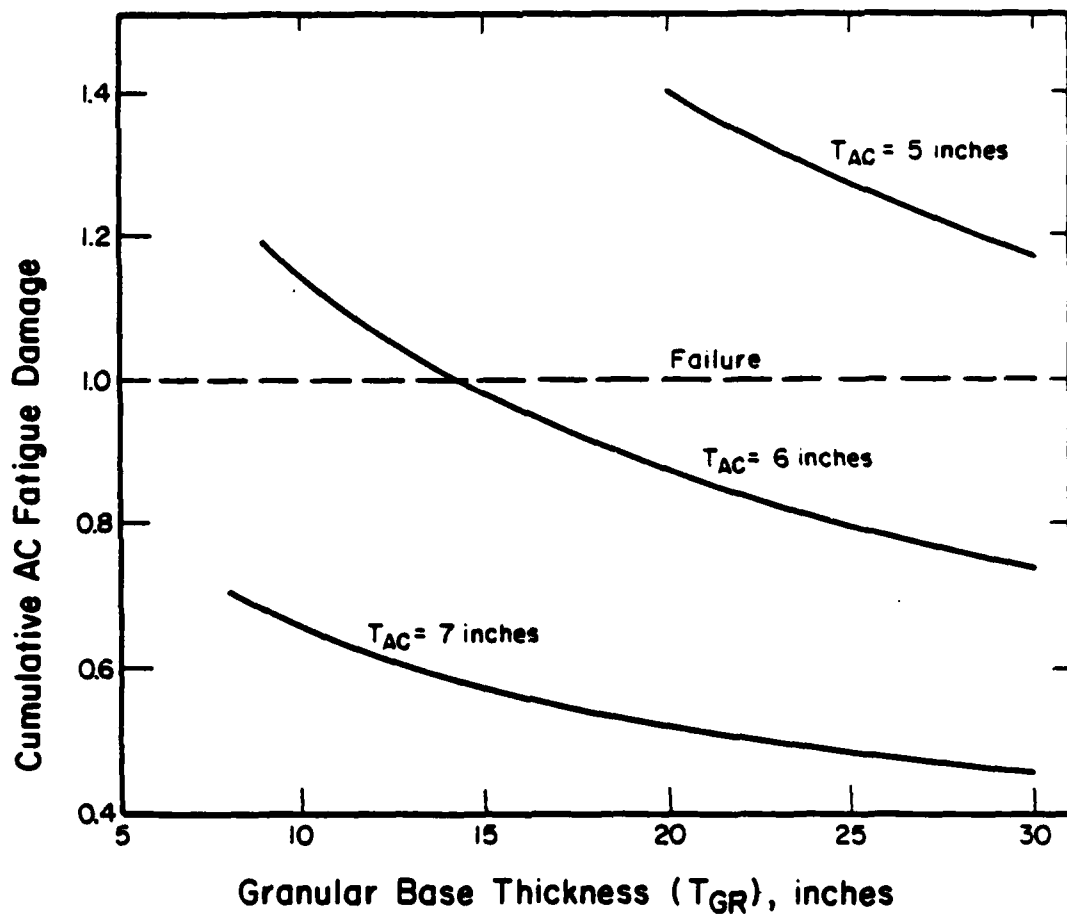


Figure 52. Cumulative AC Fatigue Damage Versus Granular Base Thickness for 32,000 Coverages of Heavyweight F-15 Aircraft.

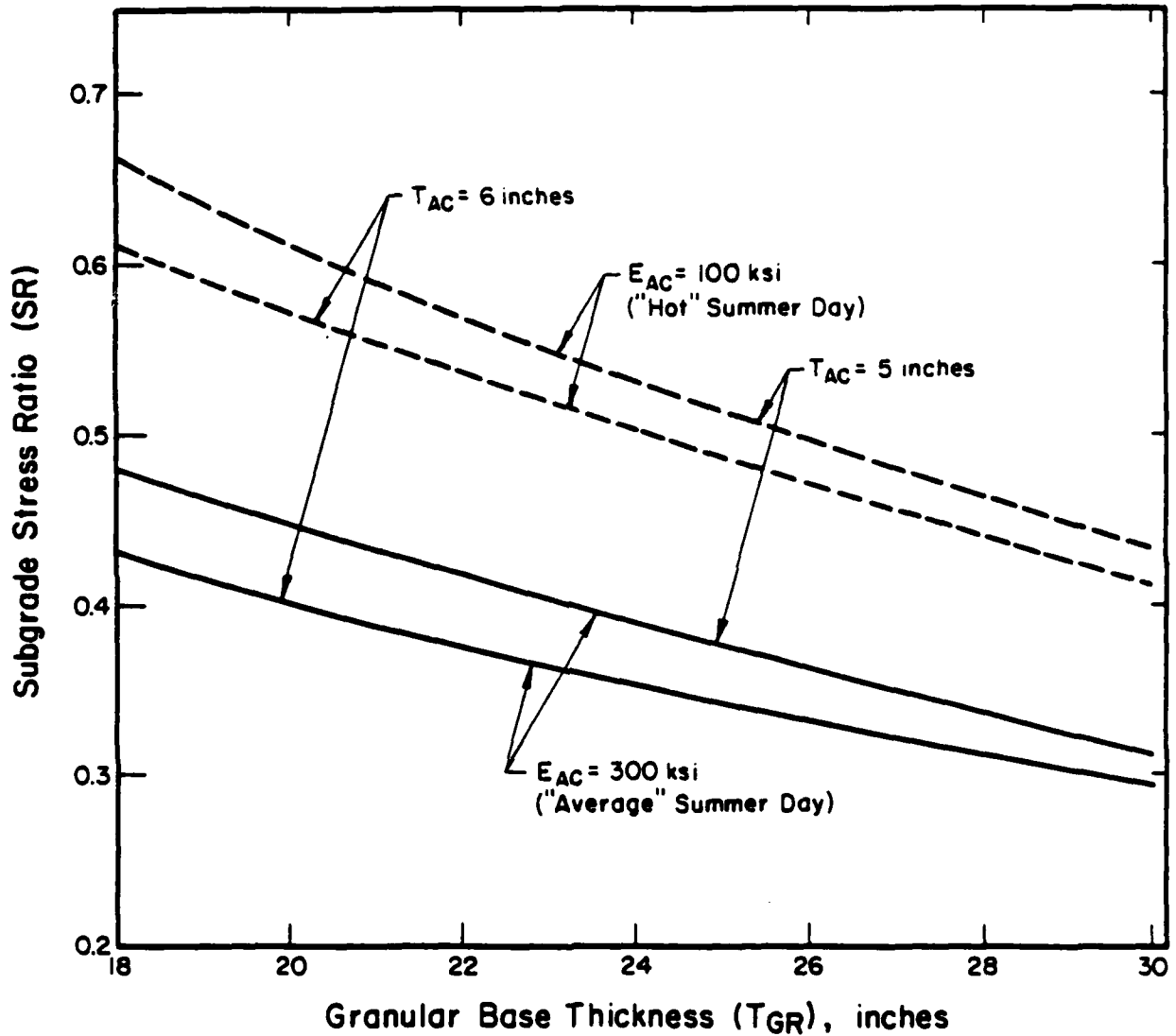


Figure 53. Summer Subgrade Stress Ratio Versus Granular Base Thickness ($E_{Ri} = 3.1$ ksi).

TABLE 9. DESIGN FOR 32,000 COVERAGES OF HEAVYWEIGHT F-15 AIRCRAFT.

Asphalt Concrete Thickness = 6 inches

Granular Base Thickness = 24 inches

Season	E_{AC}	E_{Ri}	D_0	ϵ_{AC}	ϵ_z	σ_D	SR	N	D_i
Spring	1300	1.4	50.0	398	709	2.2	0.29	40,000	0.20
Summer	300	3.1	66.7	819	1059	4.5	0.35	32,000	0.25
	100	3.1	92.1	1089	1720	6.5	0.50	60,000	
Fall	700	5.4	45.9	568	613	4.3	0.23	31,000	0.26
Winter	1800	6.5	33.1	275	381	3.5	0.17	81,000	<u>0.10</u>
$\Sigma D_i = 0.81$									

E_{AC} = Asphalt concrete modulus, in ksi

E_{Ri} = Subgrade modulus at breakpoint, in ksi

D_0 = Predicted maximum surface deflection, in mils

ϵ_{AC} = Predicted maximum radial tensile strain in asphalt concrete, in microstrain

ϵ_z = Predicted maximum subgrade vertical compressive strain, in microstrain

σ_D = Predicted maximum subgrade deviator stress, in psi

SR = Predicted maximum subgrade stress ratio

N = Predicted number of load applications (coverages) to crack appearance, from Equation (20)

D_i = Seasonal AC fatigue damage factor = 8000 coverages/N

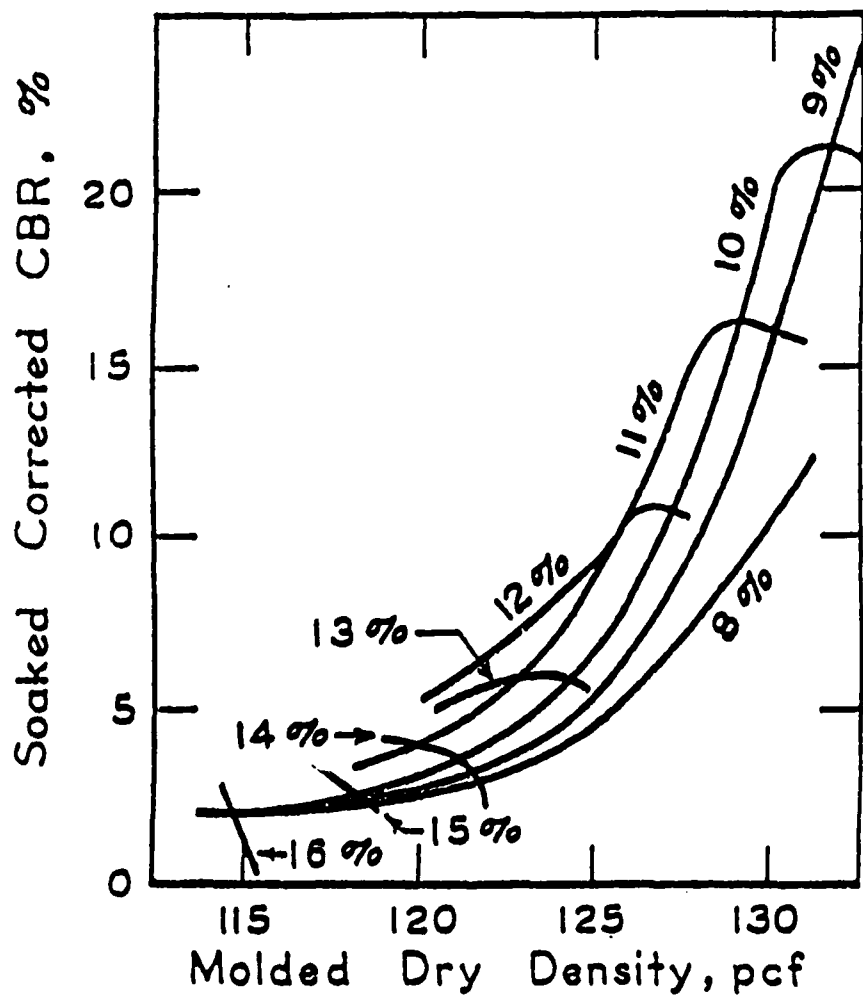


Figure 54. Soaked CBR of AASHO Road Test Subgrade Soil (Reference 85).

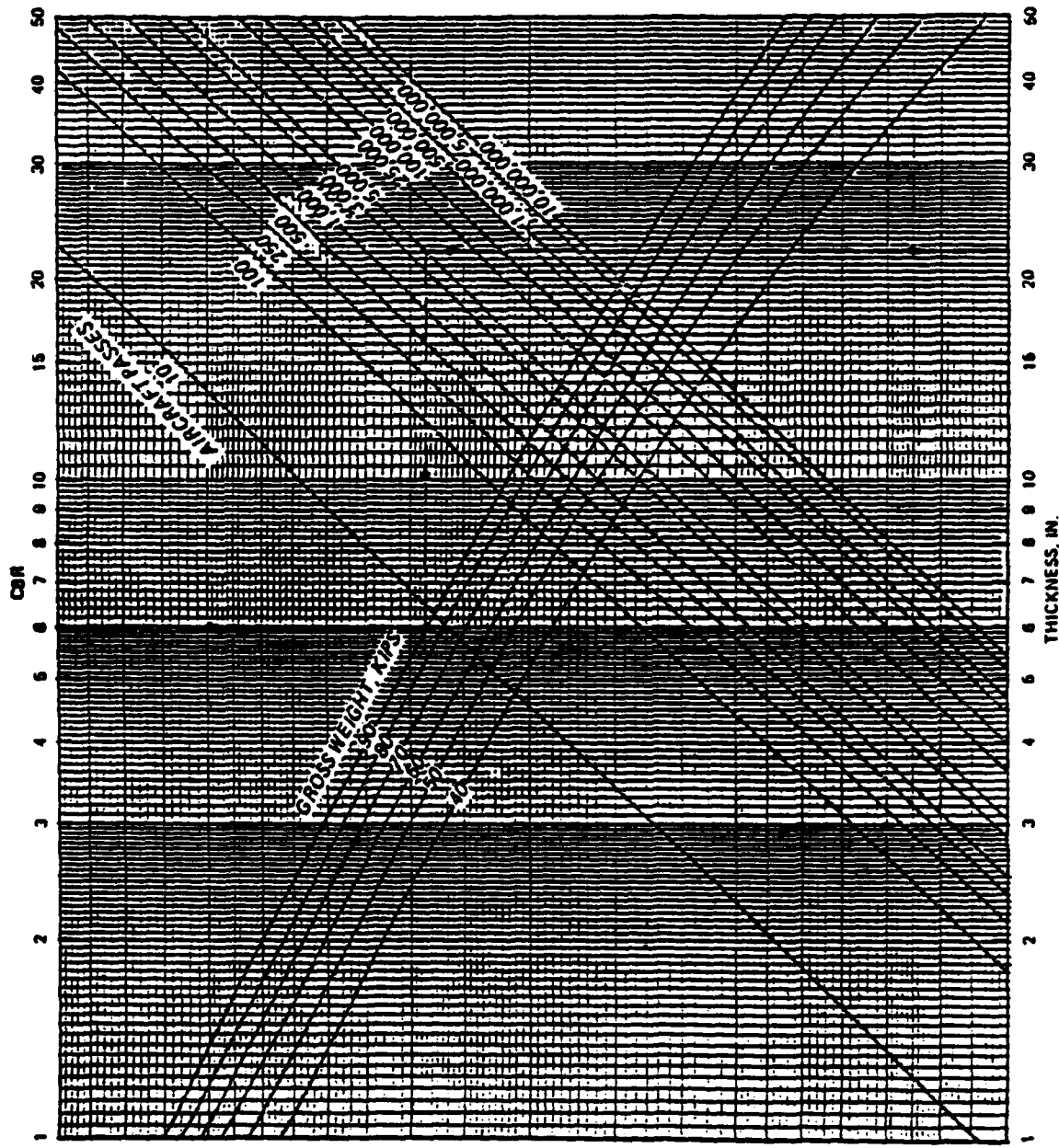


Figure 55. Flexible Pavement Design Curve for F-15, Type A Traffic Area (Reference 86).

Frost Penetration (a) = 50" (Total Pavement Thickness Required for Complete Protection)

Water content of base = 8 %

Water content of subgrade = 14 %

r = 14/8 = 1.75

c = a - p = 50" - 4" = 46"

Required Base Thickness (b) = 32" (Limited Subgrade Frost Protection)

Use structural requirement, since it is greater than Limited Subgrade Frost Protection. Design CBR for Reduced Subgrade Strength method is 3.5 for F3/F4 subgrade frost groups (Reference 78). The structural requirement still controls. The following design is acceptable according to the DOD (CBR) design procedure:

4" Asphalt concrete surface

16" Clean, well-graded, non-frost susceptible base course (0-1.5 % finer than 0.02 mm by weight)

16" Slightly frost-susceptible subbase (up to 6 % finer than 0.02 mm by weight)

13" Subbase

Mechanistic analysis of this design is presented in Table 10. This analysis shows that 4 inches of AC is insufficient to prevent premature fatigue cracking. The effect of adding AC is also shown in Table 10. Five inches of AC gives fatigue damage slightly greater than one. Six inches of AC is required to guard against early fatigue cracking. The relationship between AC thickness and fatigue damage is nonlinear; increasing thickness can increase the service life significantly.

C. CORRELATION OF COMPUTED RESPONSES WITH CBR DESIGNS

A study was accomplished to mechanistically analyze various CBR designs

TABLE 10. MECHANISTIC ANALYSIS OF CBR DESIGN FOR 32,000 COVERAGES OF HEAVYWEIGHT F-15 AIRCRAFT.

a) Asphalt Concrete Thickness = 4 inches
 Granular Base Thickness = 41 inches

Season	E _{AC} ^a	E _{Ri}	D _O	E _{AC}	E _Z	σ _D	SR	N	D _i
Spring	1300	1.4	60.8	511	468	1.4	0.19	18,000	0.44
Summer	300	3.1	73.6	863	604	2.7	0.21	27,000	0.30
	100	3.1	94.4	1055	880	3.5	0.27	66,000	
Fall	700	5.4	53.6	656	381	2.7	0.15	19,000	0.41
Winter	1800	6.5	41.2	380	260	2.3	0.11	29,000	0.27

$$\Sigma D_i = 1.42$$

b) Asphalt Concrete Thickness = 5 inches
 Granular Base Thickness = 40 inches

Season	E _{AC} ^a	E _{Ri}	D _O	E _{AC}	E _Z	σ _D	SR	N	D _i
Spring	1300	1.4	53.5	445	424	1.4	0.18	28,000	0.28
Summer	300	3.1	68.3	834	593	2.8	0.22	30,000	0.27
	100	3.1	91.2	1064	917	3.8	0.30	64,000	
Fall	700	5.4	48.2	604	357	2.7	0.15	25,000	0.31
Winter	1800	6.5	35.8	318	213	2.3	0.11	51,000	0.16

$$\Sigma D_i = 1.02$$

c) Asphalt Concrete Thickness = 6 inches
 Granular Base Thickness = 39 inches

Season	E _{AC} ^a	E _{Ri}	D _O	E _{AC}	E _Z	σ _D	SR	N	D _i
Spring	1300	1.4	47.3	375	373	1.4	0.18	48,000	0.17
Summer	300	3.1	63.0	771	557	2.8	0.22	38,000	0.21
	100	3.1	87.0	1025	906	4.0	0.31	72,000	
Fall	700	5.4	43.4	534	323	2.7	0.14	37,000	0.21
Winter	1800	6.5	31.3	259	201	2.1	0.10	98,000	0.08

$$\Sigma D_i = 0.67$$

^a Variables and units same as defined for Table 9

for the heavyweight F-15 aircraft. ILLI-PAVE was used as the structural model. The calculated pavement responses were then correlated with anticipated service life according to the CBR design. Table 11 contains the required pavement thickness (AC + base) for CBR values of 1 to 8 and pass levels of 200, 1000, 10,000, 100,000, 300,000, and 1,000,000. Total thickness requirements range from 10 to 68 inches. The minimum AC thickness of 4 inches was assumed. AC modulus values of 100, 300, 500, 1000, and 1500 ksi were used.

Regression equations were developed relating the ILLI-PAVE responses to expected service life according to the CBR design. The resulting equations are contained in Table 12. The best single variable correlation with expected service life is subgrade stress ratio (SR). Note that AC tensile strain does not correlate well with expected service life. The equation with the best precision indicators (i.e., R^2 and SEE) contains both vertical subgrade compressive strain (ϵ_z) and subgrade modulus at breakpoint (E_{Ri}). Figure 56 shows resulting best-fit plots of subgrade stress ratios for various repetition values and asphalt concrete modulus. Figure 56 also contains a plot of the best-fit line for all data (i.e., all AC moduli). Figure 57 is the same kind of plot for vertical compressive subgrade strain. The plots show that the calculated pavement response (subgrade stress ratio or strain) is dependent upon the AC modulus, which the CBR design procedure does not take into account.

The procedure outlined in the previous paragraph is similar to that used by Barker and Brabston (Reference 71) in developing their limiting subgrade vertical strain criteria presented in Figure 28. In this criteria, limiting strain is a function of subgrade modulus. Their criteria was developed from the CBR curves using the CHEVIT elastic layer program to compute strains.

TABLE 11. TOTAL PAVEMENT THICKNESS ACCORDING TO CBR
DESIGN FOR HEAVYWEIGHT F-15 AIRCRAFT.

CBR	E_{Ri} (ksi)	200 Passes	1000 Passes	10,000 Passes	100,000 Passes	300,000 Passes	1,000,000 Passes
1	1.2	28 ^a	36	48	59	63	68
2	2.8	20	26	34	42	45	49
3	4.4	17	22	28	35	37	41
4	6.0	14	19	24	30	32	35
5	7.6	13	16	22	26	28	30
6	9.2	12	15	20	24	26	28
7	10.8	11	14	18	22	24	26
8	12.4	10	13	17	21	22	24

^a Total Pavement Thickness = Asphalt Concrete Thickness + Granular Base Thickness, in inches

TABLE 12. CORRELATION OF ILLI-PAVE RESPONSES WITH CBR DESIGN.

A	B ₁	X ₁	B ₂	X ₂	R ²	SEE
122.05	-38.84	log ϵ_{AC}	-8.62x10 ⁻³	E_{AC}	0.426	1.011
16.09	-4.70	log ϵ_z	2.06	log E_{Ri}	0.708	0.721
17.95	-0.10	DO	-3.03	log E_{AC}	0.324	1.097
9.98x10 ⁻⁴	-7.39	log SR	0.06	E_{Ri}	0.594	0.849
5.56	-7.29	log σ_D	5.53	log E_{Ri}	0.586	0.858
7.56	-1.46	log ϵ_{AC}	--	--	0.016	1.320
13.93	-3.48	log ϵ_z	--	--	0.525	0.917
5.06	-0.03	DO	--	--	0.086	1.272
0.58	-7.02	log SR	--	--	0.564	0.879
4.21	-0.10	σ_D	--	--	0.185	1.201

Equations of Form: log coverages = A + B₁X₁ + B₂X₂

ϵ_{AC} = Asphalt concrete tensile strain, in microstrain

ϵ_z = Subgrade compressive strain, in microstrain

DO = Surface deflection, in mils

SR = Subgrade stress ratio

σ_D = Subgrade deviator stress, in psi

E_{AC} = Asphalt concrete modulus, in ksi

E_{Ri} = Subgrade modulus at breakpoint, in ksi

R² = Coefficient of determination

SEE = Standard error of estimate

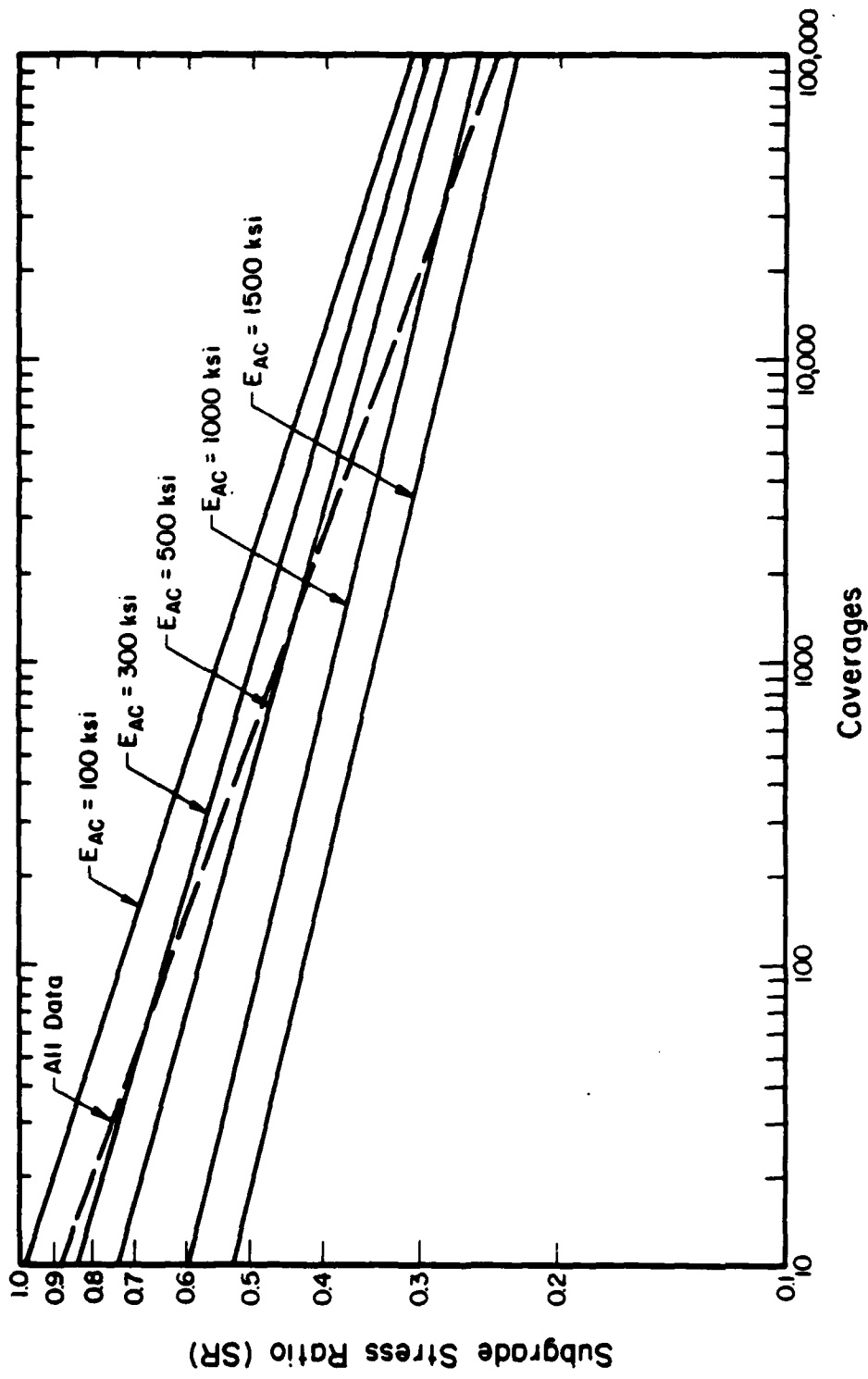


Figure 56. Effect of Asphalt Concrete Modulus Upon Repetition - Subgrade Stress Ratio Results.

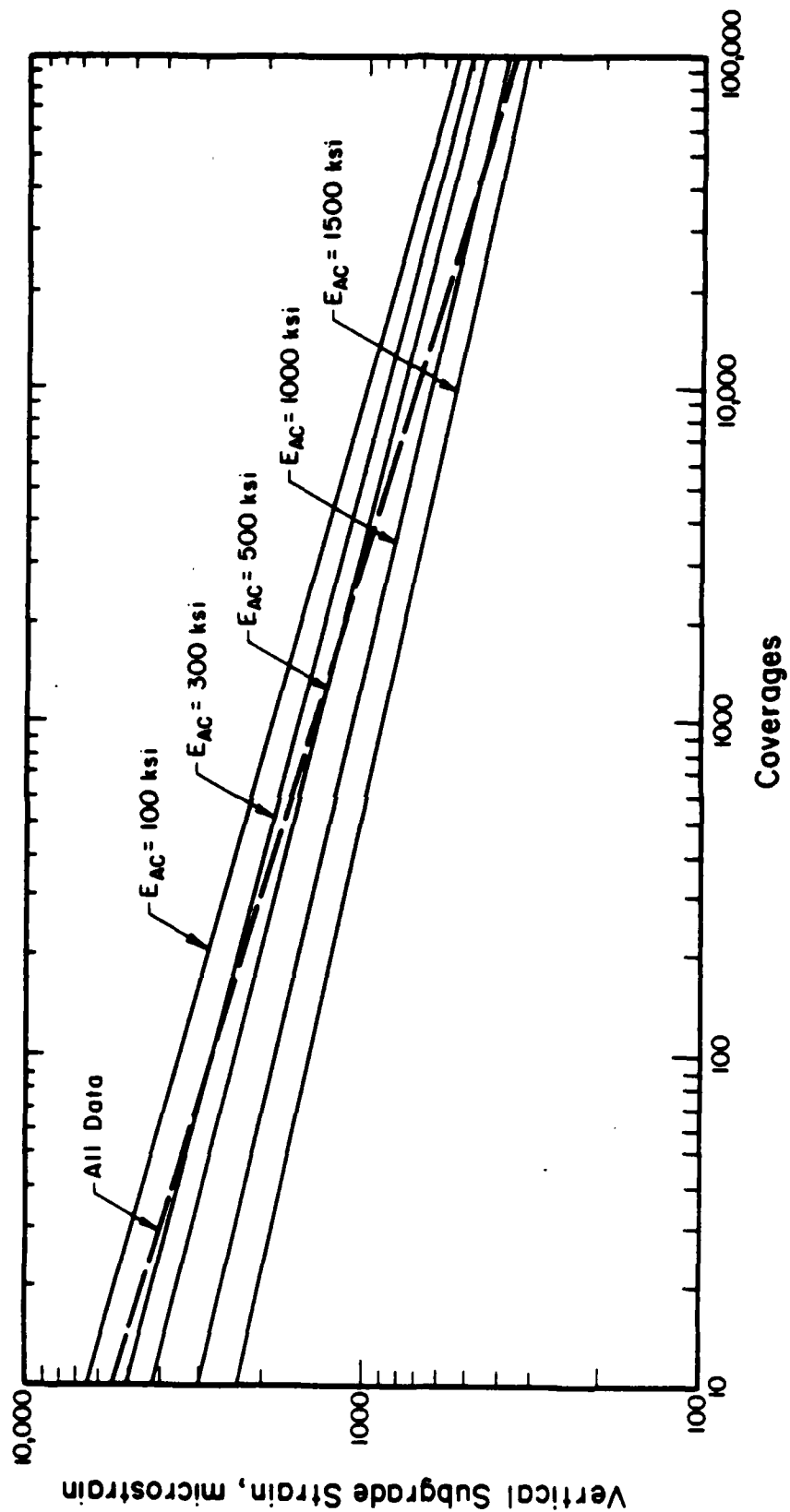


Figure 57. Effect of Asphalt Concrete Modulus Upon Repetition - Vertical Subgrade Strain Results.

AC thickness of 3 inches and modulus of 200 ksi were assumed for their analyses. Limiting subgrade vertical stress is obtained by multiplying the limiting strain by the subgrade modulus. A conservative estimate of limiting subgrade stress ratio is obtained by dividing the limiting subgrade stress by the subgrade strength. Note, subgrade deviator stress is slightly less than the vertical stress since the minor principal stress is usually low. Table 13 presents the results of limiting stress ratio calculations from the Barker and Brabston strain criteria.

D. COMPARISON OF PROPOSED PROCEDURES WITH CBR DESIGN PROCEDURE

The following comments are provided comparing the proposed mechanistic design procedures with the DOD design procedures:

1. The proposed procedures consider fatigue damage of the AC, but the CBR design procedure does not. The CBR design equation was developed from accelerated traffic tests where repetitions to failure were relatively few (5000 coverages or less). The mode of failure in these tests was primarily subgrade related. These results have been extrapolated up to ten million passes (one million coverages or more). Minimum AC surface thickness requirements may be too thin in certain cases. ILLI-PAVE analyses of pavements designed by the CBR method for the heavyweight F-15 generally show AC fatigue failure could be expected prior to 300,000 passes (see Table 14).

2. Low subgrade stress ratios were calculated using ILLI-PAVE on pavements designed by the CBR method. Using low AC modulus (i.e., 100 ksi), subgrade stress ratios are approximately 0.40 for sections designed for 300,000 passes and 0.37 for sections designed for 1,000,000 passes (see Table 15). Low stress ratios indicate designs may be overly conservative for subgrade rutting, especially considering the design CBR values is measured

TABLE 13. SUBGRADE STRESS RATIO CRITERIA FROM REFERENCE 71 STRAIN CRITERIA.

Asphalt Concrete Thickness = 3 inches

Asphalt Concrete Modulus = 200 ksi

Subgrade CBR	E_s	Qu	Passes	ϵ_z	σ_z	SR
3	4,500	15.1	100,000	0.83	3.7	0.25
4	6,000	18.8	100,000	0.89	5.4	0.29
5	7,500	22.5	100,000	0.94	7.1	0.31
6	9,000	26.2	100,000	0.98	8.8	0.34
7	10,500	30.0	100,000	1.01	10.6	0.35
8	12,000	33.7	100,000	1.04	12.4	<u>0.37</u> <u>$\bar{x}=0.32$</u>
3	4,500	15.1	300,000	0.71	3.2	0.21
4	6,000	18.8	300,000	0.79	4.7	0.25
5	7,500	22.5	300,000	0.84	6.3	0.28
6	9,000	26.2	300,000	0.88	8.0	0.30
7	10,500	30.0	300,000	0.92	9.7	0.32
8	12,000	33.7	300,000	0.95	11.4	<u>0.34</u> <u>$\bar{x}=0.28$</u>
3	4,500	15.1	1,000,000	0.61	2.7	0.18
4	6,000	18.8	1,000,000	0.68	4.1	0.22
5	7,500	22.5	1,000,000	0.74	5.6	0.25
6	9,000	26.2	1,000,000	0.79	7.1	0.27
7	10,500	30.0	1,000,000	0.83	8.7	0.29
8	12,000	33.7	1,000,000	0.86	10.4	<u>0.31</u> <u>$\bar{x}=0.25$</u>

E_s = Subgrade modulus, in psi

Qu = Subgrade unconfined compressive strength, in psi

ϵ_z = Limiting subgrade vertical strain from Reference 71, $\times 10^{-3}$ inch/inch

σ_z = Limiting subgrade vertical stress = $E_s \times \epsilon_z$, in psi

SR = Limiting subgrade stress ratio = ϵ_z/Qu

TABLE 14. ASPHALT CONCRETE FATIGUE DAMAGE EXPECTED FROM MECHANISTIC ANALYSIS OF CBR DESIGNS FOR HEAVYWEIGHT F-15.

Asphalt Concrete Thickness = 4 inches

Asphalt Concrete Modulus = 500 ksi

Subgrade CBR	Granular Base Thickness (in.)	Passes ^a	AC Strain (microstrain)	Fatigue Damage ^b
1	55	100,000	810	0.66
2	38	100,000	819	0.68
3	31	100,000	824	0.70
4	26	100,000	830	0.71
5	22	100,000	837	0.73
6	20	100,000	840	0.74
7	18	100,000	840	0.74
8	17	100,000	839	0.74
1	59	300,000	809	1.97
2	41	300,000	817	2.04
3	33	300,000	820	2.06
4	28	300,000	825	2.10
5	24	300,000	830	2.14
6	22	300,000	832	2.16
7	20	300,000	834	2.18
8	18	300,000	834	2.18
1	64	1,000,000	808	6.55
2	45	1,000,000	815	6.73
3	37	1,000,000	818	6.82
4	31	1,000,000	821	6.90
5	26	1,000,000	827	7.04
6	24	1,000,000	826	7.02
7	22	1,000,000	828	7.07
8	20	1,000,000	827	7.04

^a Coverages = 0.107 x Passes

^b Expected service life calculated using Equation (20). Crack appearance is expected when Fatigue Damage = 1.0.

TABLE 15. SUBGRADE STRESS RATIO FOR "HOT" SUMMER DAY FROM MECHANISTIC ANALYSIS OF CBR DESIGNS FOR HEAVYWEIGHT F-15.

Asphalt Concrete Thickness = 4 inches

Asphalt Concrete Modulus = 100 ksi

Subgrade CBR	Granular Base Thickness (in.)	Passes	Subgrade Stress Ratio
1	55	100,000	0.43
2	38	100,000	0.34
3	31	100,000	0.33
4	26	100,000	0.42
5	22	100,000	0.44
6	20	100,000	0.47
7	18	100,000	0.51
8	17	100,000	0.51
			$\bar{x}=0.43$
1	59	300,000	0.40
2	41	300,000	0.33
3	33	300,000	0.32
4	28	300,000	0.38
5	24	300,000	0.40
6	22	300,000	0.43
7	20	300,000	0.46
8	18	300,000	0.48
			$\bar{x}=0.40$
1	64	1,000,000	0.38
2	45	1,000,000	0.30
3	37	1,000,000	0.30
4	31	1,000,000	0.34
5	26	1,000,000	0.37
6	24	1,000,000	0.39
7	22	1,000,000	0.42
8	20	1,000,000	0.43
			$\bar{x}=0.37$

after a four-day soak test (i.e., conservative subgrade modulus).

3. Seasonal variations of pavement properties (AC and subgrade) can be considered with the proposed procedures. In the CBR design procedure, one subgrade condition is used throughout the design life. The design CBR is normally close to the worst possible field condition expected (i.e., four-day soak test).

4. In the proposed procedure, the resilient testing procedures used to characterize the pavement layers closely simulates the stress state conditions imposed by traffic loading. This difference (resilient - static CBR) can be substantial. It has been shown (Section III.B) that the resilient properties of granular materials and subgrade soils are stress-dependent under repetitive dynamic loading.

5. The proposed procedure permits extrapolation to other load configurations with minimum, or no, full-scale testing required. The transfer functions used must be validated for the range of predicted responses and required design life.

SECTION VIII

SUMMARY, FINDINGS AND CONCLUSIONS, AND RECOMMENDATIONS

A. SUMMARY

Material characterization for asphalt concrete, granular materials, and subgrade soils is discussed. The finite element program ILLI-PAVE is used to determine flexible pavement responses to the heavyweight F-15 aircraft wheel loading (30-kip/355-psi) and heavier-weight F-15 (36-kip/395-psi).

Algorithms are developed relating pavement variables (thicknesses and moduli) to pavement structural responses. Load magnitude effects and granular base quality influence on structural responses are also investigated.

A discussion of transfer functions is presented. Pavement test section data from the literature were analyzed using the ILLI-PAVE procedure. Regression analysis based transfer functions are derived relating ILLI-PAVE pavement structural responses and coverages to failure (determined from test section data).

The components of a proposed mechanistic design procedure are discussed. A mechanistic design example is presented. CBR based designs for the heavyweight F-15 aircraft are analyzed using mechanistic methods and the responses correlated with expected service life (per the CBR procedure).

B. FINDINGS AND CONCLUSIONS

Major findings and conclusions from this study are:

1. The ILLI-PAVE algorithms developed for the heavyweight and heavier-weight F-15 aircraft loadings are adequate for estimating flexible pavement structural responses.
2. ILLI-PAVE algorithms developed from a smaller data base provide

acceptable precision when compared to algorithms based on a much larger data base. A 3^4 factorial design is shown to provide an adequate data base from which to derive ILLI-PAVE algorithms for conventional flexible pavement.

3. There is little difference in calculated responses when the quality of the granular base is altered by changing the constants K and n in the resilient modulus model $E_r = K\theta^n$ (θ is the sum of principal stresses).

4. A 4-inch thick asphalt concrete surface course may not be sufficient to prevent premature fatigue cracking of pavements subjected to long term use by the heavyweight F-15 aircraft.

5. CBR designs for the heavyweight F-15 aircraft may be overly conservative for subgrade rutting as indicated by low calculated subgrade stress ratios.

6. As demonstrated by the high variability in the MWHGL test section properties (Section V.E.1), variability of paving material/soil properties and pavement structural responses/performance are expected, even under tightly controlled conditions. Therefore, variability must be anticipated and considered in the design, analysis, and testing of flexible airfield pavements.

7. Equivalent "dynamic" deflection basins can be used to backcalculate layer moduli if the pavement experiences stable responses under loading. However, if significant permanent deformations occur during loading, backcalculation of layer moduli is very difficult to accomplish (Section V.E.2).

8. There are limited flexible airfield pavement test data from which mechanistic based transfer functions can be derived.

C. RECOMMENDATIONS

The following recommendations are made:

1. Proceed with activities required to further develop the proposed mechanistic-based design procedures and consider their near-future implementation.
2. Validate/refine design criteria (transfer functions) for asphalt concrete fatigue and subgrade rutting presented in this research.
3. Develop improved design criteria/transfer functions for granular base/subbase materials.
4. Extend the concepts presented in this report to the development of design procedures for aircraft with a multiple wheel gear configuration (e.g., C-141).
5. Utilize the mechanistic design concepts developed in this research to establish flexible airfield pavement evaluation procedures based on nondestructive testing data (preferably falling weight deflectometer).
6. Closely monitor in-place flexible airfield pavements, and establish traffic conditions, in-situ soil/material properties, pavement distress and performance. This information will facilitate transfer function development under more realistic conditions (as opposed to those established under accelerated loading and assumed traffic distributions). These data will also be helpful in establishing typical seasonal effects (AC modulus and subgrade E_{Ri}) for various regions/climatic zones.
7. Consider using both cracking and rutting criteria to define failure instead of just rut depth (the present CBR criteria). The criteria should be consistent with Pavement Condition Index (PCI) system concepts (i.e., consider both the severity and amount/density of each distress).

8. Closely monitor asphalt concrete temperatures during flexible pavement testing and trafficking. Temperature is critical in nondestructive testing activities and analyzing pavement response and performance.

9. Develop improved construction subgrade stability criteria and practices to facilitate the adequate compaction of granular base/subbase layers. Adequate density is required to maximize shear strength/rutting resistance in granular materials. A minimum subgrade CBR of 6-8 is required during construction to provide a working platform and allow proper compaction of the upper layers (Reference 76). In many cases, subgrade stabilization/modification may be needed to meet this requirement.

APPENDIX A
ILLI-PAVE DATA BASE

These tables contain the response parameters in conjunction with the independent variables used in each parameter's calculation. Data was obtained using stress dependent material and the stress modification technique in the ILLI-PAVE program. Definitions of variables used in the tables:

	<u>VARIABLE</u>	<u>UNITS</u>
TAC	Thickness of Asphalt Concrete Surface	inches
TGR	Thickness of Granular Base Layer	inches
EAC	Modulus of Asphalt Concrete Surface	ksi
ERI	Subgrade Modulus at the Intercept	ksi
D0	Deflection at R= 0 in. From Center of Loaded Area	mils
D1	Deflection at R=12 in. From Center of Loaded Area	mils
D2	Deflection at R=24 in. From Center of Loaded Area	mils
D3	Deflection at R=36 in. From Center of Loaded Area	mils
AREA	Deflection Basin Area	inches
MEAC	Maximum Tensile Strain in Asphalt Concrete	microstrain
MTAC	Maximum Tensile Stress in Asphalt Concrete	psi
TOCT	Maximum Octahedral Stress in Asphalt Concrete	psi
DS	Deflection at Top of Subgrade	mils
EZ	Maximum Strain at Top of Subgrade	microstrain
SZ	Maximum Subgrade Normal Stress	psi
SDEV	Maximum Subgrade Deviator Stress	psi
SR	Subgrade Stress Ratio	

TABLE A-1. ILLI-PAVE DATA BASE, STRUCTURAL RESPONSES TO 30-KIP/355-PSI LOAD.

TAC	TGR	EAC	ERI	DO	D1	D2	D3	AREA	MEAC	MTAC	TUCT	DS	EZ	SZ	SDEV	SR	
3	6	100	1.00	255.0	159.4	73.3	32.0	17.70	1388	168	162	232.8	9294	21.2	6.2	1.00	
3	9	100	1.00	197.1	128.7	64.0	32.6	18.72	937	107	119	171.2	6615	15.1	6.2	1.00	
3	12	100	1.00	164.9	111.4	58.5	32.3	19.54	883	60	107	135.7	4830	12.0	6.2	1.00	
3	18	100	1.00	128.0	86.0	50.9	31.8	20.32	928	24	104	92.6	3062	9.4	6.2	1.00	
3	24	100	1.00	108.7	70.6	44.9	30.9	20.45	965	11	106	67.2	2377	10.1	4.8	.78	
5	6	100	1.00	178.3	117.5	64.0	33.8	19.35	1583	156	145	154.7	6492	14.4	6.2	1.00	
5	9	100	1.00	152.0	101.6	58.0	33.3	19.92	1325	101	128	124.6	4725	11.5	6.2	1.00	
5	12	100	1.00	134.0	89.8	53.3	32.6	20.28	1226	79	121	103.5	3745	10.2	6.2	1.00	
5	18	100	1.00	110.6	73.4	46.7	31.4	20.68	1170	60	116	74.6	2545	9.2	5.2	.84	
5	24	100	1.00	100.1	64.9	43.3	30.9	20.82	1153	55	117	58.8	2107	10.0	4.3	.69	
7	6	100	1.00	137.8	92.3	55.9	33.4	20.36	1478	165	131	114.1	4643	11.2	6.2	1.00	
7	7	9	100	1.00	122.1	81.6	51.6	32.7	20.69	1283	124	119	94.8	3556	9.6	6.2	1.00
7	7	12	100	1.00	111.2	74.0	48.1	32.0	20.90	1190	101	112	80.9	2881	9.1	5.9	.95
7	7	18	100	1.00	98.5	64.8	44.0	31.3	21.15	1104	79	106	62.7	2292	9.9	4.6	.74
7	7	24	100	1.00	91.9	59.7	41.7	31.0	21.27	1064	70	104	52.2	1772	9.3	3.6	.59
9	6	100	1.00	110.8	74.4	49.0	32.6	21.12	1224	159	107	87.6	3363	9.2	6.2	1.00	
9	9	100	1.00	102.1	68.1	46.2	32.0	21.32	1092	125	98	75.4	2807	9.2	5.7	.92	
9	9	12	100	1.00	96.1	63.7	44.2	31.6	21.46	1022	106	93	66.3	2556	10.0	5.1	.82
9	9	18	100	1.00	88.9	58.4	41.8	31.3	21.64	949	86	89	54.6	1950	9.4	3.9	.64
9	9	24	100	1.00	84.5	55.0	40.2	31.1	21.72	911	77	89	47.1	1497	8.7	3.2	.51
3	6	300	1.00	194.6	125.6	65.7	33.8	18.84	1509	445	318	174.5	7231	16.2	6.2	1.00	
3	9	300	1.00	162.8	108.4	59.3	33.3	19.59	1189	307	255	139.7	5311	12.6	6.2	1.00	
3	12	300	1.00	142.7	97.0	55.2	32.9	20.19	1046	245	231	116.9	4197	10.8	6.2	1.00	
3	18	300	1.00	114.2	78.4	48.3	31.8	20.98	949	198	217	82.9	2757	9.0	5.7	.91	
3	24	300	1.00	99.8	67.6	44.1	31.1	21.30	923	184	214	63.0	2259	10.1	4.6	.73	
5	6	300	1.00	123.0	87.5	53.8	33.2	21.41	1331	518	297	107.8	4218	10.6	6.2	1.00	
5	5	300	1.00	111.5	80.1	50.8	32.8	21.86	1171	430	268	92.8	3376	9.3	5.7	1.00	
5	12	300	1.00	102.3	73.8	48.1	32.4	22.20	1076	379	250	80.9	2818	8.8	5.7	.93	
5	18	300	1.00	90.1	65.1	44.3	31.6	22.68	978	327	231	63.3	2322	9.8	4.6	.75	
5	24	300	1.00	83.6	60.2	42.1	31.3	22.95	934	305	222	53.0	1810	9.2	3.7	.59	
7	6	300	1.00	88.4	66.4	46.0	32.4	23.46	980	422	224	75.9	2815	9.3	5.7	.92	
7	7	9	300	1.00	83.5	63.0	44.5	32.2	23.75	904	377	210	67.9	2626	9.8	5.2	.83
7	7	12	300	1.00	79.8	60.2	43.2	32.0	23.97	854	347	200	61.6	2321	9.6	4.6	.74
7	7	18	300	1.00	74.5	56.3	41.4	31.7	24.30	794	313	188	52.3	1790	8.9	3.6	.58
7	7	24	300	1.00	71.1	53.7	40.1	31.5	24.50	761	295	181	45.9	1405	8.3	2.9	.47
9	6	300	1.00	70.2	54.6	41.4	32.1	25.16	703	316	16.3	59.1	2283	9.3	4.4	.71	
9	9	300	1.00	68.1	53.0	40.7	32.0	25.33	666	293	156	54.7	2009	8.8	3.9	.63	
9	12	300	1.00	66.4	51.7	40.0	31.9	25.47	640	277	151	51.0	1762	8.4	3.5	.56	
9	18	300	1.00	63.7	49.6	39.0	31.7	25.68	606	257	14.4	45.1	1377	7.9	2.8	.46	
9	24	300	1.00	61.8	48.1	38.2	31.5	25.81	585	245	139	40.8	1105	7.5	2.4	.39	

TABLE A-1. ILLI-PAVE DATA BASE, STRUCTURAL RESPONSES TO 30-KIP/355-PSI LOAD (CONTINUED).

TAC	TGR	EAC	ERI	DO	D1	D2	D3	AREA	MEAC	MTAC	TOCT	DS	EZ	SZ	SDEV	SR	
3	6	500	1.00	163.4	107.6	60.1	33.7	19.56	1410	734	445	145.9	5943	13.7	6.2	1.00	
3	9	500	1.00	143.5	97.0	56.1	33.4	20.20	1167	570	380	122.5	4617	11.4	6.2	1.00	
3	12	500	1.00	127.6	87.6	52.4	32.9	20.71	1030	481	344	104.0	3759	10.1	6.2	1.00	
3	18	500	1.00	105.6	73.2	46.7	31.6	21.43	909	405	312	76.4	2613	9.1	5.3	.86	
3	24	500	1.00	94.2	65.0	43.4	31.3	21.80	867	379	302	59.9	2145	9.9	4.3	.70	
5	6	500	1.00	100.3	74.2	48.8	32.6	22.69	1057	697	365	86.6	3241	9.1	6.2	1.00	
5	9	500	1.00	93.3	69.6	46.8	32.5	23.06	961	618	337	78.3	2809	8.9	5.6	.91	
5	12	500	1.00	87.7	65.7	45.1	32.1	23.36	896	564	318	69.6	2574	9.5	5.1	.82	
5	18	500	1.00	80.2	60.3	42.7	31.8	23.80	822	507	296	57.6	2076	9.4	4.1	.67	
5	24	500	1.00	75.5	56.8	41.1	31.6	24.08	785	477	284	49.5	1617	8.7	3.3	.53	
7	6	500	1.00	72.1	57.0	42.4	32.3	25.23	714	504	254	62.8	2451	9.7	4.7	.76	
7	9	500	1.00	69.8	55.4	41.6	32.2	25.44	678	471	244	58.0	2175	9.2	4.2	.68	
7	12	500	1.00	67.6	53.9	40.9	32.1	25.61	650	448	235	53.9	1914	8.8	3.8	.60	
7	18	500	1.00	64.8	51.6	39.6	31.9	25.88	614	416	224	47.4	1501	8.1	3.0	.49	
7	24	500	1.00	62.5	49.8	38.9	31.7	26.07	592	398	216	42.5	1200	7.7	2.6	.41	
9	6	500	1.00	58.3	48.0	38.8	32.1	27.17	490	357	178	50.5	1738	8.0	3.4	.54	
9	9	500	1.00	57.3	47.2	38.4	32.1	27.29	474	342	173	47.7	1554	7.7	3.0	.49	
9	12	500	1.00	56.4	46.5	38.0	32.0	27.39	461	331	169	45.2	1385	7.4	2.8	.45	
9	18	500	1.00	54.9	45.3	37.4	31.8	27.55	443	314	163	41.1	1114	7.1	2.3	.38	
9	24	500	1.00	53.8	44.4	36.9	31.7	27.67	431	304	159	37.9	917	6.9	2.1	.33	
3	6	1000	1.00	122.5	83.8	51.5	33.0	20.87	1136	1190	627	109.2	4343	11.0	6.2	1.00	
3	9	1000	1.00	112.6	78.3	49.4	32.8	21.35	997	1022	561	95.8	3547	9.7	6.2	1.00	
3	12	1000	1.00	104.3	73.4	47.5	32.5	21.76	904	913	517	84.5	2953	8.8	6.0	.97	
3	18	1000	1.00	91.4	65.0	44.0	31.8	22.40	803	797	469	65.8	2414	9.8	4.8	.77	
3	24	1000	1.00	84.4	60.1	41.9	31.5	22.76	759	748	448	54.5	1903	9.3	3.8	.62	
5	6	1000	1.00	74.6	58.6	42.7	32.3	24.90	690	642	419	66.5	2635	10.1	5.0	.81	
5	9	1000	1.00	72.2	57.0	42.0	32.3	25.13	654	792	400	61.4	2354	9.6	4.5	.73	
5	12	1000	1.00	70.1	55.5	41.4	32.2	25.34	627	755	387	56.9	2092	5.1	4.1	.65	
5	18	1000	1.00	66.7	53.0	40.2	32.0	25.66	590	705	367	49.7	1616	8.4	3.3	.53	
5	24	1000	1.00	64.1	51.1	39.3	31.6	25.89	568	675	355	44.2	1308	7.8	2.7	.44	
7	6	1000	1.00	56.2	47.4	38.5	32.3	27.81	432	556	273	50.3	1694	7.8	3.2	.52	
7	9	1000	1.00	55.4	46.9	38.3	32.2	27.92	421	539	267	47.7	1531	7.5	3.0	.48	
7	12	1000	1.00	54.7	46.3	38.0	32.2	28.02	411	525	261	45.3	1375	7.3	2.7	.44	
7	18	1000	1.00	53.3	45.2	37.4	32.0	28.19	397	504	253	41.3	1116	7.0	2.3	.37	
7	24	1000	1.00	52.3	44.4	36.9	31.9	28.33	386	489	247	38.1	922	6.8	2.0	.33	
7	9	6	1000	1.00	47.2	41.4	36.1	32.1	29.79	285	377	184	42.5	1172	6.4	2.3	.37
9	9	9	1000	1.00	46.9	41.2	35.9	32.1	29.84	280	369	181	40.8	1070	6.3	2.1	.34
9	12	1000	1.00	46.5	40.9	35.8	32.0	29.90	276	363	179	39.3	973	6.2	2.0	.32	
9	18	1000	1.00	45.9	40.4	35.5	31.9	29.99	270	353	175	36.8	811	6.1	1.8	.28	
9	24	1000	1.00	45.4	39.9	35.2	31.8	30.06	345	172	345	36.7	687	6.2	1.6	.26	

TABLE A-1. ILLI-PAVE DATA BASE, STRUCTURAL RESPONSES TO 30-KIP/355-PSI LOAD (CONTINUED).

TAC	TGR	EAC	ERI	DO	D1	D2	D3	AREA	MEAC	MTAC	TOCT	OS	EZ	SZ	SDEV	SR
3	6	1500	1.00	101.3	71.5	47.0	32.7	21.96	929	1375	697	90.5	3461	9.6	6.2	1.00
3	9	1500	1.00	95.3	68.1	45.6	32.5	22.36	842	1233	642	81.0	2962	9.0	5.9	.96
3	12	1500	1.00	90.0	64.8	44.3	32.2	22.70	779	1133	602	72.6	2619	9.1	5.3	.85
3	15	1500	1.00	82.2	59.9	42.2	31.9	23.23	707	1019	555	59.5	2206	9.6	4.4	.70
3	24	1500	1.00	77.3	56.5	40.6	31.7	23.56	671	963	531	50.8	1710	8.8	3.5	.56
5	6	1500	1.00	63.6	51.9	40.1	32.3	26.41	515	873	428	57.2	2143	9.0	4.0	.65
5	9	1500	1.00	62.4	51.1	39.7	32.3	26.57	498	840	416	53.8	1927	8.6	3.7	.59
5	12	1500	1.00	61.2	50.2	39.3	32.2	26.71	483	813	405	50.6	1725	8.2	3.3	.54
5	15	1500	1.00	59.2	48.7	38.6	32.1	26.96	462	774	390	45.3	1378	7.6	2.8	.45
5	24	1500	1.00	57.6	47.5	38.0	31.9	27.14	448	749	380	41.1	1114	7.2	2.4	.38
7	6	1500	1.00	49.5	43.3	36.8	32.0	29.33	313	557	271	45.0	1335	6.8	2.5	.41
7	9	1500	1.00	49.1	43.0	36.7	32.2	29.40	308	546	267	43.1	1220	6.6	2.4	.36
7	12	1500	1.00	48.7	42.6	36.5	32.2	29.46	303	537	263	41.4	1107	6.5	2.2	.35
7	15	1500	1.00	47.9	42.0	36.1	32.1	29.58	295	522	257	38.4	916	6.3	1.9	.31
7	24	1500	1.00	47.3	41.5	35.8	31.9	29.68	289	510	253	36.0	769	6.3	1.7	.28
9	6	1500	1.00	42.6	38.8	35.0	32.1	31.15	204	372	180	39.2	930	5.6	1.6	.29
9	9	1500	1.00	42.6	38.6	34.9	32.1	31.15	201	367	178	39.0	857	5.6	1.7	.26
9	12	1500	1.00	42.4	38.4	34.7	32.0	31.22	199	363	177	36.9	786	5.6	1.6	.26
9	15	1500	1.00	42.1	38.1	34.5	31.9	31.27	196	355	174	34.9	669	5.7	1.5	.24
9	24	1500	1.00	41.7	37.8	34.3	31.8	31.32	193	350	172	33.3	586	5.9	1.4	.23
3	6	100	3.02	191.8	107.4	44.8	19.7	16.14	1203	137	138	170.3	9712	27.4	12.8	1.00
3	9	100	3.02	154.9	92.3	41.8	20.7	17.16	959	95	118	129.3	7173	21.4	12.6	.99
3	12	100	3.02	131.6	81.5	39.8	21.2	18.04	914	53	108	102.2	5297	17.4	9.7	.76
3	18	100	3.02	106.7	66.1	36.6	21.9	18.77	949	17	106	70.9	3082	13.5	7.6	.60
3	24	100	3.02	94.2	56.7	33.6	21.8	18.89	976	14	107	53.3	2066	11.3	5.7	.45
3	30	100	3.02	84.2	42.7	21.7	17.78	1516	139	117	46.3	1710	10.6	5.0	.39	
5	6	100	3.02	122.4	75.2	39.9	22.0	18.37	1299	93	126	95.1	6956	19.9	12.3	.96
5	9	100	3.02	101.7	63.1	37.3	22.5	19.17	1236	113	115	126	5196	16.8	9.6	.75
5	12	100	3.02	94.2	58.3	35.6	22.4	19.39	1156	93	110	64.0	3724	14.0	8.3	.65
5	18	100	3.02	84.9	52.0	33.1	22.3	19.60	1085	75	105	49.9	3891	14.7	8.5	.67
5	24	100	3.02	79.7	48.1	31.4	22.0	19.63	1053	68	103	40.6	2450	12.0	6.5	.51
7	6	100	3.02	93.1	58.1	35.9	22.7	19.58	1158	146	102	5005	16.0	9.6	.75	
7	9	100	3.02	86.8	53.9	34.4	22.6	19.77	1042	115	94	60.4	3724	14.0	8.3	.65
7	12	100	3.02	82.3	50.8	33.2	22.5	19.89	982	90	53.2	2881	12.6	7.2	.56	
7	18	100	3.02	76.5	46.6	31.2	22.3	20.00	925	82	90	43.0	2235	11.1	6.0	.47
7	24	100	3.02	73.2	44.2	30.3	22.1	20.01	897	74	90	36.1	1568	10.5	4.7	.37
9	6	100	3.02	86.8	53.9	34.4	22.6	19.77	1042	115	94	60.4	2776	12.0	6.9	.54
9	12	100	3.02	82.3	50.8	33.2	22.5	19.89	982	90	53.2	2881	12.6	7.2	.56	
9	18	100	3.02	76.5	46.6	31.2	22.3	20.00	925	82	90	43.0	2235	11.1	6.0	.47
9	24	100	3.02	73.2	44.2	30.3	22.1	20.01	897	74	90	36.1	1568	10.5	4.7	.37

TABLE A-1. ILLI-PAVE DATA BASE, STRUCTURAL RESPONSES TO 30-KIP/355-PSI LOAD (CONTINUED).

TAC	TGR	EAC	ERI	DO	D1	D2	D3	AREA	MEAC	MTAC	TOCT	DS	EZ	S2	SDEV	SR
3	6	300	3.02	153.2	90.4	43.6	21.6	17.34	1433	411	297	134.0	7750	22.2	12.8	1.00
3	9	300	3.02	131.0	80.6	40.8	21.9	16.12	1154	293	250	108.4	5976	18.4	10.5	.82
3	12	300	3.02	114.8	72.7	38.7	22.1	16.80	1027	236	229	89.0	4519	15.9	9.0	.71
3	15	300	3.02	96.0	61.6	35.7	22.3	19.55	942	195	217	64.6	2754	12.6	7.1	.55
3	18	300	3.02	85.9	54.4	33.2	22.1	19.78	921	183	215	49.8	1891	10.8	5.4	.42
3	21	300	3.02	100.8	67.6	39.0	22.8	20.05	1266	488	284	85.7	4558	15.8	9.6	.75
5	6	300	3.02	90.9	62.4	37.2	22.8	20.50	1121	407	257	73.3	3541	13.8	8.2	.64
5	9	300	3.02	85.2	58.2	35.7	22.7	20.83	1037	361	242	63.9	2820	12.5	7.3	.57
5	12	300	3.02	76.4	52.3	33.5	22.6	21.24	957	317	227	50.5	1962	10.7	5.5	.43
5	15	300	3.02	76.4	48.5	31.9	22.3	21.42	921	299	220	41.4	1432	9.9	4.4	.35
5	18	300	3.02	71.3	48.5	31.9	22.3	21.42	921	397	214	61.2	2759	12.0	7.2	.56
7	6	300	3.02	73.5	52.5	34.4	22.9	22.06	931	356	201	54.7	2335	10.9	6.1	.48
7	9	300	3.02	69.8	50.1	33.4	22.9	22.32	864	330	193	49.4	1940	10.3	5.4	.42
7	12	300	3.02	66.8	48.0	32.6	22.8	22.52	821	183	41.1	42.6	9.1	4.3	.34	
7	15	300	3.02	62.6	42.9	30.3	22.5	22.79	771	301	178	35.1	927	9.1	4.3	.34
7	18	300	3.02	59.9	42.9	30.3	22.5	22.92	746	287	155	47.2	1893	9.8	5.2	.41
9	6	300	3.02	57.9	42.8	30.9	22.8	23.64	666	277	149	43.3	1625	9.4	4.7	.36
9	9	300	3.02	56.2	41.6	30.3	22.8	23.79	635	264	145	40.0	1383	9.2	4.3	.34
9	12	300	3.02	54.9	40.6	29.9	22.7	23.91	614	247	140	34.6	902	8.7	4.2	.33
9	15	300	3.02	52.9	39.1	29.2	22.7	24.08	588	238	137	30.6	643	8.3	3.8	.30
9	18	300	3.02	51.6	36.1	28.7	22.6	24.17	573	183	178	30.6	643	8.3	3.8	.30
9	21	300	3.02	51.6	36.1	28.7	22.6	24.17	573	183	178	30.6	643	8.3	3.8	.30
3	6	500	3.02	131.5	80.5	41.8	22.3	18.17	1342	696	426	114.6	6597	19.4	11.6	.90
3	9	500	3.02	115.8	72.9	39.5	22.4	18.81	1118	543	367	95.1	5127	16.9	9.8	.76
3	12	500	3.02	104.1	67.1	37.7	22.5	19.37	995	462	334	80.4	3966	14.7	8.5	.66
3	15	500	3.02	89.1	58.2	34.9	22.5	20.05	893	397	308	60.0	2520	12.0	6.6	.52
3	18	500	3.02	80.8	52.4	32.8	22.3	20.30	860	376	300	47.3	1764	10.5	5.1	.40
3	21	500	3.02	82.8	58.3	36.1	23.0	21.36	1004	658	348	71.1	3404	13.6	8.2	.64
5	6	500	3.02	77.5	55.1	35.0	22.9	21.71	918	586	323	62.7	2786	12.3	7.2	.57
5	9	500	3.02	73.5	52.5	34.0	22.9	21.99	862	540	307	56.1	2332	11.2	6.3	.49
5	12	500	3.02	67.5	48.4	32.3	22.7	22.37	800	490	288	45.6	1693	10.0	4.9	.38
5	15	500	3.02	63.8	45.7	31.1	22.6	22.56	770	466	279	38.3	1187	9.5	4.3	.34
5	18	500	3.02	59.4	45.0	31.7	22.9	23.80	680	477	243	50.6	2035	10.2	5.6	.44
5	21	500	3.02	57.5	43.7	31.1	22.9	24.00	618	448	234	46.4	1777	9.7	5.0	.39
7	6	500	3.02	56.0	42.6	30.7	22.9	24.16	625	427	227	42.7	1536	9.4	4.5	.35
7	9	500	3.02	53.6	40.8	29.9	22.8	24.39	596	402	218	36.7	1049	8.9	4.2	.33
7	12	500	3.02	52.0	39.6	29.3	22.7	24.52	579	388	212	32.1	726	8.4	4.0	.31
7	15	500	3.02	47.1	37.1	28.7	22.8	25.67	468	338	170	39.6	1342	8.9	4.5	.35
7	18	500	3.02	46.4	36.6	28.5	22.8	25.78	455	317	163	34.8	903	8.7	4.4	.34
7	21	500	3.02	45.8	36.2	28.3	22.8	25.87	445	304	159	31.1	653	7.9	3.8	.29
9	6	500	3.02	44.8	35.4	27.9	22.8	26.01	431	297	156	28.1	491	7.6	3.3	.26
9	9	500	3.02	44.0	34.8	27.6	22.7	26.10	422	183	178	30.6	643	8.3	3.8	.30
9	12	500	3.02	44.0	34.0	27.6	22.7	26.10	422	183	178	30.6	643	8.3	3.8	.30

TABLE A-1. ILLI-PAVE DATA BASE, STRUCTURAL RESPONSES TO 30-KIP/355-PSI LOAD (CONTINUED).

TAC	TGR	EAC	ERI	DO	D1	D2	D3	AREA	MEAC	MTAC	TOCT	DS	EZ	SZ	SDEV	SR	
3	6	1000	3.02	100.9	93.2	61.2	36.4	22.6	19.56	1079	1127	597	87.7	4813	16.4	9.7	76
3	9	1000	3.02	93.2	86.6	57.7	35.2	22.6	20.04	951	972	538	76.3	3794	14.5	8.7	68
3	12	1000	3.02	77.5	52.2	33.3	22.7	21.01	20.46	867	873	499	66.7	3047	12.9	7.6	59
3	15	1000	3.02	71.9	48.4	31.8	22.6	21.26	784	776	459	52.6	2100	10.9	5.6	45	
3	24	1000	3.02	45.2	32.0	23.0	23.0	23.50	442	736	442	42.8	1525	9.9	4.6	36	
5	6	1000	3.02	59.7	45.2	31.5	23.0	23.73	659	803	401	53.9	2191	10.6	6.1	48	
5	9	1000	3.02	58.0	44.0	31.1	22.9	23.92	604	725	385	49.5	1948	10.2	5.4	42	
5	12	1000	3.02	55.2	42.1	30.3	22.9	24.21	573	682	373	45.4	1696	9.7	4.8	38	
5	15	1000	3.02	53.4	40.7	29.6	22.6	24.38	556	659	348	33.7	826	8.7	4.3	34	
5	24	1000	3.02	45.1	36.7	28.5	22.9	26.38	415	532	262	39.4	1175	9.1	5.0	39	
7	6	1000	3.02	44.6	36.3	28.4	22.9	26.49	405	517	257	37.0	1032	8.7	4.5	35	
7	9	1000	3.02	44.0	35.9	28.2	22.9	26.59	398	506	253	34.9	881	8.3	4.3	33	
7	12	1000	3.02	43.0	43.2	35.3	27.9	22.9	26.59	490	247	31.2	651	7.8	3.7	29	
7	15	1000	3.02	42.5	34.7	27.6	22.9	26.85	379	479	243	28.3	492	7.4	3.3	26	
9	6	1000	3.02	37.1	31.5	26.4	22.8	28.41	276	363	178	32.4	707	7.5	3.9	30	
9	9	1000	3.02	36.9	31.3	26.4	22.8	28.47	272	357	176	30.9	614	7.2	3.6	28	
9	12	1000	3.02	36.7	31.2	26.3	22.8	28.52	269	352	175	29.5	534	7.0	3.4	26	
9	15	1000	3.02	36.4	30.9	26.2	22.8	28.61	264	345	172	27.2	410	6.7	2.9	23	
9	18	1000	3.02	36.1	30.7	26.1	22.8	28.68	261	340	170	25.3	321	6.7	2.6	20	
9	24	1000	3.02	36.1	30.7	26.1	22.8	28.68	261	340	170	25.3	321	6.7	2.6	20	
3	6	1500	3.02	84.1	56.2	34.8	22.9	20.61	884	1305	665	73.3	3722	14.3	8.5	66	
3	9	1500	3.02	79.5	53.9	34.1	22.9	21.00	805	1176	616	65.3	3056	13.0	7.7	60	
3	12	1500	3.02	75.5	51.7	33.3	22.9	21.33	750	1088	581	58.4	2528	11.8	6.8	53	
3	15	1500	3.02	69.5	48.0	32.0	22.8	21.79	686	990	542	47.5	1827	10.3	5.2	40	
3	24	1500	3.02	65.5	45.4	30.9	22.7	22.04	656	944	522	39.6	1308	9.5	4.3	34	
5	6	1500	3.02	51.8	40.6	29.8	22.9	24.98	494	835	411	45.6	1542	10.5	6.2	49	
5	9	1500	3.02	50.9	40.0	29.6	23.0	25.13	479	806	401	42.6	1475	9.6	4.9	39	
5	12	1500	3.02	50.0	39.4	29.4	23.0	25.27	466	783	393	39.7	1262	9.2	4.6	36	
5	15	1500	3.02	48.5	36.3	28.9	23.0	25.49	449	752	381	34.8	892	8.5	4.2	33	
5	24	1500	3.02	47.4	37.5	28.5	22.5	26.64	439	732	37.3	30.9	647	8.0	3.8	29	
7	6	1500	3.02	39.2	33.1	27.1	22.9	27.95	303	538	263	34.7	833	8.1	4.4	34	
7	9	1500	3.02	38.9	32.9	27.0	22.9	28.02	299	529	260	33.0	734	7.7	4.0	31	
7	12	1500	3.02	38.6	32.7	26.9	22.9	28.09	295	521	257	31.4	638	7.4	3.7	29	
7	15	1500	3.02	38.2	32.4	26.8	23.0	28.20	289	510	252	28.7	487	7.0	3.2	25	
7	24	1500	3.02	37.6	32.1	26.7	23.0	28.29	285	502	249	26.4	378	6.9	2.8	22	
7	6	1500	3.02	33.1	29.1	25.4	22.8	29.91	199	361	176	29.5	510	6.6	3.2	25	
9	9	1500	3.02	33.0	29.0	25.4	22.6	29.95	197	358	175	28.3	447	6.4	3.0	23	
9	12	1500	3.02	32.9	29.0	25.4	22.6	29.99	195	355	174	27.3	393	6.3	2.8	22	
9	15	1500	3.02	32.8	28.9	25.4	22.6	29.99	193	350	172	26.5	308	6.2	2.4	19	
9	24	1500	3.02	32.6	28.7	25.3	22.6	29.99	191	346	170	24.1	252	6.3	2.2	17	

TABLE A-1. ILLI-PAVE DATA BASE, STRUCTURAL RESPONSES TO 30-KIP/355-PSI LOAD (CONTINUED).

TAC	TGR	EAC	ERI	DO	D1	D2	D3	AREA	MTAC	TOCT	DS	E2	SZ	SDEV	SR
3	6	100	7.68	125.4	60.9	23.7	10.8	14.61	1077	93	126	105.5	6774	33.6	22.8
3	9	100	7.68	106.7	56.3	23.7	11.5	15.64	968	51	112	81.9	4688	33.9	22.2
3	12	100	7.68	96.1	52.4	23.6	12.0	16.24	957	28	108	67.1	3595	27.7	18.2
3	15	100	7.68	84.4	46.0	23.0	12.7	16.71	984	10	108	48.3	2158	20.1	13.5
3	24	100	7.68	78.6	42.1	22.1	13.0	16.81	996	19	108	37.1	1430	15.6	10.0
5	6	100	7.68	100.2	53.2	24.2	12.0	16.01	1350	100	128	78.1	4933	33.1	22.5
5	9	100	7.68	90.6	49.2	23.9	12.4	16.51	1233	77	122	64.0	3579	27.0	18.2
5	12	100	7.68	84.5	46.4	23.6	12.7	16.83	1190	65	119	54.3	2703	22.8	15.6
5	15	100	7.68	77.3	42.3	22.7	13.1	17.10	1165	57	116	41.1	1703	17.2	11.4
5	24	100	7.68	73.4	39.7	22.0	13.3	17.16	1153	54	117	32.5	1176	13.9	8.6
7	6	100	7.68	84.1	46.1	23.9	12.8	16.89	1249	116	115	61.3	3533	26.1	18.1
7	9	100	7.68	78.7	43.4	23.3	13.1	17.17	1155	94	109	51.9	2637	22.0	15.3
7	12	100	7.68	75.1	41.4	22.9	13.2	17.34	1111	82	107	45.0	2049	19.0	13.0
7	15	100	7.68	70.5	38.6	22.2	13.4	17.50	1067	70	104	35.2	1352	14.9	9.6
7	24	100	7.68	67.9	36.8	21.6	13.5	17.53	1044	65	103	28.5	956	12.4	7.3
9	6	100	7.68	72.4	40.1	22.7	13.3	17.51	1039	118	93	49.4	2560	21.1	15.0
9	9	100	7.68	69.2	38.3	22.3	13.4	17.65	973	98	91	42.9	1979	18.2	12.7
9	12	100	7.68	67.0	36.9	21.9	13.5	17.75	939	87	90	37.8	1582	16.0	10.8
9	15	100	7.68	64.2	35.1	21.4	13.7	17.84	904	76	90	30.4	1081	13.0	8.0
9	24	100	7.68	62.5	33.9	21.0	13.7	17.86	885	72	90	25.2	782	11.3	6.2
3	6	300	7.68	104.2	55.5	24.7	11.9	15.91	1224	316	259	86.8	5542	34.1	22.8
3	9	300	7.68	92.6	51.6	24.2	12.4	16.62	1055	245	233	71.0	4119	30.0	19.8
3	12	300	7.68	85.1	49.5	23.9	12.7	17.10	982	214	223	59.8	3107	25.1	16.9
3	15	300	7.68	76.1	43.9	23.1	13.2	17.61	934	192	217	44.6	1937	18.6	12.5
3	24	300	7.68	71.3	40.9	22.3	13.4	17.76	919	183	215	34.9	1310	14.8	9.3
5	6	300	7.68	74.2	45.6	24.1	13.1	18.33	1121	415	256	60.1	3305	25.6	17.5
5	9	300	7.68	69.5	43.3	23.6	13.3	18.70	1030	362	240	51.7	2559	21.9	15.0
5	12	300	7.68	66.2	41.5	23.2	13.5	18.95	980	333	231	45.3	2040	19.0	12.9
5	15	300	7.68	61.8	38.9	22.5	13.7	19.25	930	305	222	35.7	1379	15.0	9.7
5	24	300	7.68	59.2	37.2	22.0	13.8	19.40	907	293	217	29.1	981	12.5	7.4
7	6	300	7.68	56.4	37.3	22.4	13.7	20.16	849	352	197	44.4	2069	18.7	13.0
7	9	300	7.68	54.4	36.1	22.1	13.8	20.36	806	325	190	39.5	1679	16.5	11.2
7	12	300	7.68	52.9	35.1	21.8	13.9	20.48	779	308	184	35.4	1384	14.7	9.7
7	15	300	7.68	50.7	33.6	21.4	14.0	20.72	747	289	178	29.1	984	12.3	7.4
7	24	300	7.68	49.4	32.9	21.1	14.1	20.83	731	279	175	24.4	720	10.7	5.8
9	6	300	7.68	45.2	30.9	20.5	13.9	21.49	622	271	146	34.4	1391	14.3	9.7
9	9	300	7.68	44.3	30.4	20.4	14.0	21.66	601	257	142	31.3	1156	13.0	8.4
9	12	300	7.68	43.6	29.9	20.3	14.1	21.76	588	248	140	28.6	978	11.9	7.3
9	15	300	7.68	42.7	29.3	20.1	14.2	21.88	571	238	136	24.2	710	10.4	5.8
9	24	300	7.68	42.1	28.9	20.0	14.3	21.98	562	232	134	20.9	514	9.5	4.9

TABLE A-1. ILLI-PAVE DATA BASE, STRUCTURAL RESPONSES TO 30-KIP/355-PSI LOAD (CONTINUED).

TAC	TGR	EAC	ERI	DO	D1	D2	D3	AREA	MEAC	MTAC	TGCT	DS	EZ	SZ	SDEV	SR
3	6	500	7.68	92.9	51.6	24.7	12.6	16.67	1153	579	374	77.3	4834	33.2	21.9	.96
3	9	500	7.68	84.3	48.5	24.2	12.9	17.26	1007	474	337	64.6	3601	27.6	18.5	.81
3	12	500	7.68	78.4	45.9	23.8	13.1	17.68	933	425	318	55.2	2777	23.3	15.8	.69
3	15	500	7.68	71.1	42.2	23.0	13.5	18.13	873	385	304	42.0	1775	17.6	11.7	.51
3	18	500	7.68	67.1	39.7	22.3	13.6	16.30	852	372	298	33.3	1219	14.1	8.8	.39
3	21	500	7.68	62.5	40.9	23.2	13.6	19.61	906	582	317	51.3	2558	21.9	15.0	.66
5	6	500	7.68	59.6	39.3	22.9	13.7	19.89	849	533	302	45.2	2058	19.0	12.9	.57
5	9	500	7.68	57.4	38.1	22.5	13.8	20.11	813	502	292	40.1	1685	16.7	11.2	.49
5	12	500	7.68	54.4	36.2	22.0	14.0	20.38	774	470	280	32.5	1180	13.6	8.5	.37
5	15	500	7.68	52.6	35.0	21.6	14.1	20.52	755	455	274	26.9	858	11.6	6.6	.29
5	18	500	7.68	45.9	32.5	21.1	13.9	21.81	634	438	228	37.1	1529	15.5	10.4	.45
7	6	500	7.68	44.9	31.9	20.9	14.0	21.98	612	418	222	33.7	1279	13.9	9.0	.40
7	9	500	7.68	44.1	31.4	20.8	14.1	22.10	597	404	218	30.7	1082	12.7	7.9	.35
7	12	500	7.68	43.0	30.6	20.6	14.3	22.28	578	387	212	25.9	1093	10.9	6.2	.27
7	15	500	7.68	42.0	30.1	20.4	14.4	22.40	567	376	208	22.2	579	9.8	5.2	.23
7	18	500	7.68	36.3	26.8	19.1	14.0	23.48	444	318	162	28.6	1001	11.8	7.4	.32
9	6	500	7.68	36.0	26.5	19.1	14.1	23.58	435	309	160	26.6	856	10.9	6.5	.28
9	9	500	7.68	35.7	26.4	19.1	14.2	23.67	428	303	158	24.6	728	10.2	5.8	.25
9	12	500	7.68	35.3	26.1	19.1	14.3	23.80	420	295	155	21.4	526	9.2	4.9	.21
9	15	500	7.68	35.1	26.0	19.1	14.5	23.89	415	290	154	18.9	391	8.5	4.1	.18
9	18	500	7.68	35.1	26.0	19.1	14.5	23.89	415	290	154	18.9	391	8.5	4.1	.18
3	6	1000	7.68	75.5	44.8	23.8	13.3	17.96	956	985	536	63.0	3616	27.7	18.4	.81
3	9	1000	7.68	70.7	42.8	23.4	13.5	18.38	837	873	495	54.4	2806	23.6	16.0	.70
3	12	1000	7.68	67.1	41.2	23.0	13.6	18.70	810	810	471	47.5	2236	20.3	13.7	.60
3	15	1000	7.68	62.3	38.7	22.4	13.8	19.09	757	748	447	37.3	1490	15.7	10.2	.45
3	18	1000	7.68	59.6	37.0	21.9	14.0	19.26	734	722	435	30.2	1048	12.9	7.8	.34
3	21	1000	7.68	47.7	33.6	21.3	13.9	21.59	614	742	377	39.9	1693	16.9	11.2	.49
5	6	1000	7.68	46.5	33.0	21.1	14.0	21.78	591	709	366	36.1	1429	15.1	9.8	.43
5	9	1000	7.68	46.5	33.0	21.1	14.0	21.78	591	709	366	36.1	1429	15.1	9.8	.43
5	12	1000	7.68	45.6	32.5	21.0	14.1	21.94	575	687	358	32.8	1211	13.6	8.6	.38
5	15	1000	7.68	44.2	31.6	20.8	14.3	22.16	555	659	348	27.5	889	11.5	6.8	.30
5	18	1000	7.68	43.3	31.0	20.6	14.4	22.30	544	644	342	23.4	650	10.2	5.5	.24
5	21	1000	7.68	43.3	31.0	20.6	14.4	22.30	544	644	342	23.4	650	10.2	5.5	.24
7	6	1000	7.68	34.5	26.5	19.0	14.0	24.27	396	505	262	28.8	971	11.7	7.1	.31
7	9	1000	7.68	34.3	26.3	19.0	14.2	24.38	389	494	248	26.6	841	10.9	6.3	.28
7	12	1000	7.68	34.0	26.2	19.0	14.3	24.47	384	486	246	24.7	719	10.2	5.7	.25
7	15	1000	7.68	33.7	26.0	19.1	14.4	24.62	377	476	242	21.6	526	9.1	4.8	.21
7	18	1000	7.68	33.5	25.9	19.1	14.6	24.73	372	470	239	19.1	393	8.4	4.1	.18
7	21	1000	7.68	27.6	22.1	17.4	14.1	26.24	266	349	173	22.8	602	9.2	5.1	.23
9	6	1000	7.68	27.6	22.1	17.5	14.2	26.32	264	345	172	21.5	511	8.7	4.7	.21
9	9	1000	7.68	27.6	22.1	17.5	14.3	26.38	264	342	171	20.2	438	8.2	4.3	.19
9	12	1000	7.68	27.6	22.2	17.5	14.3	26.38	264	342	171	20.2	438	8.2	4.3	.19
9	15	1000	7.68	27.6	22.2	17.7	14.5	26.49	259	338	169	18.2	329	7.6	3.6	.16
9	18	1000	7.68	27.6	22.3	17.8	14.6	26.59	257	335	168	16.6	254	7.3	3.1	.14

TABLE A-1. ILLI-PAVE DATA BASE, STRUCTURAL RESPONSES TO 30-KIP/355-PSI LOAD (CONTINUED).

TAC	TGR	EAC	ERI	DO	D1	D2	D3	AREA	MEAC	MTAC	TOCT	DS	EZ	SZ	SDEV	SR	
3	6	1500	7.68	64.7	40.0	22.7	13.6	16.89	800	1173	609	54.2	2889	24.2	16.2	.71	
3	9	1500	7.68	61.7	38.8	22.4	13.8	19.23	742	1078	574	47.7	2311	20.8	14.0	.62	
3	12	1500	7.68	59.4	37.6	22.2	13.9	19.49	705	1018	551	42.2	1878	18.1	12.1	.53	
3	15	1500	7.68	56.1	35.9	21.7	14.1	19.83	664	954	526	33.9	1288	14.3	9.1	.40	
3	18	1500	7.68	54.1	34.7	21.4	14.2	20.00	644	923	513	27.9	922	12.0	7.0	.31	
3	21	1500	7.68	52.1	40.1	29.6	20.0	14.1	22.93	469	789	392	33.9	1294	14.2	9.0	.39
5	6	1500	7.68	40.1	39.5	29.3	19.9	14.2	23.08	457	766	385	31.1	1112	12.9	8.0	.35
5	9	1500	7.68	39.5	39.0	29.0	19.9	14.3	23.21	448	750	379	28.6	958	11.6	7.1	.31
5	12	1500	7.68	39.0	38.3	28.5	19.8	14.4	23.40	437	729	371	24.4	708	10.3	5.7	.25
5	15	1500	7.68	38.3	37.9	28.2	19.8	14.6	23.53	430	717	366	21.2	515	9.2	4.8	.21
5	18	1500	7.68	37.9	37.5	28.5	17.9	14.1	25.82	292	516	254	24.8	722	10.0	5.7	.23
7	6	1500	7.68	29.3	29.3	23.5	18.0	14.2	25.91	289	510	252	23.2	617	9.4	5.2	.23
7	9	1500	7.68	29.3	29.3	23.5	18.0	14.3	25.99	287	505	251	21.8	527	8.9	4.8	.21
7	12	1500	7.68	29.2	29.2	23.5	18.0	14.3	25.99	283	499	248	19.4	394	8.1	4.1	.18
7	15	1500	7.68	29.2	29.2	23.5	18.1	14.5	26.12	281	494	246	17.5	300	7.5	3.5	.15
7	18	1500	7.68	29.1	29.1	23.5	18.2	14.7	26.22	281	493	351	17.2	430	7.9	4.2	.18
9	6	1500	7.68	23.9	23.9	20.0	16.6	14.1	27.87	193	349	171	19.2	369	7.5	3.6	.17
9	9	1500	7.68	24.0	20.1	16.7	14.2	27.93	191	347	171	18.3	319	7.2	3.5	.15	
9	12	1500	7.68	24.0	20.2	16.7	14.3	27.99	190	344	170	16.8	246	6.8	3.1	.14	
9	15	1500	7.68	24.2	20.3	16.9	14.5	28.08	189	342	169	15.6	198	6.7	3.1	.14	
9	18	1500	7.68	24.2	20.4	17.0	14.7	28.16	189	342	169	15.6	198	6.7	3.1	.14	
9	21	1500	7.68	24.2	20.4	17.0	14.7	28.16	189	342	169	15.6	198	6.7	3.1	.14	
3	6	100	12.34	96.1	42.9	16.0	7.5	13.81	1029	33	11.9	76.7	5411	56.0	32.8	1.00	
3	9	100	12.34	85.5	40.7	16.4	7.9	14.57	978	18	11.1	61.0	3837	42.9	29.5	.90	
3	12	100	12.34	79.5	39.0	16.7	8.3	15.03	962	19	10.9	50.6	2804	34.7	24.4	.74	
3	15	100	12.34	73.4	36.5	16.9	8.8	15.44	1003	16	10.9	37.3	1706	24.5	17.4	.53	
3	18	100	12.34	70.6	34.9	16.8	9.2	15.56	1008	14	10.9	28.9	1140	18.5	12.7	.39	
3	21	100	12.34	70.1	34.9	17.0	9.0	15.82	1267	82	123	59.5	3945	42.5	29.9	.91	
5	6	100	12.34	81.1	37.9	16.0	8.8	14.86	1198	67	120	49.2	2822	34.2	24.5	.75	
5	9	100	12.34	75.4	37.3	16.9	8.5	15.30	1198	67	120	49.2	2822	34.2	24.5	.75	
5	12	100	12.34	72.0	36.0	17.0	8.8	15.58	1176	61	11.9	42.0	2141	28.4	20.5	.62	
5	15	100	12.34	68.3	34.3	17.1	9.2	15.84	1163	56	11.8	32.0	1365	20.8	14.7	.45	
5	18	100	12.34	66.5	33.3	17.0	9.5	15.93	1153	53	11.7	25.4	938	16.2	10.9	.33	
5	21	100	12.34	61.8	31.2	17.0	9.8	16.31	1037	64	10.3	22.3	765	14.3	9.2	.28	
7	6	100	12.34	67.1	33.8	17.0	9.1	15.89	1107	82	10.6	40.6	2104	27.6	20.2	.62	
7	9	100	12.34	65.2	32.9	17.0	9.3	16.05	1081	74	10.5	35.2	1639	23.3	16.8	.51	
7	12	100	12.34	63.0	31.9	17.0	9.6	16.23	1054	67	10.4	27.6	1083	17.7	12.2	.37	
7	15	100	12.34	61.8	31.2	17.0	9.8	16.31	1037	64	10.3	22.3	765	14.3	9.2	.28	
9	6	100	12.34	61.8	31.2	16.6	9.3	16.18	967	100	9.2	38.9	2065	26.5	19.9	.61	
9	9	100	12.34	60.2	30.4	16.6	9.5	16.32	929	87	9.1	33.9	1595	22.5	16.5	.50	
9	12	100	12.34	59.1	29.9	16.6	9.6	16.42	910	79	9.1	29.9	1274	19.4	13.9	.42	
9	15	100	12.34	57.8	29.2	16.6	9.9	16.54	890	73	9.1	24.0	870	15.2	10.2	.31	
9	18	100	12.34	57.2	28.9	16.6	10.1	16.61	877	70	9.1	19.7	627	12.7	7.6	.24	

TABLE A-1. ILLI-PAVE DATA BASE, STRUCTURAL RESPONSES TO 30-KIP/355-PSI LOAD (CONTINUED).

IAC	IGR	EAC	ERI	DO	D1	D2	D3	AREA	MEAC	MIAC	10CI	DS	EZ	SZ	SDEV	SR
3	6	300	12.34	82.3	40.3	6.9	8.2	14.93	1123	274	243	65.9	4508	47.6	32.8	1.00
3	9	300	12.34	75.2	38.6	17.1	8.5	15.56	1006	224	226	54.3	3254	38.3	26.8	.82
3	12	300	12.34	70.9	37.3	17.2	8.8	15.97	958	204	220	46.0	2458	31.5	22.4	.68
3	18	300	12.34	66.2	35.3	17.3	9.3	16.39	927	189	216	34.7	1541	22.7	16.1	.49
3	24	300	12.34	63.9	34.2	17.2	9.5	16.54	916	182	215	27.3	1047	17.4	11.9	.36
5	6	300	12.34	60.7	34.8	17.3	9.1	17.20	1037	372	239	47.1	2674	32.9	23.7	.72
5	9	300	12.34	58.1	33.9	17.4	9.3	17.54	975	334	229	40.7	2062	27.6	19.9	.61
5	12	300	12.34	56.3	33.1	17.3	9.5	17.76	943	314	224	35.7	1643	23.5	16.8	.51
5	18	300	12.34	54.2	32.1	17.3	9.6	18.03	912	296	219	28.2	1107	17.9	12.4	.38
5	24	300	12.34	53.1	31.5	17.3	10.0	18.17	898	288	215	22.6	786	14.4	9.4	.29
7	6	300	12.34	47.3	29.4	16.7	9.7	18.92	794	321	186	35.5	1704	23.7	17.3	.53
7	9	300	12.34	46.4	29.0	16.7	9.8	19.11	767	303	182	31.6	1371	20.5	14.6	.45
7	12	300	12.34	45.7	28.7	16.7	10.0	19.25	750	292	179	28.2	1125	17.9	12.5	.36
7	18	300	12.34	44.8	28.2	16.8	10.2	19.44	731	279	175	23.0	796	14.3	9.4	.29
7	24	300	12.34	44.3	28.0	16.8	10.4	19.56	721	274	173	19.2	585	12.1	7.3	.22
9	6	300	12.34	38.5	24.9	15.6	10.0	20.15	588	251	139	27.9	1155	17.8	12.7	.39
9	9	300	12.34	38.2	24.7	15.7	10.1	20.27	576	242	137	25.1	952	15.8	10.9	.33
9	12	300	12.34	37.9	24.6	15.7	10.2	20.37	568	237	135	22.8	798	14.1	9.4	.29
9	18	300	12.34	37.7	24.5	15.9	10.5	20.52	559	231	134	19.1	582	11.8	7.2	.22
9	24	300	12.34	37.6	24.6	16.0	10.7	20.64	554	227	133	16.3	430	10.4	5.8	.18
3	6	500	12.34	74.4	38.3	17.3	8.6	15.66	1054	515	347	59.7	3914	43.1	29.6	.90
3	9	500	12.34	69.1	36.9	17.4	8.9	16.19	948	438	322	50.1	2880	35.2	24.9	.76
3	12	500	12.34	65.7	35.8	17.4	9.2	16.55	898	404	310	43.0	2217	29.3	20.9	.64
3	18	500	12.34	61.9	34.2	17.4	9.5	16.94	859	378	301	32.9	1419	21.1	15.1	.46
3	24	500	12.34	60.0	33.3	17.3	9.8	17.10	845	369	297	26.1	975	16.6	11.2	.34
5	6	500	12.34	51.7	31.9	17.1	9.5	18.47	843	532	298	40.8	2101	28.0	20.1	.61
5	9	500	12.34	50.2	31.3	17.1	9.7	18.74	803	497	288	36.0	1678	23.9	17.0	.52
5	12	500	12.34	49.1	30.8	17.1	9.8	18.92	780	477	282	31.9	1369	20.7	14.6	.44
5	18	500	12.34	47.7	30.1	17.1	10.1	19.16	756	456	275	25.7	951	16.1	10.9	.33
5	24	500	12.34	47.0	29.8	17.2	10.3	19.30	745	447	271	21.1	688	13.3	8.4	.25
7	6	500	12.34	38.8	26.1	16.0	10.0	20.56	599	409	217	30.0	1273	19.4	13.7	.42
7	9	500	12.34	38.3	25.9	16.0	10.1	20.71	585	395	214	27.1	1053	17.1	11.8	.36
7	12	500	12.34	38.0	25.8	16.1	10.2	20.83	576	386	211	21.5	885	15.2	10.2	.31
7	18	500	12.34	37.7	25.6	16.2	10.5	21.00	565	376	208	20.4	616	12.6	7.8	.24
7	24	500	12.34	37.5	25.6	16.3	10.7	21.13	559	371	206	17.3	482	10.9	6.2	.19
9	6	500	12.34	30.9	21.7	14.7	10.3	22.18	425	301	156	23.3	837	14.4	9.7	.29
9	9	500	12.34	30.8	21.7	14.8	10.3	22.18	420	296	155	21.3	705	13.0	8.4	.25
9	12	500	12.34	30.8	21.7	14.9	10.4	22.27	416	292	154	19.6	602	11.9	7.3	.22
9	18	500	12.34	30.8	21.8	15.1	10.6	22.42	412	288	153	16.8	415	10.3	5.8	.18
9	24	500	12.34	30.9	21.9	15.3	10.9	22.54	410	286	152	14.6	329	9.2	4.8	.15

TABLE A-1. ILLI-PAVE DATA BASE, STRUCTURAL RESPONSES TO 30-KIP/355-PSI LOAD (CONTINUED).

TAC	TGR	EAC	ERI	DO	D1	D2	D3	AREA	MEAC	MTAC	TOCT	DS	EZ	SZ	SDEV	SR
3	6	1000	12.34	61.9	34.4	17.2	9.3	16.91	879	499	49.9	2962	36.2	25.2	.77	
3	9	1000	12.34	59.0	33.6	17.3	9.5	17.31	812	814	470	43.1	2283	30.1	21.3	
3	12	1000	12.34	56.9	32.8	17.3	9.6	17.58	774	769	454	37.6	1811	25.4	.65	
3	15	1000	12.34	54.5	31.6	17.3	9.9	17.90	739	728	438	29.4	1200	18.9	.55	
3	18	1000	12.34	53.2	31.2	17.2	10.2	16.06	724	712	431	23.7	843	15.0	.40	
3	21	1000	12.34	51.9	30.8	16.2	10.0	20.40	580	696	358	32.4	1423	21.5	.30	
5	6	1000	12.34	40.1	27.0	16.2	10.0	20.40	564	673	351	29.1	1181	18.7	.45	
5	9	1000	12.34	39.5	26.8	16.2	10.1	20.58	554	658	346	26.3	993	16.5	.39	
5	12	1000	12.34	39.1	26.6	16.2	10.2	20.72	542	641	340	21.6	720	13.4	.34	
5	15	1000	12.34	38.6	26.4	16.4	10.5	20.92	536	633	337	18.3	535	11.4	.26	
5	18	1000	12.34	38.4	26.4	16.5	10.7	21.06	531	483	243	23.4	816	14.4	.20	
7	6	1000	12.34	29.2	21.5	14.6	10.2	22.93	381	376	476	24.1	696	13.0	.29	
7	9	1000	12.34	29.1	21.5	14.7	10.3	23.04	373	471	240	19.7	598	11.8	.25	
7	12	1000	12.34	29.1	21.6	14.8	10.5	23.14	370	466	238	16.9	444	10.2	.22	
7	15	1000	12.34	29.2	21.7	15.0	11.0	23.29	367	463	236	14.7	330	9.1	.18	
7	18	1000	12.34	29.3	21.8	15.3	11.0	23.42	361	379	337	16.8	523	10.7	.15	
9	6	1000	12.34	23.1	17.8	13.3	10.2	24.79	259	357	335	16.8	441	9.9	.19	
9	9	1000	12.34	23.2	17.9	13.5	10.4	24.88	257	334	168	17.0	376	9.2	.17	
9	12	1000	12.34	23.3	18.0	13.6	10.5	24.96	257	332	167	14.0	278	8.3	.16	
9	15	1000	12.34	23.4	18.3	13.8	10.6	25.10	256	331	166	12.6	214	7.6	.13	
9	18	1000	12.34	23.6	18.3	13.9	10.8	25.23	255	331	166	12.6	214	7.6	.11	
9	21	1000	12.34	23.8	18.5	14.1	11.0	25.31	255	331	166	12.6	214	7.6	.11	
3	6	1500	12.34	53.9	31.5	16.8	9.6	17.82	743	1083	572	43.7	2406	31.5	.67	
3	9	1500	12.34	52.1	30.9	16.9	9.8	18.12	700	1012	546	38.2	1906	26.5	.57	
3	12	1500	12.34	50.8	30.4	16.9	9.9	18.35	674	970	531	33.8	1538	22.6	.49	
3	15	1500	12.34	49.2	29.8	16.9	10.2	18.64	647	928	515	26.9	1043	17.2	.36	
3	18	1500	12.34	48.4	29.4	16.9	10.4	18.80	635	909	507	22.0	743	13.9	.27	
3	21	1500	12.34	33.9	23.9	15.3	10.1	21.67	447	750	376	27.7	1093	17.9	.20	
5	6	1500	12.34	33.7	23.9	15.4	10.3	21.82	439	735	372	25.2	925	15.8	.37	
5	9	1500	12.34	33.7	23.9	15.4	10.3	21.82	439	725	368	23.0	788	14.1	.32	
5	12	1500	12.34	33.5	23.9	15.5	10.4	21.93	434	725	368	23.0	788	14.1	.28	
5	15	1500	12.34	33.4	23.9	15.6	10.7	22.12	427	712	364	19.3	582	11.7	.22	
5	18	1500	12.34	25.0	19.4	14.3	10.9	24.77	278	490	244	15.1	334	8.9	.15	
5	21	1500	12.34	25.0	19.4	14.3	11.1	24.89	278	488	244	13.4	252	6.2	.12	
7	6	1500	12.34	24.6	19.0	13.7	10.3	24.44	283	499	247	20.1	614	11.9	.22	
7	9	1500	12.34	24.7	19.1	13.9	10.4	24.53	281	496	246	18.6	530	10.9	.20	
7	12	1500	12.34	24.8	19.2	14.0	10.6	24.62	280	493	246	17.3	452	10.1	.18	
7	15	1500	12.34	25.0	19.4	14.3	10.8	24.77	278	490	244	15.1	334	8.9	.15	
7	18	1500	12.34	25.0	19.4	14.3	11.1	24.89	278	488	244	13.4	252	6.2	.12	
7	21	1500	12.34	25.2	19.6	14.5	11.1	24.89	278	488	244	13.4	252	6.2	.12	
9	6	1500	12.34	24.6	19.0	13.7	10.3	24.44	283	499	247	20.1	614	11.9	.22	
9	9	1500	12.34	24.7	19.1	13.9	10.4	24.53	281	496	246	18.6	530	10.9	.20	
9	12	1500	12.34	25.0	19.2	14.0	10.6	24.62	280	493	246	17.3	452	10.1	.18	
9	15	1500	12.34	25.0	19.4	14.3	10.8	24.77	278	490	244	15.1	334	8.9	.15	
9	18	1500	12.34	25.0	19.4	14.3	11.1	24.89	278	488	244	13.4	252	6.2	.12	
9	21	1500	12.34	25.2	19.6	14.5	11.1	24.89	278	488	244	13.4	252	6.2	.12	
9	24	1500	12.34	25.2	19.6	14.5	11.1	24.89	278	488	244	13.4	252	6.2	.12	
9	27	1500	12.34	25.2	19.6	14.5	11.1	24.89	278	488	244	13.4	252	6.2	.12	
9	30	1500	12.34	25.2	19.6	14.5	11.1	24.89	278	488	244	13.4	252	6.2	.12	
9	33	1500	12.34	25.2	19.6	14.5	11.1	24.89	278	488	244	13.4	252	6.2	.12	
9	36	1500	12.34	25.2	19.6	14.5	11.1	24.89	278	488	244	13.4	252	6.2	.12	
9	39	1500	12.34	25.2	19.6	14.5	11.1	24.89	278	488	244	13.4	252	6.2	.12	
9	42	1500	12.34	25.2	19.6	14.5	11.1	24.89	278	488	244	13.4	252	6.2	.12	
9	45	1500	12.34	25.2	19.6	14.5	11.1	24.89	278	488	244	13.4	252	6.2	.12	
9	48	1500	12.34	25.2	19.6	14.5	11.1	24.89	278	488	244	13.4	252	6.2	.12	
9	51	1500	12.34	25.2	19.6	14.5	11.1	24.89	278	488	244	13.4	252	6.2	.12	
9	54	1500	12.34	25.2	19.6	14.5	11.1	24.89	278	488	244	13.4	252	6.2	.12	
9	57	1500	12.34	25.2	19.6	14.5	11.1	24.89	278	488	244	13.4	252	6.2	.12	
9	60	1500	12.34	25.2	19.6	14.5	11.1	24.89	278	488	244	13.4	252	6.2	.12	
9	63	1500	12.34	25.2	19.6	14.5	11.1	24.89	278	488	244	13.4	252	6.2	.12	
9	66	1500	12.34	25.2	19.6	14.5	11.1	24.89	278	488	244	13.4	252	6.2	.12	
9	69	1500	12.34	25.2	19.6	14.5	11.1	24.89	278	488	244	13.4	252	6.2	.12	
9	72	1500	12.34	25.2	19.6	14.5	11.1	24.89	278	488	244	13.4	252	6.2	.12	
9	75	1500	12.34	25.2	19.6	14.5	11.1	24.89	278	488	244	13.4	252	6.2	.12	
9	78	1500	12.34	25.2	19.6	14.5	11.1	24.89	278	488	244	13.4	252	6.2	.12	
9	81	1500	12.34	25.2	19.6	14.5	11.1	24.89	278	488	244	13.4	252	6.2	.12	
9	84	1500	12.34	25.2	19.6	14.5	11.1	24.89	278	488	244	13.4	252	6.2	.12	
9	87	1500	12.34	25.2	19.6	14.5	11.1	24.89	278	488	244	13.4	252	6.2	.12	
9	90	1500	12.34	25.2	19.6	14.5	11.1	24.89	278	488	244	13.4	252	6.2	.12	
9	93	1500	12.34	25.2	19.6	14.5	11.1	24.89	278	488	244	13.4	252	6.2	.12	
9	96	1500	12.34	25.2	19.6	14.5	11.1	24.89	278	488	244	13.4	252	6.2	.12	
9	99	1500	12.34	25.2	19.6	14.5	11.1	24.89	278	488	244	13.4	252	6.2	.12	
9	102	1500	12.34	25.2	19.6	14.5	11.1	24.89	278	488	244	13.4	252	6.2	.12	
9	105	1500	12.34	25.2	19.6	14.5	11.1	24.89	278	488	244	13.4	252	6.2	.12	
9	108	1500	12.34	25.2	19.6	14.5	11.1	24.89	278	488	244	13.4	252	6.2	.12	
9	111	1500	12.34	25.2	19.6	14.5	11.1	24.89	278	488	244	13.4	252	6.2	.12	
9	114	1500	12.34	25.2	19.6	14.5	11.1	24.89	278	488	244	13.4	252	6.2	.12	
9	117	1500	12.34	25.2	19.6	14.5	11.1	24.89	278	488	244	13.4	252	6.2	.12	
9</td																

TABLE A-2. ILLI-PAVE DATA BASE, STRUCTURAL RESPONSES TO 24-KIP/355-PSI LOAD.

TAC	TGR	EAC	ERI	DO	D1	D2	D3	AREA	MEAC	MTAC	TOCT	DS	EZ	SZ	SDEV	SR	
3	6	100	1.00	202.2	119.6	53.7	24.0	17.00	1245	136	181.1	7931	16.0	6.2	1.00		
3	12	100	1.00	136.0	67.1	45.2	24.8	16.77	975	50	108.0	4176	10.9	6.2	1.00		
3	24	100	1.00	93.4	57.1	35.6	24.2	19.47	1029	14	108	54.0	2141	9.7	4.3	.70	
3	5	6	100	1.00	144.6	91.5	46.6	25.7	18.70	1507	146	137	122.6	5392	12.5	6.2	1.00
5	12	100	1.00	110.2	70.4	41.2	25.1	19.52	1217	79	119	81.6	3108	8.9	6.2	1.00	
5	24	100	1.00	85.6	52.8	34.5	24.3	19.94	1137	59	114	47.3	1815	9.0	3.7	.60	
5	9	6	100	1.00	90.2	56.1	38.1	25.3	20.48	1070	142	93	66.5	2876	9.0	5.6	.94
9	12	100	1.00	80.3	51.2	35.2	24.9	20.77	915	100	86	52.9	2242	9.4	4.6	.72	
9	24	100	1.00	71.6	44.7	32.2	24.5	20.94	823	77	86	37.6	1252	7.7	2.7	.44	
3	6	500	1.00	129.2	82.6	45.6	25.6	19.08	1308	690	414	113.8	4939	11.9	6.2	1.00	
3	12	500	1.00	103.0	68.5	40.6	25.3	20.18	1001	482	333	81.5	3110	8.9	6.2	1.00	
3	24	500	1.00	79.0	52.6	34.6	24.7	21.10	865	397	297	47.0	1854	9.0	3.8	.61	
5	6	500	1.00	79.9	56.1	38.0	25.5	22.35	926	612	320	69.6	2783	8.8	5.5	.89	
5	12	500	1.00	71.4	52.5	35.7	25.3	22.95	807	513	285	55.3	2303	9.2	4.5	.73	
5	24	500	1.00	62.6	46.1	33.0	25.0	23.56	721	445	259	39.5	1353	7.7	2.8	.46	
9	6	500	1.00	47.1	38.2	30.6	25.5	26.83	412	300	149	40.2	1432	6.8	2.8	.45	
9	12	500	1.00	45.6	37.2	30.3	25.4	27.01	391	281	143	35.9	1134	6.4	2.3	.37	
9	24	500	1.00	43.6	35.5	29.4	25.1	27.25	368	261	135	30.0	739	6.1	1.7	.28	
3	6	1500	1.00	80.7	56.0	36.7	25.5	21.67	822	1217	617	71.3	3000	9.3	5.9	.96	
3	12	1500	1.00	72.9	51.6	35.0	25.3	22.34	710	1036	546	57.3	2474	9.5	4.6	.78	
3	24	1500	1.00	64.0	45.6	32.7	25.1	23.07	628	906	444	40.6	1434	7.8	3.0	.46	
5	6	1500	1.00	51.1	41.3	31.6	25.6	26.18	444	751	368	45.5	1785	7.8	3.4	.55	
5	12	1500	1.00	49.5	40.2	31.3	25.6	26.45	421	708	353	40.3	1424	7.0	2.6	.45	
5	24	1500	1.00	46.8	38.1	30.3	25.4	26.82	395	661	333	32.6	908	6.3	2.0	.32	
9	6	1500	1.00	34.3	30.6	27.7	25.5	30.94	170	310	150	31.2	748	4.7	1.5	.24	
9	12	1500	1.00	34.0	30.6	27.6	25.4	31.00	167	303	148	29.2	627	4.8	1.4	.22	
9	24	1500	1.00	33.5	30.1	27.3	25.2	31.08	162	294	144	26.4	469	5.3	1.2	.20	
3	6	100	7	68	102.7	47.4	18.2	8.5	14.16	1111	34	120	83.2	5839	38.7	22.8	1.00
3	12	100	7	68	81.9	41.3	18.4	9.4	15.44	1028	20	110	54.0	2994	24.4	16.4	.72
3	24	100	7	68	69.0	34.3	17.5	10.2	15.91	1051	13	111	29.8	1190	13.7	8.7	.36
5	6	100	7	68	83.5	41.8	18.8	9.4	15.38	1306	99	124	62.5	4108	29.0	19.7	.86
5	12	100	7	68	72.1	37.1	18.5	10.0	16.09	1176	68	116	43.6	2227	19.9	13.7	.60
5	24	100	7	68	64.0	32.4	17.5	10.4	16.35	1132	58	114	26.0	969	12.2	7.4	.32
9	6	100	7	68	60.5	31.7	17.9	10.5	16.87	915	107	90	39.2	2050	18.0	12.9	.57
9	12	100	7	68	56.9	29.6	17.4	10.7	17.06	841	84	89	30.1	1280	13.7	9.1	.40
9	24	100	7	68	53.6	27.7	16.9	10.9	17.16	798	72	69	20.0	616	9.9	5.4	.24

TABLE A-2. ILLI-PAVE DATA BASE, STRUCTURAL RESPONSES TO 24-KIP/355-PSI LOAD (CONTINUED).

TAC	TGR	EAC	ERI	DO	D1	D2	D3	AREA	MEAC	MTAC	TOCT	DS	EZ	SZ	SEV	SR
3	6	500	7.68	75.7	40.5	19.1	9.8	16.23	1091	558	354	61.7	4001	29.1	19.3	.85
3	12	500	7.68	65.3	36.7	16.7	10.3	17.12	917	434	311	44.2	2275	20.3	13.9	.61
3	24	500	7.68	57.3	32.4	17.6	10.7	17.65	849	293	26.6	1001	12.3	7.5	.33	
5	6	500	7.68	50.6	32.2	18.3	10.7	19.24	804	618	281	40.7	2052	16.7	12.9	.57
5	12	500	7.68	47.3	30.5	17.9	10.9	19.68	737	460	263	32.0	1362	14.4	9.5	.42
5	24	500	7.68	44.1	28.6	17.4	11.2	20.03	694	425	250	21.3	681	10.1	5.7	.25
9	6	500	7.68	29.6	21.3	15.2	11.1	23.07	374	267	137	22.8	802	10.1	6.1	.27
9	9	500	7.68	29.3	21.2	15.3	11.3	23.24	364	258	134	19.5	558	8.8	5.0	.22
9	12	500	7.68	29.0	21.0	15.4	11.6	23.46	355	250	131	14.9	300	7.3	3.5	.15
9	24	500	7.68	29.0	21.0	15.4	11.6	23.46								
3	6	1500	7.68	52.3	31.7	17.9	10.8	18.59	717	1053	546	43.2	2325	20.8	14.0	.61
3	12	1500	7.68	48.7	30.1	17.6	11.0	19.12	648	939	504	33.6	1520	15.5	10.3	.45
3	24	1500	7.68	45.3	28.3	17.2	11.3	19.56	603	670	476	22.1	741	10.4	5.9	.26
5	6	1500	7.68	32.3	23.5	15.9	11.2	22.70	406	680	339	26.9	1040	12.1	7.5	.33
5	12	1500	7.68	31.7	23.2	15.9	11.4	22.94	391	655	330	22.6	761	10.1	5.9	.26
5	24	1500	7.68	31.1	22.9	15.9	11.7	23.23	380	634	322	16.7	394	8.0	4.1	.18
9	6	1500	7.68	19.4	16.0	13.2	11.2	27.58	162	293	144	16.1	332	6.7	3.5	.16
9	9	1500	7.68	19.4	16.0	13.2	11.4	27.69	161	291	143	14.5	245	6.1	2.9	.13
9	12	1500	7.68	19.5	16.2	13.4	11.4	27.69	161	291	143	14.5	245	6.1	2.9	.13
9	24	1500	7.68	19.6	16.4	13.7	11.6	27.88	159	288	142	12.3	153	5.9	2.2	.10
3	6	100	12.34	81.2	33.5	12.3	5.9	13.21	1080	31	117	62.2	4690	49.3	32.8	1.00
3	12	100	12.34	68.9	31.2	13.0	6.5	14.25	1043	12	111	41.1	2351	30.4	21.8	.66
3	24	100	12.34	62.6	28.6	13.3	7.2	14.72	1059	9	111	23.3	945	16.0	10.9	.33
5	6	100	12.34	68.5	30.8	13.1	6.4	14.25	1234	82	119	48.0	3257	37.2	26.6	.81
5	12	100	12.34	62.2	29.0	13.4	6.9	14.85	1160	64	116	33.9	1768	24.5	17.8	.54
5	24	100	12.34	58.5	27.4	13.6	7.5	15.19	1131	57	114	20.3	771	14.0	9.2	.28
9	6	100	12.34	52.3	24.6	13.1	7.3	15.54	857	93	90	31.0	1662	22.5	17.0	.52
9	9	100	12.34	50.7	24.2	13.2	7.6	15.76	817	78	89	23.9	1029	16.5	11.7	.36
9	12	100	12.34	49.7	23.8	13.5	8.0	15.97	802	70	89	15.7	506	10.9	6.5	.20
9	24	100	12.34	49.7	23.8	13.5	8.0	15.97								
3	6	500	12.34	61.5	30.3	13.5	6.8	15.21	1008	504	332	48.1	3218	37.8	26.5	.81
3	12	500	12.34	55.4	28.8	13.7	7.2	15.99	886	415	304	34.6	1822	25.3	18.2	.55
3	24	500	12.34	51.7	27.4	13.9	7.7	16.48	843	386	292	20.9	799	14.2	9.5	.29
5	6	500	12.34	42.3	25.4	13.5	7.5	18.09	754	479	266	32.6	1693	23.8	17.1	.52
5	12	500	12.34	40.7	24.8	13.7	7.8	18.49	710	440	255	25.5	1100	17.5	12.2	.37
5	24	500	12.34	39.7	24.5	13.9	8.2	18.85	686	419	248	16.8	555	11.4	6.9	.21
9	6	500	12.34	25.3	17.3	11.7	8.1	21.65	359	255	132	18.5	667	12.1	7.9	.24
9	9	500	12.34	25.4	17.5	11.9	8.3	21.64	354	249	131	15.5	474	10.0	6.0	.18
9	12	500	12.34	25.6	17.8	12.4	8.6	22.12	351	246	130	11.5	251	7.9	4.0	.12

TABLE A-2. ILLI-PAVE DATA BASE, STRUCTURAL RESPONSES TO 24-KIP/355-PSI LOAD (CONTINUED).

TAC	TGR	EAC	ERI	DO	D1	D2	D3	AREA	MEAC	MTAC	TOCT	DS	EZ	SZ	SDEV	SR
3	6	1500	12.34	43.9	25.0	13.3	7.6	17.50	671	961	516	34.9	1942	26.9	18.9	.58
3	12	1500	12.34	42.0	24.5	13.4	7.9	17.97	623	901	488	26.9	1237	19.1	13.4	.41
3	24	1500	12.34	40.7	24.1	13.7	6.3	16.36	595	858	471	17.4	598	11.6	7.4	.23
5	6	1500	12.34	27.5	19.1	12.2	6.1	21.42	368	650	327	22.0	673	15.0	9.9	.30
5	12	1500	12.34	27.4	19.2	12.4	6.3	21.66	380	635	322	18.2	626	11.9	7.5	.23
5	24	1500	12.34	27.6	19.5	12.6	6.6	21.97	375	625	318	13.0	331	8.7	4.6	.15
9	6	1500	12.34	16.1	12.7	10.1	6.2	26.13	158	286	141	12.7	289	7.6	4.2	.13
9	12	1500	12.34	16.3	13.0	10.4	6.5	26.29	158	286	141	11.3	210	6.7	3.4	.10
9	24	1500	12.34	16.8	13.5	10.6	6.9	26.56	158	286	141	9.3	128	6.2	2.4	.07

TABLE A-3. ILLI-PAVE DATA BASE, STRUCTURAL RESPONSES TO 36-KIP/355-PSI LOAD.

TAC	TGR	EAC	ERI	DO	D1	D2	D3	AREA	MEAC	MTAC	TOCT	DS	EZ	SZ	SDEV	SR
3	6	100	1.00	306.9	203.6	98.2	42.7	18.63	1291	148	181	283.5	10783	24.3	6.2	1.00
3	12	100	1.00	191.0	134.8	72.3	40.3	20.27	812	53	106	160.7	5473	13.2	6.2	1.00
3	24	100	1.00	123.9	84.5	54.8	38.0	21.32	909	14	103	81.3	2455	9.5	5.1	.81
5	6	100	1.00	213.4	145.4	80.7	42.5	19.91	1653	173	153	188.3	7576	16.6	6.2	1.00
5	12	100	1.00	155.5	108.3	65.5	40.4	20.98	1212	77	122	123.5	4189	10.8	6.2	1.00
5	24	100	1.00	113.6	76.8	52.1	37.7	21.59	1149	50	116	70.4	2324	10.5	4.7	.76
9	6	100	1.00	131.2	90.9	60.3	40.2	21.67	1355	174	119	106.5	3949	10.2	6.2	1.00
9	12	100	1.00	111.7	76.6	53.6	38.7	22.07	1106	109	102	80.3	2664	9.4	5.4	.88
9	24	100	1.00	96.8	65.3	48.3	37.7	22.41	979	76	93	56.6	1719	9.5	3.5	.57
3	6	500	1.00	196.5	133.3	75.0	42.1	20.00	1489	770	478	176.9	7021	15.7	6.2	1.00
3	12	500	1.00	149.7	106.0	64.2	40.7	21.27	1033	473	345	124.0	4202	10.8	6.2	1.00
3	24	500	1.00	108.6	77.3	52.3	38.2	22.43	856	360	301	72.0	2330	10.2	4.7	.76
5	6	500	1.00	120.4	90.5	59.9	40.4	23.01	1168	769	403	107.4	3798	10.0	6.2	1.00
5	12	500	1.00	104.0	79.2	54.6	39.3	23.74	967	605	344	84.5	2742	9.1	5.5	.89
5	24	500	1.00	88.0	67.5	49.4	38.3	24.55	831	497	302	59.5	1850	9.6	3.7	.60
9	6	500	1.00	69.3	57.8	46.8	38.9	27.47	561	408	203	60.9	2017	9.0	3.9	.62
9	12	500	1.00	66.9	55.9	45.9	38.7	27.72	523	374	192	54.5	1618	8.3	3.2	.51
9	24	500	1.00	63.6	53.2	44.4	38.3	28.03	485	340	179	45.8	1082	7.7	2.3	.38
3	6	1500	1.00	121.3	86.9	57.4	40.0	22.25	1017	1502	762	109.1	4034	10.7	6.2	1.00
3	12	1500	1.00	107.1	78.6	54.0	39.5	23.06	835	1208	646	88.2	2856	8.9	5.6	.93
3	24	1500	1.00	90.2	67.2	49.0	38.4	24.02	700	999	558	61.1	1950	9.7	3.9	.63
5	6	1500	1.00	75.9	62.4	48.4	39.2	26.61	579	981	480	68.8	2464	10.1	4.6	.75
5	12	1500	1.00	72.8	60.3	47.4	39.0	26.96	537	904	451	60.9	1994	9.1	3.6	.62
5	24	1500	1.00	68.2	56.8	45.7	38.6	27.44	492	822	418	49.7	1307	8.1	2.7	.43
9	6	1500	1.00	51.4	46.8	42.2	38.9	31.33	235	428	207	47.4	1103	6.4	2.1	.34
9	12	1500	1.00	50.9	46.4	42.0	38.6	31.41	229	416	203	44.6	940	6.4	1.9	.30
9	24	1500	1.00	50.0	45.6	41.4	38.4	31.52	221	400	197	40.4	701	6.5	1.6	.26
3	6	100	7.68	143.9	76.2	29.9	13.2	15.39	1033	55	126	123.5	7528	49.0	22.8	1.00
3	12	100	7.68	109.5	63.3	29.1	14.7	16.93	906	40	108	79.7	4147	30.6	20.0	.88
3	24	100	7.68	87.4	49.7	26.7	15.8	17.59	949	12	106	44.1	1654	17.4	11.1	.49
5	6	100	7.68	116.3	64.8	30.2	14.7	16.57	1371	104	133	93.4	5623	36.9	22.8	1.00
5	12	100	7.68	96.2	55.5	28.7	15.6	17.48	1184	63	120	64.6	3153	25.4	17.1	.75
5	24	100	7.68	82.0	46.6	26.4	16.1	17.86	1153	49	119	38.8	1370	15.5	9.7	.42
9	6	100	7.68	63.8	48.4	27.7	16.2	18.06	1142	126	103	59.4	3053	23.7	16.6	.73
9	12	100	7.68	76.5	44.0	26.4	16.4	18.34	1016	88	95	45.4	1870	18.0	12.2	.53
9	24	100	7.68	70.4	49.0	25.0	16.6	18.46	951	70	94	30.3	922	12.5	7.1	.31

TABLE A-3. ILLI-PAVE DATA BASE, STRUCTURAL RESPONSES TO 36-KIP/355-PSI LOAD (CONTINUED).

TAC	TGR	EAC	ERI	DO	D1	D2	D3	AREA	MEAC	MTAC	TOCT	DS	EZ	SZ	SDEV	SR	
3	6	500	7.68	109.1	63.0	30.4	15.4	17.1	1194	589	386	92.3	5498	36.8	22.8	1.00	
3	12	500	7.68	90.8	55.3	28.9	16.0	16.19	935	415	320	65.9	3247	26.0	17.4	.76	
3	24	500	7.68	76.1	46.7	26.7	16.5	16.66	841	353	298	39.7	1423	15.6	9.9	.44	
3	5	6	500	7.68	74.0	49.4	28.3	16.5	19.94	990	634	347	61.7	3042	24.7	16.7	.73
5	12	500	7.68	67.2	45.6	27.2	16.7	20.49	872	534	314	48.2	1999	19.0	12.7	.56	
5	24	500	7.68	60.6	41.3	25.6	16.9	16.95	799	474	292	32.4	1015	13.0	7.6	.33	
5	9	6	500	7.68	42.9	32.2	23.1	16.9	23.61	506	363	186	34.7	1196	13.4	8.5	.37
9	12	500	7.68	41.9	31.5	22.9	17.1	24.02	486	342	179	29.7	882	11.5	6.7	.29	
9	24	500	7.68	40.8	30.8	22.7	17.3	24.26	467	325	173	22.8	484	9.5	4.7	.21	
3	6	1500	7.68	76.7	46.4	27.6	16.6	19.19	866	1270	661	65.1	3423	27.1	17.9	.78	
3	12	1500	7.68	69.5	45.1	26.7	16.6	19.84	747	1074	587	50.6	2224	20.5	13.7	.60	
3	24	1500	7.68	62.4	40.9	25.5	17.0	20.42	672	956	539	33.5	1089	13.4	8.0	.35	
3	5	6	1500	7.68	47.7	35.6	24.1	17.0	23.15	525	884	439	40.8	1544	16.2	10.3	.45
5	12	1500	7.68	46.1	34.7	23.9	17.2	23.45	497	831	421	34.5	1144	13.4	8.2	.36	
5	24	1500	7.68	44.3	33.5	23.5	17.4	23.60	472	786	403	25.6	639	10.4	5.4	.24	
5	9	6	1500	7.68	28.4	24.0	19.9	16.9	26.11	222	404	198	24.4	529	9.0	4.8	.21
9	12	1500	7.68	28.5	24.1	20.1	17.1	26.22	220	398	196	22.1	396	8.2	4.0	.18	
9	24	1500	7.68	28.6	24.3	20.3	17.5	26.39	216	391	193	18.8	243	7.5	3.0	.13	
3	6	100	12.34	110.3	52.6	19.8	9.1	14.37	991	34	121	90.7	6041	61.8	32.8	1.00	
3	12	100	12.34	89.6	47.1	20.5	10.1	15.73	935	25	108	59.9	3237	38.5	26.8	.82	
3	24	100	12.34	77.8	41.0	20.2	11.1	16.30	964	16	107	34.3	1321	20.8	14.3	.44	
3	5	6	100	12.34	93.0	47.2	20.7	10.0	15.40	1279	83	126	70.8	4538	47.2	32.8	1.00
5	12	100	12.34	81.2	42.9	20.8	10.6	16.21	1171	58	120	49.8	2493	31.8	22.7	.69	
5	24	100	12.34	73.7	39.0	20.3	11.5	16.59	1155	49	119	30.3	1096	18.3	12.4	.38	
5	9	6	100	12.34	70.8	37.5	20.2	11.2	16.72	1057	106	97	46.7	2455	30.1	22.4	.68
9	12	100	12.34	66.9	35.5	20.0	11.6	16.99	982	79	93	35.8	1508	22.1	15.8	.48	
9	24	100	12.34	64.0	33.8	19.8	12.1	17.18	943	67	94	23.7	742	14.3	9.0	.27	
3	6	500	12.34	86.8	46.5	21.2	10.5	16.07	1084	519	356	71.0	4506	47.8	32.8	1.00	
3	12	500	12.34	75.4	42.8	21.1	11.1	17.07	897	391	311	51.0	2584	32.8	23.2	.71	
3	24	500	12.34	67.6	39.0	20.7	11.8	17.65	834	350	297	31.1	1142	16.7	12.7	.39	
3	5	6	500	12.34	60.8	38.4	20.8	11.5	16.81	915	575	324	48.9	2491	31.8	22.6	.69
5	12	500	12.34	57.0	36.6	20.6	11.9	19.31	833	504	302	38.2	1624	23.6	16.7	.51	
5	24	500	12.34	53.8	34.9	20.4	12.4	19.72	787	465	288	25.4	817	15.1	9.7	.29	
5	9	6	500	12.34	36.3	26.0	17.6	12.2	22.43	485	343	178	28.1	1005	16.5	11.3	.34
9	12	500	12.34	36.0	25.8	17.8	12.5	22.63	471	329	175	23.6	724	13.6	8.6	.26	
9	24	500	12.34	35.8	25.9	18.1	13.0	22.90	460	319	171	17.6	406	10.4	5.5	.17	

TABLE A-3. ILLI-PAVE DATA BASE, STRUCTURAL RESPONSES TO 36-KIP/355-PSI LOAD (CONTINUED).

TAC	TGR	EAC	ERI	DO	D1	D2	D3	AREA	MEAC	MTAC	TOCT	DS	EZ	SZ	SDEV	SR
3	6	1500	12.34	63.4	37.9	20.4	11.6	16.12	801	1164	616	52.2	2842	35.6	24.5	.75
3	12	1500	12.34	59.0	36.3	20.3	12.0	16.71	710	1018	562	40.4	1820	25.8	18.1	.65
3	24	1500	12.34	55.4	34.5	20.1	12.5	19.19	660	940	531	26.4	881	15.7	10.2	.31
5	6	1500	12.34	40.2	28.6	16.4	12.2	21.90	499	637	420	33.3	1307	20.6	13.9	.42
5	12	1500	12.34	39.4	28.4	16.5	12.5	22.16	479	800	408	27.7	946	16.3	10.7	.33
5	24	1500	12.34	36.9	26.2	16.7	13.0	22.51	464	772	397	20.0	529	11.6	6.6	.20
9	6	1500	12.34	23.4	19.1	15.1	12.3	26.69	217	394	194	19.3	464	10.4	5.8	.18
9	12	1500	12.34	23.6	19.3	15.4	12.6	26.84	216	391	193	17.1	339	9.1	4.7	.14
9	24	1500	12.34	24.1	19.9	15.9	13.2	27.06	214	368	192	14.1	204	8.0	3.4	.10

TABLE A-4. COMPARISON OF AC TENSILE STRAIN (MEAC) AT
24-, 30-, AND 36-KIP LOAD.

TAC	TGR	EAC	ERI	24 KIP, 355 PSI		30 KIP, 355 PSI		36 KIP, 355 PSI	
				MEAC (% CHANGE)		MEAC		MEAC (% CHANGE)	
3	6	100	1.00	1245	(-10.3)	1366		1291	(-7.0)
3	12	100	1.00	976	(10.5)	863		812	(-6.0)
3	24	100	1.00	1029	(6.6)	965		909	(-5.6)
5	6	100	1.00	1507	(-4.6)	1563		1653	(4.4)
5	12	100	1.00	1217	(-7.1)	1226		1212	(-1.1)
5	24	100	1.00	1137	(-1.4)	1153		1149	(-4.4)
5	6	100	1.00	1070	(-12.6)	1224		1355	(10.6)
5	12	100	1.00	915	(-10.5)	1022		1106	(8.2)
5	24	100	1.00	823	(-9.7)	911		979	(7.5)
6	6	500	1.00	1308	(-7.3)	1410		1489	(5.6)
6	12	500	1.00	1001	(-2.6)	1030		1033	(-3)
6	24	500	1.00	865	(-2)	867		856	(-1.2)
6	5	500	1.00	926	(-12.4)	1057		1168	(10.5)
6	12	500	1.00	807	(-9.9)	896		967	(8.0)
6	24	500	1.00	721	(-6.1)	785		831	(5.9)
6	9	500	1.00	412	(-15.9)	490		561	(14.4)
6	12	500	1.00	391	(-15.1)	461		523	(13.4)
6	24	500	1.00	368	(-14.5)	431		485	(12.6)
6	1500	1.00		822	(-11.6)	929		1017	(9.5)
6	12	1500	1.00	710	(-8.9)	779		835	(7.1)
6	24	1500	1.00	628	(-6.5)	671		700	(4.3)
6	5	1500	1.00	444	(-13.8)	515		579	(12.3)
6	12	1500	1.00	421	(-12.9)	483		537	(11.1)
6	24	1500	1.00	395	(-11.8)	448		492	(9.8)
6	9	1500	1.00	170	(-16.5)	204		235	(15.1)
6	12	1500	1.00	167	(-16.3)	199		229	(14.6)
6	24	1500	1.00	162	(-16.0)	193		221	(14.4)
6	100	7.68		1111	(-3.1)	1077		1033	(-4.1)
6	12	100	7.68	1028	(7.5)	957		906	(-5.3)
6	24	100	7.68	1051	(5.6)	996		949	(-4.7)
6	5	100	7.68	1306	(-3.2)	1350		1371	(1.6)
6	12	100	7.68	1176	(-1.2)	1190		1184	(-5)
6	24	100	7.68	1132	(-1.8)	1153		1153	(0)
6	9	100	7.68	915	(-12.0)	1039		1142	(9.9)
6	12	100	7.68	841	(-10.4)	939		1016	(8.2)
6	24	100	7.68	798	(-9.8)	885		951	(7.5)

TABLE A-4. COMPARISON OF AC TENSILE STRAIN (MEAC) AT 24-, 30-, AND 36-KIP LOAD (CONTINUED).

TAC	TGR	EAC	ERI	24 KIP, 355 PSI		30 KIP, 355 PSI		36 KIP, 355 PSI	
				MEAC (% CHANGE)		MEAC		MEAC (% CHANGE)	
3	6	500	7.68	1091	(-5.4)	1153		1194	(3.5)
3	12	500	7.68	917	(-1.7)	933		935	(-3)
3	24	500	7.68	849	(-4)	852		841	(-1.3)
5	6	500	7.68	804	(-11.3)	906		990	(9.3)
5	12	500	7.68	737	(-9.4)	813		872	(7.3)
5	24	500	7.68	634	(-8.0)	755		799	(5.6)
9	6	500	7.68	574	(-15.9)	444		508	(14.3)
9	12	500	7.68	364	(-15.0)	428		486	(13.4)
9	24	500	7.68	355	(-14.3)	415		467	(12.5)
9	6	1500	7.68	717	(-10.4)	800		868	(8.5)
3	12	1500	7.68	648	(-8.1)	705		747	(6.0)
3	24	1500	7.68	603	(-6.4)	644		672	(4.2)
5	6	1500	7.68	405	(-13.7)	469		525	(11.9)
5	12	1500	7.68	391	(-12.7)	446		497	(10.9)
5	24	1500	7.68	380	(-11.7)	430		472	(9.7)
9	6	1500	7.68	162	(-16.4)	193		222	(15.0)
9	12	1500	7.68	161	(-16.1)	191		220	(14.7)
9	24	1500	7.68	159	(-15.9)	189		216	(14.2)
3	6	100	12.34	1080	(4.9)	1029		991	(-3.7)
3	12	100	12.34	1043	(6.2)	982		935	(-4.8)
3	24	100	12.34	1059	(5.1)	1008		964	(-4.3)
5	6	100	12.34	1234	(-2.6)	1267		1279	(-1.0)
5	12	100	12.34	1160	(-1.3)	1176		1171	(-4)
5	24	100	12.34	1131	(-1.9)	1153		1155	(-1)
9	6	100	12.34	857	(-11.4)	967		1057	(9.3)
9	12	100	12.34	817	(-10.2)	910		982	(7.9)
9	24	100	12.34	802	(-8.6)	877		943	(7.5)
3	6	500	12.34	1008	(-4.4)	1054		1084	(2.8)
3	12	500	12.34	886	(-1.3)	898		897	(-1)
3	24	500	12.34	843	(-3)	845		834	(-1.3)
5	6	500	12.34	754	(-10.5)	843		915	(8.6)
5	12	500	12.34	710	(-9.0)	780		833	(6.6)
5	24	500	12.34	686	(-7.9)	745		787	(5.7)
9	6	500	12.34	359	(-15.6)	425		485	(13.9)
9	12	500	12.34	354	(-14.9)	416		471	(13.0)
9	24	500	12.34	351	(-14.3)	410		460	(12.3)

TABLE A-4. COMPARISON OF AC TENSILE STRAIN (MEAC) AT
24-, 30-, AND 36-KIP LOAD (CONTINUED).

TAC	TGR	EAC	ERI	24 KIP, 355 PSI		30 KIP, 355 PSI		36 KIP, 355 PSI		MEAC (% CHANGE)
				MEAC	(% CHANGE)	MEAC	(% CHANGE)	MEAC	(% CHANGE)	
3	6	1500	12.34	671	(-9.7)	743		801	(7.7)	
3	12	1500	12.34	623	(-7.6)	674		710	(5.5)	
3	24	1500	12.34	595	(-6.2)	635		660	(4.0)	
5	6	1500	12.34	368	(-13.2)	447		499	(11.5)	
5	12	1500	12.34	380	(-12.4)	434		479	(10.5)	
5	24	1500	12.34	375	(-11.5)	424		464	(9.5)	
9	6	1500	12.34	156	(-16.3)	189		217	(14.9)	
9	12	1500	12.34	158	(-16.0)	186		216	(14.6)	
9	24	1500	12.34	158	(-15.8)	188		214	(14.2)	

TABLE A-5. COMPARISON OF SUBGRADE STRAIN (EZ) AT
24-, 30-, AND 36-KIP LOAD.

TAC	TGR	EAC	ERI	24 KIP, 355 PSI		30 KIP, 355 PSI		36 KIP, 355 PSI	
				EZ (% CHANGE)		EZ		EZ (% CHANGE)	
3	6	100	1.00	7931	(-14.7)	9294		10783	(16.0)
3	12	100	1.00	4176	(-13.5)	4830		5473	(13.3)
3	24	100	1.00	2141	(-9.9)	2377		2455	(3.3)
3	6	100	1.00	5392	(-16.9)	6492		7578	(16.7)
5	12	100	1.00	3108	(-17.0)	3745		4189	(11.8)
5	24	100	1.00	1615	(-13.9)	2107		2324	(10.3)
5	6	100	1.00	2876	(-14.5)	3363		3949	(17.4)
9	12	100	1.00	2242	(-12.3)	2556		2664	(4.2)
9	24	100	1.00	1252	(-16.4)	1497		1719	(14.8)
3	6	500	1.00	4939	(-16.9)	5943		7021	(18.1)
3	12	500	1.00	3110	(-17.3)	3759		4202	(11.8)
3	24	500	1.00	1854	(-13.5)	2145		2330	(8.6)
5	6	500	1.00	2783	(-14.1)	3241		3798	(17.2)
5	12	500	1.00	2303	(-10.5)	2574		2742	(6.5)
5	24	500	1.00	1353	(-16.3)	1617		1850	(14.4)
5	6	500	1.00	1432	(-17.6)	1738		2017	(16.0)
9	12	500	1.00	1134	(-18.2)	1385		1618	(16.8)
9	24	500	1.00	739	(-19.4)	917		1082	(18.0)
3	6	1500	1.00	3000	(-13.3)	3461		4034	(16.5)
3	12	1500	1.00	2474	(-5.5)	2619		2856	(9.0)
3	24	1500	1.00	1434	(-16.1)	1710		1950	(14.0)
5	6	1500	1.00	1785	(-16.7)	2143		2464	(14.9)
5	12	1500	1.00	1424	(-17.4)	1725		1994	(15.6)
5	24	1500	1.00	908	(-18.5)	1114		1307	(17.2)
5	6	1500	1.00	748	(-19.6)	930		1103	(18.6)
9	12	1500	1.00	627	(-20.2)	786		940	(19.6)
9	24	1500	1.00	469	(-20.0)	586		701	(19.6)
3	6	100	7.68	5839	(-13.8)	6774		7528	(11.1)
3	12	100	7.68	2994	(-16.7)	3595		4147	(15.3)
3	24	100	7.68	1190	(-16.8)	1430		1654	(15.6)
5	6	100	7.68	4108	(-16.7)	4933		5623	(14.0)
5	12	100	7.68	2227	(-17.6)	2703		3153	(16.6)
5	24	100	7.68	969	(-17.6)	1176		1370	(16.5)
9	6	100	7.68	2050	(-19.9)	2560		3053	(19.3)
9	12	100	7.68	1280	(-19.1)	1582		1870	(18.3)
9	24	100	7.68	616	(-21.3)	782		922	(18.0)

TABLE A-5. COMPARISON OF SUBGRADE STRAIN (EZ) AT 24-, 30-, AND 36-KIP LOAD (CONTINUED).

TAC	TGR	EAC	ERI	24 KIP, 355 PSI		30 KIP, 355 PSI		36 KIP, 355 PSI	
				EZ	(% CHANGE)	EZ	(% CHANGE)	EZ	(% CHANGE)
3	6	500	7.68	4001	(-17.2)	4834		5498	(13.7)
3	12	500	7.68	2275	(-16.1)	2777		3247	(16.9)
3	24	500	7.68	1001	(-17.9)	1219		1423	(16.7)
5	6	500	7.68	2052	(-19.6)	2558		3042	(16.9)
5	12	500	7.68	1362	(-19.2)	1685		1999	(16.7)
5	24	500	7.68	681	(-20.6)	858		1015	(16.3)
9	6	500	7.68	802	(-19.9)	1001		1196	(19.4)
9	12	500	7.68	558	(-23.3)	728		882	(21.1)
9	24	500	7.68	300	(-23.1)	391		484	(23.6)
3	6	1500	7.68	2325	(-19.5)	2869		3423	(18.5)
3	12	1500	7.68	1520	(-19.1)	1878		2224	(18.4)
3	24	1500	7.68	741	(-19.7)	922		1089	(16.1)
5	6	1500	7.68	1040	(-19.6)	1294		1544	(19.4)
5	12	1500	7.68	761	(-20.6)	958		1144	(19.4)
5	24	1500	7.68	394	(-23.5)	515		639	(24.1)
9	6	1500	7.68	332	(-22.8)	430		529	(23.0)
9	12	1500	7.68	245	(-23.3)	319		396	(24.1)
9	24	1500	7.68	153	(-22.4)	198		243	(22.9)
3	6	100	12.34	4690	(-13.3)	5411		6041	(11.7)
3	12	100	12.34	2351	(-16.3)	2808		3237	(15.3)
3	24	100	12.34	945	(-17.1)	1140		1321	(15.9)
5	6	100	12.34	3257	(-17.4)	3945		4536	(15.0)
5	12	100	12.34	1768	(-17.4)	2141		2493	(16.4)
5	24	100	12.34	771	(-17.8)	938		1096	(16.6)
9	6	100	12.34	1662	(-19.5)	2065		2455	(16.9)
9	12	100	12.34	1029	(-19.3)	1274		1508	(16.3)
9	24	100	12.34	506	(-19.3)	627		742	(16.4)
3	6	500	12.34	3218	(-17.6)	3914		4506	(15.1)
3	12	500	12.34	1822	(-17.6)	2217		2584	(16.6)
3	24	500	12.34	799	(-16.1)	975		1142	(17.2)
5	6	500	12.34	1693	(-19.4)	2101		2491	(18.6)
5	12	500	12.34	1100	(-19.7)	1369		1624	(18.6)
5	24	500	12.34	555	(-19.4)	668		817	(16.6)
9	6	500	12.34	667	(-20.3)	837		1005	(20.0)
9	12	500	12.34	474	(-21.3)	602		724	(20.2)
9	24	500	12.34	251	(-23.7)	329		406	(23.6)

TABLE A-5. COMPARISON OF SUBGRADE STRAIN (EZ) AT 24-, 30-, AND 36-KIP LOAD (CONTINUED).

TAC	TGR	EAC	ERI	24 KIP, 355 PSI		30 KIP, 355 PSI		36 KIP, 355 PSI	
				EZ (% CHANGE)		EZ		EZ (% CHANGE)	
3	6	1500	12.34	1942	(-19.3)	2406		2842	(16.2)
3	12	1500	12.34	1237	(-19.6)	1538		1820	(16.3)
3	24	1500	12.34	598	(-19.5)	743		881	(16.5)
5	6	1500	12.34	873	(-20.1)	1093		1307	(19.6)
5	12	1500	12.34	626	(-20.6)	788		946	(20.1)
5	24	1500	12.34	331	(-23.4)	432		529	(22.7)
9	6	1500	12.34	289	(-23.2)	377		464	(23.2)
9	12	1500	12.34	210	(-23.0)	273		339	(24.2)
9	24	1500	12.34	126	(-22.5)	166		204	(23.0)

TABLE A-6. COMPARISON OF SUBGRAPH^a DEVIATOR STRESS (SDEV)
AT 24-, 30-, AND 36-KIP LOAD.

TAC	TGR	EAC	ERI	24 KIP, 355 PSI		30 KIP, 355 PSI		36 KIP, 355 PSI	
				SDEV (% CHANGE)		SDEV		SDEV (% CHANGE)	
3	6	100	1.00	6.2	(0.0)	6.2	(0.0)	6.2	(0.0)
3	12	100	1.00	6.2	(0.0)	6.2	(0.0)	6.2	(0.0)
3	24	100	1.00	4.3	(-10.4)	4.8	(6.2)	5.1	(6.2)
5	6	100	1.00	6.2	(0.0)	6.2	(0.0)	6.2	(0.0)
5	12	100	1.00	6.2	(0.0)	6.2	(0.0)	6.2	(0.0)
5	24	100	1.00	3.7	(-14.0)	4.3	(9.3)	4.7	(9.3)
9	6	100	1.00	5.8	(-6.5)	6.2	(0.0)	6.2	(0.0)
9	12	100	1.00	4.5	(-11.8)	5.1	(5.9)	5.4	(5.9)
9	24	100	1.00	2.7	(-15.6)	3.2	(9.4)	3.5	(9.4)
3	6	500	1.00	6.2	(0.0)	6.2	(0.0)	6.2	(0.0)
3	12	500	1.00	6.2	(0.0)	6.2	(0.0)	6.2	(0.0)
3	24	500	1.00	3.8	(-11.6)	4.3	(9.3)	4.7	(9.3)
5	6	500	1.00	5.5	(-11.3)	6.2	(0.0)	6.2	(0.0)
5	12	500	1.00	4.5	(-11.8)	5.1	(7.8)	5.5	(7.8)
5	24	500	1.00	2.8	(-15.2)	3.3	(12.1)	3.7	(12.1)
9	6	500	1.00	2.8	(-17.6)	3.4	(14.7)	3.9	(14.7)
9	12	500	1.00	2.3	(-17.9)	2.8	(14.3)	3.2	(14.3)
9	24	500	1.00	1.7	(-19.0)	2.1	(9.5)	2.3	(9.5)
3	6	1500	1.00	5.9	(-4.8)	6.2	(0.0)	6.2	(0.0)
3	12	1500	1.00	4.8	(-9.4)	5.3	(9.4)	5.8	(9.4)
3	24	1500	1.00	3.0	(-14.3)	3.5	(11.4)	3.9	(11.4)
5	6	1500	1.00	3.4	(-15.0)	4.0	(15.0)	4.6	(15.0)
5	12	1500	1.00	2.8	(-15.2)	3.3	(15.2)	3.8	(15.2)
5	24	1500	1.00	2.0	(-16.7)	2.4	(12.5)	2.7	(12.5)
9	6	1500	1.00	1.5	(-16.7)	1.8	(16.7)	2.1	(16.7)
9	12	1500	1.00	1.4	(-12.5)	1.6	(18.8)	1.9	(18.8)
9	24	1500	1.00	1.2	(-14.3)	1.4	(14.3)	1.6	(14.3)
3	6	100	7.68	22.8	(0.0)	22.8	(0.0)	22.8	(0.0)
3	12	100	7.68	16.4	(-9.9)	16.2	(20.0)	20.0	(9.9)
3	24	100	7.68	8.7	(-13.0)	10.0	(11.0)	11.1	(11.0)
5	6	100	7.68	19.7	(-12.4)	22.5	(22.8)	22.8	(1.3)
5	12	100	7.68	13.7	(-12.2)	15.6	(17.1)	17.1	(9.6)
5	24	100	7.68	7.4	(-14.0)	8.6	(9.7)	9.7	(12.8)
9	6	100	7.68	12.9	(-14.0)	15.0	(16.6)	16.6	(10.7)
9	12	100	7.68	9.1	(-15.7)	10.8	(12.2)	12.2	(13.0)
9	24	100	7.68	5.4	(-12.9)	6.2	(7.1)	7.1	(14.5)

TABLE A-6. COMPARISON OF SUBGRADE DEVIATOR STRESS (SDEV)
AT 24-, 30-, AND 36-KIP LOAD (CONTINUED).

TAC	TGR	EAC	ERI	24 KIP, 355 PSI		30 KIP, 355 PSI		36 KIP, 355 PSI	
				***	****	*****	*****	*****	*****
3	6	500	7.68	19.3	(-11.9)	21.9	22.8	(-4.1)	
3	12	500	7.68	13.9	(-12.0)	15.8	17.4	(10.1)	
3	24	500	7.68	7.5	(-14.8)	8.8	9.9	(12.5)	
5	6	500	7.68	12.9	(-14.0)	15.0	16.7	(11.3)	
5	12	500	7.68	9.5	(-15.2)	11.2	12.7	(13.4)	
5	24	500	7.68	5.7	(-13.6)	6.6	7.6	(15.2)	
9	6	500	7.68	6.1	(-17.6)	7.4	8.5	(14.9)	
9	12	500	7.68	5.0	(-13.8)	5.8	6.7	(15.5)	
9	24	500	7.68	3.5	(-14.6)	4.1	4.7	(14.6)	
3	6	1500	7.68	14.0	(-13.6)	16.2	17.9	(10.5)	
3	12	1500	7.68	10.3	(-14.9)	12.1	13.7	(13.2)	
3	24	1500	7.68	5.9	(-15.7)	7.0	8.0	(14.3)	
5	6	1500	7.68	7.5	(-16.7)	9.0	10.3	(14.4)	
5	12	1500	7.68	5.9	(-16.9)	7.1	8.2	(15.5)	
5	24	1500	7.68	4.1	(-14.6)	4.8	5.4	(12.5)	
9	6	1500	7.68	3.5	(-16.7)	4.2	4.8	(14.3)	
9	12	1500	7.68	2.9	(-17.1)	3.5	4.0	(14.3)	
9	24	1500	7.68	2.2	(-29.0)	3.1	3.0	(-3.2)	
3	6	100	12.34	32.8	(0.0)	32.8	32.8	(0.0)	
3	12	100	12.34	21.8	(-10.7)	24.4	26.8	(9.8)	
3	24	100	12.34	10.9	(-14.2)	12.7	14.3	(12.6)	
5	6	100	12.34	26.6	(-11.0)	29.9	32.8	(9.7)	
5	12	100	12.34	17.8	(-13.2)	20.5	22.7	(10.7)	
5	24	100	12.34	9.2	(-15.6)	10.9	12.4	(13.8)	
9	6	100	12.34	17.0	(-14.6)	19.9	22.4	(12.6)	
9	12	100	12.34	11.7	(-15.8)	13.9	15.8	(13.7)	
9	24	100	12.34	6.5	(-16.7)	7.8	9.0	(15.4)	
3	6	500	12.34	26.5	(-10.5)	29.6	32.8	(10.8)	
3	12	500	12.34	18.2	(-12.9)	20.9	23.2	(11.0)	
3	24	500	12.34	9.5	(-15.2)	11.2	12.7	(13.4)	
5	6	500	12.34	17.1	(-14.9)	20.1	22.6	(12.4)	
5	12	500	12.34	12.2	(-16.4)	14.6	16.7	(14.4)	
5	24	500	12.34	6.9	(-17.9)	8.4	9.7	(15.5)	
9	6	500	12.34	7.9	(-18.6)	9.7	11.3	(16.5)	
9	12	500	12.34	6.0	(-17.8)	7.3	8.6	(17.8)	
9	24	500	12.34	4.0	(-16.7)	4.8	5.5	(14.6)	

TABLE A-6. COMPARISON OF SUBGRADE DEVIATOR STRESS (SDEV)
AT 24-, 30-, AND 36-KIP LOAD (CONTINUED).

TAC	TGR	EAC	ERI	24 KIP, 355 PSI		30 KIP, 355 PSI		36 KIP, 355 PSI	
				SDEV	SDEV (% CHANGE)	SDEV	SDEV	SDEV	SDEV (% CHANGE)
3	6	1500	12.34	16.9	(-14.1)	22.0		24.5	(11.4)
3	12	1500	12.34	13.4	(-15.7)	15.9		16.1	(13.6)
3	24	1500	12.34	7.4	(-16.9)	6.9		10.2	(14.6)
5	6	1500	12.34	9.9	(-17.5)	12.0		13.9	(15.6)
5	12	1500	12.34	7.5	(-18.5)	9.2		10.7	(16.3)
5	24	1500	12.34	4.8	(-15.8)	5.7		6.6	(15.8)
9	6	1500	12.34	4.2	(-16.0)	5.0		5.9	(16.0)
9	12	1500	12.34	3.4	(-17.1)	4.1		4.7	(14.6)
9	24	1500	12.34	2.4	(-17.2)	2.9		3.4	(17.2)

TABLE A-7. ILLI-PAVE DATA BASE, STRUCTURAL RESPONSES TO 30-KIP/355-PSI LOAD (LOW-QUALITY BASE COURSE).

TAC	TGR	EAC	ERI	DO	D1	D2	D3	AREA	MEAC	MTAC	TOCT	DS	E2	S2	SDEV	SR
3	6	100	1.00	259.6	165.0	73.7	31.5	17.76	1780	219	165	240.7	8799	20.9	6.2	1.00
3	12	100	1.00	174.6	123.7	61.4	31.8	19.81	1055	116	109	150.1	4823	12.4	6.2	1.00
3	24	100	1.00	110.1	77.2	48.0	31.4	21.36	764	98	74.0	2450	10.0	5.0	.61	
5	6	100	1.00	181.5	120.9	65.1	33.6	19.42	1524	193	145	159.5	6384	14.6	6.2	1.00
5	12	100	1.00	139.5	96.8	56.1	33.0	20.58	1043	100	112	111.6	3758	10.3	6.2	1.00
5	24	100	1.00	102.1	69.5	45.7	31.4	21.39	1017	52	109	63.4	2270	10.4	4.6	.74
9	6	100	1.00	112.7	76.0	49.8	32.7	21.13	1194	152	106	89.5	3383	9.4	6.2	1.00
9	9	100	1.00	98.6	66.1	45.4	31.9	21.52	976	104	92	69.0	2633	10.2	5.2	.85
9	12	100	1.00	87.0	57.6	41.7	31.5	21.87	879	74	91	49.3	1620	9.1	3.4	.54
9	24	100	1.00	164.6	109.6	60.8	33.8	19.65	1282	705	417	148.7	5889	13.8	6.2	1.00
3	6	500	1.00	132.5	93.1	54.7	33.3	20.89	897	427	312	111.4	3743	10.3	6.2	1.00
3	12	500	1.00	96.2	69.2	45.6	31.8	22.30	718	294	266	64.8	2306	10.3	4.6	.75
3	24	500	1.00	101.7	75.4	49.4	33.0	22.67	1047	687	365	90.4	3248	9.2	6.2	1.00
5	6	500	1.00	90.1	67.9	46.2	32.5	23.36	872	541	315	72.6	2598	9.5	5.2	.83
5	12	500	1.00	77.8	59.3	42.6	32.0	24.18	747	439	277	51.6	1743	9.1	3.6	.57
5	24	500	1.00	58.7	48.3	39.0	32.3	27.15	496	362	180	50.8	1752	8.1	3.4	.54
9	6	500	1.00	57.2	47.2	38.5	32.2	27.34	470	337	172	45.7	1421	7.5	2.8	.46
9	9	500	1.00	55.0	45.5	37.6	32.1	27.62	440	311	162	38.3	952	7.0	2.1	.34
9	12	500	1.00	55.0	45.5	37.6	32.1	27.62	440	311	162	38.3	952	7.0	2.1	.34
9	24	500	1.00	55.0	45.5	37.6	32.1	27.62	440	311	162	38.3	952	7.0	2.1	.34
3	6	1500	1.00	102.4	72.3	47.4	32.8	21.94	916	1353	694	92.1	3458	9.7	6.2	1.00
3	12	1500	1.00	92.2	66.8	45.2	32.6	22.70	753	1087	593	75.9	2652	9.0	5.3	.86
3	24	1500	1.00	79.3	58.8	42.0	32.2	23.69	626	885	510	53.4	1848	9.3	3.7	.60
5	6	1500	1.00	64.0	52.2	40.3	32.5	26.39	519	881	431	57.6	2159	9.1	4.1	.65
5	12	1500	1.00	62.1	51.0	39.8	32.5	26.67	488	822	411	51.3	1772	8.3	3.4	.55
5	24	1500	1.00	59.0	48.7	38.8	32.8	27.09	452	756	385	41.8	1172	7.4	2.5	.40
9	6	1500	1.00	43.0	38.9	35.1	32.3	31.15	205	374	181	39.2	929	5.6	1.8	.29
9	9	1500	1.00	42.8	38.8	35.0	32.3	31.21	202	367	179	36.8	784	5.6	1.6	.26
9	12	1500	1.00	42.3	38.4	34.8	32.2	31.31	196	356	174	33.4	589	5.9	1.4	.23
9	24	1500	1.00	42.3	38.4	34.8	32.2	31.31	196	356	174	33.4	589	5.9	1.4	.23
3	6	100	7.68	122.9	62.7	23.6	10.6	14.94	955	111	123	106.4	6306	44.1	22.8	1.00
3	12	100	7.68	94.0	55.1	24.3	11.9	16.89	727	61	105	69.8	3494	28.2	18.0	.79
3	24	100	7.68	76.1	45.1	23.5	13.2	17.86	808	8	100	40.0	1528	16.6	10.5	.46
5	6	100	7.68	99.2	54.1	24.6	11.9	16.24	1109	99	120	79.0	4777	33.2	21.7	.95
5	12	100	7.68	84.2	48.5	24.4	12.8	17.31	1030	65	109	56.8	2720	23.6	15.7	.69
5	24	100	7.68	72.9	42.0	23.4	13.6	17.87	1026	51	111	34.8	1271	14.9	9.1	.40
9	6	100	7.68	72.9	40.7	23.1	13.4	17.59	986	106	91	50.2	2556	21.5	14.9	.65
9	12	100	7.68	68.0	38.1	22.6	13.7	17.92	879	80	90	39.2	1628	16.6	11.0	.48
9	24	100	7.68	63.8	35.6	22.0	14.1	18.16	878	66	66	26.6	845	11.9	6.6	.29

TABLE A-7. ILLI-PAVE DATA BASE, STRUCTURAL RESPONSES TO 30-KIP/355-PSI LOAD (LOW-QUALITY BASE COURSE) (CONTINUED).

TAC	TGR	EAC	ERI	DO	D1	D2	D3	AREA	MEAC	MTAC	TOCT	DS	EZ	SZ	SDEV	SR	
3	6	500	7.68	92.2	52.3	24.9	12.6	16.85	1016	495	340	78.4	4692	33.4	21.1	.93	
3	12	500	7.68	76.1	47.7	24.5	13.2	18.1	781	342	281	57.9	2808	24.3	15.9	.70	
3	24	500	7.68	66.5	41.6	23.5	14.0	19.05	698	280	262	35.8	1320	15.1	9.4	.41	
5	6	500	7.68	62.8	41.2	23.5	13.6	19.67	879	558	312	52.0	2564	22.3	15.0	.66	
5	12	500	7.68	58.2	39.1	23.1	14.0	20.27	773	466	283	41.6	1737	17.5	11.4	.50	
5	24	500	7.68	53.7	36.5	22.6	14.5	20.83	708	411	265	28.3	925	12.2	7.1	.31	
9	6	500	7.68	36.7	27.0	19.3	14.1	23.49	447	320	164	29.0	1002	12.0	7.3	.32	
9	9	12	500	7.68	36.3	26.9	19.5	14.4	23.71	433	306	160	25.0	743	10.5	5.9	.26
9	9	24	500	7.68	36.1	26.9	19.7	14.9	23.97	420	294	156	19.2	406	8.7	4.2	.19
3	6	1500	7.68	64.9	40.3	22.9	13.7	18.96	773	1127	596	55.0	2880	24.6	16.1	.71	
3	12	1500	7.68	59.8	38.5	22.7	14.1	19.68	661	944	529	43.6	1935	18.9	12.4	.54	
3	24	1500	7.68	54.8	36.1	22.3	14.6	20.36	591	833	486	29.4	998	12.7	7.5	.33	
5	6	1500	7.68	40.3	29.8	20.1	14.2	22.96	469	790	393	34.2	1301	14.4	9.0	.40	
5	12	1500	7.68	39.6	29.5	20.3	14.5	23.26	448	750	381	29.1	982	12.2	7.2	.32	
5	24	1500	7.68	38.9	29.2	20.5	15.0	23.63	430	716	368	21.7	545	9.5	5.0	.22	
9	6	1500	7.68	24.1	20.2	16.7	14.2	27.89	194	353	173	20.3	421	7.9	4.1	.18	
9	9	12	1500	7.68	24.4	20.5	17.0	14.5	28.03	193	351	172	18.3	312	7.2	3.4	.15
9	9	24	1500	7.68	24.8	20.9	17.5	15.1	28.24	192	347	171	15.6	197	6.8	2.6	.11
3	6	100	12.34	.92.4	43.6	16.1	7.4	14.24	805	54	112	76.4	5022	54.5	32.8	1.00	
3	12	100	12.34	76.0	40.7	17.1	8.3	15.76	769	45	107	52.1	2718	35.1	23.9	.73	
3	24	100	12.34	67.2	37.1	17.6	9.3	16.63	826	15	101	31.1	1216	19.9	13.4	.41	
5	6	100	12.34	79.4	39.5	17.0	8.2	15.16	1053	77	113	59.8	3781	42.5	28.9	.88	
5	12	100	12.34	70.6	37.3	17.6	8.9	16.09	1029	53	110	43.5	2141	29.3	20.4	.62	
5	24	100	12.34	65.3	35.1	16.1	9.7	16.67	1030	51	111	27.2	1011	17.5	11.6	.35	
9	6	100	12.34	62.0	31.6	16.9	9.3	16.29	905	87	91	39.5	2057	27.0	19.8	.60	
9	9	12	100	12.34	59.6	30.8	17.1	9.8	16.63	872	71	91	31.0	1310	20.3	14.1	.43
9	9	24	100	12.34	58.2	30.3	17.6	10.4	16.95	879	63	92	20.8	676	13.5	8.3	.25
3	6	500	12.34	72.9	38.6	17.4	8.6	15.93	910	424	311	60.1	3770	43.2	28.8	.88	
3	12	500	12.34	64.3	36.8	17.9	9.3	17.08	744	315	272	44.5	2230	30.3	21.0	.64	
3	24	500	12.34	58.7	34.8	18.3	10.1	17.90	690	275	260	28.0	1054	17.9	11.9	.36	
5	6	500	12.34	51.7	32.2	17.3	9.6	18.58	809	503	290	41.4	2107	28.6	20.1	.61	
5	12	500	12.34	49.4	31.5	17.6	10.0	19.16	734	135	272	33.1	1412	21.7	14.9	.46	
5	24	500	12.34	47.7	31.1	18.0	10.7	19.69	695	401	260	22.3	744	14.2	8.9	.27	
9	6	500	12.34	31.2	21.9	14.8	10.2	22.11	427	302	157	23.5	640	14.6	9.7	.29	
9	9	12	500	12.34	31.3	22.2	15.2	10.6	22.35	419	294	155	20.0	615	12.2	7.4	.23
9	9	24	500	12.34	31.9	22.6	15.9	11.3	22.68	414	288	154	14.8	340	9.4	4.9	.15

TABLE A-7. ILLI-PAVE DATA BASE, STRUCTURAL RESPONSES TO 30-KIP/355-PSI LOAD (LOW-QUALITY BASE COURSE) (CONTINUED).

TAC	TGR	EAC	ERI	DO	D1	D2	D3	AREA	MEAC	MTAC	TOCT	DS	EZ	SZ	SDEV	SR
3	6	1500	12.34	53.8	31.7	17.0	9.7	17.94	709	1026	553	44.3	2403	32.2	21.9	.67
3	12	1500	12.34	50.7	31.0	17.3	10.1	18.62	624	887	505	34.9	1586	23.7	16.3	.50
3	24	1500	12.34	48.7	30.6	17.8	10.8	19.24	578	814	478	23.3	805	14.9	9.5	.29
5	6	1500	12.34	34.1	24.1	15.4	10.2	21.72	446	748	377	28.0	1102	18.3	12.1	.37
5	12	1500	12.34	34.0	24.3	15.8	10.6	22.03	432	721	369	23.5	810	14.7	9.4	.29
5	24	1500	12.34	34.3	24.8	16.5	11.3	22.42	422	703	363	16.9	457	10.6	5.9	.18
9	6	1500	12.34	19.9	16.1	12.7	10.4	26.48	190	344	169	16.0	368	9.0	4.9	.15
9	12	1500	12.34	20.4	16.5	13.2	10.8	26.67	190	344	170	14.2	268	8.0	4.0	.12
9	24	1500	12.34	21.1	17.3	13.9	11.5	26.97	190	344	170	11.7	165	7.2	2.9	.09

TABLE A-8. ILLI-PAVE DATA BASE, STRUCTURAL RESPONSES TO 30-KIP/355-PSI LOAD (HIGH-QUALITY BASE COURSE).

TAC	TGR	EAC	ERI	DO	D1	D2	D3	AREA	MEAC	MTAC	TOCT	DS	EZ	SZ	SDEV	SR
3	6	100	1.00	245.7	149.5	72.3	32.8	17.63	1530	113	159	219.3	9868	21.1	6.2	1.00
3	12	100	1.00	157.9	99.9	55.6	32.5	19.05	1221	33	115	122.9	4798	11.6	6.2	1.00
3	24	100	1.00	108.4	63.6	41.9	30.5	19.39	1301	11	120	60.6	2223	9.9	4.5	.72
3	48	100	1.00	175.2	113.6	62.7	33.7	19.23	1814	159	155	150.0	6584	14.2	6.2	1.00
5	12	100	1.00	127.6	82.0	50.4	32.1	19.97	1467	84	133	94.4	3586	9.6	6.2	1.00
5	24	100	1.00	97.8	60.0	40.7	30.5	20.22	1386	64	129	54.1	1914	9.4	3.9	.63
5	48	100	1.00	108.5	72.4	48.1	32.3	21.11	1239	164	107	85.2	3334	9.1	6.2	1.00
9	6	100	1.00	93.0	61.0	42.9	31.4	21.42	1051	116	94	63.3	2466	9.8	4.9	.79
9	12	100	1.00	93.0	61.0	42.9	31.4	21.42	1051	91	91	44.7	1366	8.2	2.9	.47
9	24	100	1.00	81.6	52.1	38.5	30.6	21.59	950	91	44.7	63.3	2466	8.2	2.9	.47
3	6	500	1.00	160.0	104.8	59.1	33.6	19.55	1517	820	469	140.6	6098	13.5	6.2	1.00
3	12	500	1.00	120.6	80.6	49.7	32.3	20.57	1161	582	374	94.0	3577	9.5	6.2	1.00
3	24	500	1.00	91.8	60.3	41.1	30.8	21.28	1026	499	339	54.9	1950	9.3	3.9	.64
5	6	500	1.00	98.4	72.7	48.1	32.6	22.72	1059	701	363	86.6	3231	9.0	6.2	1.00
5	12	500	1.00	84.8	63.1	43.9	31.8	23.40	907	578	318	66.5	2527	9.5	5.0	.61
5	24	500	1.00	72.7	54.0	39.6	31.1	24.02	810	503	288	46.9	1479	6.3	3.1	.49
9	6	500	1.00	57.7	47.5	38.5	32.0	27.22	482	350	175	50.2	1722	7.9	3.3	.54
9	12	500	1.00	55.4	45.7	37.5	31.7	27.46	450	321	165	44.6	1344	7.3	2.7	.43
9	24	500	1.00	52.4	43.2	36.1	31.3	27.75	419	294	154	37.3	875	6.8	2.0	.32
3	6	1500	1.00	99.9	70.4	46.4	32.5	21.99	934	696	88.7	3476	9.6	6.2	1.00	
3	12	1500	1.00	87.2	62.5	43.2	31.9	22.74	796	606	69.0	2636	9.4	5.2	.85	
3	24	1500	1.00	74.8	53.9	39.4	31.2	23.46	705	1022	546	48.1	1563	6.3	3.2	.51
5	6	1500	1.00	63.0	51.4	39.9	32.2	26.45	509	862	423	56.7	2124	8.9	4.0	.65
5	12	1500	1.00	60.1	49.3	38.8	32.0	26.79	475	799	398	49.7	1670	8.0	3.2	.52
5	24	1500	1.00	55.9	46.0	37.1	31.5	27.23	440	736	372	40.3	1052	7.0	2.2	.36
9	6	1500	1.00	42.6	38.6	34.8	32.0	31.16	202	368	179	39.2	930	5.6	1.8	.29
9	12	1500	1.00	42.0	38.1	34.4	31.8	31.24	196	356	174	36.8	783	5.6	1.6	.26
9	24	1500	1.00	41.1	37.2	33.8	31.4	31.34	189	342	169	33.3	581	5.9	1.4	.23
3	6	100	7.68	127.3	59.8	23.8	11.0	14.40	1425	33	132	102.8	7210	45.0	22.8	1.00
3	12	100	7.68	98.7	48.8	23.0	12.2	15.46	1305	29	121	63.3	3620	26.8	18.4	.81
3	24	100	7.68	81.8	38.7	20.7	12.8	15.64	1330	16	123	33.9	1308	14.4	9.3	.41
5	6	100	7.68	101.2	52.2	24.1	12.0	15.76	1600	117	142	77.1	5074	32.9	22.8	1.00
5	12	100	7.68	84.8	44.1	22.7	12.7	16.34	1439	77	133	51.6	2659	21.9	15.4	.68
5	24	100	7.68	73.6	36.9	20.5	13.0	16.41	1389	65	130	29.9	1069	12.9	8.0	.35
9	6	100	7.68	71.7	39.3	22.4	13.2	17.43	1081	129	95	48.4	2550	20.6	15.0	.66
9	12	100	7.68	65.6	35.4	21.2	13.3	17.57	987	101	92	36.2	1525	15.3	10.5	.46
9	24	100	7.68	60.7	31.9	19.8	13.4	17.54	933	87	92	23.7	708	10.6	5.8	.26

TABLE A-8. ILLI-PAVE DATA BASE, STRUCTURAL RESPONSES TO 30-KIP/355-PSI LOAD (HIGH-QUALITY BASE COURSE) (CONTINUED).

TAC	TGR	EAC	ERI	DO	D1	D2	D3	AREA	MEAC	MTAC	TOCT	DS	EZ	S2	SDEV	SR
3	6	500	7.68	93.5	51.0	24.4	12.6	16.48	1291	681	408	76.2	4945	32.9	22.6	.99
3	12	500	7.68	78.5	44.0	23.0	13.0	17.24	1091	543	357	52.3	2714	22.3	15.6	.68
3	24	500	7.68	67.2	37.2	20.9	13.3	17.54	1014	494	337	30.6	1105	13.0	6.2	.36
5	6	500	7.68	62.0	40.3	23.0	13.5	19.55	925	599	321	50.4	2546	21.4	15.0	.66
5	12	500	7.68	56.3	36.8	21.9	13.6	19.96	842	529	297	38.6	1625	16.0	10.9	.48
5	24	500	7.68	51.0	33.2	20.5	13.7	20.23	789	488	281	25.4	788	10.9	6.2	.27
9	6	500	7.68	35.9	26.4	18.9	13.9	23.47	439	314	161	28.5	1000	11.6	7.4	.32
9	12	500	7.68	35.0	25.8	18.7	14.0	23.65	422	298	155	24.2	712	10.0	5.7	.25
9	24	500	7.68	33.9	24.9	18.4	14.1	23.83	407	284	150	18.5	374	8.3	4.0	.18
3	6	1500	7.68	64.4	39.6	22.5	13.5	16.83	822	1209	620	53.4	2885	23.7	16.2	.71
3	12	1500	7.68	58.6	36.6	21.6	13.7	19.32	738	1074	567	40.6	1011	17.2	11.8	.52
3	24	1500	7.68	52.9	33.0	20.4	13.8	19.67	686	994	533	26.3	846	11.2	6.5	.29
5	6	1500	7.68	39.7	29.3	19.8	13.9	22.92	467	785	390	33.5	1288	13.9	9.0	.39
5	12	1500	7.68	38.3	28.3	19.5	14.0	23.19	445	746	375	28.0	935	11.4	7.0	.31
5	24	1500	7.68	36.6	27.1	19.0	14.2	23.46	427	712	362	20.6	486	8.9	4.7	.20
9	6	1500	7.68	23.7	19.9	16.4	14.0	27.86	192	348	171	20.2	439	7.9	4.3	.19
9	12	1500	7.68	23.7	19.8	16.5	14.1	27.96	189	342	169	18.3	326	7.2	3.5	.16
9	24	1500	7.68	23.6	19.8	16.6	14.3	28.11	186	335	166	15.5	199	6.7	2.6	.11
3	6	100	12.34	101.2	42.1	15.9	7.5	13.33	1390	51	130	77.2	5818	57.4	32.8	1.00
3	12	100	12.34	84.1	37.1	16.2	8.4	14.20	1328	18	124	48.6	2862	33.8	24.8	.76
3	24	100	12.34	74.8	32.3	15.7	9.0	14.42	1342	12	124	26.5	1047	16.9	11.9	.36
5	6	100	12.34	82.9	38.4	16.6	8.2	14.56	1521	100	137	59.1	4086	42.3	30.9	.94
5	12	100	12.34	73.4	34.6	16.4	8.8	15.06	1426	73	132	40.2	2116	27.2	20.3	.62
5	24	100	12.34	67.5	31.2	15.8	9.2	15.18	1390	65	130	23.4	858	14.9	10.1	.31
9	6	100	12.34	61.5	30.7	16.4	9.2	16.07	1020	113	93	38.2	2064	25.9	20.0	.61
9	12	100	12.34	58.2	28.8	16.0	9.5	16.21	965	95	92	28.7	1232	18.4	13.5	.41
9	24	100	12.34	55.8	27.2	15.6	9.7	16.26	928	86	92	18.6	576	11.9	7.2	.22
3	6	500	12.34	75.9	37.9	17.1	6.6	15.38	1200	623	384	59.2	4021	42.8	30.4	.93
3	12	500	12.34	67.0	34.6	16.6	9.1	16.03	1061	525	350	41.1	2176	28.0	20.7	.63
3	24	500	12.34	60.9	31.4	16.2	9.5	16.31	1009	492	336	24.1	891	15.2	10.4	.32
5	6	500	12.34	51.6	31.5	16.9	9.4	18.38	869	556	304	40.2	2088	27.3	20.0	.61
5	12	500	12.34	48.5	29.9	16.6	9.7	18.71	815	509	289	30.7	1319	19.6	14.2	.43
5	24	500	12.34	45.8	28.2	16.2	10.0	18.95	782	482	279	19.9	635	12.4	7.8	.24
9	6	500	12.34	30.6	21.4	14.5	10.0	22.05	422	299	155	23.1	836	14.1	9.7	.30
9	12	500	12.34	30.2	21.1	14.5	10.2	22.21	411	289	152	19.2	591	11.5	7.2	.22
9	24	500	12.34	29.8	21.0	14.6	10.5	22.42	402	280	149	14.3	315	9.0	4.7	.14

TABLE A-8. ILLI-PAVE DATA BASE, STRUCTURAL RESPONSES TO 30-KIP/355-PSI LOAD (HIGH-QUALITY BASE COURSE) (CONTINUED).

TAC	TGR	EAC	ERI	DO	D1	D2	D3	AREA	MEAC	MTAC	TOCT	DS	EZ	SZ	SDEV	SR
3	6	1500	12.34	54.0	31.2	16.7	9.5	17.71	771	1130	586	43.1	2396	30.8	21.9	.67
3	12	1500	12.34	50.5	29.7	16.4	9.6	18.11	713	1036	551	32.5	1482	21.5	15.5	.47
3	24	1500	12.34	47.6	28.0	16.1	10.1	18.40	679	983	529	20.7	683	12.6	6.3	.26
5	6	1500	12.34	33.6	23.7	15.1	10.0	21.64	447	750	376	27.3	1085	17.5	11.9	.36
5	12	1500	12.34	32.9	23.3	15.1	10.2	21.86	433	724	366	22.4	767	13.6	9.0	.27
5	24	1500	12.34	32.2	22.9	15.1	10.5	22.12	422	703	358	16.0	408	9.6	5.5	.17
9	6	1500	12.34	19.6	15.8	12.5	10.1	26.41	188	339	168	16.0	385	9.0	5.1	.16
9	12	1500	12.34	19.7	15.9	12.6	10.3	26.54	186	336	166	14.1	280	7.9	4.2	.13
9	24	1500	12.34	19.9	16.2	12.9	10.7	26.74	184	333	165	11.7	167	7.1	2.9	.09

TABLE A-9. COMPARISON OF AC TENSILE STRAIN (MEAC) AT 30-KIP/355-PSI LOAD
WITH LOW-, MEDIUM-, AND HIGH-QUALITY BASE COURSE.

TAC	TGR	EAC	ERI	30 KIP, 355 PSI		30 KIP, 355 PSI		30 KIP, 355 PSI	
				K=3000, N=.65	MEAC (% CHANGE)	K=5000, N=.50	MEAC	K=9000, N=.33	MEAC (% CHANGE)
3	6	100	1.00	1780	(28.3)	1368		1530	(10.3)
3	12	100	1.00	1055	(19.5)	863		1221	(38.4)
3	24	100	1.00	764	(-20.9)	965		1301	(34.6)
5	6	100	1.00	1524	(-3.7)	1583		1814	(14.6)
5	12	100	1.00	1043	(-14.9)	1226		1467	(19.7)
5	24	100	1.00	1017	(-11.6)	1153		1386	(20.2)
9	6	100	1.00	1194	(-2.5)	1224		1239	(1.2)
9	12	100	1.00	976	(-4.5)	1022		1051	(2.8)
9	24	100	1.00	879	(-3.5)	911		950	(4.3)
3	6	500	1.00	1282	(-9.1)	1410		1517	(7.6)
3	12	500	1.00	897	(-12.9)	1030		1161	(12.8)
3	24	500	1.00	718	(-17.2)	867		1026	(18.3)
5	6	500	1.00	1047	(-1.0)	1057		1059	(-2)
5	12	500	1.00	872	(-2.6)	896		907	(1.3)
5	24	500	1.00	747	(-4.9)	785		810	(3.2)
9	6	500	1.00	496	(1.3)	490		482	(-1.7)
9	12	500	1.00	470	(1.8)	461		450	(-2.5)
9	24	500	1.00	440	(2.1)	431		419	(-2.8)
3	6	1500	1.00	916	(-1.4)	929		934	(6)
3	12	1500	1.00	753	(-3.4)	779		796	(2.1)
3	24	1500	1.00	626	(-6.8)	671		705	(5.1)
5	6	1500	1.00	519	(8)	515		509	(-1.1)
5	12	1500	1.00	488	(1.1)	483		475	(-1.6)
5	24	1500	1.00	452	(1.0)	448		440	(-1.7)
9	6	1500	1.00	205	(7)	204		202	(-9)
9	12	1500	1.00	202	(1.1)	199		196	(-1.6)
9	24	1500	1.00	196	(1.5)	193		189	(-2.1)
3	6	100	7.68	955	(-11.4)	1077		1425	(32.3)
3	12	100	7.68	727	(-24.1)	957		1305	(36.4)
3	24	100	7.68	808	(-18.8)	996		1330	(33.6)
5	6	100	7.68	1109	(-17.9)	1350		1600	(18.6)
5	12	100	7.68	1030	(-13.5)	1190		1439	(20.9)
5	24	100	7.68	1026	(-11.0)	1153		1389	(20.5)
9	6	100	7.68	986	(-5.1)	1039		1081	(4.0)
9	12	100	7.68	879	(-6.4)	939		987	(5.1)
9	24	100	7.68	878	(-8)	865		933	(5.5)

TABLE A-9. COMPARISON OF AC TENSILE STRAIN (MEAC) AT 30-KIP/355-PSI LOAD
WITH LOW-, MEDIUM-, AND HIGH-QUALITY BASE COURSE (CONTINUED).

TAC	TGR	EAC	ERI	30 KIP, 355 PSI K=3000, N=.65 MEAC (% CHANGE)			30 KIP, 355 PSI K=5000, N=.50 MEAC			30 KIP, 355 PSI K=9000, N=.33 MEAC (% CHANGE)		
				30	355	PSI	30	355	PSI	30	355	PSI
3	6	500	7.68	1016	(-11.9)		1153			1291	(11.9)	
3	12	500	7.68	781	(-16.3)		933			1091	(16.9)	
3	24	500	7.68	698	(-16.1)		852			1014	(19.1)	
5	6	500	7.68	879	(-3.0)		906			925	(2.2)	
5	12	500	7.68	773	(-4.9)		813			842	(3.5)	
5	24	500	7.68	708	(-6.2)		755			789	(4.6)	
9	6	500	7.68	447	(-7.7)		444			439	(-1.1)	
9	12	500	7.68	433	(-1.0)		428			422	(-1.5)	
9	24	500	7.68	420	(-1.4)		415			407	(-2.0)	
3	6	1500	7.68	773	(-3.4)		800			822	(2.6)	
3	12	1500	7.68	661	(-6.2)		705			738	(4.7)	
3	24	1500	7.68	591	(-8.3)		644			686	(6.4)	
5	6	1500	7.68	469	(-1)		469			467	(-4)	
5	12	1500	7.68	448	(-1)		448			445	(-6)	
5	24	1500	7.68	430	(0.0)		430			427	(-7)	
9	6	1500	7.68	194	(-6)		193			192	(-8)	
9	12	1500	7.68	193	(-9)		191			189	(-1.3)	
9	24	1500	7.68	192	(-1.4)		189			186	(-1.9)	
3	6	100	12.34	805	(-21.8)		1029			1390	(35.1)	
3	12	100	12.34	769	(-21.8)		982			1328	(35.2)	
3	24	100	12.34	826	(-1.8)		1008			1342	(33.2)	
5	6	100	12.34	1053	(-1.9)		1267			1521	(20.1)	
5	12	100	12.34	1029	(-12.5)		1176			1426	(21.3)	
5	24	100	12.34	1030	(-10.7)		1153			1390	(20.5)	
9	6	100	12.34	905	(-6.4)		967			1020	(5.4)	
9	12	100	12.34	872	(-4.2)		910			965	(6.0)	
9	24	100	12.34	879	(-2)		877			928	(5.6)	
3	6	500	12.34	910	(-13.6)		1054			1200	(13.6)	
3	12	500	12.34	744	(-17.2)		898			1061	(18.2)	
3	24	500	12.34	690	(-18.4)		845			1009	(19.4)	
5	6	500	12.34	809	(-4.0)		843			869	(3.2)	
5	12	500	12.34	734	(-5.9)		780			815	(4.4)	
5	24	500	12.34	695	(-6.7)		745			782	(5.0)	
9	6	500	12.34	427	(-3)		425			422	(-7)	
9	12	500	12.34	419	(-6)		416			411	(-1.2)	
9	24	500	12.34	414	(-1)		402			402	(-6)	

TABLE A-9. COMPARISON OF AC TENSILE STRAIN (MEAC) AT 30-KIP/355-PSI LOAD
WITH LOW-, MEDIUM-, AND HIGH-QUALITY BASE COURSE (CONTINUED).

TAC	TGR	EAC	ERI	30 KIP, 355 PSI K=3000, N=.65		30 KIP, 355 PSI K=5000, N=.50		30 KIP, 355 PSI K=9000, N=.33	
				MEAC	(% CHANGE)	MEAC	(% CHANGE)	MEAC	(% CHANGE)
3	6	1500	12.34	709	(-4.6)	743		771	(3.8)
3	12	1500	12.34	624	(-7.3)	674		713	(5.6)
3	24	1500	12.34	578	(-8.9)	635		679	(6.9)
5	6	1500	12.34	446	(-2)	447		447	(0)
5	12	1500	12.34	432	(-4)	434		433	(-2)
5	24	1500	12.34	422	(-3)	424		422	(-4)
9	6	1500	12.34	190	(.5)	189		188	(-7)
9	12	1500	12.34	190	(.6)	188		186	(-1.2)
9	24	1500	12.34	190	(1.3)	186		184	(-1.8)

TABLE A-10. COMPARISON OF SUBGRADE STRAIN (EZ) AT 30-KIP/355-PSI LOAD WITH LOW-, MEDIUM-, AND HIGH-QUALITY BASE COURSE.

TAC	TGR	EAC	ERI	30 KIP, 355 PSI		30 KIP, 355 PSI		30 KIP, 355 PSI	
				K=3000, N=.65	EZ (% CHANGE)	K=5000, N=.50	EZ	K=9000, N=.33	EZ (% CHANGE)
3	6	100	1.00	8799	(-5.3)	9294		9868	(-6.2)
3	12	100	1.00	4823	(-2)	4830		4798	(-7)
3	24	100	1.00	2450	(3.0)	2377		2223	(-6.5)
5	6	100	1.00	6384	(-1.7)	6492		6584	(-1.4)
5	12	100	1.00	3758	(-3)	3745		3586	(-4.3)
5	24	100	1.00	2270	(7.7)	2107		1914	(-9.2)
9	6	100	1.00	3383	(-6)	3363		3334	(-9)
9	12	100	1.00	2633	(3.0)	2556		2466	(-3.5)
9	24	100	1.00	1620	(6.2)	1497		1366	(-8.7)
3	6	500	1.00	5889	(-9)	5943		6098	(-2.6)
3	12	500	1.00	3743	(-4)	3759		3577	(-4.6)
3	24	500	1.00	2306	(7.5)	2145		1950	(-9.1)
5	6	500	1.00	3248	(-2)	3241		3231	(-3)
5	12	500	1.00	2598	(-9)	2574		2527	(-1.6)
5	24	500	1.00	1743	(7.8)	1617		1479	(-8.5)
9	6	500	1.00	1752	(-6)	1738		1722	(-1.0)
9	12	500	1.00	1421	(2.6)	1385		1344	(-3.0)
9	24	500	1.00	952	(3.8)	917		875	(-4.6)
3	6	1500	1.00	3458	(-1)	3461		3476	(-4)
3	12	1500	1.00	2652	(1.3)	2619		2636	(-6)
3	24	1500	1.00	1848	(6.1)	1710		1563	(-8.6)
5	6	1500	1.00	2159	(-7)	2143		2124	(-9)
5	12	1500	1.00	1772	(2.6)	1725		1670	(-3.2)
5	24	1500	1.00	1172	(5.1)	1114		1052	(-5.6)
9	6	1500	1.00	929	(-1)	930		930	(-1)
9	12	1500	1.00	784	(-3)	786		783	(-5)
9	24	1500	1.00	589	(.5)	586		581	(-9)
3	6	100	7.68	6306	(-6.9)	6774		7210	(6.4)
3	12	100	7.68	3494	(-2.8)	3595		3620	(-7)
3	24	100	7.68	1528	(6.8)	1430		1308	(-8.6)
5	6	100	7.68	4777	(-3.2)	4933		5074	(2.9)
5	12	100	7.68	2720	(.6)	2703		2659	(-1.6)
5	24	100	7.68	1271	(8.0)	1176		1069	(-9.1)
9	6	100	7.68	2558	(-0)	2560		2550	(-4)
9	12	100	7.68	1628	(2.9)	1582		1525	(-3.5)
9	24	100	7.68	845	(6.1)	782		708	(-9.4)

TABLE A-10. COMPARISON OF SUBGRADE STRAIN (EZ) AT 30-KIP/355-PSI LOAD WITH
LOW-, MEDIUM-, AND HIGH-QUALITY BASE COURSE (CONTINUED).

TAC	TGR	EAC	ERI	30 KIP, 355 PSI			30 KIP, 355 PSI			30 KIP, 355 PSI		
				K=3000, N=.65	EZ (X CHANGE)	EZ	K=5000, N=.50	EZ	K=9000, N=.33	EZ	EZ (% CHANGE)	
3	6	500	7.68	4692	(-2.9)		4834		4945	(-2.3)		
3	12	500	7.68	2808	(1.1)		2777		2714	(-2.3)		
3	24	500	7.68	1320	(6.3)		1219		1105	(-9.3)		
5	6	500	7.68	2564	(-2)		2558		2546	(-5)		
5	12	500	7.68	1737	(3.1)		1685		1625	(-3.6)		
5	24	500	7.68	925	(7.6)		858		788	(-8.2)		
9	6	500	7.68	1002	(-1)		1001		1000	(-1)		
9	12	500	7.68	743	(2.0)		728		712	(-2.2)		
9	24	500	7.68	406	(3.9)		391		374	(-4.2)		
3	6	1500	7.68	2880	(-3)		2889		2885	(-1)		
3	12	1500	7.68	1935	(3.0)		1878		1811	(-3.6)		
3	24	1500	7.68	998	(6.2)		922		846	(-8.3)		
5	6	1500	7.68	1301	(6)		1294		1286	(-4)		
5	12	1500	7.68	982	(2.5)		958		935	(-2.5)		
5	24	1500	7.68	545	(5.6)		515		486	(-5.7)		
9	6	1500	7.68	421	(-2.1)		430		439	(2.1)		
9	12	1500	7.68	312	(-2.3)		319		326	(2.2)		
9	24	1500	7.68	197	(-6)		198		199	(.6)		
3	6	100	12.34	5022	(-7.2)		5411		5818	(7.5)		
3	12	100	12.34	2718	(-3.2)		2808		2862	(1.9)		
3	24	100	12.34	1216	(6.7)		1140		1047	(-8.2)		
5	6	100	12.34	3781	(-4.2)		3945		4086	(3.6)		
5	12	100	12.34	2141	(0)		2141		2116	(-1.2)		
5	24	100	12.34	1011	(7.8)		938		858	(-8.5)		
9	6	100	12.34	2057	(-4)		2065		2064	(-1)		
9	12	100	12.34	1310	(2.6)		1274		1232	(-3.3)		
9	24	100	12.34	676	(7.9)		627		576	(-8.1)		
3	6	500	12.34	3770	(-3.7)		3914		4021	(2.7)		
3	12	500	12.34	2230	(6)		2217		2176	(-1.6)		
3	24	500	12.34	1054	(6.1)		975		891	(-8.6)		
5	6	500	12.34	2107	(3)		2101		2088	(-6)		
5	12	500	12.34	1412	(3.1)		1369		1319	(-3.7)		
5	24	500	12.34	744	(6)		688		635	(-7.6)		
9	6	500	12.34	840	(4)		837		836	(-1)		
9	12	500	12.34	615	(2.2)		602		591	(-1.9)		
9	24	500	12.34	340	(3.6)		329		315	(-4.1)		

TABLE A-10. COMPARISON OF SUBGRADE STRAIN (EZ) AT 30-KIP/355-PSI LOAD WITH
LOW-, MEDIUM-, AND HIGH-QUALITY BASE COURSE (CONTINUED).

TAC	TGR	EAC	ERI	30 KIP, 355 PSI		30 KIP, 355 PSI		30 KIP, 355 PSI	
				K=3000, N=.65		K=5000, N=.50		K=9000, N=.33	
				EZ (% CHANGE)		EZ		EZ (% CHANGE)	
3	6	1500	12.34	2403	(-1)	2406	(-1)	2396	(-4)
3	12	1500	12.34	1586	(3.1)	1538	(-3.7)	1482	(-3.7)
3	24	1500	12.34	805	(8.3)	743	(-8.2)	683	(-8.2)
5	6	1500	12.34	1102	(-1.9)	1093	(-1.7)	1085	(-1.7)
5	12	1500	12.34	810	(2.6)	788	(-2.6)	767	(-2.6)
5	24	1500	12.34	457	(5.9)	432	(-5.5)	408	(-5.5)
9	6	1500	12.34	368	(-2.4)	377	(2.3)	385	(2.3)
9	12	1500	12.34	268	(-1.6)	273	(2.5)	280	(2.5)
9	24	1500	12.34	165	(-.5)	166	(.6)	167	(.6)

AD-A181 596

DEVELOPMENT OF MECHANISTIC FLEXIBLE PAVEMENT DESIGN
CONCEPTS FOR THE HEAV. (U) ILLINOIS UNIV AT URBANA
NEWMARK CIVIL ENGINEERING LAB H F KELLY SEP 86

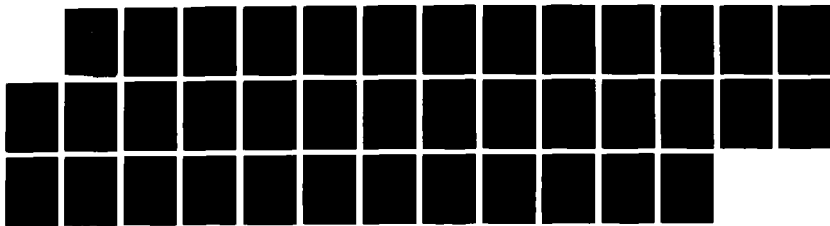
UNCLASSIFIED

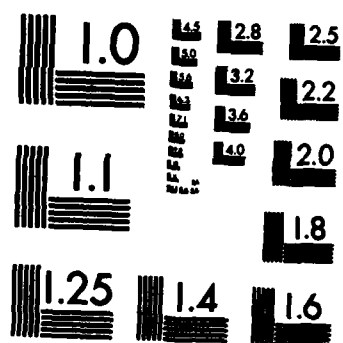
AFESC/ESL-TR-86-32 F08637-85-M-6023

3/3

F/G 1/5

NL





MICROCOPY RESOLUTION TEST CHART
NATIONAL BUREAU OF STANDARDS-1963-A

TABLE A-11. COMPARISON OF SUBGRADE DEVIATOR STRESS (SDEV) AT 30-KIP/355-PSI LOAD
WITH LOW-, MEDIUM-, AND HIGH-QUALITY BASE COURSE.

TAC	TGR	EAC	ERI	30 KIP, 355 PSI K=3000, N=.65		30 KIP, 355 PSI K=5000, N=.50		30 KIP, 355 PSI K=9000, N=.33		SDEV (% CHANGE)	SDEV (% CHANGE)
				30	SDEV (% CHANGE)	30	SDEV	30	SDEV		
3	6	100	1.00	6.2 (0.0)		6.2 (0.0)		6.2 (0.0)		6.2 (0.0)	
3	12	100	1.00	6.2 (0.0)		6.2 (0.0)		6.2 (0.0)		6.2 (0.0)	
3	24	100	1.00	5.0 (4.2)		4.8 (4.2)		4.5 (-6.3)		4.5 (-6.3)	
3	6	100	1.00	6.2 (0.0)		6.2 (0.0)		6.2 (0.0)		6.2 (0.0)	
5	6	100	1.00	6.2 (0.0)		6.2 (0.0)		6.2 (0.0)		6.2 (0.0)	
5	12	100	1.00	6.2 (0.0)		6.2 (0.0)		6.2 (0.0)		6.2 (0.0)	
5	24	100	1.00	4.6 (7.0)		4.3 (7.0)		3.9 (-9.3)		3.9 (-9.3)	
5	6	100	1.00	6.2 (0.0)		6.2 (0.0)		6.2 (0.0)		6.2 (0.0)	
9	6	100	1.00	6.2 (0.0)		5.2 (2.0)		5.1 (-3.9)		4.9 (-3.9)	
9	12	100	1.00	5.2 (2.0)		5.1 (2.0)		5.1 (-3.9)		4.9 (-3.9)	
9	24	100	1.00	3.4 (6.3)		3.2 (6.3)		3.2 (-9.4)		2.9 (-9.4)	
9	6	500	1.00	6.2 (0.0)		6.2 (0.0)		6.2 (0.0)		6.2 (0.0)	
9	12	500	1.00	6.2 (0.0)		6.2 (0.0)		6.2 (0.0)		6.2 (0.0)	
9	24	500	1.00	4.6 (7.0)		4.3 (7.0)		3.9 (-9.3)		3.9 (-9.3)	
9	6	500	1.00	6.2 (0.0)		6.2 (0.0)		6.2 (0.0)		6.2 (0.0)	
5	12	500	1.00	5.2 (2.0)		5.1 (2.0)		5.0 (-2.0)		5.0 (-2.0)	
5	24	500	1.00	3.6 (9.1)		3.3 (9.1)		3.1 (-6.1)		3.1 (-6.1)	
5	6	500	1.00	3.4 (9.1)		3.4 (9.1)		3.3 (-2.9)		3.3 (-2.9)	
9	12	500	1.00	2.8 (0.0)		2.6 (0.0)		2.7 (-3.6)		2.7 (-3.6)	
9	24	500	1.00	2.1 (0.0)		2.1 (0.0)		2.1 (-4.8)		2.0 (-4.8)	
9	6	1500	1.00	6.2 (0.0)		6.2 (0.0)		6.2 (0.0)		6.2 (0.0)	
9	12	1500	1.00	5.3 (0.0)		5.3 (0.0)		5.3 (0.0)		5.2 (0.0)	
9	24	1500	1.00	3.7 (5.7)		3.7 (5.7)		3.5 (-8.6)		3.2 (-8.6)	
5	6	1500	1.00	4.1 (2.5)		4.0 (2.5)		4.0 (0.0)		4.0 (0.0)	
5	12	1500	1.00	3.4 (3.0)		3.3 (3.0)		3.2 (-3.0)		3.2 (-3.0)	
5	24	1500	1.00	2.5 (4.2)		2.4 (4.2)		2.2 (-8.3)		2.2 (-8.3)	
5	6	1500	1.00	1.8 (0.0)		1.8 (0.0)		1.8 (0.0)		1.8 (0.0)	
9	12	1500	1.00	1.6 (0.0)		1.6 (0.0)		1.6 (0.0)		1.6 (0.0)	
9	24	1500	1.00	1.4 (0.0)		1.4 (0.0)		1.4 (0.0)		1.4 (0.0)	
3	6	100	7.68	22.8 (0.0)		22.8 (0.0)		22.8 (0.0)		22.8 (0.0)	
3	12	100	7.68	18.0 (-1.1)		18.2 (-1.1)		18.4 (-1.1)		18.4 (-1.1)	
3	24	100	7.68	10.5 (-5.0)		10.5 (-5.0)		9.3 (-7.0)		9.3 (-7.0)	
3	6	100	7.68	21.7 (-3.6)		21.7 (-3.6)		22.5 (-1.3)		22.5 (-1.3)	
5	12	100	7.68	15.7 (-6.1)		15.6 (-6.1)		15.4 (-1.3)		15.4 (-1.3)	
5	24	100	7.68	9.1 (5.6)		8.6 (5.6)		8.0 (-7.0)		8.0 (-7.0)	
5	6	100	7.68	14.9 (-7.1)		15.0 (-7.1)		15.0 (0.0)		15.0 (0.0)	
9	12	100	7.68	11.0 (1.9)		10.8 (1.9)		10.5 (-2.8)		10.5 (-2.8)	
9	24	100	7.68	6.6 (6.5)		6.2 (6.5)		5.8 (-6.5)		5.8 (-6.5)	

TABLE A-11. COMPARISON OF SUBGRADE DEVIATOR STRESS (SDEV) AT 30-KIP/355-PSI LOAD
WITH LOW-, MEDIUM-, AND HIGH-QUALITY BASE COURSE (CONTINUED).

TAC	TGR	EAC	ERI	30 KIP, 355 PSI K=3000, N=.65 SDEV (% CHANGE)			30 KIP, 355 PSI K=5000, N=.50 SDEV			30 KIP, 355 PSI K=9000, N=.33 SDEV (% CHANGE)			
				***	***	***	***	***	***	***	***	***	***
3	6	500	7.68	21.1	(-3.7)		21.9			22.5	(-2.7)		
3	12	500	7.68	15.9	(-6)		15.6			15.6	(-1.3)		
3	24	500	7.68	9.4	(-6.6)		8.6			8.2	(-6.6)		
5	6	500	7.68	15.0	(0.0)		15.0			15.0	(0.0)		
5	12	500	7.68	11.4	(-1.6)		11.2			10.9	(-2.7)		
5	24	500	7.68	7.1	(-7.6)		6.6			6.2	(-6.1)		
6	6	500	7.68	7.3	(-1.4)		7.4			7.4	(0.0)		
6	12	500	7.68	5.9	(-1.7)		5.8			5.7	(-1.7)		
6	24	500	7.68	4.2	(-2.4)		4.1			4.0	(-2.4)		
9	6	1500	7.68	16.1	(-6)		16.2			16.2	(0.0)		
9	12	1500	7.68	12.4	(-5)		12.1			11.8	(-2.5)		
9	24	1500	7.68	7.5	(-7.1)		7.0			6.5	(-7.1)		
9	6	1500	7.68	9.0	(0.0)		9.0			9.0	(0.0)		
9	12	1500	7.68	7.2	(-1.4)		7.1			7.0	(-1.4)		
9	24	1500	7.68	5.0	(-4.2)		4.8			4.7	(-2.1)		
9	6	1500	7.68	4.1	(-2.4)		4.2			4.3	(-2.4)		
9	12	1500	7.68	3.4	(-2.9)		3.5			3.5	(0.0)		
9	24	1500	7.68	2.6	(-16.1)		3.1			2.6	(-16.1)		
9	6	100	12.34	32.8	(0.0)		32.8			32.8	(0.0)		
9	12	100	12.34	23.9	(-2.0)		24.4			24.8	(-1.6)		
9	24	100	12.34	13.4	(-5.5)		12.7			11.9	(-6.3)		
9	6	100	12.34	28.9	(-3.3)		29.9			30.9	(-3.3)		
9	12	100	12.34	20.4	(-5)		20.5			20.3	(-1.0)		
9	24	100	12.34	11.6	(-6.4)		10.9			10.1	(-7.3)		
9	9	6	100	12.34	19.8	(-5)	19.9			20.0	(-5)		
9	9	12	100	12.34	14.1	(-1.4)	13.9			13.5	(-2.9)		
9	9	24	100	12.34	8.3	(-6.4)	7.8			7.2	(-7.7)		
9	9	6	500	12.34	28.8	(-2.7)	29.6			30.4	(-2.7)		
9	9	12	500	12.34	21.0	(-5)	20.9			20.7	(-1.0)		
9	9	24	500	12.34	11.9	(-6.2)	11.2			10.4	(-7.1)		
9	6	500	12.34	20.1	(0.0)		20.1			20.0	(-5)		
9	12	500	12.34	14.9	(-2.1)		14.6			14.2	(-2.7)		
9	24	500	12.34	8.9	(-6.0)		8.4			7.8	(-7.1)		
9	6	500	12.34	9.7	(0.0)		9.7			9.7	(0.0)		
9	12	500	12.34	7.4	(-1.4)		7.3			7.2	(-1.4)		
9	24	500	12.34	4.9	(-2.1)		4.8			4.7	(-2.1)		

TABLE A-11. COMPARISON OF SUBGRADE DEVIATOR STRESS (SDEV) AT 30-KIP/355-PSI LOAD
WITH LOW-, MEDIUM-, AND HIGH-QUALITY BASE COURSE (CONTINUED).

TAC	TGR	EAC	ERI	30 KIP, 355 PSI K=3000, N=.65		30 KIP, 355 PSI K=5000, N=.50		30 KIP, 355 PSI K=9000, N=.33	
				SDEV	(% CHANGE)	SDEV	(% CHANGE)	SDEV	(% CHANGE)
3	6	1500	12.34	21.9	(-5)	22.0		21.9	(-5)
3	12	1500	12.34	16.3	(2.5)	15.9		15.5	(-2.5)
3	24	1500	12.34	9.5	(6.7)	8.9		8.3	(-6.7)
5	6	1500	12.34	12.1	(.8)	12.0		11.9	(-8)
5	12	1500	12.34	9.4	(2.2)	9.2		9.0	(-2.2)
5	24	1500	12.34	5.9	(3.5)	5.7		5.5	(-3.5)
9	6	1500	12.34	4.9	(-2.0)	5.0		5.1	(2.0)
9	12	1500	12.34	4.0	(-2.4)	4.1		4.2	(2.4)
9	24	1500	12.34	2.9	(0.0)	2.9		2.9	(0.0)

TABLE A-12. ILLI-PAVE DATA BASE, STRUCTURAL RESPONSES TO 36-KIP/395-PSI LOAD.

TAC	TGR	EAC	ERI	DO	D1	D2	D3	AREA	MEAC	MITAC	TOCT	DS	EZ	SZ	SDEV	SR	
3	6	100	100	100	313.8	203.3	96.2	41.7	16.25	1795	204	191	289.5	10924	25.0	6.2	1.00
3	12	100	100	100	195.8	135.9	71.6	39.9	19.93	884	79	118	164.2	5622	13.6	6.2	1.00
3	24	100	100	100	125.4	84.1	54.4	37.6	21.06	991	14	113	80.6	2590	10.5	6.3	.65
3	5	6	100	100	214.0	143.9	79.6	42.1	19.72	1724	160	162	187.6	7647	16.6	6.2	1.00
5	12	100	100	100	157.4	108.2	65.3	40.3	20.76	1292	79	131	123.7	4269	11.1	6.2	1.00
5	24	100	100	100	115.8	76.9	52.1	37.7	21.34	1223	52	127	70.4	2400	11.0	4.8	.75
5	9	6	100	100	132.5	90.4	59.9	40.0	21.43	1389	177	122	106.2	3961	10.3	6.2	1.00
9	12	100	100	100	113.3	76.4	53.5	36.6	21.60	1139	111	105	79.9	2867	10.6	5.8	.93
9	24	100	100	100	98.6	65.4	48.4	37.6	22.12	1009	78	100	56.7	1735	9.6	3.6	.58
3	6	500	100	100	195.5	130.6	73.5	41.5	19.61	1567	606	496	175.7	6689	15.6	6.2	1.00
3	12	500	100	100	152.3	106.5	64.1	40.5	21.04	1107	506	372	126.0	4307	11.1	6.2	1.00
3	24	500	100	100	109.7	77.3	52.3	38.1	22.27	919	385	324	72.0	2432	10.6	4.8	.78
5	6	500	100	100	120.5	90.0	59.5	40.1	22.66	1212	796	419	107.1	3825	10.3	6.2	1.00
5	12	500	100	100	104.3	78.9	54.6	39.2	23.62	1008	629	359	84.0	2890	10.1	5.8	.93
5	24	500	100	100	88.6	67.7	49.5	38.4	24.42	871	521	317	59.6	1873	9.7	3.6	.61
5	9	6	500	100	69.9	57.9	46.9	39.0	27.34	575	418	208	61.1	2044	9.1	3.9	.63
9	12	500	100	100	67.5	56.0	46.0	38.8	27.56	536	383	197	54.7	1631	8.4	3.2	.52
9	24	500	100	100	64.2	53.3	44.5	38.4	27.89	498	349	184	46.0	1087	7.7	2.3	.38
3	6	1500	100	100	121.6	86.5	57.0	39.8	22.13	1063	1570	799	109.1	4062	11.0	6.2	1.00
3	12	1500	100	100	107.6	78.4	53.8	39.3	22.93	876	1267	680	88.2	2994	9.6	6.0	.97
3	24	1500	100	100	91.0	67.4	49.1	38.5	23.90	739	1054	590	61.3	1979	9.8	4.0	.64
5	6	1500	100	100	76.4	62.6	48.5	39.2	26.53	600	1016	498	69.0	2525	10.4	4.7	.76
5	12	1500	100	100	73.3	60.4	47.1	39.1	26.67	557	937	469	61.1	2022	9.3	3.9	.63
5	24	1500	100	100	68.7	56.9	45.6	38.7	27.35	512	854	436	49.9	1314	8.1	2.7	.44
9	6	1500	100	100	51.6	46.9	42.3	38.9	31.25	240	438	212	47.5	1111	6.5	2.1	.34
9	12	1500	100	100	51.2	46.5	42.1	38.8	31.33	234	426	208	44.7	945	6.4	1.9	.31
9	24	1500	100	100	50.2	45.7	41.5	38.5	31.43	226	410	202	40.5	703	6.5	1.6	.26
3	6	100	7.6	149.0	75.3	29.8	13.2	15.00	1118	115	142	127.5	7763	51.2	22.8	1.00	
3	12	100	7.6	112.0	63.6	29.0	14.7	16.71	976	46	118	80.8	4221	31.1	20.2	.89	
3	24	100	7.6	89.3	49.8	26.8	15.9	17.35	1029	12	116	44.4	1671	17.5	11.3	.49	
5	6	100	7.6	118.5	64.9	30.3	14.7	16.38	1451	110	141	94.2	5728	37.6	22.8	1.00	
5	12	100	7.6	98.3	55.6	28.7	15.6	17.25	1263	67	129	65.0	3188	25.8	17.5	.77	
5	24	100	7.6	84.0	46.7	26.4	16.1	17.61	1226	52	127	38.9	1382	15.6	9.8	.43	
9	6	100	7.6	85.7	48.5	27.7	16.2	17.61	1175	129	106	59.8	3087	24.0	16.9	.74	
9	12	100	7.6	78.4	44.1	26.5	16.4	18.06	1048	90	101	45.6	1888	18.2	12.3	.54	
9	24	100	7.6	72.3	39.9	25.0	16.6	18.17	981	71	101	30.4	928	12.6	7.1	.31	

TABLE A-12. ILLI-PAVE DATA BASE, STRUCTURAL RESPONSES TO 36-KIP/395-PSI LOAD (CONTINUED).

TAC	TGR	EAC	ERI	DO	D1	D2	D3	AREA	MEAC	MTAC	TOCT	DS	EZ	SZ	SDEV	SR
3	6	500	7.68	110.9	63.1	30.4	15.4	16.95	1269	624	412	93.4	5619	37.7	22.8	1.00
3	12	500	7.68	92.0	55.3	28.9	16.0	16.04	1000	441	344	66.3	3286	26.4	17.7	.76
3	24	500	7.68	77.2	46.6	26.7	16.5	16.72	904	376	321	39.9	1436	16.9	10.0	.44
3	5	6	500	7.68	49.6	28.3	16.5	19.81	1034	661	363	62.1	3067	25.0	17.0	.75
5	12	500	7.68	68.0	45.7	27.3	16.7	20.36	914	558	330	48.6	2021	19.2	12.6	.56
5	24	500	7.68	61.3	41.4	25.6	17.0	20.81	639	497	327	48.5	1022	13.1	7.7	.34
9	6	500	7.68	43.4	32.3	23.1	16.9	23.64	521	372	191	34.6	1210	13.5	8.6	.39
9	12	500	7.68	42.4	31.6	22.9	17.1	23.84	499	351	184	29.6	889	11.6	6.7	.29
9	24	500	7.68	41.4	30.9	22.6	17.4	24.08	479	333	178	22.9	485	9.6	4.7	.21
3	6	1500	7.68	77.6	48.6	27.6	16.6	19.08	912	1333	695	65.6	3478	27.6	16.3	.80
3	12	1500	7.68	70.3	45.2	26.6	16.6	19.72	787	1131	619	51.0	2254	20.7	13.8	.61
3	24	1500	7.68	63.1	41.0	25.5	17.1	20.29	710	1011	570	33.7	1099	13.5	8.1	.36
5	6	1500	7.68	48.1	35.7	24.5	17.0	23.05	545	918	457	41.0	1567	16.4	10.5	.46
5	12	1500	7.68	46.6	34.6	23.9	17.2	23.35	517	865	438	34.6	1156	13.5	8.3	.36
5	24	1500	7.68	44.7	33.6	23.6	17.5	23.69	491	818	420	25.7	643	10.5	5.5	.24
9	6	1500	7.68	28.7	24.1	19.9	17.0	27.98	228	414	203	24.5	533	9.0	4.8	.21
9	12	1500	7.68	24.2	20.1	17.2	17.2	28.10	225	408	201	22.1	398	8.2	4.0	.16
9	24	1500	7.68	28.8	24.4	20.4	17.5	28.27	221	401	198	18.8	244	7.5	3.0	.13
3	6	100	12.34	112.8	52.5	19.6	9.1	14.17	1062	36	131	91.9	6207	63.5	32.8	1.00
3	12	100	12.34	91.6	47.0	20.5	10.1	15.50	1007	25	118	60.4	3287	39.1	27.3	.83
3	24	100	12.34	79.6	41.0	20.2	11.2	16.07	1044	18	117	34.7	1335	21.0	14.5	.44
5	6	100	12.34	95.2	47.3	20.7	10.6	15.20	1356	88	135	71.5	4637	48.1	32.8	1.00
5	12	100	12.34	83.2	43.0	20.6	10.6	15.98	1246	61	129	50.2	2528	32.2	23.1	.70
5	24	100	12.34	75.6	39.0	20.4	11.5	16.34	1226	51	128	30.4	1106	18.4	12.5	.38
9	6	100	12.34	72.7	37.6	20.2	11.3	16.46	1090	108	103	47.0	2490	30.5	22.7	.69
9	12	100	12.34	68.6	35.6	20.0	11.6	16.71	1014	81	101	36.0	1524	22.3	16.0	.49
9	24	100	12.34	65.9	33.9	19.6	12.1	16.89	972	69	102	23.8	747	14.4	9.0	.27
3	6	500	12.34	88.2	46.6	21.2	10.5	15.94	1153	551	381	71.8	4609	48.8	32.8	1.00
3	12	500	12.34	76.5	42.9	21.1	11.2	16.91	961	417	335	51.4	2626	33.3	23.6	.72
3	24	500	12.34	68.6	39.1	20.7	11.9	17.49	897	375	320	31.3	1153	16.9	12.8	.39
5	6	500	12.34	61.6	38.5	20.8	11.5	16.68	957	601	340	49.3	2535	32.2	23.0	.70
5	12	500	12.34	57.7	36.8	20.6	11.9	19.17	874	528	318	38.4	1644	23.8	16.9	.51
5	24	500	12.34	54.5	35.0	20.4	12.4	19.57	826	488	303	25.5	824	15.2	9.7	.30
9	6	500	12.34	36.8	26.1	17.7	12.2	22.24	498	352	183	28.2	1017	16.7	11.4	.35
9	12	500	12.34	36.5	25.9	17.8	12.5	22.44	484	338	179	23.7	730	13.6	8.6	.26
9	24	500	12.34	36.3	26.0	18.1	13.0	22.71	473	328	176	17.7	408	10.5	5.5	.17

TABLE A-12. ILLI-PAVE DATA BASE, STRUCTURAL RESPONSES TO 36-KIP/395-PSI LOAD (CONTINUED).

TAC	TGR	EAC	ERI	DO	D1	D2	D3	AREA	MEAC	MTAC	TOCT	DS	EZ	SZ	SDEV	SR
3	6	1500	12.34	64.2	36.0	20.4	11.6	16.00	643	1225	649	52.7	2898	36.1	25.0	.76
3	12	1500	12.34	59.6	36.4	20.3	12.0	16.59	750	1074	595	40.7	1846	26.1	18.3	.66
3	24	1500	12.34	56.1	34.6	20.2	12.5	19.06	699	994	563	26.5	869	15.9	10.3	.32
5	6	1500	12.34	40.6	28.9	18.4	12.2	21.79	519	870	437	33.5	1328	20.8	14.1	.43
5	12	1500	12.34	39.8	28.5	18.5	12.5	22.07	499	833	425	27.6	956	16.4	10.6	.33
5	24	1500	12.34	39.2	28.3	18.6	13.0	22.40	484	805	415	20.0	533	11.7	6.6	.20
9	6	1500	12.34	23.6	19.1	15.1	12.3	26.55	223	403	199	19.3	469	10.4	5.8	.16
9	12	1500	12.34	23.9	19.4	15.4	12.6	26.70	221	400	196	17.1	341	9.1	4.8	.16
9	24	1500	12.34	24.3	19.9	16.0	13.2	26.95	220	397	197	14.1	205	8.0	3.4	.10

TABLE A-13. COMPARISON OF AC TENSILE STRAIN (MEAC) AT 30-KIP/355-PSI AND 36-KIP/355-PSI LOAD TO 36-KIP/395-PSI LOAD.

TAC	TGR	EAC	ERI	30 KIP, 355 PSI		36 KIP, 395 PSI		36 KIP, 355 PSI	
				MEAC	(% CHANGE)	MEAC	(% CHANGE)	MEAC	(% CHANGE)
3	6	100	1.00	1386	(-22.7)	1795	1291	(-28.1)	
3	12	100	1.00	883	(-1)	884	812	(-8.1)	
3	24	100	1.00	965	(-2.6)	991	909	(-8.3)	
5	6	100	1.00	1583	(-8.2)	1724	1653	(-4.1)	
5	12	100	1.00	1226	(-5.1)	1292	1212	(-6.2)	
5	24	100	1.00	1153	(-5.7)	1223	1149	(-6.0)	
9	6	100	1.00	1224	(-11.9)	1369	1355	(-2.4)	
9	12	100	1.00	1022	(-10.3)	1139	1106	(-3.0)	
9	24	100	1.00	911	(-9.7)	1009	979	(-3.0)	
3	6	500	1.00	1410	(-10.0)	1567	1489	(-5.0)	
3	12	500	1.00	1030	(-7.0)	1107	1033	(-6.7)	
3	24	500	1.00	867	(-5.6)	919	856	(-6.8)	
5	6	500	1.00	1057	(-12.6)	1212	1168	(-3.6)	
5	12	500	1.00	896	(-11.1)	1008	967	(-4.0)	
5	24	500	1.00	785	(-9.9)	871	831	(-4.6)	
9	6	500	1.00	490	(-14.7)	575	561	(-2.4)	
9	12	500	1.00	461	(-14.0)	536	523	(-2.5)	
9	24	500	1.00	431	(-13.5)	498	485	(-2.6)	
3	6	1500	1.00	929	(-12.6)	1063	1017	(-4.3)	
3	12	1500	1.00	779	(-11.0)	876	835	(-4.7)	
3	24	1500	1.00	671	(-9.2)	739	700	(-5.3)	
5	6	1500	1.00	515	(-14.1)	600	579	(-3.5)	
5	12	1500	1.00	483	(-13.3)	557	537	(-3.7)	
5	24	1500	1.00	416	(-12.5)	512	492	(-3.9)	
9	6	1500	1.00	204	(-15.2)	240	235	(-2.3)	
9	12	1500	1.00	199	(-14.9)	234	229	(-2.4)	
9	24	1500	1.00	193	(-14.7)	226	221	(-2.4)	
3	6	100	7.68	1077	(-3.7)	1118	1033	(-7.7)	
3	12	100	7.68	957	(-2.0)	976	906	(-7.2)	
3	24	100	7.68	996	(-3.2)	1029	949	(-7.8)	
5	6	100	7.68	1350	(-7.0)	1451	1371	(-5.5)	
5	12	100	7.68	1190	(-5.7)	1263	1184	(-6.2)	
5	24	100	7.68	1153	(-6.0)	1226	1153	(-6.0)	
9	6	100	7.68	1039	(-11.6)	1175	1142	(-2.8)	
9	12	100	7.68	939	(-10.4)	1048	1016	(-3.0)	
9	24	100	7.68	885	(-9.8)	981	951	(-3.0)	

TABLE A-13. COMPARISON OF AC TENSILE STRAIN (MEAC) AT 30-KIP/355-PSI AND 36-KIP/355-PSI LOAD TO 36-KIP/395-PSI LOAD (CONTINUED).

TAC	TGR	EAC	ERI	30 KIP, 355 PSI		36 KIP, 395 PSI		36 KIP, 395 PSI	
				MEAC	(% CHANGE)	MEAC	(% CHANGE)	MEAC	(% CHANGE)
3	6	500	7.68	1153	(-9.1)	1269	(-5.9)	1194	(-5.9)
3	12	500	7.68	933	(-6.7)	1000	(-6.4)	935	(-6.9)
3	24	500	7.68	852	(-5.6)	904	(-6.1)	841	(-6.9)
5	6	500	7.68	906	(-12.4)	1034	(-9.2)	990	(-4.2)
5	12	500	7.68	813	(-11.0)	914	(-4.5)	872	(-4.7)
5	24	500	7.68	755	(-10.0)	839	(-4.7)	799	(-4.7)
9	6	500	7.68	444	(-14.7)	521	(-2.6)	508	(-2.6)
9	12	500	7.68	428	(-14.1)	499	(-2.6)	486	(-2.6)
9	24	500	7.68	415	(-13.5)	479	(-2.7)	467	(-2.7)
9	6	1500	7.68	800	(-12.2)	912	(-4.6)	868	(-4.6)
9	12	1500	7.68	705	(-10.5)	787	(-5.1)	747	(-5.1)
9	24	1500	7.68	644	(-9.3)	710	(-5.4)	672	(-5.4)
5	6	1500	7.68	469	(-14.0)	545	(-3.6)	525	(-3.6)
5	12	1500	7.68	448	(-13.3)	517	(-3.9)	497	(-3.9)
5	24	1500	7.68	430	(-12.5)	491	(-4.0)	472	(-4.0)
9	6	1500	7.68	193	(-15.2)	228	(-2.5)	222	(-2.5)
9	12	1500	7.68	191	(-14.9)	225	(-2.4)	220	(-2.4)
9	24	1500	7.68	189	(-14.6)	221	(-2.5)	216	(-2.5)
9	6	100	12.34	1029	(-3.1)	1062	(-6.6)	991	(-6.6)
9	12	100	12.34	982	(-2.5)	1007	(-7.2)	935	(-7.6)
9	24	100	12.34	1008	(-3.5)	1044	(-6.6)	964	(-7.6)
5	6	100	12.34	1267	(-6.7)	1358	(-5.8)	1279	(-5.8)
5	12	100	12.34	1176	(-5.6)	1248	(-6.2)	1171	(-6.2)
5	24	100	12.34	1153	(-6.1)	1228	(-6.0)	1155	(-6.0)
9	6	100	12.34	967	(-11.2)	1090	(-3.0)	1057	(-3.0)
9	12	100	12.34	910	(-10.2)	1014	(-3.1)	982	(-3.1)
9	24	100	12.34	877	(-9.6)	972	(-3.0)	943	(-3.0)
9	6	500	12.34	1054	(-8.6)	1153	(-6.0)	1084	(-6.0)
9	12	500	12.34	898	(-6.5)	961	(-6.7)	897	(-6.7)
9	24	500	12.34	845	(-5.6)	897	(-7.0)	834	(-7.0)
5	6	500	12.34	843	(-12.0)	957	(-4.5)	915	(-4.5)
5	12	500	12.34	780	(-10.7)	874	(-4.7)	833	(-4.7)
5	24	500	12.34	745	(-9.9)	826	(-4.6)	787	(-4.6)
9	6	500	12.34	425	(-14.5)	498	(-2.6)	485	(-2.6)
9	12	500	12.34	416	(-13.9)	484	(-2.7)	471	(-2.7)
9	24	500	12.34	410	(-13.4)	473	(-2.7)	460	(-2.7)

TABLE A-13. COMPARISON OF AC TENSILE STRAIN (MEAC) AT 30-KIP/355-PSI AND 36-KIP/355-PSI LOAD TO 36-KIP/395-PSI LOAD (CONTINUED).

TAC	TGR	EAC	ERI	30 KIP, 355 PSI		36 KIP, 395 PSI		36 KIP, 355 PSI	
				MEAC	(% CHANGE)	MEAC	(% CHANGE)	MEAC	(% CHANGE)
3	6	1500	12.34	743	(-11.6)	843		801	(-5.0)
3	12	1500	12.34	674	(-10.2)	750		710	(-5.3)
3	24	1500	12.34	635	(-9.2)	699		660	(-5.5)
5	6	1500	12.34	447	(-13.6)	519		499	(-3.9)
5	12	1500	12.34	434	(-13.1)	499		479	(-4.0)
5	24	1500	12.34	424	(-12.4)	464		464	(-4.1)
9	6	1500	12.34	189	(-15.1)	223		217	(-2.5)
9	12	1500	12.34	188	(-14.9)	221		216	(-2.5)
9	24	1500	12.34	188	(-14.6)	220		214	(-2.5)

TABLE A-14. COMPARISON OF SUBGRADE STRAIN (EZ) AT 30-KIP/355-PSI AND 36-KIP/355-PSI LOAD TO 36-KIP/395-PSI LOAD.

TAC	TGR	EAC	ERI	30 KIP, 355 PSI		36 KIP, 395 PSI		36 KIP, 355 PSI	
				EZ (% CHANGE)		EZ		EZ (% CHANGE)	
3	6	100	1.00	9294	(-14.9)	10924		10763	(-1.3)
3	12	100	1.00	4830	(-14.1)	5622		5473	(-2.7)
3	24	100	1.00	2377	(-6.2)	2590		2455	(-5.2)
5	6	100	1.00	6492	(-15.1)	7647		7578	(-1.9)
5	12	100	1.00	3745	(-12.3)	4269		4189	(-1.9)
5	24	100	1.00	2107	(-12.2)	2400		2324	(-3.2)
9	6	100	1.00	3363	(-15.1)	3961		3949	(-1.3)
9	12	100	1.00	2556	(-10.9)	2867		2664	(-7.1)
9	24	100	1.00	1497	(-13.7)	1735		1719	(-1.9)
3	6	500	1.00	5943	(-13.7)	6889		7021	(-1.9)
3	12	500	1.00	3759	(-12.7)	4307		4202	(-2.4)
3	24	500	1.00	2145	(-11.6)	2432		2330	(-4.2)
5	6	500	1.00	3241	(-15.3)	3825		3798	(-1.7)
5	12	500	1.00	2574	(-10.9)	2890		2742	(-5.1)
5	24	500	1.00	1617	(-13.7)	1873		1850	(-1.2)
9	6	500	1.00	1738	(-14.9)	2044		2017	(-1.3)
9	12	500	1.00	1385	(-15.1)	1631		1618	(-1.8)
9	24	500	1.00	917	(-15.6)	1087		1082	(-1.4)
3	6	1500	1.00	3461	(-14.8)	4062		4034	(-1.7)
3	12	1500	1.00	2619	(-12.5)	2994		2856	(-4.6)
3	24	1500	1.00	1710	(-13.6)	1979		1950	(-1.5)
5	6	1500	1.00	2143	(-15.1)	2525		2464	(-2.4)
5	12	1500	1.00	1725	(-14.7)	2022		1994	(-1.4)
5	24	1500	1.00	1114	(-15.2)	1314		1307	(-1.6)
9	6	1500	1.00	930	(-16.3)	1111		1103	(-1.7)
9	12	1500	1.00	786	(-16.8)	945		940	(-1.5)
9	24	1500	1.00	586	(-16.7)	703		701	(-1.3)
3	6	100	7.68	6774	(-12.7)	7763		7528	(-3.0)
3	12	100	7.68	3595	(-14.8)	4221		4147	(-1.6)
3	24	100	7.68	1430	(-14.4)	1671		1654	(-1.0)
5	6	100	7.68	4933	(-13.9)	5728		5623	(-1.6)
5	12	100	7.68	2703	(-15.2)	3188		3153	(-1.1)
5	24	100	7.68	1176	(-14.9)	1382		1370	(-1.9)
9	6	100	7.68	2560	(-17.1)	3087		3053	(-1.1)
9	12	100	7.68	1582	(-16.2)	1888		1870	(-1.9)
9	24	100	7.68	782	(-15.6)	928		922	(-1.7)

TABLE A-14. COMPARISON OF SUBGRADE STRAIN (EZ) AT 30-KIP/355-PSI AND 36-KIP/355-PSI LOAD TO 36 KIP/395-PSI LOAD (CONTINUED).

TAC	TGR	EAC	30 KIP, 355 PSI		36 KIP, 395 PSI		36 KIP, 355 PSI	
			ERI	EZ (% CHANGE)	ERI	EZ (% CHANGE)	ERI	EZ (% CHANGE)
3	6	500	7.66	4634 (-14.0)	5619	5498 (-2.2)		
3	12	500	7.66	2777 (-15.6)	3288	3247 (-1.2)		
3	24	500	7.66	1219 (-15.1)	1436	1423 (-1.9)		
5	6	500	7.66	2558 (-17.1)	3087	3042 (-1.4)		
5	12	500	7.66	1685 (-16.7)	2021	1999 (-1.1)		
5	24	500	7.66	856 (-16.1)	1022	1015 (-.7)		
6	6	500	7.66	1001 (-17.3)	1210	1196 (-1.2)		
6	12	500	7.66	726 (-16.1)	889	882 (-.9)		
6	24	500	7.66	391 (-19.5)	485	484 (-.4)		
3	6	1500	7.66	2869 (-16.9)	3478	3423 (-1.6)		
3	12	1500	7.66	1976 (-16.7)	2254	2224 (-1.3)		
3	24	1500	7.66	922 (-16.1)	1099	1089 (-.9)		
5	6	1500	7.66	1294 (-17.4)	1567	1544 (-1.4)		
5	12	1500	7.66	958 (-17.1)	1156	1144 (-1.1)		
5	24	1500	7.66	515 (-19.9)	643	639 (-.6)		
9	6	1500	7.66	430 (-19.4)	533	529 (-.6)		
9	12	1500	7.66	319 (-20.0)	398	396 (-.7)		
9	24	1500	7.66	198 (-19.0)	244	243 (-.5)		
3	6	100	12.34	5411 (-12.6)	6207	6041 (-2.7)		
3	12	100	12.34	2808 (-14.6)	3237	3237 (-1.5)		
3	24	100	12.34	1140 (-14.6)	1335	1321 (-1.1)		
5	6	100	12.34	3945 (-14.9)	4637	4538 (-2.1)		
5	12	100	12.34	2141 (-15.3)	2528	2493 (-1.4)		
5	24	100	12.34	938 (-15.2)	1106	1096 (-.9)		
9	6	100	12.34	2065 (-17.1)	2490	2455 (-1.4)		
9	12	100	12.34	1274 (-16.4)	1524	1508 (-1.1)		
9	24	100	12.34	627 (-16.1)	747	742 (-.7)		
3	6	500	12.34	3914 (-15.1)	4609	4506 (-2.2)		
3	12	500	12.34	2217 (-15.6)	2626	2584 (-1.6)		
3	24	500	12.34	975 (-15.4)	1153	1142 (-.9)		
5	6	500	12.34	2101 (-17.1)	2535	2491 (-1.7)		
5	12	500	12.34	1369 (-16.7)	1644	1624 (-1.2)		
5	24	500	12.34	688 (-16.4)	824	817 (-.8)		
9	6	500	12.34	837 (-17.7)	1017	1005 (-1.2)		
9	12	500	12.34	602 (-17.5)	730	724 (-.9)		
9	24	500	12.34	329 (-19.5)	408	406 (-.5)		

TABLE A-14. COMPARISON OF SUBGRADE STRAIN (EZ) AT 30-KIP/355-PSI AND 36-KIP/355-PSI LOAD TO 36-KIP/395-PSI LOAD (CONTINUED).

TAC	TGR	EAC	ERI	30 KIP, 355 PSI		36 KIP, 395 PSI		36 KIP, 355 PSI	
				EZ	(% CHANGE)	EZ	(% CHANGE)	EZ	(% CHANGE)
3	6	1500	12.34	2406	(-17.0)	2896		2842	(-1.9)
3	12	1500	12.34	1538	(-16.7)	1846		1820	(-1.4)
3	24	1500	12.34	743	(-16.3)	889		881	(-1.9)
5	6	1500	12.34	1093	(-17.7)	1326		1307	(-1.6)
5	12	1500	12.34	786	(-17.6)	956		946	(-1.1)
5	24	1500	12.34	432	(-19.0)	533		529	(-1.6)
9	6	1500	12.34	377	(-19.6)	469		464	(-1.2)
9	12	1500	12.34	273	(-20.1)	341		339	(-1.6)
9	24	1500	12.34	166	(-19.1)	205		204	(-1.5)

TABLE A-15. COMPARISON OF SUBGRADE DEVIATOR STRESS (SDEV) AT 30-KIP/355-PSI AND 36-KIP/355-PSI LOAD TO 36-KIP/395-PSI LOAD.

TAC	IGR	EAC	ERI	30 KIP, 355 PSI		36 KIP, 395 PSI		36 KIP, 355 PSI	
				SDEV	SDEV (% CHANGE)	SDEV	SDEV (% CHANGE)	SDEV	SDEV (% CHANGE)
3	6	100	1.00	6.2 (0.0)		6.2 (0.0)		6.2 (0.0)	
3	12	100	1.00	6.2 (0.0)		6.2 (0.0)		6.2 (0.0)	
3	24	100	1.00	4.8 (-9.4)		5.3		5.1 (-3.8)	
5	6	100	1.00	6.2 (0.0)		6.2		6.2 (0.0)	
5	12	100	1.00	6.2 (0.0)		6.2		6.2 (0.0)	
5	24	100	1.00	4.3 (-10.4)		4.8		4.7 (-2.1)	
9	6	100	1.00	6.2 (0.0)		6.2		6.2 (0.0)	
9	12	100	1.00	5.1 (-12.1)		5.8		5.4 (-6.9)	
9	24	100	1.00	3.2 (-11.1)		3.6		3.5 (-2.8)	
3	6	500	1.00	6.2 (0.0)		6.2		6.2 (0.0)	
3	12	500	1.00	6.2 (0.0)		6.2		6.2 (0.0)	
3	24	500	1.00	4.3 (-12.2)		4.9		4.7 (-4.1)	
5	6	500	1.00	6.2 (0.0)		6.2		6.2 (0.0)	
5	12	500	1.00	5.1 (-12.1)		5.6		5.5 (-5.2)	
5	24	500	1.00	3.3 (-13.2)		3.8		3.7 (-2.6)	
9	6	500	1.00	3.4 (-12.8)		3.9		3.9 (0.0)	
9	12	500	1.00	2.8 (-12.5)		3.2		3.2 (0.0)	
9	24	500	1.00	2.1 (-8.7)		2.3		2.3 (0.0)	
3	6	1500	1.00	6.2 (0.0)		6.2		6.2 (0.0)	
3	12	1500	1.00	5.3 (-11.7)		6.0		5.8 (-3.3)	
3	24	1500	1.00	3.5 (-12.5)		4.0		3.9 (-2.5)	
5	6	1500	1.00	4.0 (-14.9)		4.7		4.6 (-2.1)	
5	12	1500	1.00	3.3 (-15.4)		3.9		3.8 (-2.6)	
5	24	1500	1.00	2.4 (-11.1)		2.7		2.7 (0.0)	
9	6	1500	1.00	1.8 (-14.3)		2.1		2.1 (0.0)	
9	12	1500	1.00	1.6 (-15.8)		1.9		1.9 (0.0)	
9	24	1500	1.00	1.4 (-12.5)		1.6		1.6 (0.0)	
3	6	100	7.68	22.8 (0.0)		22.8		22.8 (0.0)	
3	12	100	7.68	18.2 (9.9)		20.2		20.2 (0.0)	
3	24	100	7.68	10.0 (-11.5)		11.3		11.1 (-1.8)	
5	6	100	7.68	22.5 (-1.3)		22.8		22.8 (0.0)	
5	12	100	7.68	15.6 (-10.9)		17.5		17.1 (-3.3)	
5	24	100	7.68	8.6 (-12.2)		9.8		9.7 (-1.0)	
9	6	100	7.68	15.0 (-11.2)		16.9		16.6 (-1.8)	
9	12	100	7.68	10.8 (-12.2)		12.3		12.2 (-1.8)	
9	24	100	7.68	6.2 (-12.7)		7.1		7.1 (0.0)	

TABLE A-15. COMPARISON OF SUBGRADE DEVIATOR STRESS (SDEV) AT 30-KIP/355 PSI AND 36-KIP/355-PSI LOAD TO 36-KIP/395-PSI LOAD (CONTINUED).

TAC	TGR	EAC	ERI	30 KIP, 355 PSI		36 KIP, 395 PSI		36 KIP, 355 PSI	
				***	***	***	***	SDEV (%) CHANGE)	SDEV
3	6	500	7.68	21.9	(-3.9)	22.8	22.8	(0.0)	(0.0)
3	12	500	7.68	15.6	(-10.7)	17.7	17.4	(-1.7)	(-1.7)
3	24	500	7.68	8.8	(-12.0)	10.0	9.9	(-1.0)	(-1.0)
3	6	500	7.68	15.0	(-11.8)	17.0	16.7	(-1.8)	(-1.8)
5	12	500	7.68	11.2	(-12.5)	12.6	12.7	(-1.6)	(-1.6)
5	24	500	7.68	6.6	(-14.3)	7.7	7.6	(-1.3)	(-1.3)
5	6	500	7.68	7.4	(-14.0)	8.6	8.5	(-1.2)	(-1.2)
9	12	500	7.68	5.8	(-13.4)	6.7	6.7	(0.0)	(0.0)
9	24	500	7.68	4.1	(-12.6)	4.7	4.7	(0.0)	(0.0)
9	6	1500	7.68	16.2	(-11.6)	19.3	17.9	(-2.2)	(-2.2)
9	12	1500	7.68	12.1	(-12.3)	13.6	13.7	(-1.7)	(-1.7)
9	24	1500	7.68	7.0	(-13.6)	8.1	8.0	(-1.2)	(-1.2)
5	6	1500	7.68	9.0	(-14.3)	10.5	10.3	(-1.9)	(-1.9)
5	12	1500	7.68	7.1	(-14.5)	8.3	8.2	(-1.2)	(-1.2)
5	24	1500	7.68	4.6	(-12.7)	5.5	5.4	(-1.6)	(-1.6)
5	6	1500	7.68	4.2	(-12.5)	4.8	4.8	(0.0)	(0.0)
9	12	1500	7.68	3.5	(-12.5)	4.0	4.0	(0.0)	(0.0)
9	24	1500	7.68	3.1	(-13.3)	3.0	3.0	(0.0)	(0.0)
9	6	100	12.34	32.6	(0.0)	32.6	32.6	(0.0)	(0.0)
9	12	100	12.34	24.4	(-10.6)	27.3	26.8	(-1.6)	(-1.6)
9	24	100	12.34	12.7	(-12.4)	14.5	14.3	(-1.4)	(-1.4)
6	100	12.34	29.9	(-6.6)	32.6	32.6	(0.0)	(0.0)	
6	12	100	12.34	20.5	(-11.3)	23.1	22.7	(-1.7)	(-1.7)
6	24	100	12.34	10.9	(-12.8)	12.5	12.4	(-1.6)	(-1.6)
6	6	100	12.34	19.9	(-12.3)	22.7	22.4	(-1.3)	(-1.3)
12	100	12.34	13.9	(-13.1)	16.0	15.8	(-1.2)	(-1.2)	
12	24	100	12.34	7.6	(-13.3)	9.0	9.0	(0.0)	(0.0)
6	6	500	12.34	29.6	(-9.6)	32.6	32.6	(0.0)	(0.0)
6	12	500	12.34	20.9	(-11.4)	23.6	23.2	(-1.7)	(-1.7)
6	24	500	12.34	11.2	(-12.5)	12.6	12.7	(-1.6)	(-1.6)
6	6	500	12.34	20.1	(-12.6)	23.0	22.6	(-1.7)	(-1.7)
12	500	12.34	14.6	(-13.6)	16.9	16.7	(-1.2)	(-1.2)	
12	24	500	12.34	6.4	(-13.4)	9.7	9.7	(0.0)	(0.0)
6	6	500	12.34	9.7	(-14.9)	11.4	11.3	(-1.9)	(-1.9)
12	500	12.34	7.3	(-15.1)	8.6	8.6	(0.0)	(0.0)	
12	24	500	12.34	4.6	(-12.7)	5.5	5.5	(0.0)	(0.0)

TABLE A-15. COMPARISON OF SUBGRADE DEVIATOR STRESS (SDEV) AT 30-KIP/355-PSI AND 36-KIP/355-PSI LOAD TO 36-KIP/395-PSI LOAD (CONTINUED).

TAC	TGR	EAC	ERI	30 KIP, 355 PSI		36 KIP, 395 PSI		36 KIP, 355 PSI	
				***	***	*****	*****	*****	*****
3	6	1500	12.34	22.0	(-12.0)	25.0		24.5	(-2.0)
3	12	1500	12.34	15.9	(-13.1)	16.3		16.1	(-1.1)
3	24	1500	12.34	6.9	(-13.6)	10.3		10.2	(-1.0)
5	6	1500	12.34	12.0	(-14.9)	14.1		13.9	(-1.4)
5	12	1500	12.34	9.2	(-14.6)	10.6		10.7	(-.9)
5	24	1500	12.34	5.7	(-13.6)	6.6		6.6	(0.0)
9	6	1500	12.34	5.0	(-13.6)	5.6		5.8	(0.0)
9	12	1500	12.34	4.1	(-14.6)	4.6		4.7	(-2.1)
9	24	1500	12.34	2.9	(-14.7)	3.4		3.4	(0.0)

APPENDIX B
ILLI-PAVE DESIGN ALGORITHMS

These tables contain the design algorithms developed by regression analysis of ILLI-PAVE data base (Appendix A). Description of the technique and statistics associated with the equations are contained in Sections III.D, III.E, and III.G of the text. Definitions of variables and statistics used in the equations:

	<u>VARIABLE</u>	<u>UNITS</u>
T _{AC}	Thickness of Asphalt Concrete Surface	inches
T _{GR}	Thickness of Granular Base Layer	inches
E _{AC}	Modulus of Asphalt Concrete Surface	ksi
E _{Ri}	Subgrade Modulus at the Intercept	ksi
MEAC	Maximum Tensile Strain in Asphalt Concrete	microstrain
EZ	Maximum Compressive Strain in Subgrade	microstrain
SDEV	Maximum Subgrade Deviator Stress	psi
SR	Subgrade Stress Ratio = SDEV/Compressive Strength	
DO	Maximum Surface Deflection	mils
P	Magnitude of Load on Wheel	kips
R ²	Coefficient of Determination	
SEE	Standard Error of Estimate	

TABLE B-1. REGRESSION EQUATIONS WITH "ENGINEERING MEANINGFUL" VARIABLES DEVELOPED FROM FULL FACTORIAL MINUS SUBGRADE FAILURES (372 CASES).

$$\text{Log MEAC} = 3.5818 - .0276(\text{Log TAC})(\text{Log EAC}) - 2.85 \times 10^{-4}(\text{log TAC})(\text{EAC}) - .7465(\text{Log TGR}/\text{Log TAC}) - .0403(\text{Log E}_{\text{Ri}})$$

$R^2 = .980$ SEE = .0320 (1.076)

$R^2 = .950$ SEE = 67.9 microstrain

$$\text{Log EZ} = 4.9989 - .5677(\text{Log TAC})(\text{Log EAC}) - .2701(\text{Log TGR}) - .0115(\text{Log TGR}/\text{Log TAC}) - .3099(\text{Log E}_{\text{Ri}})$$

$R^2 = .969$ SEE = .0576 (1.142)

$R^2 = .940$ SEE = 290.1 microstrain

$$\text{Log SDEV} = 1.6190 - .4104(\text{Log TAC})(\text{Log EAC}) - .0110(\text{Log TGR}/\text{Log TAC}) + .2358(\text{log E}_{\text{Ri}}) + .0170(\text{E}_{\text{Ri}})$$

$R^2 = .970$ SEE = .0488 (1.119)

$R^2 = .966$ SEE = 1.1 psi

$$\text{Log SR} = 0.8243 - .4095(\text{Log TAC})(\text{Log EAC}) - .0110(\text{Log TGR}/\text{Log TAC}) + .0132(\text{E}_{\text{Ri}}) - .3811(\text{Log E}_{\text{Ri}})$$

$R^2 = .947$ SEE = .0506 (1.124)

$R^2 = .923$ SEE = .06

$$\text{Log DO} = 2.8066 - .3766(\text{Log TAC})(\text{Log EAC}) - .7032(\text{Log TGR}/\text{Log TAC}) - .0101(\text{E}_{\text{Ri}}) - .1290(\text{Log E}_{\text{Ri}})$$

$R^2 = .981$ SEE = .0250 (1.059)

$R^2 = .969$ SEE = 4.3 mils

TABLE B-2. REGRESSION EQUATIONS WITH MORE "COMPLICATED" VARIABLES DEVELOPED FROM FULL FACTORIAL MINUS SUBGRADE FAILURES (372 CASES).

$$\text{Log MEAC} = 3.4422 - .0092(\text{TAC})(\text{Log EAC})^2 - 1.83 \times 10^{-4}(\text{EAC})(\text{Log TAC})^2 \\ - .6304(\text{Log TGR}/\text{TAC}) - .0037(\text{ERi}/\text{Log TGR})$$

$R^2 = .987$ SEE = .0254 (1.060)
 $R^2 = .968$ SEE = 53.9 microstrain

$$\text{Log EZ} = 4.7361 - .5634(\text{Log TAC})(\text{Log EAC}) - .2178(\text{Log TGR})(\text{Log ERi}) \\ - .0140(\text{TGR}/\text{Log TAC}) - .0011(\text{TAC})(\text{ERi})$$

$R^2 = .971$ SEE = .0551 (1.135)
 $R^2 = .937$ SEE = 299.3 microstrain

$$\text{Log SDEV} = 1.5465 - .3945(\text{Log TAC})(\text{Log EAC}) - .0091(\text{TGR}/\text{Log TAC}) \\ + .2359(\text{Log ERi}) + .0182(\text{ERi}/\text{Log TGR})$$

$R^2 = .975$ SEE = .0442 (1.107)
 $R^2 = .977$ SEE = 0.9 psi

$$\text{Log SR} = 0.6509 - .3622(\text{Log TAC})(\text{Log EAC}) - .0077(\text{TGR}/\text{Log TAC}) \\ + .0048(\text{ERi}/\text{Log TAC}) - .2756(\text{Log TGR})(\text{Log ERi})$$

$R^2 = .956$ SEE = .0462 (1.112)
 $R^2 = .930$ SEE = .06

$$\text{Log DO} = 2.7282 - .3503(\text{Log TAC})(\text{Log EAC}) - .5970(\text{Log TGR}/\text{TAC}) \\ - .0110(\text{ERi}) - .0436(\text{Log EAC})(\text{Log ERi})$$

$R^2 = .984$ SEE = .0234 (1.055)
 $R^2 = .967$ SEE = 4.5 mils

TABLE B-3. REGRESSION EQUATIONS DEVELOPED FROM 3⁴ FACTORIAL
MINUS SUBGRADE FAILURES (70 CASES).

$$\text{Log MEAC} = 3.5354 - .0263(\text{T}_{\text{AC}})(\text{Log E}_{\text{AC}}) - 2.80 \times 10^{-4}(\text{E}_{\text{AC}})(\text{Log T}_{\text{AC}}) \\ - .6722(\text{Log T}_{\text{GR}}/\text{Log T}_{\text{AC}}) - .0328(\text{Log E}_{\text{Ri}})$$

$$R^2 = .980 \quad \text{SEE} = .0328 \quad (1.078)$$

$$R^2 = .947 \quad \text{SEE} = 69.9 \text{ microstrain}$$

$$\text{Log EZ} = 4.9927 - .5443(\text{Log T}_{\text{AC}})(\text{Log E}_{\text{AC}}) - .3307(\text{Log T}_{\text{GR}}) \\ - .0104(\text{T}_{\text{GR}}/\text{Log T}_{\text{AC}}) - .3158(\text{Log E}_{\text{Ri}})$$

$$R^2 = .968 \quad \text{SEE} = .0576 \quad (1.142)$$

$$R^2 = .939 \quad \text{SEE} = 299.9 \text{ microstrain}$$

$$\text{Log SDEV} = 1.7011 - .4388(\text{Log T}_{\text{AC}})(\text{Log E}_{\text{AC}}) - .0115(\text{T}_{\text{GR}}/\text{Log T}_{\text{AC}}) \\ + .3034(\text{Log E}_{\text{Ri}}) + .0087(\text{E}_{\text{Ri}})$$

$$R^2 = .966 \quad \text{SEE} = .0530 \quad (1.130)$$

$$R^2 = .955 \quad \text{SEE} = 1.2 \text{ psi}$$

$$\text{Log SR} = 0.5783 + .0350(\text{T}_{\text{AC}}) - .0472(\text{T}_{\text{AC}})(\text{Log E}_{\text{AC}}) \\ - .0109(\text{T}_{\text{GR}}/\text{Log T}_{\text{AC}}) - .0262(\text{Log E}_{\text{Ri}})$$

$$R^2 = .925 \quad \text{SEE} = .0642 \quad (1.159)$$

$$R^2 = .888 \quad \text{SEE} = .08$$

$$\text{Log DO} = 2.6884 - .2816(\text{Log T}_{\text{AC}})(\text{Log E}_{\text{AC}}) - .0687(\text{Log E}_{\text{AC}}) \\ - .0200(\text{T}_{\text{GR}}/\text{Log T}_{\text{AC}}) - .2164(\text{Log E}_{\text{Ri}})$$

$$R^2 = .975 \quad \text{SEE} = .0315 \quad (1.075)$$

$$R^2 = .951 \quad \text{SEE} = 5.8 \text{ mils}$$

Note: All statistics are based on full 4x5x5x4 factorial (372 cases).

TABLE B-4. REGRESSION EQUATIONS DEVELOPED FOR 24-KIP/355-PSI LOADING
DEVELOPED FROM 3⁴ FACTORIAL MINUS SUBGRADE FAILURES (73 CASES).

$$\text{Log MEAC} = 3.5269 - .0280(\text{Log T}_{\text{AC}})(\text{Log E}_{\text{AC}}) - 3.00 \times 10^{-4}(\text{E}_{\text{AC}})(\text{Log T}_{\text{AC}}) \\ - .6059(\text{Log T}_{\text{GR}}/\text{Log T}_{\text{AC}}) - .0380(\text{Log E}_{\text{Ri}})$$

$$R^2 = .987 \quad \text{SEE} = .0319 \quad (1.076)$$

$$R^2 = .968 \quad \text{SEE} = 59.0 \text{ microstrain}$$

$$\text{Log EZ} = 4.8858 - .5578(\text{Log T}_{\text{AC}})(\text{Log E}_{\text{AC}}) - .2972(\text{Log T}_{\text{GR}}) \\ - .0105(\text{Log T}_{\text{GR}}/\text{Log T}_{\text{AC}}) - .3188(\text{Log E}_{\text{Ri}})$$

$$R^2 = .967 \quad \text{SEE} = .0649 \quad (1.161)$$

$$R^2 = .898 \quad \text{SEE} = 319.4 \text{ microstrain}$$

$$\text{Log SDEV} = 1.6766 - .4564(\text{Log T}_{\text{AC}})(\text{Log E}_{\text{AC}}) - .0118(\text{Log T}_{\text{GR}}/\text{Log T}_{\text{AC}}) \\ + .3014(\text{Log E}_{\text{Ri}}) + .0082(\text{E}_{\text{Ri}})$$

$$R^2 = .980 \quad \text{SEE} = .0476 \quad (1.116)$$

$$R^2 = .970 \quad \text{SEE} = 1.1 \text{ psi}$$

$$\text{Log SR} = 0.5340 + .0392(\text{Log T}_{\text{AC}}) - .0497(\text{Log T}_{\text{AC}})(\text{Log E}_{\text{AC}}) \\ - .0111(\text{Log T}_{\text{GR}}/\text{Log T}_{\text{AC}}) - .2697(\text{Log E}_{\text{Ri}})$$

$$R^2 = .952 \quad \text{SEE} = .0601 \quad (1.148)$$

$$R^2 = .934 \quad \text{SEE} = .06$$

$$\text{Log DO} = 2.6519 - .2815(\text{Log T}_{\text{AC}})(\text{Log E}_{\text{AC}}) - .0879(\text{Log E}_{\text{AC}}) \\ - .0180(\text{Log T}_{\text{GR}}/\text{Log T}_{\text{AC}}) - .2136(\text{Log E}_{\text{Ri}})$$

$$R^2 = .974 \quad \text{SEE} = .0320 \quad (1.078)$$

$$R^2 = .953 \quad \text{SEE} = 4.7 \text{ mils}$$

TABLE B-5. REGRESSION EQUATIONS DEVELOPED FOR 36-KIP/355-PSI LOADING
DEVELOPED FROM 3⁴ FACTORIAL MINUS SUBGRADE FAILURES (66 CASES).

$$\text{Log MEAC} = 3.5691 - .0256(\text{Log EAC})(\text{Log TAC}) - 2.50 \times 10^{-4}(\text{EAC})(\text{Log TAC}) \\ - .7786(\text{Log TGR}/\text{Log TAC}) - .0344(\text{Log E}_{\text{Ri}})$$

$$R^2 = .970 \quad \text{SEE} = .0397 \quad (1.096)$$

$$R^2 = .926 \quad \text{SEE} = 83.1 \text{ microstrain}$$

$$\text{Log EZ} = 4.9419 - .5118(\text{Log TAC})(\text{Log EAC}) - .3178(\text{Log TGR}) \\ - .0098(\text{TGR}/\text{Log TAC}) - .2924(\text{Log E}_{\text{Ri}})$$

$$R^2 = .957 \quad \text{SEE} = .0638 \quad (1.158)$$

$$R^2 = .919 \quad \text{SEE} = 281.8 \text{ microstrain}$$

$$\text{Log SDEV} = 1.7074 - .4234(\text{Log TAC})(\text{Log EAC}) - .0112(\text{TGR}/\text{Log TAC}) \\ + .2943(\text{Log E}_{\text{Ri}}) + .0103(\text{E}_{\text{Ri}})$$

$$R^2 = .977 \quad \text{SEE} = .0484 \quad (1.118)$$

$$R^2 = .960 \quad \text{SEE} = 1.3 \text{ psi}$$

$$\text{Log SR} = 0.5915 + .0336(\text{Log TAC}) - .0452(\text{Log EAC}) \\ - .0105(\text{TGR}/\text{Log TAC}) - .2574(\text{Log E}_{\text{Ri}})$$

$$R^2 = .947 \quad \text{SEE} = .0554 \quad (1.136)$$

$$R^2 = .926 \quad \text{SEE} = .06$$

$$\text{Log DO} = 2.7051 - .2721(\text{Log TAC})(\text{Log EAC}) - .0569(\text{Log EAC}) \\ - .0197(\text{TGR}/\text{Log TAC}) - .2237(\text{Log E}_{\text{Ri}})$$

$$R^2 = .970 \quad \text{SEE} = .0321 \quad (1.077)$$

$$R^2 = .957 \quad \text{SEE} = 5.8 \text{ mils}$$

TABLE B-6. REGRESSION EQUATIONS DEVELOPED INCLUDING LOAD VARIABLE FROM 3⁵ FACTORIAL MINUS SUBGRADE FAILURES (209 CASES).

$$\begin{aligned}\text{Log MEAC} = & 3.3692 - .0337(\text{T}_{\text{AC}})(\text{Log E}_{\text{AC}}) - 2.71 \times 10^{-5}(\text{T}_{\text{AC}})(\text{E}_{\text{AC}}) \\ & - .5157(\text{Log T}_{\text{GR}}/\text{T}_{\text{AC}}) - .0011(\text{T}_{\text{AC}})(\text{P})\end{aligned}$$

$$\begin{aligned}R^2 = .982 & \quad \text{SEE} = .0343 \text{ (1.082)} \\ R^2 = .957 & \quad \text{SEE} = 65.2 \text{ microstrain}\end{aligned}$$

$$\begin{aligned}\text{Log ME}_{\text{AC}} = & 3.2398 - .0205(\text{T}_{\text{AC}})(\text{Log E}_{\text{AC}}) - 3.68 \times 10^{-5}(\text{T}_{\text{AC}})(\text{E}_{\text{AC}}) \\ & - .5835(\text{Log T}_{\text{GR}}/\text{T}_{\text{AC}}) + .0056(\text{P})\end{aligned}$$

$$\begin{aligned}R^2 = .972 & \quad \text{SEE} = .0419 \text{ (1.101)} \\ R^2 = .944 & \quad \text{SEE} = 74.5 \text{ microstrain}\end{aligned}$$

$$\begin{aligned}\text{Log EZ} = & 4.4023 - .5824(\text{Log T}_{\text{AC}})(\text{Log E}_{\text{AC}}) - .0158(\text{T}_{\text{GR}}/\text{Log T}_{\text{AC}}) \\ & - .3089(\text{Log E}_{\text{Ri}}) + .0133(\text{P})\end{aligned}$$

$$\begin{aligned}R^2 = .952 & \quad \text{SEE} = .0726 \text{ (1.182)} \\ R^2 = .894 & \quad \text{SEE} = 330.1 \text{ microstrain}\end{aligned}$$

$$\begin{aligned}\text{Log SDEV} = & 1.4000 - .4401(\text{Log T}_{\text{AC}})(\text{Log E}_{\text{AC}}) - .0115(\text{T}_{\text{GR}}/\text{Log T}_{\text{AC}}) \\ & + .3870(\text{Log E}_{\text{Ri}}) + .0101(\text{P})\end{aligned}$$

$$\begin{aligned}R^2 = .977 & \quad \text{SEE} = .0491 \text{ (1.120)} \\ R^2 = .959 & \quad \text{SEE} = 1.4 \text{ psi}\end{aligned}$$

$$\begin{aligned}\text{Log SR} = & 0.6155 - .4411(\text{Log T}_{\text{AC}})(\text{Log E}_{\text{AC}}) - .0115(\text{T}_{\text{GR}}/\text{Log T}_{\text{AC}}) \\ & - .2704(\text{Log E}_{\text{Ri}}) + .0100(\text{P})\end{aligned}$$

$$\begin{aligned}R^2 = .963 & \quad \text{SEE} = .0487 \text{ (1.119)} \\ R^2 = .994 & \quad \text{SEE} = .06\end{aligned}$$

$$\begin{aligned}\text{Log DO} = & 2.3903 - .3628(\text{Log T}_{\text{AC}})(\text{Log E}_{\text{AC}}) - .6754(\text{Log T}_{\text{GR}}/\text{T}_{\text{AC}}) \\ & - .2173(\text{Log E}_{\text{Ri}}) + .0120(\text{P})\end{aligned}$$

$$\begin{aligned}R^2 = .972 & \quad \text{SEE} = .0327 \text{ (1.078)} \\ R^2 = .961 & \quad \text{SEE} = 4.8 \text{ mils}\end{aligned}$$

TABLE B-7. REGRESSION EQUATIONS DEVELOPED FOR HEAVIER-WEIGHT F-15 DEVELOPED FROM 3⁴ FACTORIAL MINUS SUBGRADE FAILURES (56 CASES).

$$\text{Log MEAC} = 2.4215 + 1.228(\text{Log T}_{\text{AC}}) - .0486(\text{Log T}_{\text{AC}})(\text{Log E}_{\text{AC}}) \\ - 2.50 \times 10^{-4}(\text{Log T}_{\text{AC}})(\text{E}_{\text{AC}}) + .1584(\text{Log E}_{\text{AC}})$$

$$R^2 = .981 \quad \text{SEE} = .0323 \quad (1.077) \\ R^2 = .967 \quad \text{SEE} = 58.6 \text{ microstrain}$$

$$\text{Log EZ} = 4.7280 - .5016(\text{Log T}_{\text{AC}})(\text{Log E}_{\text{AC}}) - .0318(\text{T}_{\text{GR}}/\text{Log T}_{\text{AC}}) \\ + .1093(\text{T}_{\text{GR}}/\text{T}_{\text{AC}}) - .2974(\text{Log E}_{\text{Ri}})$$

$$R^2 = .961 \quad \text{SEE} = .0614 \quad (1.152) \\ R^2 = .923 \quad \text{SEE} = 282.8 \text{ microstrain}$$

$$\text{Log SDEV} = 1.3149 - .0201(\text{T}_{\text{AC}})(\text{Log E}_{\text{AC}}) - 1.78 \times 10^{-4}(\text{Log T}_{\text{AC}})(\text{E}_{\text{AC}}) \\ - .0173(\text{T}_{\text{GR}}) + .3940(\text{Log E}_{\text{Ri}})$$

$$R^2 = .985 \quad \text{SEE} = .0396 \quad (1.095) \\ R^2 = .978 \quad \text{SEE} = 1.2 \text{ psi}$$

$$\text{Log SR} = 0.5264 + .0201(\text{T}_{\text{AC}})(\text{log E}_{\text{AC}}) - 1.77 \times 10^{-4}(\text{Log T}_{\text{AC}})(\text{E}_{\text{AC}}) \\ - .0174(\text{T}_{\text{GR}}) - .2631(\text{Log E}_{\text{Ri}})$$

$$R^2 = .976 \quad \text{SEE} = .0376 \quad (1.090) \\ R^2 = .968 \quad \text{SEE} = .04$$

$$\text{Log DO} = 2.5250 + .2623(\text{Log T}_{\text{AC}}) - .3581(\text{Log T}_{\text{AC}})(\text{Log E}_{\text{AC}}) \\ - .0175(\text{T}_{\text{GR}}/\text{T}_{\text{AC}}) - .2200(\text{Log E}_{\text{Ri}})$$

$$R^2 = .976 \quad \text{SEE} = .0291 \quad (1.069) \\ R^2 = .964 \quad \text{SEE} = 5.3 \text{ mils}$$

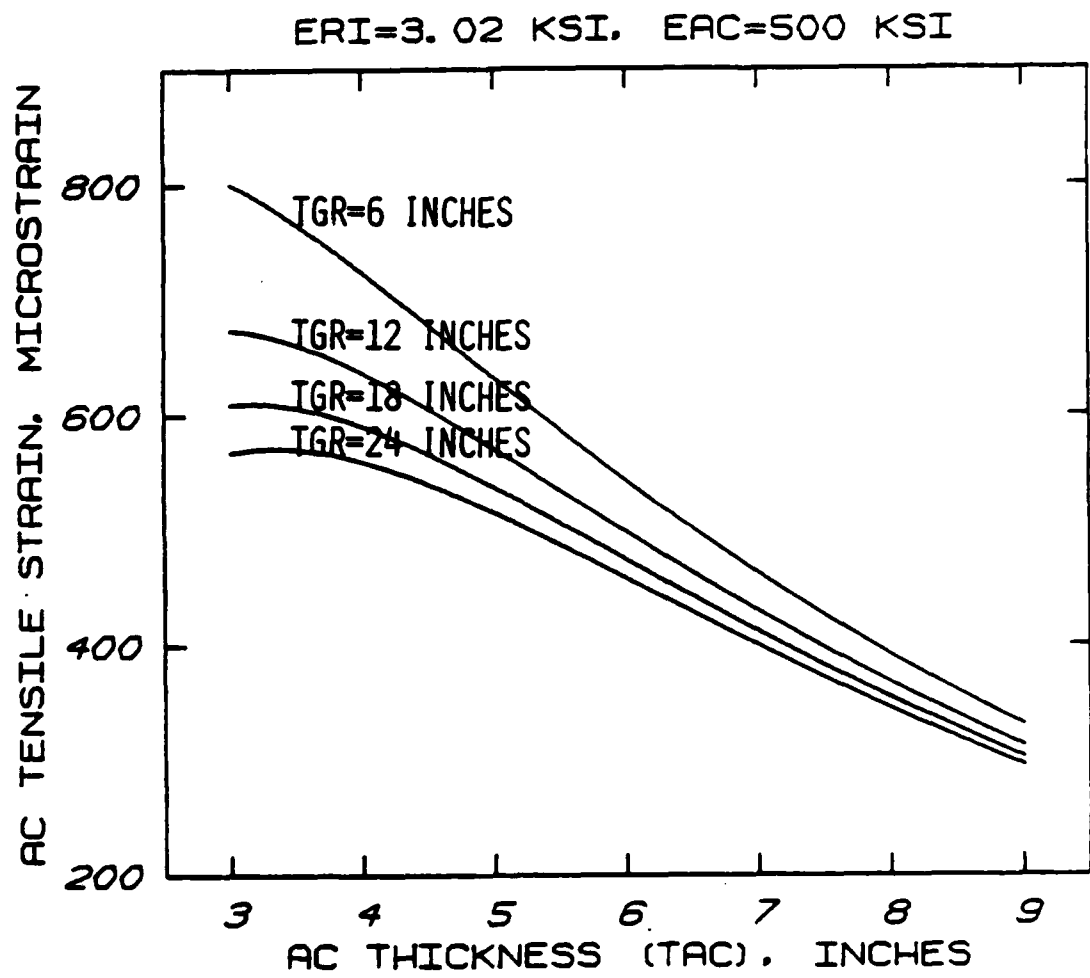


Figure B-1. AC Tensile Strain Versus AC Thickness, Varying Granular Base Thickness.

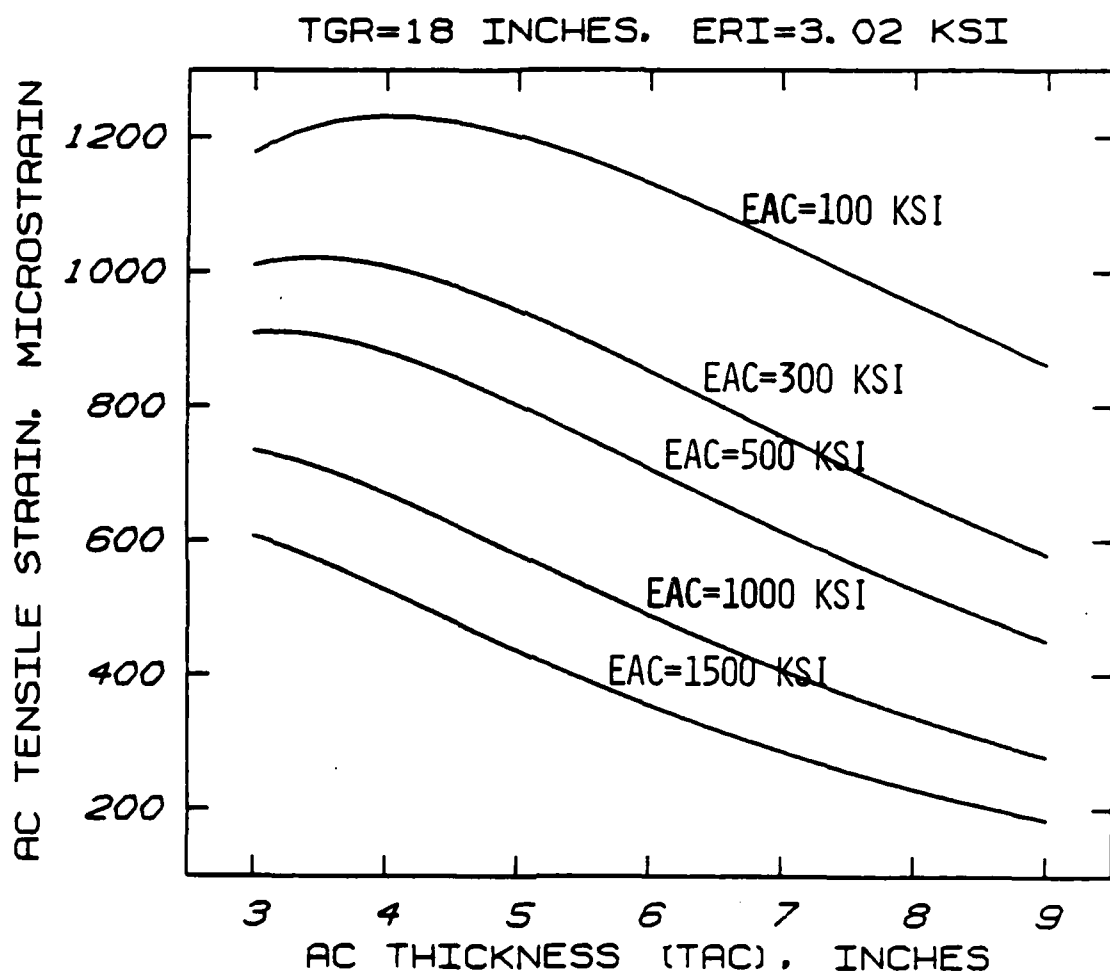


Figure B-2. AC Tensile Strain Versus AC Thickness,
Varying AC Modulus.

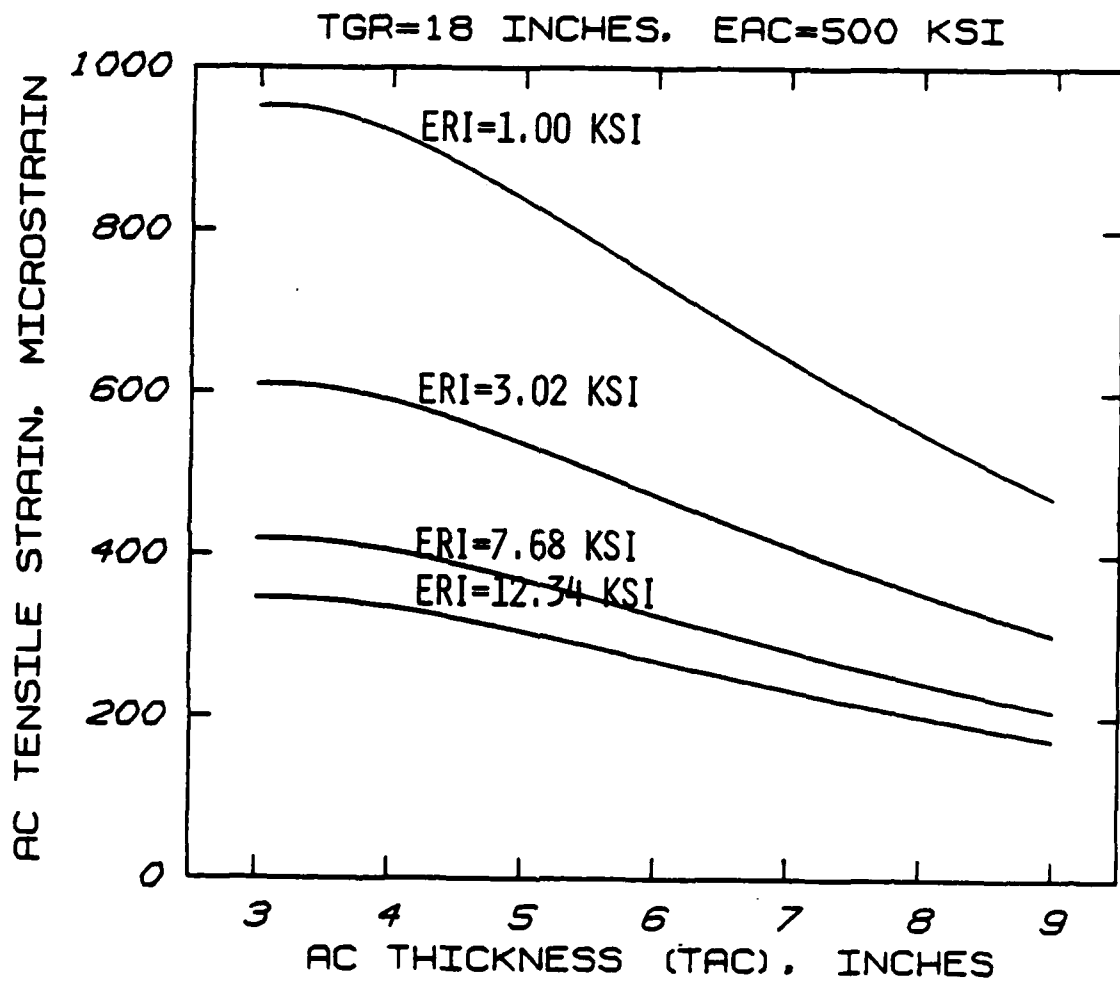


Figure B-3. AC Tensile Strain Versus AC Thickness, Varying Subgrade Modulus.

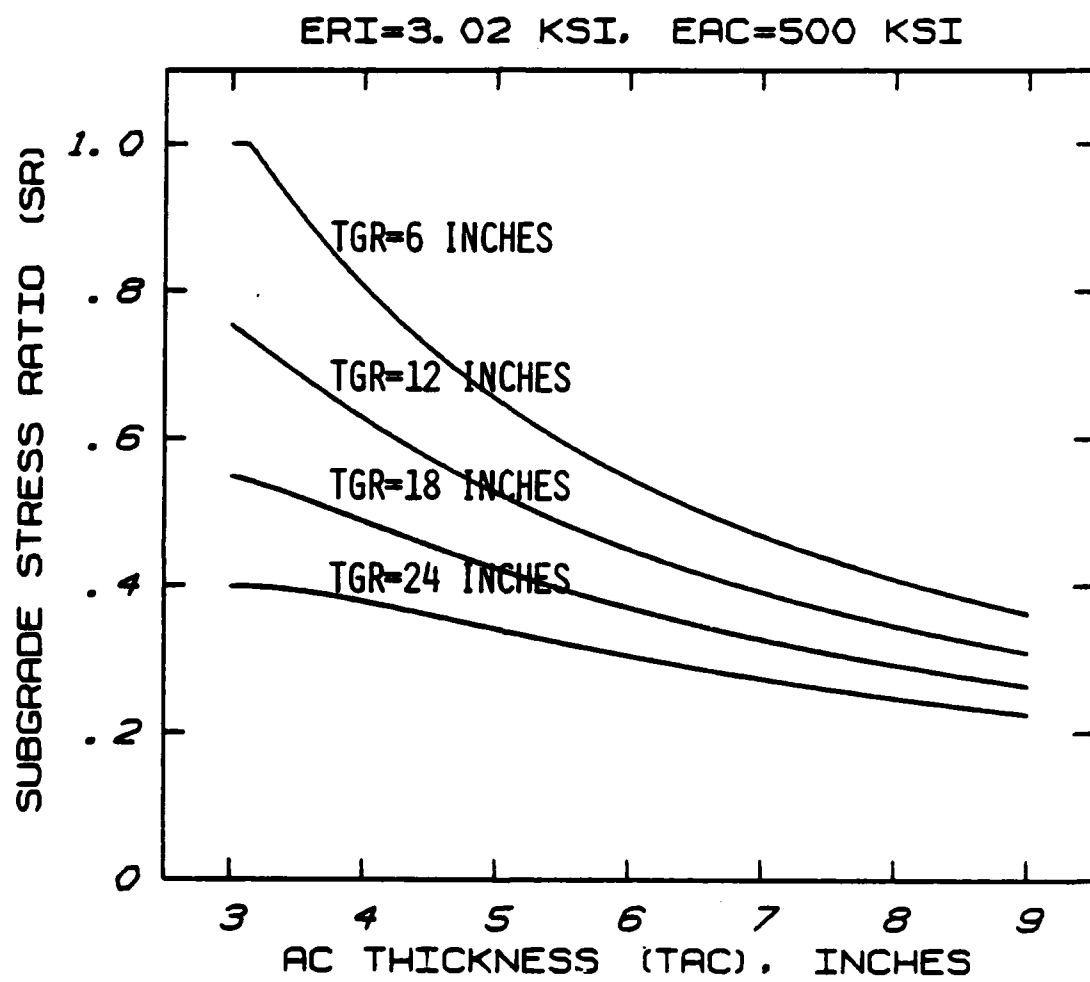


Figure B-4. Subgrade Stress Ratio Versus AC Thickness, Varying Granular Base Thickness.

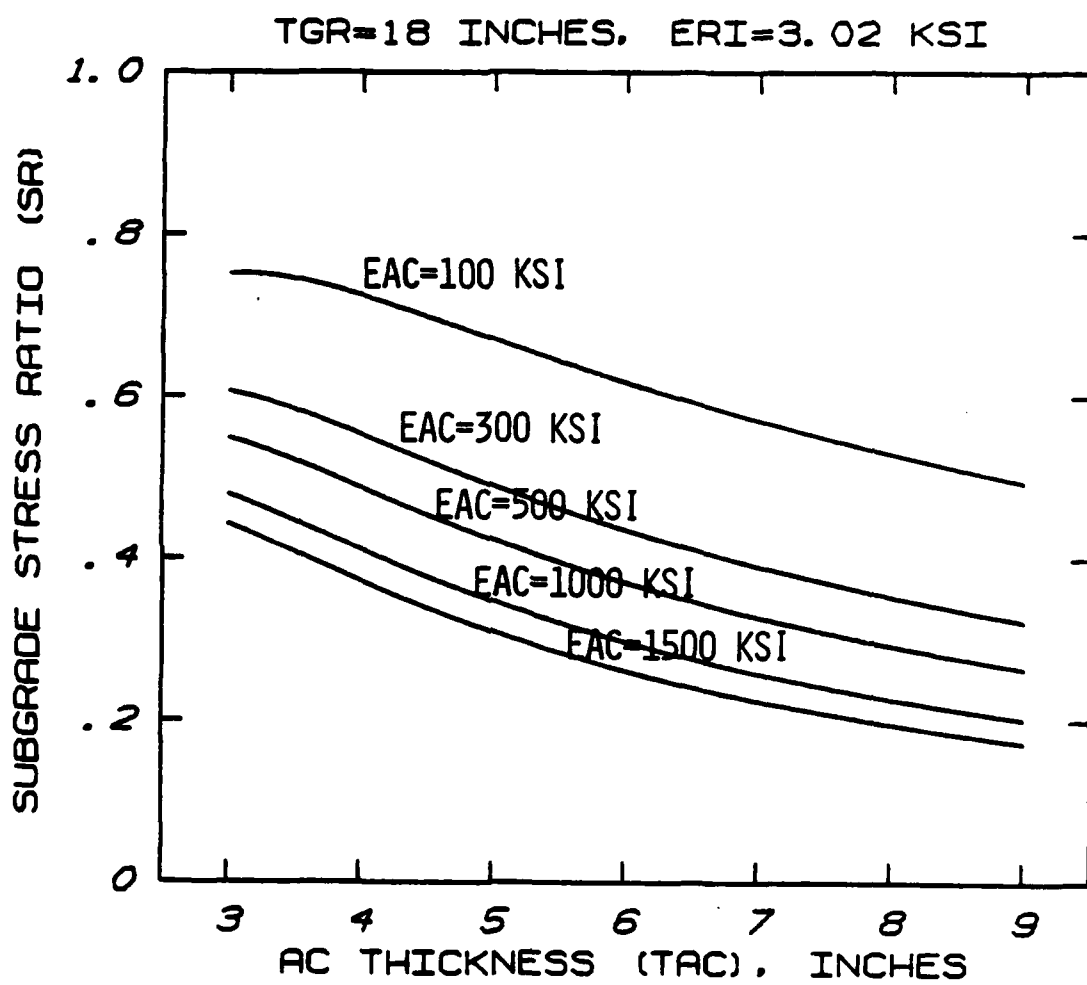


Figure B-5. Subgrade Stress Ratio Versus AC Thickness, Varying AC Modulus.

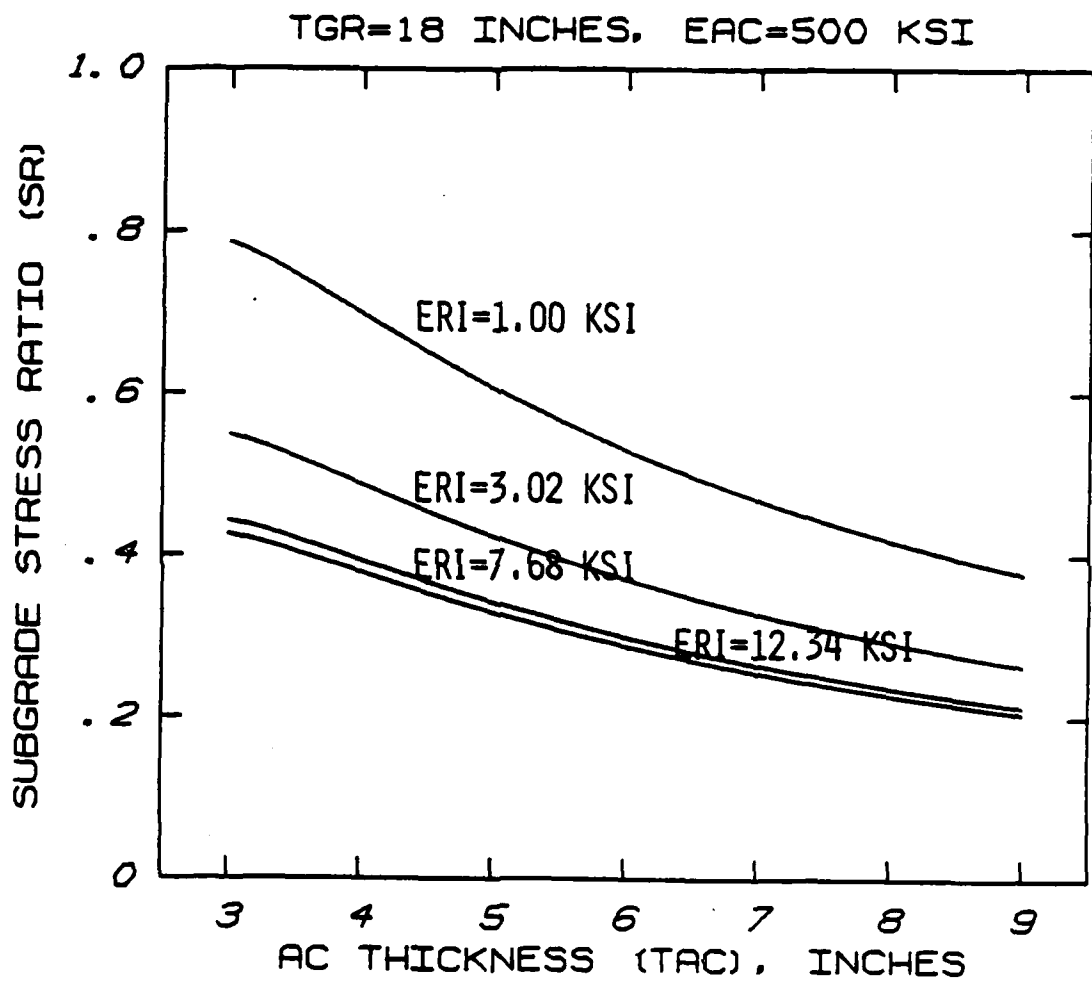


Figure B-6. Subgrade Stress Ratio Versus AC Thickness, Varying Subgrade Modulus.

LIST OF REFERENCES

1. Millard, K. Aircraft Characteristics for Airfield Pavement Design and Evaluation, Air Force Engineering and Services Center, Tyndall AFB, FL, January 1983.
2. Army Technical Manual 5-824-1, Air Force Manual 88-6 Chapter 1, General Provisions for Airfield Design, 1977.
3. Navy Design Manual 21.3, Army Technical Manual 5-825-2, Air Force manual 88-6 Chapter 2, Flexible Pavement Design for Airfields, 1979.
4. Raad, Lutfi and Figueroa, Jose L., "Load Response of Transportation Support Facilities," Transportation Engineering Journal, Vol. 106, No. TE1, ASCE, New York, pp. 111-128, January 1980.
5. Traylor, M.L., Characterization of Flexible Pavements by Non-Destructive Testing, Ph.D. Thesis, University of Illinois, Urbana-Champaign, 1978.
6. Hoffman, N.S. and Thompson, M.R., Mechanistic Interpretation of Nondestructive Pavement Testing Deflections, Civil Engineering Studies, Transportation Engineering Studies No. 32, University of Illinois, Urbana-Champaign, June 1981.
7. Elliott, R.P. and Thompson, M.R., Mechanistic Design Concepts for Conventional Flexible Pavements, Civil Engineering Studies, Transportation Engineering Studies No. 42, University of Illinois, Urbana-Champaign, February 1985.
8. Gomez, N.S. and Thompson, M.R., Mechanistic Design Concepts for Full-Depth Asphalt Concrete Pavements, Civil Engineering Studies, Transportation Engineering Series No. 41, University of Illinois, Urbana-Champaign, August 1984.
9. Suddath, L.P. and Thompson, M.R., Load-Deflection Behavior of Lime-Stabilized Layers, TR M-118, U.S. Army Construction Engineering Research Laboratory, Champaign, IL, 1975.
10. Costigan, Robert R., Response and Performance of Contingency Airfield Pavements Containing Stabilized Material Layers, Ph.D. Thesis, University of Illinois, Urbana-Champaign, 1984.
11. Foster, Charles R. and Ahlvin, R.G., "Notes on the Corps of Engineers' CBR Design Procedure," Highway Research Board Bulletin 210, Washington, D.C., pp. 1-12, 1959.
12. Army Technical Manual 5-824-2, Air Force Manual 88-6 Chapter 2, Airfield - Flexible Pavements Air Force, 1969.
13. Yoder, E.J. and Witczak, M.W., Principles of Pavement Design, 2nd Ed., John Wiley & Sons, Inc., New York, 1975.
14. "Development of CBR Flexible Pavement Design Methods for Airfields, A

Symposium," Transactions, Vol. 115, ASCE, New York, pp. 453-589, 1950.

15. Stockton Runway Test Section, Corps of Engineers, Sacramento District, September 1942.

16. Supplement to Stockton Runway Test Section, Corps of Engineers, Sacramento District, May 1944.

17. Service Behavior Test, Barksdale Field, Louisiana, Corps of Engineers, Little Rock District, Comprehensive report with five appendixes (July 1944) and published report (October 1944).

18. Accelerated Traffic Tests, Eglin Field, Florida, Corps of Engineers, Mobile District, 15 January 1945.

19. Accelerated Traffic Tests, Langley Field, Virginia, Corps of Engineers, Norfolk District, June 1945.

20. Summary Report Accelerated Traffic Tests, Corps of Engineers, Waterways Experiment Station, February 1947.

21. Accelerated Traffic Test at Stockton Airfield, Stockton, California (Stockton Test No. 2), 7 vol, Corps of Engineers, Sacramento District, May 1948.

22. Investigation of the Design and Control of Asphalt Paving Mixtures, Vols. 1, 2, and 3, TM 3-254, Corps of Engineers, Waterways Experiment Station, May 1948.

23. Chou, Yu T., "Analysis of Pavements Designed by CBR Equation," Transportation Engineering Journal, Vol. 104, No. TE4, ASCE, New York, pp. 457-474, July 1978.

24. Design of Flexible Airfield Pavements for Multiple-Wheel Landing Gear Assemblies, Report No. 1, Test Section with Lean-Clay Subgrade, TM 3-349, Corps of Engineers, Waterways Experiment Station, September 1952.

25. Design of Flexible Airfield Pavements for Multiple-Wheel Landing Gear Assemblies, Report No. 2, Analysis of Existing Data, TM 3-349, Corps of Engineers, Waterways Experiment Station, June 1955.

26. Collection of Letter Reports on Flexible Pavement Design Curves, MP 4-61, Corps of Engineers, Waterways Experiment Station, June 1951.

27. Investigation of Effects of Traffic with High-Pressure Tires on Asphalt Pavements, TM 3-312, Corps of Engineers, Waterways Experiment Station, May 1950.

28. Effects of Traffic with Small High-Pressure Tires on Asphalt Pavements, TM 3-314, Corps of Engineers, Waterways Experiment Station, June 1950.

29. Design of Upper Base Courses for High Pressure Tires, Report No. 1 Base Courses Requirements as Related to Contact Pressure, TM 3-373, Corps of Engineers, Waterways Experiment Station, December 1953.

30. Mathematical Expression of the CBR Relations, TR 3-441, Corps of Engineers, Waterways Experiment Station, November 1956.

31. Ahlvin, R.G., Hammit, G.M., Hutchinson, R.L., Ledbetter, R.H., Rice, J.L., and Ulery, H.H., Multiple-Wheel Heavy Gear Load Pavement Tests, Vols. 1-4, TR S-71-17, Corps of Engineers, Waterways Experiment Station, November 1971.

32. Pereira, A. Taboza, Procedures for Development of CBR Design Curves, IR S-77-1, Corps of Engineers, Waterways Experiment Station, June 1977.

33. Brown, D.N. and Thompson, O.O., Lateral Distribution of Aircraft Traffic, MP S-73-56, Corps of Engineers, Waterways Experiment Station, July 1973.

34. Field Moisture Content Investigation, Report No. 2, October 1945-November 1952 Phase, TM 3-401, Corps of Engineers, Waterways Experiment Station, April 1955.

35. Field Moisture Content Investigation, Report No. 3, November 1952-May 1956 Phase, TM 3-401, Corps of Engineers, Waterways Experiment Station, May 1961.

36. Field Moisture Content Investigation, Report No. 4, August 1955-March 1959 Phase, TM 3-401, Corps of Engineers, Waterways Experiment Station, November 1963.

37. Chou, Y.T., Engineering Behavior of Pavement Materials: State of the Art, TR S-77-9, Corps of Engineers, Waterways Experiment Station, February 1977.

38. Thompson, M.R. and Robnett, Q.L., Final Report-Resilient Properties of Subgrade Soils, Civil Engineering Studies, Transportation Engineering Series No. 14, Illinois Cooperative Highway and Transportation Series No. 160, University of Illinois, Urbana-Champaign, June 1976.

39. Wilson, E.L., A Digital Computer Program for the Finite Element Analysis of Solids With Non-Linear Material Properties, University of California, 1965.

40. Barksdale, R.D., Analysis of Layered Systems, Georgia Institute of Technology, 1969.

41. Duncan, J.M., Monismith, C.L., and Wilson, E.L., "Finite Element Analysis of Pavement", Highway Research Record 228, Highway Research Board, Washington, D.C., pp. 18-33, 1968.

42. ILLI-PAVE Users Manual, Civil Engineering Department, University of Illinois, Urbana-Champaign, May 1982.

43. Brown, S.F., "Determination of Young's Modulus for Bituminous Materials in Pavement Design," Highway Research Record 431, Highway Research Board, Washington, D.C., pp. 38-49, 1973.

44. Asphalt Concrete Overlays of Flexible Pavement, Vol. I, Development of

New Design Criteria, Report No. FHWA-RD-75-75, Austin Research Engineers, Inc., Federal Highway Administration, Washington, D.C., 1975.

45. Rada, G. and Witzczak, M.W., "Comprehensive Evaluation of Laboratory Resilient Moduli Results for Granular Material," Transportation Research Record 810, Transportation Research Board, Washington, D.C., pp. 23-33, 1981.

46. Figueroa, Jose L., Resilient Based Flexible Pavement Design Procedure for Secondary Road, Ph.D. Thesis, University of Illinois, Urbana-Champaign, 1979.

47. Nie, N.H., Hull, C.H., Jenkins, J.G., Steinbrenner, K., and Bent, D.H., Statistical Package for the Social Sciences (SPSS), 2nd ed., McGraw-Hill Book Company, 1975.

48. Allen, John J. and Thompson, Marshall R., "Significance of Variably Confined Triaxial Testing," Transportation Engineering Journal, Vol. 100, No. TE4, ASCE, New York, pp. 827-843, November 1974.

49. Bonnaure, F., Gravois, A., and Udrone, J., "A New Method for Predicting the Fatigue Life of Bituminous Mixes," Proceedings, Association of Asphalt Paving Technologists, Volume 49, 1980.

50. Finn, F., Saraf, C.L. Kulkarni, R., Nair, K., Smith, W., and Abdullah, A., Development of Pavement Structural Subsystems, National Cooperative Highway Research Program, Volume 1, Final Report, Project 1-10B, February 1977.

51. Kingham, R.I., "Failure Criteria Developed from AASHO Road Test Data," Proceedings, Third International Conference on the Structural Design of Asphalt Pavements, pp. 656-669, 1972.

52. Witzczak, M.W., "Design of Full-Depth Asphalt Airfield Pavements," Proceedings, Third International Conference on the Structural Design of Asphalt Pavements, pp. 550-567, 1972.

53. Research and Development of The Asphalt Institutes' Thickness Design Manual (MS-1) Ninth Edition, Research Report No. 82-2, The Asphalt Institute, College Park, MD, August 1982.

54. Pell, P.S., "Dynamic Stiffness and Fatigue Strength of Bituminous Materials," lecture notes presented on a residential course on Analytical Design of Bituminous Pavements, University of Nottingham, England, March 1982.

55. Thompson, M.R., Concepts for Developing a Nondestructive Testing Based Asphalt Overlay Thickness Design Procedure, Civil Engineering Studies, Transportation Series No. 34, Illinois Cooperative Highway Research Program Series No. 194, University of Illinois, Urbana-Champaign, June 1982.

56. Flexible Pavement Overlay Thickness Design Procedures, Vol. 1, Evaluation and Modification of the Design Methods, Report No. FHWA/RD-81/032, Federal Highway Administration, Washington, D.C., August 1981.

57. Brown, S.F. and Pell, P.S., "A Fundamental Structural Design Procedure

for Flexible Pavements," Proceedings, Third International Conference on the Structural Design of Asphalt Pavements, pp. 369-381, 1972.

58. Deacon, J.A. and Monismith, C.L., "Laboratory Flexural-Fatigue Testing of Asphalt-Concrete With Emphasis on Compound-Loading Tests," Transportation Research Record 158, Highway Research Board, Washington, D.C., pp. 1-31, 1967.

59. Monismith, C.L. and Epps, J.A., Asphalt Mixture Behavior in Repeated Flexure, Report No. TE-69-6, Institute of Transportation and Traffic Engineering, University of California, Berkeley, December 1969.

60. Monismith, C.L., "Rutting Prediction in Asphalt Concrete Pavements," Transportation Research Record 616, Highway Research Board, Washington, D.C., pp. 2-8, 1976.

61. Barksdale, R.D., "Laboratory Evaluation of Rutting in Base Course Materials," Proceedings, Third International Conference on the Structural Design of Asphalt Pavements, pp. 161-174, 1972.

62. Baladi, G.Y., Valleyjo, L.E., and Goitom, T., "Normalized Characterization Model of Pavement Materials," Properties of Flexible Pavement Materials, ASTM STP 807, J.J. Emery, Ed., American Society for Testing and Materials, pp. 55-64, 1983.

63. Chou, Yu T., Analysis of Permanent Deformations of Flexible Airport Pavements, TR S-77-8, Corps of Engineers, Waterways Experiment Station, February 1977.

64. Hyde, A.F.L., Repeated Load Triaxial Testing of Soils, Ph.D. Thesis, University of Nottingham, England, 1974.

65. Kalcheff, I.V., "Characteristics of Graded Aggregates as Related to Their Behavior Under Varying Loads and Environments," paper presented at Conference of Graded Aggregate Base Materials in Flexible Pavement, Oak Brook, IL, March 1976.

66. Thompson, Marshall, R., "Repeated Load Testing of Soils and Granular Materials," paper presented at Soil Mechanics and Foundation Engineering Conference, Minneapolis, MN, January 1984.

67. Monismith, C.L., Ogawa, N., and Freeme, C.R., "Permanent Deformation Characteristics of Subgrade Soils Due to Repeated Loads," Transportation Research Record 537, Transportation Research Board, Washington, D.C., pp. 1-17, 1975.

68. Santucci, L.E., "Thickness Design Procedure for Asphalt and Emulsified Asphalt Mixes," Proceedings, Fourth International Conference on the Structural Design of Asphalt Pavements, pp. 424-456, 1977.

69. Shell Pavement Design Manual, Shell Internation Petroleum Company Limited, London, 1978.

70. Poulsen, J. and Stubstad R.N., "Laboratory Testing of Cohesive Subgrades:

Results and Implications Relative to Structural Pavement Design and Distress Models," Transportation Research Record 671, Transportation Research Board, Washington, D.C., pp. 84-91, 1978.

71. Barker, Walter R. and Brabston, William N., Development of a Structural Design Procedure for Flexible Airport Pavements, TR S-75-17, Corps of Engineers, Waterways Experiment Station, September 1975.

72. A Limited Study of Effects of Mixed Traffic on Flexible Pavements, TR 3-587, Corps of Engineers, Waterways Experiment Station, January 1962.

73. Burns, C.D., Ledbetter, R.H., and Grau, R.W., Study of Behavior of Bituminous-Stabilized Pavement Layers, MP S-73-4, Corps of Engineers, Waterways Experiment Station, March 1973.

74. Grau, R.W., Evaluation of Structural Layers in Flexible Pavement, MP S-73-26, Corps of Engineers, Waterways Experiment Station, May 1973.

75. Bush, A.J., Gunkel, R.C., Regan, G.L., and Berg, R.L., Design of Alternate Launch and Recovery Surfaces for Environmental Effects, ESL-TR-83-64, Air Force Engineering and Services Center, July 1984.

76. Thompson, M.R., Kinney, T.C., Traylor, M.L., Bullard, J.R., and Figueira, J.L., Final Report - Subgrade Stability, Civil Engineering Studies, Transportation Series No. 18, University of Illinois, Urbana-Champaign, June 1977.

77. Ruschman, D.J. "Muck 'n Mire," Air Force Engineering and Services Quarterly, AFRP 85-1, Vol 26, No. 3, Air Force Engineering and Services Center, Tyndall AFB, FL, pp. 12-16, 1985.

78. Army Technical Manual 5-818-2, Air Force Manual 88-6 Chapter 4, Pavement Design for Seasonal Frost Conditions, 1985.

79. Bergan, A.T. and Culley, R.W., "Some Fatigue Considerations in the Design of Asphalt Concrete Pavement," Symposium on Frost Action on Roads, Report Volume II, Organization for Economic Cooperation and Development, Oslo, Norway, 1973.

80. Bergan, A.T. and Fredlund, D.G., "Characterization of Freeze-Thaw Effects on Subgrade Soils," Symposium on Frost Action on Roads, Report Volume II, Organization for Economic Cooperation and Development, Oslo, Norway, 1973.

81. Chamberlain, E.J., "A Model for Predicting the Influence of Closed System Freeze-Thaw on the Strength of Thawed Clays, Symposium on Frost Action on Roads, Report Volume III, Organization for Economic Cooperation and Development, Oslo, Norway, 1973.

82. Bergan, A.T. and Monsmith, C.L., "Characterization of Subgrade Soils in Cold Regions for Pavement Design Purposes," Highway Research Board 431, Highway Research Board, Washington, D.C., 1973

83. Culley, R. W., "Effect of Freeze-Thaw Cycling on Stress-Strain Characteristics and Volume Change of a Till Subjected to Repetitive Loading,"

Technical Report 13, Saskatchewan Department of Highways, Regina, Saskatchewan, Canada, September 1970.

84. Robnett, W.L. and Thompson, M.R., "Effect of Lime Treatment on the Resilient Behavior of Fine-grained Soils," Highway Research Board 560, Transportation Research Board, Washington, D.C., 1976.

85. AASHO Road Test, Report 2, Materials and Construction, Special Report 61B, Highway Research Board, Washington, D.C., 1962.

86. Air Force Engineering and Services Center/Pavements Division Letter, Subject: Airfield Pavement Design, 17 July 1985.

END

7 - 82

Dot/c